SUPPORTED LIPID MONOLAYERS FOR THE INVESTIGATION OF SPECIFIC INTERACTIONS BETWEEN PROTEINS AND LIGANDS

THÈSE N° 1728 (1997)

PRÉSENTÉE AU DÉPARTEMENT DE CHIMIE

ÉCOLE POLYTECHNIQUE FÉDÉRALE DE LAUSANNE

POUR L'OBTENTION DU GRADE DE DOCTEUR ÈS SCIENCES

PAR

Michaela KIESS

Dipl. Chem. ETH

originaire de Männedorf (ZH)

acceptée sur proposition du jury:

Prof. H. Vogel, directeur de thèse
Prof. H.J. Mathieu, corapporteur
Prof. J. Sagiv, corapporteur
Prof. U. Spichiger, corapporteur

Lausanne, EPFL
1997

Peter, Stefi und meinen Eltern gewidmet

Para ser un buen ganador
hay primero que ser un buen perdedor.

Eduardo Pascual

Contents

Summary

In this work, the specific and nonspecific binding of proteins to planar surfaces was investigated. The surfaces were first modified by the spontaneous adsorption of a number of synthesized 1,2-diacyl-*sn*-glycero-3-phosphatidylcholine lipids with different ω-mercapto fatty acids. The influence of packing density, order, fluidity, and mobility of the head groups of these supported thiolipid monolayers on the nonspecific adsorption of proteins was systematically investigated. Nonspecific binding of fibrinogen, IgG, BSA, and rabbit serum to such surfaces was monitored on-line by surface plasmon resonance spectroscopy (SPR) and was found to be exceptionally low. Characterization of the supported thiolipid monolayers by grazing incidence infrared spectroscopy, wetting, impedance spectroscopy, calorimetry, and SPR indicates that protein adsorption is influenced by the nature of the fatty acids and suggests that besides the molecular structure of the layer-forming molecules, other supramolecular aspects such as flexibility of the immobilized lipid layer or protrusion of the lipid head groups play a role. These investigations point the way for the construction of even more highly protein repellent surfaces with potential technical applications in the medical (implants) and diagnostic fields (biosensors).

To investigate specific protein-surface interactions, acetylcholine containing ligand molecules of the general molecular structure $HS(CH_2)_{15}(CO)O(CH_2CH_2O)_nCH_2(CO)OCH_2CH_2N^+(CH_3)_3$ X^- (n = 4, 6, 13) were synthesized. They allow acetylcholine, the natural agonist of the acetylcholine receptor, to be covalently immobilized on a surface. Mixed layers of thiolipids and ligand molecules were formed by self-assembly on planar gold substrates and specific interactions between the immobilized acetylcholine and the nicotinic acetylcholine receptor (nAchR) from *Torpedo Californica* have were investigated on-line by SPR. Though it seems that the receptor binds specifically, bound receptor could be only partially displaced from the surface by excess free ligand. However, further improvement of the sensor surfaces will surely provide in the future a powerful tool for the investigation of membrane proteins and transmembrane communication.

Zusammenfassung

Diese Arbeit befasst sich mit der Untersuchung von spezifischer und unspezifischer Bindung von Proteinen an planare Oberflächen, welche durch spontane Adsorption organischer Schwefelverbindungen an dünne Goldschichten gezielt verändert wurden. Selbstorganisierte Lipidmonoschichten aus synthetisierten 1,2-Diacyl-*sn*-glycero-3-phosphatidylcholinen mit ω-ständigen Thiolgruppen an verschiedenen Fettsäuren ermöglichten die systematische Variation von Packungsdichte, Ordnung und Beweglichkeit der immobilisierten Thiolipide und erlaubten so, den Einfluss dieser Eigenschaften auf die unspezifische Proteinadsorption zu erforschen. Die Thiolipidmonoschichten zeigten bemerkenswert geringe Adsorption von Fibrinogen, Serumalbumin, Immunoglobulin G und Blutserum, welche on-line mit Oberflächenplasmonen-spektroskopie (SPR) verfolgt wurde. Die ausführliche Charakterisierung der kovalent gebundenen Lipidmonoschichten mittels Reflektions-Absorptions-Infrarotspektroskopie (GI-FTIR), Impedanzspektroskopie, Oberflächenplasmonenspektros-kopie, Kalorimetrie und Kontaktwinkelmessungen lässt vermuten, dass die Struktur der Fettsäuren der Thiolipide die Proteinadsorption beeinflussen, und dass neben der Molekülstruktur der adsorbierten Lipide auch andere, supramolekulare Aspekte wie die Flexibilität der Schicht dazu beitragen. Die angewendeten Strategien zur Reduktion der unspezifischen Proteinadsorption scheinen also erfolgreich zu sein und erlauben wohl in Zukunft, noch bessere Schichten mit technischem Anwendungspotential im medizinischen (Implantate) und diagnostischen Bereich (Biosensoren) herzustellen.

Ausserdem wurden über Thiolgruppe verankerbare "Ligandmoleküle" mit der allgemeinen Strukturformel $HS(CH_2)_{15}(CO)O(CH_2CH_2O)_nCH_2(CO)OCH_2CH_2N^+(CH_3)_3\ X^-$(n = 4, 6, 13) synthetisiert. Diese erlaubten die Fixierung von Acetylcholin, dem natürlichen Agonisten des Acetylcholinrezeptors, an der Oberfläche. Gemischte Schichten wurden durch spontane Adsorption dieser Ligandmoleküle und der oben beschriebenen Thiolipide an Goldoberflächen hergestellt und mit verschiedenen Präparationen von nikotinischem Acetylcholinrezeptor inkubiert, der aus dem elektrischen Organ des *Torpedo Californica* Aals isoliert wurde. Die Proteinadsorption wurde wiederum mit Oberflächenplasmonen Spektroskopie verfolgt. Die Ergebnisse deuten zwar auf spezifische, aber meistens irreversible Bindung des Membranrezeptors hin. Verbesserte Sensoroberflächen werden in Zukunft sicher einen wertvollen Beitrag zur Erforschung der transmembranen Kommunikation sowie Struktur und Funktionsweise von Membranproteinen leisten können!

Remerciements

Je tiens à remercier toutes les personnes qui ont contribué à ma thèse.

En particulier je tiens à remercier mon directeur de thèse, le Professeur Horst Vogel, de m'avoir admise dans son groupe de recherche me permettant de faire la connaissance des domaines fascinants des biocapteurs et des analyses de surfaces.

Je tiens aussi à remercier les corapporteurs, Madame la Professeur Ursula Spichiger et Messieurs les Professeurs Jakob Sagiv et Hans Jörg Mathieu, pour la correction du manuscrit, leurs propositions d'amélioration et l'encouragement. Mes remerciements pour les corrections vont également à Sarah Shephard et Peter Vischer ainsi qu'à Madame Verena Tabet pour le support administratif.

De plus j'aimerais remercier très chaleureusement Monsieur Andreas Heusler pour la collaboration. Son calme et sa patience, ses connaissances techniques, sa capacité d'écouter et d'analyser et sa volonté perpétuelle de "démystifier la chimie" ont contribué beaucoup au succès des nombreuses synthèses décrites dans cette thèse. Dans ce contexte, je remercie aussi les Messieurs Peter Pèchy, Roland Cloux et Laurenz Kellenberger pour les bons conseils. Je tiens à remercier aussi Monsieur Häberli de l'EPF de Zürich pour les nombreux spectres de masses fiables et ultra rapides et Monsieur Theo Schürholz ainsi que le Professeur Ferdinand Hucho pour le récepteur d'acétylcholine et les nombreux conseils.

Ma gratitude va également à mes collègues de l'institut, en particulier à Martha Liley, Claus Duschl, Mila Bontcheva, Stephan Heyse et Thierry Stora pour l'introduction dans les différentes techniques d'analyses de surfaces, les bonnes idées et les conseils, à Serge Cattarinussi pour les nombreuses discussions ainsi qu'à Sibylle Vuillemin qui a contribué à ce travail dans comme assistante étudiante.

Finalement, je remercie mon ami Peter et ma famille pour l'encouragement et le soutien tout au long de cette thèse.

Ce travail a été rendu possible grâce à la bourse "Le doctorat dans l'autre EPF" du conseil des écoles polytechniques fédérales. Dans ce contexte je tiens à remercier aussi Cornelia Sommer qui a introduit une suite de ce projet à l'EPFZ dans le cadre de son travail de diplôme.

Abbreviations

Lipids, Thiolipids and Ligand molecules

DLPE	1,2-dilauroyl-*sn*-glycero-3-phosphatidylethanolamine
DMPC	1,2-dimyristoyl-*sn*-glycero-3-phosphatidylcholine
DPPC	1,2-dipalmitoyl-*sn*-glycero-3-phosphatidylcholine
DOPC	1,2-dioleoyl-*sn*-glycero-3-phosphatidylcholine
DPhyPC	1,2-diphytanoyl-*sn*-glycero-3-phosphatidylcholine
DMPSH	1,2-dimyristoyl-*sn*-glycero-3-phosphothioethanol
PyP	16-(2-pyridyldithio)hexadecanoic acid
BPyPPC	1,2-bis[16-(2-pyridyldithio)hexadecanoyl]-*sn*-glycero-3-phosphatidylcholine
BmPPC	1,2-bis(16-mercaptohexadecanoyl)-*sn*-glycero-3-phosphatidylcholine
PmPPC	1-palmitoyl-2-[16-mercaptohexadecanoyl]-*sn*-glycero-3-phosphatidylcholine
LmPPC	1-lauroyl-2-[16-mercaptohexadecanoyl]-*sn*-glycero-3-phosphatidylcholine
PhymPPC	1-phytanoyl-2-[16-mercaptohexadecanoyl]-*sn*-glycero-3-phosphatidylcholine
mPPhyPC	1-[16-mercaptohexadecanoyl]-2-phytanoyl-*sn*-glycero-3-phosphatidylcholine
PyP-PEG$_4$-ACh	3,6,9,12,15-pentaoxa-16-carbonyl-31-(2-pyridyldithio)-hentriacontanoic acid choline ester bromide salt
PyP-PEG$_6$-ACh	3,6,9,12,15,18,21-heptaoxa-22-carbonyl-37-(2-pyridyldithio)-heptatriacontanoic acid choline ester tosylate salt
PyP-PEG$_{13}$-ACh	3,6,9,12,15,18,21,24,27,30,33,36,39,42-tetradecaoxa-43-carbonyl-58-(2-pyridyldithio)-octapentacontanoic acid choline ester bromide salt

General Chemicals

ACh	acetylcholine
CDI	1,1'-carbonyl-diimidazol
CHAPS	3-[(3-cholamidopropyl) dimethylammonio]-1-propane sulfonate
DMAP	4-(dimethylamino)pyridine
DCC	dicyclohexylcarbodiimide
DTT	1,4-dithio-DL-threitol
EDC	N-(3-dimethylaminopropyl)-N'-ethyl-carbodiimid
EDTA	ethylenediaminetetraacetic acid
EtOH	ethanol

HEPES	4-(2-hydroxyethyl)piperazine-1-ethanesulfonic acid
hr	*hour*
MetOH	methanol
nAchR	*nicotinic acetylcholine receptor*
OG	n-octyl-β-D-glucopyranoside
PC	phosphatidylcholine
RT	ambient temperature
TFA	trifluoroacetic acid
THF	tetrahydrofurane
tosylate	p-toluenesulfonate
Tris	tris(hydroxymethyl) aminomethane
Trityl	triphenylmethyl-

Analytical

AFM	atomic force microscopy
ATR	attenuated total reflection
CI	chemical ionization
FTIR	Fourier transformation infrared spectroscopy
GI	grazing incidence
IS	impedance spectroscopy
LB	Langmuir-Blodgett
m.p.	*melting point*
MS	mass spectrometry
SA	self-assembly
SPR	surface plasmon resonance spectroscopy
ToF-SIMS	time-off-flight secondary ion mass spectrometry
TIRF	total internal reflection fluorescence spectroscopy
TLC	thin layer chromatography
XPS	X-ray photoelectron spectroscopy

Part I. Background

1. Introduction

This investigation deals with **specific interactions** between **acetylcholine immobilized** on a **planar surface** and the **nicotinic acetylcholine receptor** (nAchR) in solution using surface analytical techniques based on evanescent waves. The membrane receptor-ligand system studied is a prototype for interactions occurring at cell surfaces, which allow communication between the inside and the outside of a cell across the membrane bilayer. The investigation of specific protein-surface interactions requires, however, the elimination of nonspecific interactions contributing to the measurement signal. One of the main objectives of this work was therefore the development of surfaces with very low nonspecific protein adsorption, which could be functionalized without loss of their protein-repellent character. Functionalization of a surface means the introduction of chemical moieties such as ligands, which allow the surface to be specifically addressed. This goal was achieved by coating planar gold surfaces with chemisorbed, self-organized monolayers of synthesized phosphatidylcholine lipids bearing ω-standing thiols on their fatty acids. Self-assembly of such thiolipids in the presence of a synthesized, immobilizable ligand molecule containing an acetylcholine moiety yielded surfaces to which the nicotinic acetylcholine receptor could specifically bind.

Understanding and control of **interactions between proteins and solid surfaces** is a challenging topic of great importance in current biophysical research. The preparation of surfaces with low nonspecific adsorption of proteins is crucial for many applications requiring contact with proteins or cells. Highly selective biosensors and diagnostic products, new biocompatible implant materials, the production, processing and purification of proteins as well as their storage and transport in non-adsorbing containers and tubing without depletion of the solution and without cross-contamination in analytical systems, site directed drug delivery, and mediation of cell adhesion to surfaces in biotechnology are just a few examples illustrating the widespread field of applications for protein-repellent surfaces [And85a]. **Biosensors** occupy in this context a special position as they not only require surfaces with low nonspecific protein adsorption, but in addition take advantage of the highly selective molecular recognition processes between biomolecules such as receptors and enzymes and their ligands and substrates by immobilizing them at the interface between a conventional optical, electronic, acoustic, etc. detection system and the analyte. They are so interesting because the selectivity of biological molecules by far surpasses "man-made selectivity", particularly in the case of organic analytes in complicated samples. Biological and environmental samples, for example, are very complicated from an analytical point of view: they are usually mixtures of a great variety of compounds with different properties and concentrations, often containing the analyte at very low concentration.

The value of an analytical instrument, however, increases with decreasing need for sample preparation and thus with increasing selectivity of the detection system.

Biological molecules have been immobilized on sensor surfaces by various methods ranging from covalent attachment to activated surfaces [Lie93, Fäg90, Löf90], to entrapment in polymer matrices, to simple physisorption. With the improvement of **surface analytical tools** [DeG85, Swa85, Mac87, Ulm91, Kno91], immobilization of biomolecules at surfaces could be better controlled. Generally, custom-made **modification of the surface properties** of materials has become of increasing interest as the surface properties determine molecular interactions at interfaces and thus many macroscopic properties of a material. Thereby, the formation of **self-organized monolayers** by immobilization of **organic** molecules on ***inorganic*** substrates has proved to have a great potential, as organic synthesis allows an unlimited variation of the chemical structure of the molecules [Swa87]. Their adsorption to materials' surfaces allow the construction of planned supramolecular structures [Mao88] and the subtle modulation of interfacial properties without affecting valuable bulk characteristics of a material.

Self-organized monolayers on solid substrates are formed by **physisorption** (ionic or hydrogen bonding) or **chemisorption** (covalent bonding) of organic molecules. Organic acids can be physisorbed to glass [Mao84] or metals and metal oxides such as aluminum [All85a, Che89] and silver oxide [All82, Sch86] and zirconium phosphonates can be physisorbed to silicon [Din81, Lee88a, Lee88b]. Organic silanechlorides or -ethers can be chemisorbed to activated SiO_2 [Sag80, Net83a, Net83b, Mao84, Fin86], silicon [Was89], germanium, aluminum, zinkselenide and mica [Kes91] and organic sulfur compounds to metal substrates such as gold [Nuz83, Nuz87, Nuz90, Ulm88, Eva91, Ulm92, Tro88, Whi88, Lai89, Bai89a-c], silver [Wal91], copper [Lai92b], and gallium arsenide [She92].

Silanization has a longer tradition than the immobilization of organo-sulfur compounds as it is commonly used to hydrophobize silica gels for reversed phase chromatography (for example [Bok76, Sza84, Bla85, Sch90]). Surface modification is thereby quantitated for example by determining surface areas to be modified via the adsorption of gas to evacuated silica gels followed by elemental analysis of silanized SiO_2 after digestion with HF. Silanization is a nucleophilic substitution reaction. Handling of the reagents is very delicate since omnipresent water has the same type of reactivity and competes thus with the hydroxyl groups on the surface. Vapor phase deposition of silanes [Jön85] is therefore often used rather than immersion of the solid substrate into a solution of silanes. Synthesis of organo-silane compounds is delicate for the same reasons and the choice of intramolecular functional groups is restricted to non-nucleophiles (polymerization!). Formation of densely packed monolayers by silanization is more difficult than by self-assembly of sulfur compounds on metal substrates. However, the Si-O

bond formed is very stable (Si-O bond strength: 191 kcal/mole [Wea73]) and allows chemical modification of the immobilized organic layers and controlled multilayer formation [Net83b, Net83c, Mao85, Mao87a, Mao87b, Mao88, Ulm89, Til89, Was89b]. The possibility of using optically transparent substrates allows detection by optical methods such as total internal reflection fluorescence spectroscopy (TIRF) and attenuated total reflection infrared spectroscopy (ATR-FTIR). Formation of ordered mono- and multilayers with chromophoric groups at defined positions as organic π-donor-acceptor systems is of particular interest for the development of media exhibiting high second order polarization susceptibility [Ulm88, Til90, Eva91].

In the case of spontaneous self-organization of thiocompounds, gold is a particularly suitable substrate due to the instability of gold oxides allowing thus good control of the substrate's surface. The driving forces are the at least partial formation of a strong Au-S bond by a redox mechanism (bond strength of Au-S: 100 kcal/mole (40 kcal/mole at the surface); Ag-S: 52; Cu-S: 66 [Wea73]) and the hydrophobic interactions between long hydrocarbon chains. Packing densities of the self-organized monolayers depend on the molecular structure of the thiocompounds. The adsorption of sulfur to metal surfaces is little competed by other chemical moieties. The choice of functional groups in the layer-forming molecules is therefore much less restricted. Thiols are susceptible to oxidation upon exposure to air, but disulfides have been shown to adsorb as well to metal substrates. Handling of such molecules is therefore easier than in the case of silanes.

Up to now, mainly water-soluble proteins such as antibodies [Fäg90] and enzymes have been immobilized at interfaces of biosensors since they are quite stable, relatively easy to handle and to procure. This work, however, aims at the development of a new concept for a biosensor and model membrane system based on membrane receptors. Investigation of the relationship between the structure and the biological function of membrane receptors not only provides understanding of the communication between cells, but may contribute also to the development of new drugs since many of these receptors are potential targets for new pharmaceuticals. Membrane receptors can be located at the surface of the membrane, partially inserted or membrane spanning with sometimes large extra-membranous parts. They interact with chemical messengers such as hormones, neurotransmitters etc. and transmit signals in various ways to second messengers across the membrane. Membrane proteins are generally much more difficult to handle than water-soluble proteins. Preservation of their structural and functional properties during purification and handling requires for example the use of appropriate detergents to stabilize the structure by protecting hydrophobic parts usually located within the lipid membrane from contact with water.

So far, membrane-spanning proteins have been investigated when reconstituted in lipid vesicles or inserted into planar lipid membranes spanning either holes in a teflon septum [Paw94,

Mes96] or in the openings of patch-clamp pipettes [Sak92]. However, the latter two model membrane systems are restricted to the investigation of proteins which influence the electrical properties of the membrane. Incorporation of membrane proteins into supported lipid bilayers is very promising [Lan92a, Hey97]. Such supported lipid bilayers are more stable, easy to produce once the appropriate molecules are synthesized and their handling is more facile. Yet, preservation of structural and functional integrity of the proteins upon their insertion into the supported membranes is difficult.

The "reversed" system established in this work (fig. 1.1) is supposedly simpler and may provide useful complementary information on membrane receptor-ligand interactions. In analogy to affinity chromatography, not the protein, but a small ligand is thereby immobilized on a surface. It interacts specifically with a membrane receptor protein in solution. Upon addition of excess free ligand, the bound receptor is displaced from the surface. Such a process can be monitored for example by surface plasmon resonance spectroscopy. It yields information on the relative binding strengths of the competing free ligand and may be useful for the screening of new drugs, which, as mentioned above, often target membrane receptors.

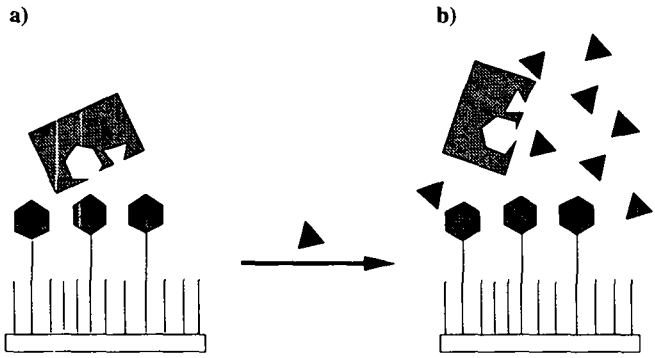

Fig. 1.1. Concept of the biosensor. Specific interaction of a membrane receptor with a functionalized surface (a) and displacement of the adsorbed protein by excess free ligand (b).

In addition, this kind of system could also provide information on the binding properties of mutant receptors, on the number and distribution of binding sites, the mechanism of ligand binding, as well as possible conformational changes upon ligand binding and general information on the structure of the protein by serving as a substrate for 2D-crystallization. The structural aspects may be probed using methods such as ATR-FTIR, surface enhanced Raman spectroscopy, or atomic force microscopy (AFM). As purification of receptor proteins is a very

tedious task, such a system may also be valuable for the systematic optimization of affinity chromatography, the success of which can so far only be determined on a trial-and-error base, using time consuming, conventional binding assays to probe receptor activity after each purification step.

The construction of this new tool for membrane-receptor investigations is described in this work. In the first part, principles of nonspecific interactions between proteins and surfaces are discussed. Based on these a surface was designed, which is optimized with respect to low nonspecific protein binding. Different possibilities of immobilizing small ligands are evaluated and the chemical structure of molecules to be synthesized are elaborated. In the second part of this work, the experimental results are presented and discussed. This includes the synthesis of "matrix and ligand molecules", the characterization of the self-assembled monolayers formed thereof, as well as nonspecific and specific protein binding to these surfaces. In the third part, the experimental procedures used are described. The appendices include infrared-spectra, reagents used for the development of analytical thin layer chromatograms, various sets of measurement parameters and the synthesis of an affinity matrix for the purification of the serotonin (5-HT_3) receptor as another mean to investigate protein-ligand interactions.

1.1. Nonspecific Binding of Proteins to Surfaces

Selectivity, sensitivity, and reproducibility are some of the most important criteria for an analytical tool. Among the major problems encountered when using proteins for analytical purposes is their nonspecific adsorption to surfaces, which prevents the detection of specific signals, leads to depletion of analytes and to crosscontamination between samples. However, as discussed above, surfaces with low nonspecific protein adsorption are important for many other applications as well. Much effort has been made to relate the structural properties of a surface with its protein adsorption characteristics. In this chapter, current theories about the interaction of proteins with surfaces and the minimization of protein adsorption are briefly summarized. Surfaces reported in literature to show the lowest nonspecific adsorption are selected. They are used as a starting point for the optimization of molecular structures based on theoretical perceptions so as to reduce further the nonspecific adsorption of proteins to the surface produced by their immobilization. In light of the intended investigation of specific protein-surface interactions, the possibility to functionalize these surfaces without loss of their protein repellent character is an important additional constraint.

1.1.1. Protein Adsorption and Biocompatibility

In the most general model proposed for protein adsorption to a surface, the protein diffuses to a surface and increasingly denatures with prolonged residence there [And, 87, And92]. The driving force of denaturation is the improvement of the interaction between protein and surface. The probability of dissociation decreases accordingly.

Adsorption of proteins to solid surfaces may be explained by similar free-energy considerations as conformational stability and aggregation of proteins [And86]. Table 1.1 lists the noncovalent forces determining such interactions in aqueous solutions. The interactions usually involve surface complementarity. In this context it is also important to note that the conformation of a protein is usually only marginally stable: For an average globular protein of 150 amino acid residues, the free energy of two adjacent conformational states differs only by about 10 kcal/mole [And86]. The conformation of a protein is dynamic since it is continuously subjected to small changes induced by Brownian motion. The presence of a surface changes the environment of a protein and thereby influences the energy of a conformational state and its probability.

type of interaction	description	effect of increasing ionic strength?	directional?
ionic	Coulomb interactions	-	-
H-bonding	donor-acceptor	-	+
charge-transfer	π-π interactions (aromatic compounds)	+	+
hydrophobic or entropic	forced order of water molecules next to apolar surface	+	-

Tab. 1.1. Major forces acting on proteins in aqueous solutions (modified after [And86]).

Under normal physiological conditions, the salt concentration is 150 mM. Charges are thus screened by counterions beyond a distance of about 10 Å. By the time a protein is within 10 Å of a charge, specific interactions dominate over the electrostatic interactions [And86].

The literature on biocompatibility of materials is a rich source of information on protein adsorption, since this is one of the first events occurring when a material comes into contact with a biological fluid [Hof82, And86, Rat96, Ima92]. It is only preceded by adsorption and possibly absorption of water (hydration) and low molecular weight solutes (amino acids etc.), ion binding and formation of an electrical double layer [And86]. Protein adsorption influencing the structure and properties of a protein is therefore believed to be crucial for the biocompatibility

of a material [And86, Hor87, And92]. And yet, in Switzerland for example, none of the recognized tests currently required for the evaluation of biological safety and certification of conformity of new medical devices investigates protein adsorption to its surface nor is there any intention to introduce such tests in the testing norms currently in preparation.

Biocompatibility distinguishes between blood compatibility and tissue compatibility, which can be further divided into soft-tissue compatibility and hard-tissue compatibility [Ima92]. Blood compatibility is usually more problematic than tissue compatibility. At an early stage of blood/material contact, non-thrombogenicity of a surface is crucial, whereas on the long term, cell growth is also important. Whole blood consists of 45 % (v/v) red and white blood cells and blood platelets and 55 % (v/v) plasma containing salts, hormones and proteins.

Both bulk (mechanical, chemical, physical) and surface properties are thought to influence the biocompatibility of a material [Win96, Ima92]. Surface modification, however, allows the biocompatibility of a material to be improved without changing bulk properties and handling characteristics of a device. Up to date, blood compatible materials are predominantly soft and hydrophilic [Rat96b].

Figure 1.3 summarizes the strategies employed in the design of biocompatible implant materials. Thromboresistance was found to be improved by immobilizing antithrombogenic moieties on surfaces, by their inclusion into a polymer lattice, or by mimicking surfaces that are not thrombogenic.

However, according to Ratner, there are no established rules for the biocompatibility of materials [Rat96a] and there is a big discrepancy between *in vitro* and *in vivo* studies of implant materials. *In vivo*, all implants end up being encapsulated at the end of the inflammatory cascade [Hof82, Rat96a] whereas *in vitro* differences can be observed [Pet83]. Ratner therefore proposed as a general strategy for the development of biocompatible materials the minimization of nonspecific interactions between implant and body fluid and the enhancement of specific interactions, which may even induce specific healing pathways [Rat96b].

Which protein is thus adsorbed preferentially to which surface and why? What are the general rules?

Factors influencing interactions of blood with foreign materials can be divided into three categories: the nature of the biomaterial itself, blood flow effects (hemodynamics), and the biological environment [Hof82]. Hydrophobicity, hydrophilicity, surface charge density, charge transfer properties, ionizability (acidity), surface dynamics, surface heterogeneity, domains and topography are considered to be the properties of surfaces and proteins that determine their

interactions [And92]. Generally, proteins tend to adsorb more strongly to hydrophobic than to hydrophilic surfaces [And86, And92]. Consequently, protein-resistant surfaces are preferentially neutral in order to avoid electrostatic interactions and hydrophilic in order to avoid hydrophobic interactions [And86]. Reversibility of protein adsorption is more likely for hydrophilic surfaces, from which proteins can be desorbed by exposure to extreme pH or high ionic strength. The time of interaction between a protein and a surface is also thought to be important for the reversibility of protein adsorption as the protein tends to adapt orientationally and conformationally in order to maximize favorable interactions with the surface [And92]. For the investigation of reversible protein-surface interactions kinetic measurements may thus be preferable to equilibrium measurements as in the latter the signal is only read when it is constant [Spi95]. For low analyte concentrations, this can take a long time allowing already adsorbed proteins to change their conformation. In the case of kinetic measurements, the equilibrium signal is calculated from the slope of the linear region [Spi95].

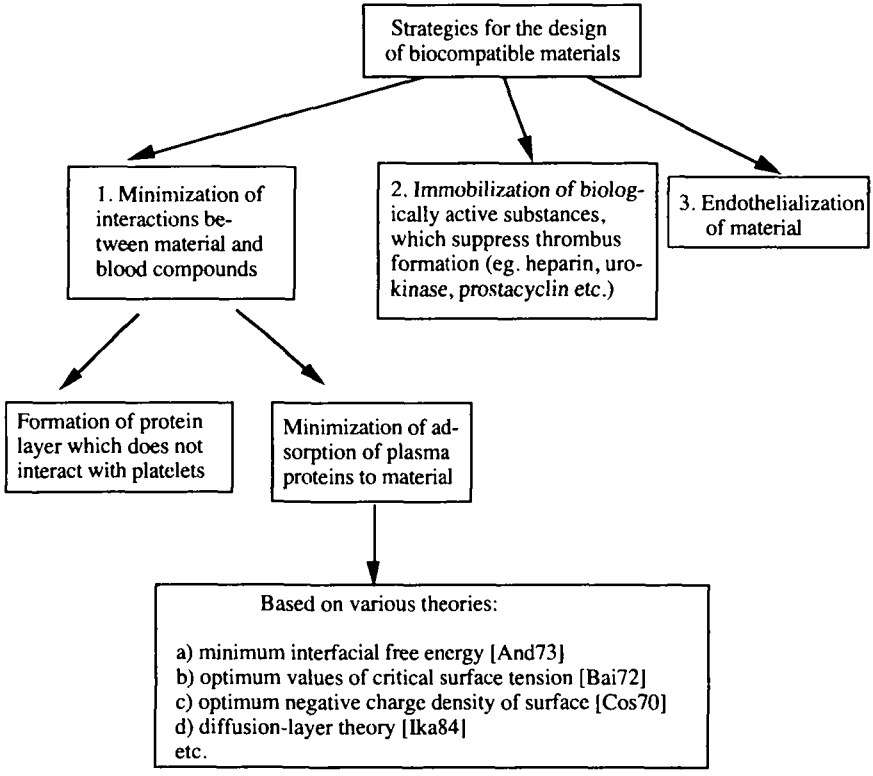

Fig. 1.3. Strategies for the design of biocompatible materials [Ima92].

Many theories have been established trying to relate physical and chemical properties of surfaces to the low nonspecific adsorption of proteins. One of the most credible is certainly that of Andrade, who postulated that the free energy at the interface of implant and blood must be zero if the introduced surface is not to disturb the equilibrium of the blood system and adsorb proteins [And76, And83, And95]. He argues that the driving force for protein adsorption and denaturation of a surface decreases with the surface being water-like in energetic terms. This may explain the low protein-affinity of hydrogels and polysaccharides used for protein chromatography. Other theories for low nonspecific adsorption of proteins suggest for example optimal values for critical surface tension [Bai72] or that the free energy of a surface must be minimal in order to avoid minimization of its free energy by protein adsorption [Lym65]. This leads to conclusions which are somewhat contradictory to the ones above since metals and inorganic materials in general have the highest surface free energies, but are hydrophilic, whereas Teflon and fluorophores, which are hydrophobic, have generally the lowest surface free energies [Rat82].

However, some generally accepted findings on protein adsorption to surfaces are listed below:

- The adsorption process is often entropically driven. Entropy is thereby gained from dehydration of hydrophobic surfaces and structural rearrangements of the protein [And86].
- The composition of an adsorbed protein layer depends on the surface exposed to the protein mixture. Thrombogenicity depends on the protein layer, the composition of which changes with time (Vroman effect, e.g. [Wil91]). Shear rates may influence protein adsorption [Ima92] and type of thrombus formed [Hof82].
- Conformational changes of proteins during adsorption have been investigated by CD and FTIR [Gen82, Oka78, Sak80]. Loss of α-helix content and increase of β-sheet content upon adsorption have been reported. Less conformational change has been observed for surfaces forming hydrogen bonds [Ito86, San86, Lei87, Len89]. Ito claims that increase of β-structure increases platelet adhesion [Ito90].

Throughout the literature, materials presenting poly(ethylene glycol) (PEG) and phosphatidylcholine (PC) on their surfaces are repeatedly reported to show the lowest nonspecific binding of proteins.

Poly(ethylene glycol) is a water-soluble, very flexible, and rapidly moving polymer. Protein adsorption was shown to be strongly reduced upon coating of surfaces with poly(ethylene glycol) derivatives [Lee89, Jeo91, Pri91, Gom91, Ber92, Pri93, Thi97]. Prime et al. for example reported very low adsorption of various proteins to mixed self-assembled monolayers

of $HS(CH_2)_{11}H$/ $HS(CH_2)_{11}(OCH_2CH_2)_nOR$ with n = 0 - 17 and R = H or CH_3 investigated by ellipsometry [Pri91, Pri93]. Blood compatibility of PEG has also been repeatedly described [Nag84, Lee95]. Protein-surface interactions in the presence of poly(ethylene glycol) have also been theoretically studied [Jeo91]. "Steric repulsion" [And86, Jeo91] or "steric (or overlap) forces" [Isr92a] are thought to be responsible for the repulsive forces acting on proteins when they approach a surface with terminally attached PEG chains. The forces are attributed to one or both of two phenomena: On the one hand, poly(ethylene glycol) chains are compressed upon collision with a protein. This leads to a reduced number of conformational states accessible to the polymer chains and hence to an unfavorable loss of entropy. The protein is thus entering "the excluded volume", which is determined by the volume usually occupied by the polymer chain. On the other hand, the collision expels solvent from the polymer layer at the interface. When the free energy of the solvent is lower in the solvent-swollen polymer layer than in the bulk, the energy required to desolvate the polymer layer disfavors its compression [Pri93]. Such arguments are commonly used to explain the stability of colloidal dispersions [Sat80]. In addition, poly(ethylene oxide)/ water interfaces are thought to have very low interfacial free energies, and thus low driving forces for protein adsorption [And73, Col82, Lee88]. Other characteristics of PEG, such as weak hydrogen bonding, low van der Waals interactions, and a stereochemical structure which hardly perturbs the structure of the water, are considered to contribute as well [And92]. Protein adsorption to PEG surfaces depends on the type of protein, its radius, as well as the molecular weight of the PEG chains and their packing density [Jeo91]. The concentration of PEG chains required at an interface to resist protein adsorption was found to decrease with increasing size of the protein. Yet, too densely packed, rigid poly(ethylene glycol) layers do not resist protein adsorption. Force profiles between PEG coated surfaces have been directly measured using the Surface Force Apparatus [Kuh94]. Systematic variation of the poly(ethylene glycol) content in phosphatidylethanolamine bilayers showed that the force is repulsive at all separation distances and that the thickness of the steric barrier could be easily controlled by adjusting the concentration of poly(ethylene glycol) lipids [Kuh94].

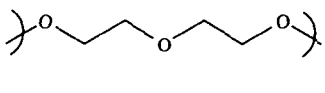

poly(ethylene glycol)
or
poly(ethylene oxide)

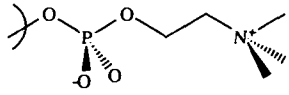

phosphatidylcholine
or
phosphorylcholine

Fig 1.2. Chemical moieties reported to resist protein adsorption best.

Interest in the phosphatidylcholine (PC) moiety arose in the course of the search for improved implant materials when it was discovered that chemical inertness is not sufficient to make a material thromboresistant [Alb82]. Hayward and Chapman wondered why blood plasma

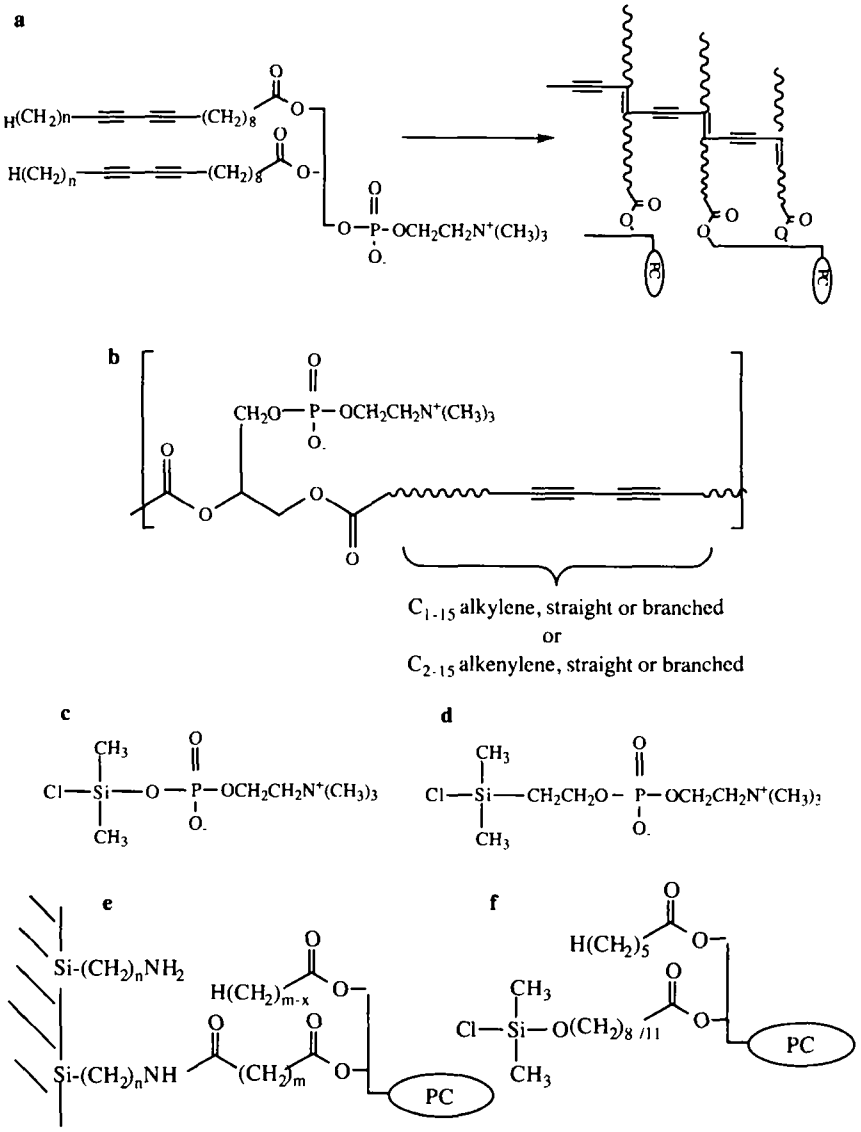

Fig. 1.4. Examples of synthetic derivatives of phosphatidylcholine (PC). a) PC-polymers as model membrane systems [Joh80]; b) biocompatible polyesters [Dur87]; c , d) immobilizable PC-derivatives for biocompatible surfaces [Dur86]; e) PC-derivatives for the modification of chromatography materials for protein purification ("immobilized artificial membranes") [Pid89, Pid90]; f) immobilizable lipids for use as model membrane systems [Kal87].

erythrocytes and blood platelet cells do not induce blood coagulation. Searching for biological arguments, they found an asymmetric distribution of lipids in the latter's cell membranes [Hay85] with phosphatidylcholines and sphingomyelins dominating in the outer lamella of the membranes and phosphatidylserine and phosphatidylethanolamine prevailing in the inner lamella. The hypothesis that this asymmetry serves to maintain the delicate balance between homeostasis and thrombosis was tested in blood coagulation assays and here PC proved to be the least coagulating [Hay84]. Since then Chapman's and other groups have synthesized various derivatives of phosphatidylcholine, some of which are shown in figure 1.4.

The synthesis of the thiolipids depicted in figure 1.5 has been described by group doing research in the field of drug delivery [Sam85, Sad86, Chu91]. These lipids have a sulfur group in their hydrocarbon chains, originally intended to stabilize vesicles by mild and reversible formation of intermolecular disulfide bonds. Later, such lipids were also reported to form self-organized monolayers on planar gold substrates [Die86, Fab89, Coy89].

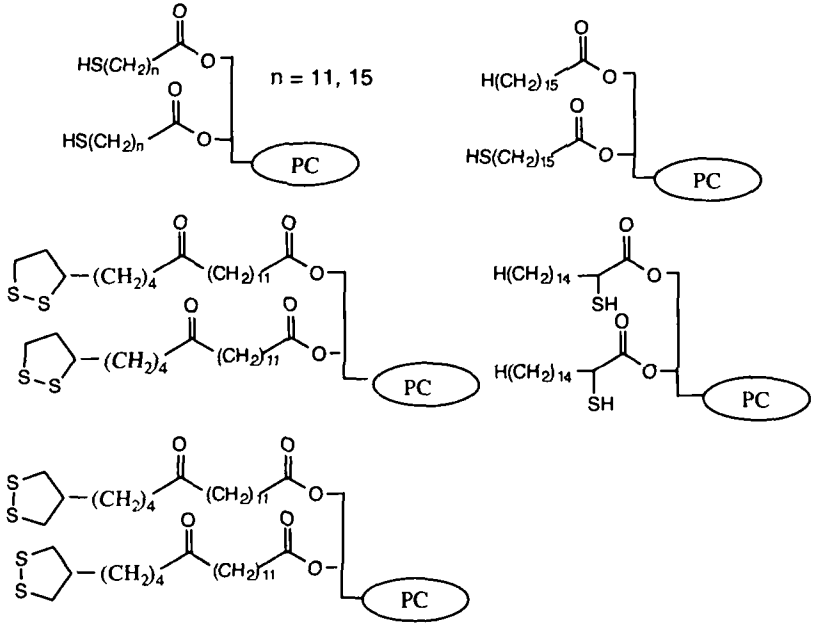

Fig. 1.5. Thiolipids with phosphatidylcholine (PC) head groups.

The biological arguments of Hayward and Chapman explaining the protein repellent character of PC (see previous pages) may be supported by the general investigations on the interactions of

lipid bilayers, where the lack of strong adhesion or aggregation of bilayers and vesicles composed of uncharged lipids with phosphatidylcholine, poly(ethylene glycol) and sugar head groups is attributed to *repulsive hydration and steric forces* [Isr92a]. Repulsive hydration forces are thought to arise whenever water is strongly bound to *hydrophilic* groups at a surface because of the energy required to dehydrate these groups as two surfaces approach. Choline derivatives are known to be extremely hygroscopic. Different types of repulsive steric forces (thermal fluctuation forces) occurring between two approaching lipid bilayers can be distinguished: They are the undulation force, the peristaltic force, and the protrusion force [Isr92a]. It is still not clear whether these steric repulsion forces may even include the repulsive hydration forces mentioned above [Isr92a].

The optimized functionalized surface

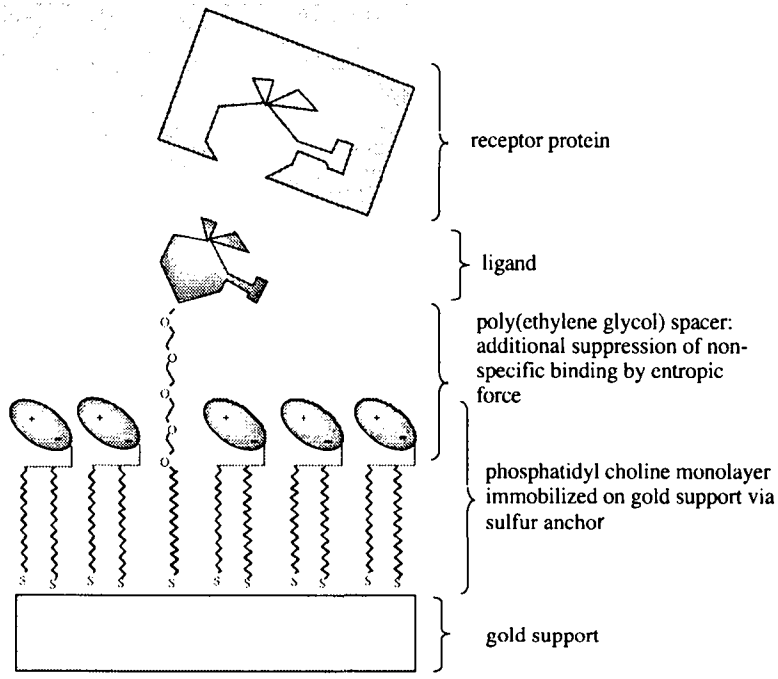

Fig. 1.6. Design of an optimized functionalized surface for the investigation of specific protein-ligand interactions.

In the supported thiolipid monolayers investigated in this work, the undulation and the peristaltic force are certainly excluded, but a repulsive protrusion force could still be imagined in the case of "loosely attached" lipid molecules as this force arises when two lipid bilayer surfaces come so close together that their protruding lipid molecules sterically overlap [Isr92a].

Three routes have so far been described for the formation of polar, supported lipid monolayers composed of derivatives of 1,2-diacyl-3-glycero-phosphatidylcholine. Two of them use SiO_2 as a solid support (fig. 1.4.e [Pid89, Pid90], fig. 1.4.f [Kal87], the third one thin gold films (fig. 1.5 [Die86, Fab89, Coy89]).

For the present work, thiolipids of the kind depicted in figure 1.5 were judged to be suitable as "matrix molecules". They unite the two most important properties required for the investigation of specific protein-surface interactions by surface plasmon resonance spectroscopy: immobilizability on thin gold films and potentially low protein adsorption due to the phosphatidylcholine head group. Figure 1.6 shows the type of functionalized surface used in this work for the investigation of specific protein-ligand interactions.

In summary, this concept offers the following advantages:

- low nonspecific protein binding to the surface due to the presence of PC groups and PEG
- known layer-forming properties of such kinds of lipids on gold [Die86, Coy89, Fab89]
- chemical and mechanical stability of covalently attached lipid layers allows good characterization of the surface
- simplified model of a biological membrane (surface)
- investigation by SPR possible (no labeling of protein or ligand required)

1.1.2. Optimization of the Chemical Structure of Thiolipids

Many theories have been established trying to relate the physical and chemical properties of a surface and its resistance to nonspecific protein adsorption (cf. chapter 1.1.1). This chapter deals with the relationship between the chemical structure of thiolipids and nonspecific binding of proteins to the corresponding self-assembled monolayers. Possible strategies for the reduction of nonspecific protein-binding to such surfaces by varying the chemical structure of the thiolipids are evaluated and improved molecular structures proposed.

The simplest common feature of non-thrombogenic lipids is the phosphatidylcholine head group [Hay84]. Besides low thrombogenicity, low nonspecific protein binding has been attributed to the PC-moiety [Ish90, Koj91, Ish93]. Functionalization of some conventional materials with PC yielded some successful implant materials[Cha84, Val85, Dur87].

However, there are indications that besides the chemical structure of the head groups the nature of the fatty acids contributes as well to reduce nonspecific protein binding [Mar85, Isr92a, Isr92b, Ish92]. In analogy to poly(ethylene glycol) chains attached to a surface [Jeo91], fluid lipid layers may namely show as well steric repulsion of proteins due to the reduced number of conformations accessible to the fatty acids upon collision with a protein. It was therefore attempted to reduce nonspecific binding to monolayers formed by self-assembling thiolipids of the type depicted in figure 1.5 by varying their molecular structure, in particular the nature of their fatty acids.

As protein adsorption to surfaces is often irreversible (chapter 1.1.1), a protein should not enter in physical contact with a surface [And86, And92]. The concepts described below are thought to contribute to the minimization of protein-surface interactions by influencing the force profile between the surface and an approaching protein. In summary, they aim at:

- minimizing hydrophobic attraction by preservation of the natural lipid conformation with a hydrophilic surface
- minimizing electrostatic attraction due to a net surface charge of zero
- maximizing steric repulsion due to fluid bilayers (fatty acids)
- maximizing repulsive hydration forces due to highly hydrated PC head groups
- maximizing thermal (steric) repulsion due to protrusion of PC head groups in "loosely attached" lipids

In the following, structural elements of the thiolipids to be synthesized are discussed in detail. Generally, the single crystal structure of DMPC has thereby been used as a guideline for the optimization o the structure of the thiolipids. This approach is very common also for the interpretation of spectroscopic and low-resolution structural data of lipids, which normally yield limited information [Bül81].

a) The head group

Even though equal signs of surface charges and protein charges do not necessarily prevent a protein from adsorbing to a surface [Van81, And86], opposite charges are subjected to coulombic attraction. Phosphatidylcholine is a zwitterion and has thus a net charge of zero.

As mentioned above, the presence of the PC-moiety is considered to decrease nonspecific binding of proteins. Chapman's biological arguments may be supported by investigations using the surface force apparatus: it could be shown by measuring the force as a function of the distance between two approaching, supported lipid bilayers that PC-lipids give rise to a repulsive force at a greater distance than for example PE-lipids [Mar85, Isr94].

One may speculate thus that a protein is repelled for the same reason at a greater distance when approaching a PC-surface. Phosphatidylcholine was therefore the head group of choice in this work. Efforts were made to preserve its natural conformation in the supported layers.

b) The hydrocarbon chains

Fatty acids were chosen according to the following three criteria:

i) Resulting thiolipids should form a "good" layer.
ii) Resulting layers should be "fluid".
iii) Synthesis and handling should be easy.

Overall, the resulting lipids should be as natural as possible and as artificial as necessary.

i) Formation of a **"good" layer** comprises all **geometrical** factors which contribute to a protein-repellent surface. Biological arguments suggest an optimized system in nature. Covalent attachment of the lipids to a planar solid support should therefore distort the conformation of the polar head group region as little as possible in order to avoid "protein attracting defects". Hydrocarbon chains should not be exposed to the water phase since they give rise to an additional attractive force ("hydrophobic force") as had been shown experimentally by comparing force profiles of stressed and unstressed bilayers of lecithin [Isr92a]. The hydrophobic or entropic force is attributed to water, which cannot interact with apolar groups via H-bonds [And86, Isr92a]. This leads to ordering of the water molecules adjacent to the apolar surface. Upon binding of a protein's hydrophobic patches to the hydrophobic regions on a surface such ordered water is released. The enthalpic contribution of such interaction is small, but the entropy change is positive. A perfectly hydrophilic surface is thus aimed at as this avoids hydrophobic interactions between a protein and a surface.

Volume of the Hydrocarbon chains

The selection of the best fatty acids for the thiolipids is based on general structural data of lipids. Biological phospholipids spontaneously aggregate in aqueous solutions [Isr92a, Gen89]. Thermodynamics or simple geometric considerations allow the aggregate preferentially formed to be predicted [Isr92a]. In thermodynamic terms, it is the one which minimizes the free energy of the system. The most stable type of aggregate is determined by the *fixed molecular volume V* and the *maximal length l* of the hydrocarbon chains as well as by the *optimum surface area* required by the polar head group [Isr92a]. Thiolipids should thus be tailored such that conformation and intermolecular interactions induced by their attachment to a planar surface correspond to those of the preferred aggregate formed in solution (thermodynamic condition). They should therefore preferably form very large liposomes with little curvature or even black lipid membranes (BLM). These types of aggregates are formed if the cross-sectional area of the hydrocarbon chains and of the polar head group are similar. Bilayers are the type of aggregates with the lowest surface-to-volume ratio. They are favored by lipids with a large molecular volume of the hydrocarbon chains. Lipids like diphytanoyl phosphatidylcholine (DPhyPC) and dioleyl phosphatidylcholines (DOPC) have a large molecular volume of the hydrocarbon chains and form stable black lipid membranes, whereas lipids like DPPC do not. For lipids with saturated straight-chain acyl substituents longer than palmitic acid, such planar bilayers cannot be formed below 50^0 C [Red71] since the minimal cross-section of two all-trans hydrocarbon chains in the gel phase is about 38 $Å^2$ whereas the one of the PC head group about 50 $Å^2$ [Gen89]. Such differences lead to curved aggregates and a tilting of the hydrocarbon chains. Fatty acids generally have a tilt angle of 30^0 in the gel phase of PC-lipids and of 12^0 in the single-crystal of DMPC [Hau81] In the liquid-crystalline phase, gauche conformations increase the hydrocarbon chain cross-section to ≥ 50 $Å^2$ and chains are thus not tilted. Fatty acid chains are not tilted in the 3D-crystal of DLPE nor in the gel phase of phosphatidylethanolamine lipids in general. Bilayers are always less thick in the liquid-crystalline state than in the gel state [Cev93].

In agreement with such predictions [Isr92a], DPPC forms liposomes. The molecular volume of its fatty acids is therefore the minimum required for "good" thiolipid monolayers on planar supports. Lipid mixtures, DOPC or DPhyPC can be used to form planar bilayers such as BLM's. The molecular volume of the hydrocarbon chains of DPhyPC and DOPC may therefore correspond best to that required for thiolipid monolayers on planar supports. Phytanic acid (scheme 2.1) is chemically stable whereas unsaturated fatty acids are susceptible to oxidation. Two thiolipids containing one branched fatty acid, namely phytanic acid (fig. 2.1), have therefore been synthesized (PhymPPC, mPPhyPC, fig. 2.1).

Hydrocarbon chain length

The influence of the hydrocarbon chain length of alkylthiols on the properties of monolayers self-assembled on planar gold surfaces has been investigated systematically [Bai88]. It could be shown that the layer properties are almost independent of the chain length for more

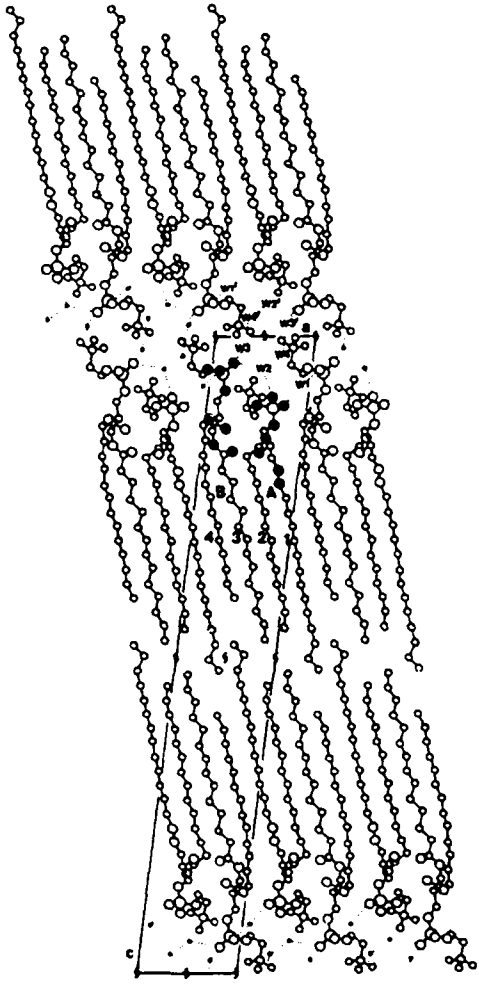

Fig. 1.7.a. Crystal structure of 1,2-dimyristoyl-sn-glycero-3-phosphocholine·2H_2O, projected onto the a-c plane from [Pea79]. The two letters A and B designate the two conformations of the asymmetric unit. The dotted lines indicate the hydrogen bonds.

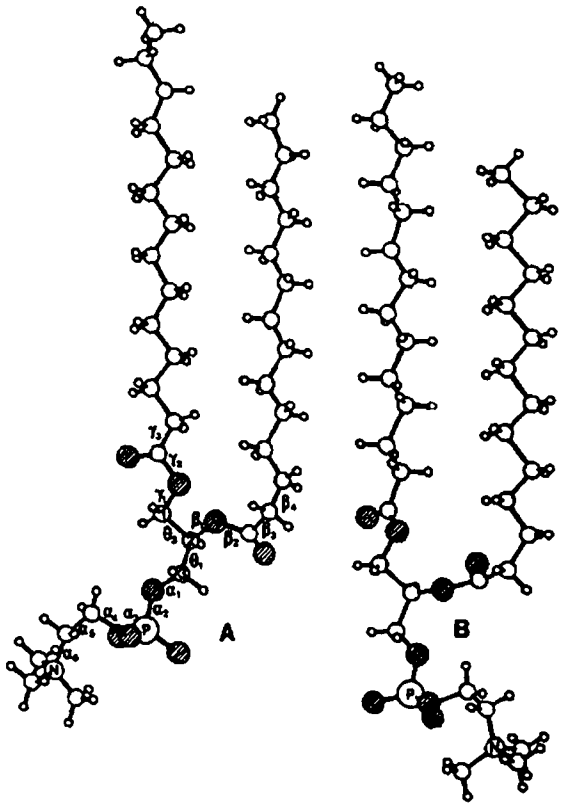

Fig. 1.7.b. The two conformations of 1,2-dimyristoyl-sn-glycero-3-phosphocholine·2H_2O in the asymmetric unit cell projected onto the a-c plane (from [Pea79]).

than ten methylene units. In the case of the thiolipids to be synthesized, longer hydrocarbon chains allow better decoupling of the polar head group region from the rigid, on a molecular scale rough polycrystalline gold surface. Structural integrity of the head group region is thus better preserved and defects in the layer due to the covalent immobilization may be better avoided. A hydrocarbon chain length of C_{16} was thus chosen for the thiolipids to synthesize since this is the longest *bifunctional* hydrocarbon chain, which is commercially available.

Three-dimensional lipid crystals contain very little water (two water molecules per lipid molecule in the case of DMPC [Pea79, Hau81]). However, conformations and orientations lipids adopt in fully hydrated membranes are very similar both in the gel and liquid-

crystalline phase as determined by ^{2}H-NMR, ^{31}P-NMR, ATR-FTIR, and neutron diffraction [See77, Fri77, See80, Bül81, Jac89, Whi94, Gen89]. Crystal structures may therefore be used as a rough starting point for the optimization of the thiolipids to be synthesized. In the DMPC crystal [Pas77, Hau81], molecules adopt alternatingly two different conformations (fig. 1.7 a and b).

As the glycerol backbone is oriented almost perpendicular to the surface of the crystal bilayer, the fatty acid in the *sn-1* position, which continues in this direction, extends further into the bilayer for both conformations. It is obvious that a plane representing the planar gold substrate used for self-assembly cannot be placed in the hydrophobic part of the crystal without cutting through at least some of the hydrocarbon chains. Distortion of the lipids must be expected upon attachment to a planar surface via ω-standing thiols on the linear, equally long fatty acids (fig. 1.8). A thiolipid with a fatty acid in the *sn-1* position, which is four methylene units shorter than the one in the *sn-2* position, has therefore been synthesized (LmPPC).

ii) Self-assembled layers should be "**fluid**" or rather "**flexible**" as the term fluidity of lipid layers comprises diffusional mobility to an extent, which is certainly not possible in the case of a supported monolayer. Flexibility of the supported thiolipid monolayer is thought to be important because measurement of the force between two approaching, supported lipid bilayers as a function of the distance between the layers using the Surface Forces Apparatus had shown that fluid phosphatidylcholine bilayers give rise to a repulsive force at a greater distance than PC-layers in the gel state [Isr92a]. As already mentioned this could be due to **steric repulsion** similar to that attributed to poly(ethylene glycol) chains attached to a surface [Jeo91] (cf. chapter 1.1.1). As for PEG chains the number of conformations accessible to the fatty acids in a fluid lipid layer may be reduced upon collision with a protein. In addition, it has been shown that densely packed, crystalline-like PEG surfaces are less resistant to protein adsorption than more loosely packed chains [Jeo91]. High flexibility of the hydrophobic part of the supported thiolipid monolayers is therefore thought to be a promising source for an improved protein-repellent character of the surface. Natural membranes are also fluid. An additional advantage of the flexibility of the anchoring hydrocarbon chains may again also be the better decoupling of the polar head group region from the solid support and thus better preservation of its structural integrity. Ligand binding to the functionalized layer could also be facilitated as had been observed in the case of monolayers at the air-water interface.

Generally, phase transitions can be induced by changes in temperature, pressure, ionic strength, or pH, depending on the lipid [Gen89]. The molecular volume increases in going from the gel to the liquid-crystalline phase [Mar90]. Decrease of crystallinity in the polar part

of the lipid with increasing number of methyl groups in going from DPPE to DPPC has been observed by FTIR [Fri79]. A selection of long-chain 1,2-diacyl *sn*-glycero-3-phosphatidylcholine lipids forming fluid layers at ambient temperature is shown in table 1.2. Considering the structural requirements discussed above, the number of possible fatty acids decreases further, as the long chain lengths required for structural integrity and decoupling of the polar head groups from the surface increase transition temperatures. As discussed above, an additional criteria for the selection of the fatty acids is the formation of planar lipid bilayers such as BLM's. DOPC and DPhyPC form BLM's, crystalline lipids usually don't.

class of PC-lipids	fatty acids	phase transition temperature [^{0}C]	
a) symmetric saturated	12:0	- 1.1 ± 0.8	
	13:0	13.7	
	14:0	*23.5 ± 0.4*	
	16:0	*41.54 ± 0.5*	
b) symmetric unsaturated	16:1 cΔ^9	-36	
	16:1 tΔ^9	- 4	
	18:1 cΔ^9	-19	
	18:1 tΔ^9	12	
c) symmetric branched		isoacyl	anteisoacyl
	12:0	-40.0	-
	14:0	- 5.2	-33.7 (±)
	15:0	5.9	-14.8 (±) / -16.5 (-)
	16:0	18.9	- 3.0 (±)
	17:0	-	8.0 (±)/ 7.6 (-)
	diphytanoyl	<< RT	
d) asymmetric saturated	16:0 - 12:0	9.6	
	16:0 - 14:0	*27*	
	18:0 - 9:0	*12.3*	
e) asymmetric unsaturated/ saturated	C1 C2		
	16:0 - 18:1 cΔ^9	- 4	
	18:1 cΔ^9 - 16:0	- 10	
	18:1 cΔ^9 - 16:0	6	
	18:1 cΔ^9 - 18:0	9	

Tab. 1.2. Phase transition temperatures of 1,2-diacyl-sn-glycero-3-phosphatidylcholines forming fluid lipid layers at room temperature for salt concentrations ≤ 1 M [Mar90].

iii) Synthesis of the fatty acids as well as their handling (stability) should be easy. For ω-Mercapto fatty acids precursors of the same chain length are commercially available up to C_{16}. Longer chains must be composed of shorter fragments. Double bonds and in particular conjugated double bonds are susceptible to oxidation upon exposure to air. It is almost impossible to buy enantiomerically pure phytol, the commercially available precursor of phytanic acid (scheme 2.1), and stereoselective synthesis is demanding [Fuj81, Sch82]. However, the use of a mixture of isomers could even be an advantage as the disorder of the chains increases.

-> Target structures of thiolipids

The chemical structure of the thiolipid mPPhyPC (fig. 2.1) is thus thought to fulfill best the requirements previously established for the formation of a self-assembled monolayer with low

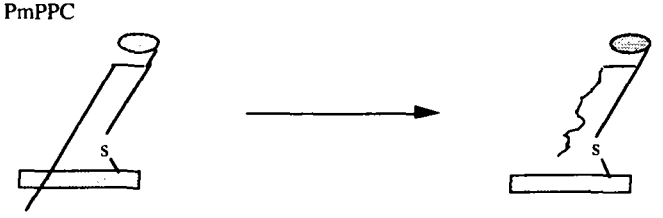

-> Shortening of hydrocarbon chain by formation of gauche conformers upon attachment to a solid substrate possibly leads to distortion of the headgroup region and thus eventually to exposure of the hydrophobic region to the water phase ("stressed system").

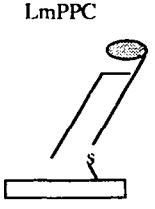

-> Conformation of the headgroup region is less disturbed upon immobilization of a thiolipid with a shorter fatty acid in the sn-1 position than in the sn-2 position.

Fig. 1.8. Hypothesis for the effect of the length of the sn-1 hydrocarbon chain on the structure of a self-assembled thiolipid monolayer based on the crystal structure of DMPC [Pea79, Hau81].

nonspecific protein binding: A molecular volume of the hydrocarbon chains, which is larger than that of DPPC, should decrease the tilt and attachment via the *sn-1* fatty acid means attachment via the fatty acid protruding further into the lipid bilayer in the case of crystalline DMPC (fig. 1.7). In addition, a lipid attached to the solid support via the fatty acid at the *sn-1* position should be mechanically more mobile than a lipid attached via the hydrocarbon chain at the *sn-2* position. The greater the mobility of the attached molecule, the more the PC head groups can also protrude.

As the fatty acid in the *sn-1* position of the DMPC crystal extends further into the bilayer (fig. 1.7), it is to be expected that the *sn-1* palmitic acid chains in BmPPC and PmPPC are "compressed" upon attachment to a solid surface. Lauric acid is four methylene units shorter than palmitic acid and should thus be more easily accommodated upon attachment to the solid substrate leading to less distortion of the polar head group region (fig. 1.8).

Considering the forces listed in table 1.1, ionic interactions, charge-transfer and hydrophobic or entropic interactions are forces not expected to act between a protein and a perfectly hydrophilic surface of a self-assembled thiolipid monolayer of the kind discussed above meanwhile hydrogen bonding cannot be completely excluded. However, the methyl groups of the

self-assembly				
lipid	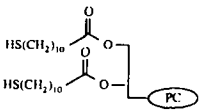	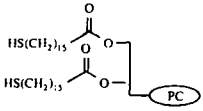 BmPPC		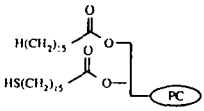 PmPPC
reference	[Die86]	[Fab89]	[Coy89]	[Die86]
SA time	60 min	24 hr		60 min
SA temperature	RT	20 - 25 ^{0}C		RT
-> rinsing	agitate in MetOH/ 2 min.	move 20 x in and out of 3 ml MetOH		agitate in MetOH/ 2 min.
-> drying	air/ 30 min	air/ 10 min		air/ 30 min

analysis of layers						
lipid	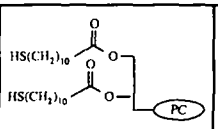		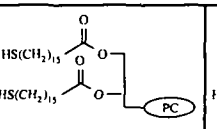 BmPPC		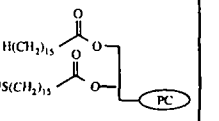 PmPPC	
reference	[Die86]	[Fab89]		[Coy89]		[Die86]
contact angle $\Theta_a H_2O$	$0^0/17^{0\ 1,6)}$	$10\text{-}15^{0\ 3)}$	$< 10^{0\ 3)}$	19 ± 3^0	46 ± 2^0	47 ± 6^0
rel. humidity	-	50 - 70 %	50 - 70 %	50 - 70 %	50 - 70 %	
time of measurement	30 sec	15 sec	15 sec			
thickness by ellipsometry [Å]						
for n = 1.50	22 ± 2	17 - 19 [3)]	21 - 24	25 ± 2	28 ± 1	17.7
for n = 1.53	21.6 ± 1.9	-	-	-	-	-
thickness by XPS [Å]	*lipid present*	-	22 Å	-	-	-
theoret. thickness	24 Å	-	-	-	-	28 Å
collision area (LB)	82 Å²/ molecule (ca. 33 dyn/ cm)	-	40 Å²/ molecule (ca. 23 dyn/ cm)[4)]	-	-	-
max. density (lipid/cm²)	$1.2\ 10^{14}$	-	$2.5\ 10^{14}$		-	$1.0\ 10^{14}$
density by P-det.[2)]	-	-	$4.3\text{-}5.4 \cdot 10^{14}$	-	-	-
IR	lipid present	-	-	-	-	-
LB-transfer : $\Theta_a H_2O$			-	-	-	-
on Au from top:	-> 58 ± 6⁰ (d = 17 ± 3 Å) *(severe disruption!)*					
on Au from bottom:	-> flips over: 44⁰ (t = 0 hr) 25 ⁰(t = 42 hr, air)					
on glass from bottom:	-> 55⁰ (stable)					

scanning electron microscopy	no morphology detectable	-	-	-	-
phase transition temp. in polymerized vesicles [Sam85][7]	-	none detected between 10 - 60[0]	-	-	-
CHO cell adhesion (% of total cells)[5]					
lipid		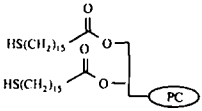 BmPPC		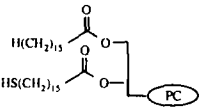 PmPPC	
fibronectin (1 µg/ ml)	91.7 ± 6.5	-	93 ± 4.3	94.4 ± 3.4	-
vitronectin (5 µg/ ml)	100 ± 2.5	-	75 ± 5.2	86.3 ± 4.1	-

Tab. 1.3. Properties of self-assembled thiolipid monolayers reported in literature [Die86, Fab89, Coy89].

1) *Θ_a measured as a function of time: equilibrium reached within 5 minutes.*
2) *Self-assembled layer hydrolyzed in 5.4 M HCl/ ≤ 6 hr/ 40 °C*
3) *stability of layer: no change of contact angle or film thickness upon immersion of layer in pure solvent (MetOH or EtOH/ 24 hr/ RT).*
4) *spread from hexane/ EtOH 9:1, 25°C; water subphase purged with N_2, LB-layer experiments all performed under N_2.*
5) *incubation of layers with different proteins/ 1 hr/ 37 °C -> blocking with 3 % of bovine albumin -> cell adhesion (37 ° C/ α-MEM/ 20 mM HEPES/ 1 % albumin)*
6) *for $CHCl_3$ instead of MetOH (also used for washing)*
7) *determined by measuring the absorbance at 400 nm*

quarternary amine aren't good proton donors. In addition, a layer of water molecules solvating the permanent cation must be removed before direct interaction with the methyl protons is possible. This implies an energy barrier to overcome. The large cationic group sterically hinders hydrogen bonding with a bond length of only about 3 Å with the oxygen atoms of the phosphate group as acceptors. Hydrogen bonding also decreases with increasing ionic strength and investigations of protein binding are usually conducted at elevated salt concentrations. From a

theoretical point of view, such self-assembled thiolipid monolayers should be very promising candidates for surfaces with low nonspecific protein adsorption.

Table 1.3 summarizes the properties of self-assembled monolayers of BmPPC and PmPPC (fig. 2.1) so far reported in literature.

1.2. Specific Interactions of Proteins with Surfaces

Molecular recognition at surfaces is a topic, which includes many aspects ranging from dynamics of ad- and desorption to geometrical considerations and conformational changes upon adsorption to force profiles, catalysis and substrates for 2D-crystallization of proteins. Figure 1.9 shows some classes of specific interactions, which have been investigated using appropriately functionalized surfaces. The "specificity" of a surface is determined by its shape, its pattern of H-bond donors and acceptors, the charge distribution and the pattern of hydrophobic patches [And86]. The "lock-and-key" interaction between receptors and ligands are extremely efficient binding mechanisms of nature, which can have the strength of covalent bonds [Isr92a]. The binding between biotin and streptavidin belongs thereby to the ligand-receptor interactions with the highest binding energy (88 kJ/mole) [Isr92a].

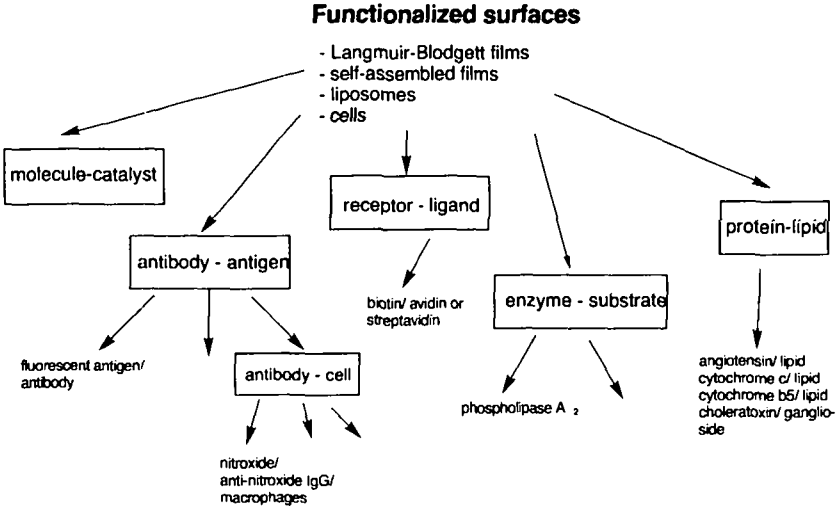

Fig. 1.9. Molecular recognition investigated at surfaces of model systems.

There are several general requirements for strong specific interactions between *immobilized* ligands and proteins [Lec94]. The ligand should for example be laterally mobile and this mobility is, off course, greatly restricted in the case of supported layers, which are covalently attached to the support. However, for the construction of a stable device, covalent attachment of the molecules to the solid support is a big advantage.

For the specific protein-ligand interactions investigated in this work, lateral mobility was attempted by the formation of flexible supported thiolipid layers and by the use of a long, dynamic, and water-soluble spacer in the ligand molecule. In the future, non-covalent attachment of the ligand molecule by complex formation could be not only a mean to increase lateral mobility, but also to prefabricate uniform layers with a great potential of simple variability for commercial purposes (fig. 1.10).

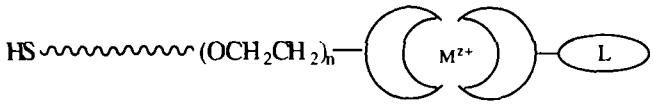

Fig. 1.10. Immobilization of a ligand by complex formation.

1.2.1. Functionalization of Surfaces

Functionalization of a surface means the introduction of chemical moieties such as ligands, which allow the surface to be specifically addressed. The synthesis of affinity chromatography gels is thereby a good source of information for the functionalization of planar surfaces. Generally, efficient functionalization of surfaces requires reactive reagents. However, the selection thereof is limited and inter- and intramolecular reactions restrict the number of functional groups admitted in the same molecule. The immobilization of sulfur compounds on metal surfaces is therefore a good compromise for these contradictory requirements.

A ligand molecule should consist of an anchoring and layer-forming part and a spacer region, to which the ligand is attached (fig. 1.11 a). The role of the spacer is even more important in the case of planar surfaces as opposed to chromatography gels, where the intrinsic roughness of the surface can contribute to optimize the presentation of the immobilized ligand. A good spacer should be water soluble, flexible, structurally simple, heterobifunctional, and chemically inert once attached to the anchoring part and the ligand. Only few elongated molecules fulfill these criteria. Poly(glycine) for example has been used as a spacer. It is water-soluble,

heterobifunctional, and well-established amide chemistry can be used to link it to other molecules. However, it is not soluble in apolar solvents and the resonance structure of the peptide bonds make it more rigid than for example poly(ethylene glycol) (PEG). The latter is a very flexible polyether. Unlike its homologues poly(methylene glycol) and poly(propylene glycol) it is well soluble in water and at the same time in many other solvents used for organic synthesis. A big disadvantage from a synthetic point of view is its homobifunctionality. Antibodies have been covalently linked to solid surfaces of biosensors via long PEG spacers providing a means of transducing binding events into a measurement signal [And90].

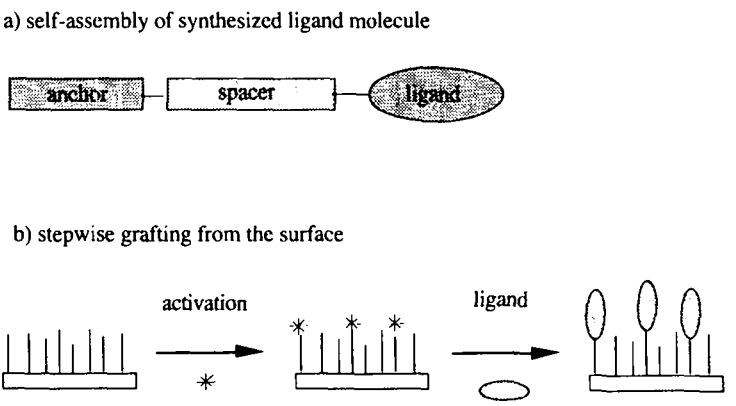

Fig. 1.11. Immobilization of a small ligand on a surface.

However, in principle there are two ways to attach a small ligand molecule to a surface: Either the entire ligand molecule including the anchoring part, the spacer part, and the ligand itself is synthesized and then attached to the surface (fig. 1.11 a) or the ligand is attached by stepwise grafting from the surface (fig. 1.11 b).

Both methods have their advantages and disadvantages and are worthwhile to be evaluated and compared (tab. 1.3). The choice of the immobilization method depends strongly on the structure of the ligand to be immobilized and its chemical reactivity. Procedure a) in figure 1.11 may also serve to "calibrate" measurements obtained with method b) since hardly any surface analytical method is capable of qualitative, but particularly not of quantitative analysis of complicated surface modifications at sub-monolayer concentrations. Such surface modifications can therefore usually only qualitatively and indirectly be confirmed, for example by specific binding of proteins. Interpretation of observed binding events, however, can sometimes be difficult as many different effects can show the same "phenotype" (see chapter 5).

a) self-assembly of synthesized molecule	b) in-situ modification of surfaces
advantages:	
- well characterized ligand molecule with known properties -> observed binding events easier to interpret	- synthesis in analogy to chromatography matrices
- functionalized surface easy to prepare, e.g. by self-assembly	- use of commercial products in multistep synthesis
- well characterized surface	- purification by rinsing
- ligand density at surface easily adjustable	- no loss of expensive ligands during multistep synthesis
- no unwanted functionalities influencing specific and non- specific binding of proteins	
- flat surface/ optimized ligand density -> substrate for 2D crystallization of receptor -> investigation of protein structure (AFM etc.)	
disadvantages:	
- ev. laborious synthesis	- functionalization ev. more laborious (several cycles)
- molecules ev. delicate to handle	- low surface area, which can be modified (-> use of dextranes to increase it)
- ev. problems to find a common solvent for different molecules	- low yields of reactions at surfaces (high reactivity needed -> reduces number of compatible functional groups)
	- reactive sites ev. sterically not accessible
	- concentration ev. difficult to adjust
	- difficult to monitor and to quantitate reaction (yield, completeness of reaction) -> only indirect monitoring (e.g. by protein binding)
	- incomplete reaction or side reactions may produce unwanted functionalities (-> increased nonspecific binding/ decreased specific binding of proteins; more complex surface -> interpretation of observations difficult!); control of reaction difficult, theoretical expectations must be trusted
	- less knowledge about general reactivity of system (susceptibility to hydrolysis, oxidation etc.) -> interpretation of observations may be wrong
	- products from side reactions are not eliminated
	- some solvents ev. incompatible with the surface to functionalize

Tab. 1.3. Summary of advantages and disadvantages of methods for ligand immobilization shown in figure 1.11.

In summary: Using method a) it may take longer until protein-ligand interactions can be investigated, but the surface modification is better controllable and better defined than with method b). Method b) yields surfaces with well adjustable properties and better interpretable binding events. For the "fine tuning" of surface properties such as their optimization with respect to low nonspecific binding of proteins and for experiments attempting to probe complicated analytes with many variable parameters such as membrane receptors, procedure a) was therefore decided to be the method to start with in this work.

Structurally, the anchoring part of a ligand molecule should be very similar to the thiolipids in order to integrate well into the thiolipid layer without distortion of the optimized, protein-repulsive surface. Structural differences of the anchoring and layer-forming parts such as mismatch of chain lengths, chain tilts, and physical state may lead to domain formation, which is very common in Langmuir-Blodgett films, and which leads to reduced accessibility of the ligands to the proteins and may increase nonspecific adsorption of proteins.

1.2.2. The Nicotinic Acetylcholine Receptor

Membrane receptors are generally not commercially available. One of the most important criteria for the selection of the membrane receptor-ligand system is therefore the availability of the protein, which should be delivered in a purified form and in sufficient amounts. A purification procedure including an affinity chromatography step is a big advantage since it demonstrates that *specific and reversible* interaction between the receptor protein and the immobilized ligand is possible. In addition, ligands should be cheap. Their chemical structure should be simple and synthesis of immobilizable derivatives should be easy.

The nicotinic acetylcholine receptor (nAChR) was used as a prototype membrane protein for the investigation of receptor-ligand interactions at surfaces. It occurs highly concentrated in the tissue of the electric organs of the eels *Electrophorus* and *Torpedo Californica*. The nAChR from the latter is the best characterized example of a neurotransmitter-stimulated channel protein. It is structurally and functionally very closely related to that in postsynaptic membranes of the skeletal muscles of higher vertebrates [Her90], where it exists also in densely packed clusters. Upon excitation of a neuron, acetylcholine is liberated. The interaction of acetylcholine with the nAChR leads to the opening of the channel and allows selective passage of cations, which induces muscle contraction. The nAChR from the neuromuscular junction is structurally and

functionally very different from the muscarinic AChR from brain cells and even from some nAChR found in the brain [Gen89]!

The nAChR is a heteropentameric glycoprotein. Five associated subunits ($\alpha_2\beta\gamma\delta$) form the channel, which has a total mass of 290 kDa. A binding site for acetylcholine is located on each α-subunit. Binding sites for other agonists and competitive antagonists are also located on the α-subunits, whereas the ones for certain local anesthetics, neurotoxins and channel blocking ligands are located within the channel. In *Torpedo*, the channel occurs as a dimer held together by a disulfide bond between the δ-subunits. The nAChR is about 140 Å long, extending over 70 Å beyond the bilayer surface on the extracellular side where the binding sites of the acetylcholine are located. Simultaneous binding of two acetylcholine molecules is required for the channel to open. Several proteins are associated with the nAChR, some of which can influence the quality of the receptor preparation significantly. The receptor can be purified by affinity chromatography using acetylcholine[Her90], naja naja siamensis toxin [Her90], methyl[N-(6-aminocaproyl-6'-aminocaproyl)-3-amino]pyridinium bromide [Sch92] and other compounds as immobilized ligands. Acetylcholine, the natural agonist of the nAChR, has a dissociation constant of $2 \cdot 10^{-8}$ M meanwhile snake venom toxins such as α-bungarotoxin bind almost irreversibly with dissociation constants K_d of 10^{-9} to 10^{-10} M [Her90].

1.2.3. Acetylcholine Containing Ligand Molecules

According to the criteria established in section 1.2.1., the ligand molecule described below was synthesized in order to render a surface specifically addressable by the nicotinic acetylcholine receptor.

Acetylcholine was chosen as the ligand to be immobilized on the surface (fig. 1.12). It is commercially available in many different salt forms. Selective and reversible binding of the nicotinic acetylcholine receptor to immobilized acetylcholine has been demonstrated by its use for affinity chromatography. Scheme 1.1 shows the synthesis of this affinity matrix [Her90]. A commercially available agarose gel is used, the reactive moiety of which is a thiol group (Affi-

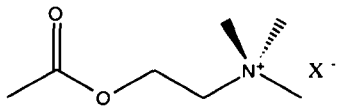

Fig. 1.12. Acetylcholine.

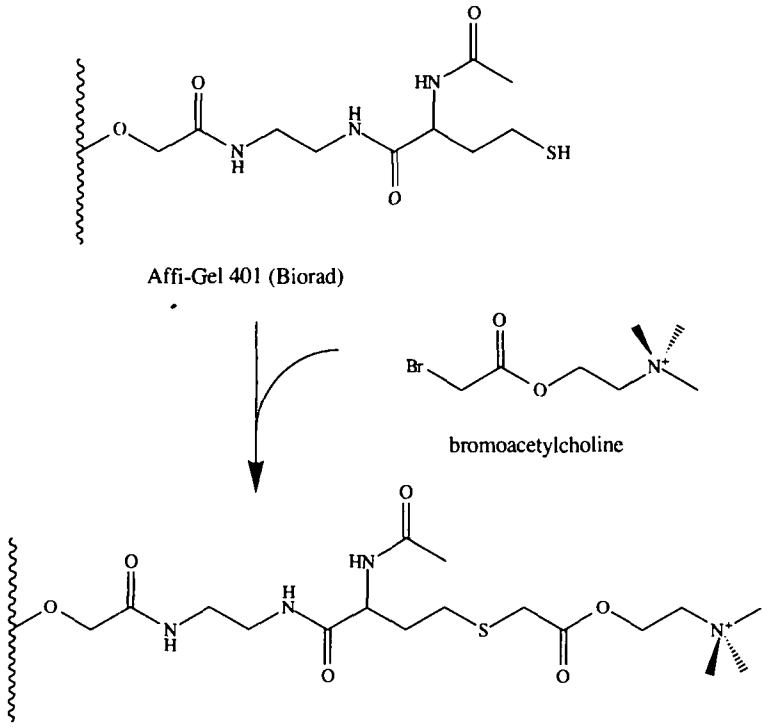

Scheme 1.1. Synthesis of an acetylcholine affinity gel using commercially available Affi-Gel 401 (Biorad) and synthesized bromoacetylcholine [Her90].

Gel 401, BioRad). Synthesized bromoacetylcholine is reacted with the thiol group of the affinity matrix in an aqueous buffer at neutral pH.

Acetylcholine fulfills thus at least some of the requirements listed above for a ligand to be suitable for the investigation of receptor-ligand interactions at solid-liquid interfaces. Its chemical structure is simple. However, acetylcholine has an ester group sensitive to hydrolysis and several reactive sites allowing for example Hoffmann-elimination of the quarternary amine. The quarternary amine itself is susceptible to nucleophilic attack. In addition, it can strongly complicate purification of synthetic intermediates as well as their characterization using standard analytical techniques. In mass spectrometry for example, quarternary amines can show very special fragmentation and secondary reactions in the gas phase and in NMR, strong solvent and counter ion dependence of chemical shifts are observed. This clearly demonstrates the limited

analogy between stepwise grafting of a surface in solid phase synthesis and synthesis of the complete ligand molecule prior to its attachment to the surface.

A poly(ethylene glycol) spacer with thirteen ethylene oxide units (PEG_{13}) was chosen for the ligand molecule to synthesize since this is the longest ethylene glycol oligomer with defined molecular weight described in literature [Jay90]. All longer poly(ethylene oxides) have average molecular weights with more or less narrow distributions, making purification and analysis of multistep derivatives difficult. However, longer PEG spacers may be of interest as they can contribute to reduce nonspecific binding of proteins [Jco91, Pri91, Pri93].

In order to avoid phase separation and distortion of the thiolipid monolayers described in chapter 1.1.2., a C_{16}-fatty acid was finally chosen as layer-forming and anchoring part of the ligand molecule.

Part II. Discussion of Experimental Results

2. Synthesis

Experimental procedures and analytical data of the synthesized compounds are given in part III of this work. Some NMR spectra are shown in annex F. Spraying reagents used to develop analytical thin layer chromatograms are described in annex E.

2.1. Lipids (Matrix Molecules)

2.1.1. Introduction

Lipids are a class of molecules, which is special with respect to synthesis and purification. Slow reactions due to steric hindrance of long-chain compounds, incompatibility of solubilities in reactions involving apolar hydrocarbon chains and polar reactants, and the need for extensive chromatographic purification are just a few of the problems encountered. Lipids are large molecules where classical methods of purification like fractionated distillation, crystallization, or sometimes even extraction fail. Often starting material and product are very similar just differing in a very small part of the molecule resulting in similar properties, which makes even chromatographic purification difficult. In addition they are susceptible to hydrolysis, oxidation of double bonds and acyl migration.

2.1.2. Discussion of the Syntheses

a) Fatty Acids

16-(2-pyridyldithio)hexadecanoic acid was synthesized according to scheme 2.1 as described earlier [Coy89] using the commercially available lactone as a starting material. Its final purification, however, was greatly simplified as compared to literature upon substitution of chromatography by recrystallization from methanol.

Phytanic acid is very widespread in nature (tab. 2.1). It accumulates for example in tissue lipids of humans suffering from a rare neurological disease, the Refsum's disease, where it can make up to 30 to 50 % of the total fatty acids in certain tissues. The diterpenoid acid is a derivative of phytol, which is the alcohol moiety of chlorophyll (configuration 7(R), 11(R)). The

multibranched structure of isoprenoid acids influences strongly their physical properties. The melting point of phytanic acid for example is lowered by 130 ^{0} as compared to n-hexadecanoic acid.

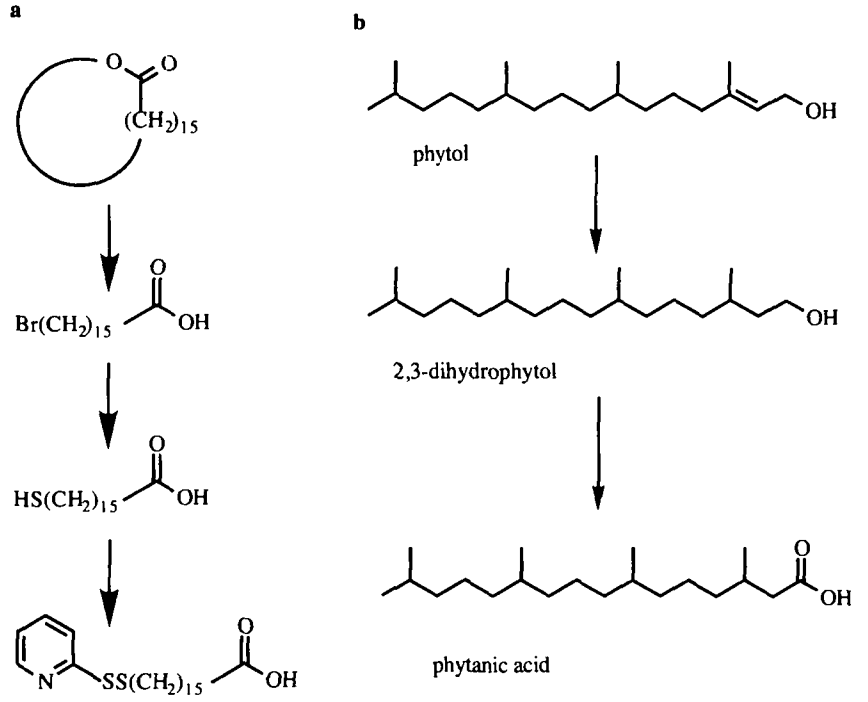

Scheme 2.1. a) Synthesis of 16-(2-pyridyldithio)hexadecanoic acid. b) Synthesis of phytanic acid.

Phytanic acid was synthesized by reducing the double bond of commercially available phytol with hydrogen in presence of PtO_2 as a catalyst followed by oxidation of the alcohol dissolved in acetone using CrO_3 in concentrated sulfuric acid as an oxidant [Red71]. The product was purified by silica gel chromatography. The starting material being not enantiomerically pure the synthesis yielded a mixture of four diastereomeric pairs of enantiomers. This may be an advantage with respect to fluidization of the supported thiolipid monolayers. The ^{1}H-NMR spectrum was better resolved than that reported in literature for methyl phytanate, but otherwise agreed well [Lou75]. The doublets below 1.0 ppm can thereby be attributed to the five methyl groups, the wide, unresolved band at 1.4 ppm as well as the nonet at 1.54 ppm to the methylene and methinyl groups except the one in the 3-position, which has a chemical shift of 1.9 ppm. The α-methylene groups finally are well resolved at 2.15 and 2.38 ppm. Mass spectrometry

showed the typical fragmentation pattern observed for saturated isoprenoid structures with the preferred fragmentation next to the tertiary carbons before and after McLafferty fragmentation [Lou75]. The base peak of m/z = 87 is characteristic for the 3-methyl structure of a saturated acid. Typical features expected for isoprenoid acids were also observed in the infrared. So for example the doublet around 1170 cm^{-1} attributed to skeletal vibrations associated with the isopropyl group and the doublet at around 1370 cm^{-1} assigned to C-H deformation modes of the $-CH(CH_3)_2$ group.

source	concentration [µg/ml]	% of total fatty acids	reference
human serum	2.1	0.1	[Cib79]
rabbit serum	0.9	-	[Lou75]
rat serum	1.9	-	"
krill	-	1.4	"
whale oil	-	1.22	"

Tab. 2.1. Concentration of phytanic acid occurring in nature.

b) Thiolipids

The chemical structures of the five synthesized thiolipids are shown in figure 2.1. (Their names correspond to the usual trivial names for lipids with the small 'm' standing for the mercapto group, which is attached in ω-position of the fatty acid designated by the following letter.) They have been synthesized according to the classical method shown in scheme 2.2.

Thereby the fatty acids with the thiol group in the ω-position protected as a mixed disulfide were esterified with the cadmium chloride salt of sn-glycero-3-phosphorylcholine in presence of dicyclohexylcarbodiimide (DCC) and 4-(dimethylamino)pyridine (DMAP) in dry dichloromethane. Purification of the protected intermediates by silica gel chromatography was followed by reductive deprotection of the thiols using 1,4-dithio-DL-threitol. BmPPC proved to be extremely susceptible to oxidation and thus polymerization upon exposure to air.

For PmPPC and LmPPC the corresponding precursors with a free alcohol group in the *sn-2* position are commercially available, whereas in the case of PhymPPC and mPPhyPC they had to be synthesized.

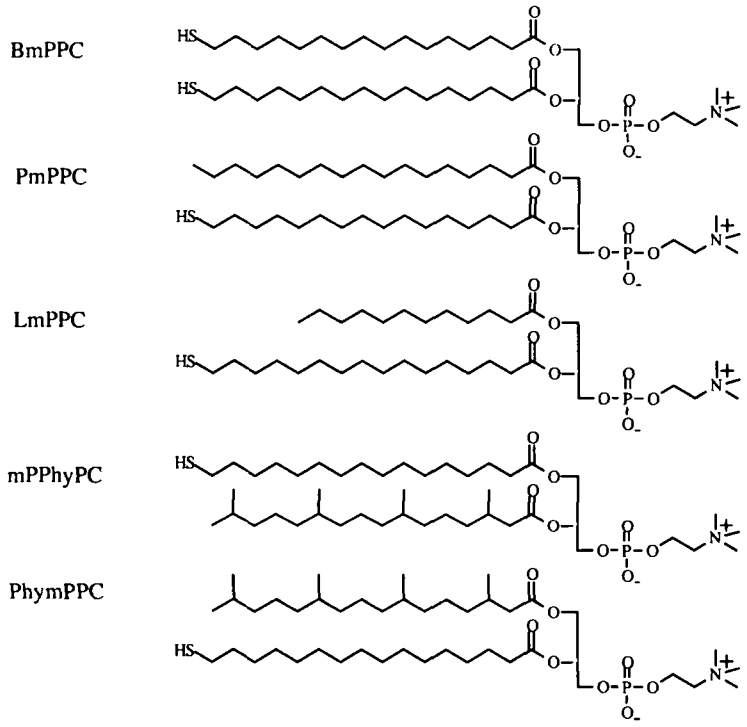

Fig. 2.1. The five thiolipids synthesized in this work.

In principle, phosphatidylcholine lipids with different fatty acids in the *sn-1* and *sn-2* position can be synthesized in two ways: For total synthesis a commercially available enantiomerically pure derivative of glycerol with different protection groups on two of the alcohol groups can be used [Eib81, Ter88]. Selective removal of the fatty acid in the *sn-2* position can be achieved by enzymatic hydrolysis using phospholipase A_2 (scheme 2.3). The resulting lysolipid is more resistant to acyl-migration than that formed by hydrolysis of the *sn-1* fatty acid [Eib81]. Since the physical properties of position isomers are quite similar, chromatographic separation and analytical distinction is quite cumbersome. In order to obtain pure lipids synthetic routes which allow the stepwise selective introduction of fatty acids are therefore preferable to time consuming and ineffective purification steps.

Ester hydrolysis in aqueous buffer using phospholipase A_2 works well for highly curved surfaces and above the phase transition temperature of the lipid to be hydrolyzed. The latter was determined by calorimetry for 1,2-bis[16-(2-pyridyldithio)hexadecanoyl]-*sn*-glycero-3-phosphatidylcholine (BPyPPC) to be 44.5 ^{0}C. BPyPPC could therefore be easily hydrolyzed at 45 ^{0} C whereas hydrolysis of DPhyPC was very difficult. Even after repeated sonication and

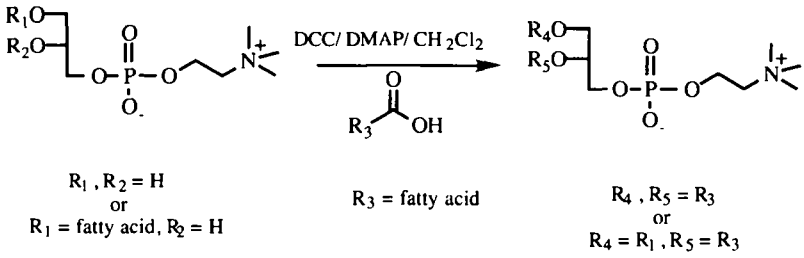

Scheme 2.2. General reaction scheme for lipid synthesis.

addition of fresh enzyme the yield of lyso-lipid was low. This may be attributed to DPhyPC forming large liposomes with little curvature. In fact, it has been shown that phopholipase A_2 hydrolyzes lipids in a monolayer at the air-water interface only up to a certain lateral pressure, which depends on the source of the enzyme [Dem75]. Phospholipase A_2 from bee venom worked until the highest pressures! The interfacial tension of the interfaces of a DPhyPC black lipid membrane, however, was determined to be 1.5 ± 0.1 dyne/cm at 24^{0}C in 0.1 M KCl [Red71]. In general, a marked reduction of the rate of hydrolysis of phytanic acid containing lipids as compared to other lipids containing other long-chain fatty acids has also been observed by other workers [Lou75].

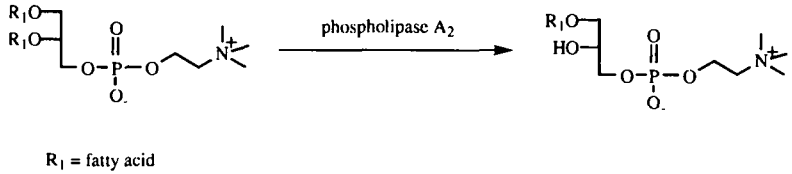

Scheme 2.3. Selective hydrolysis of diacyl phosphatidylcholines by phospholipase A_2.

Addition of detergents or melittin is known to increase hydrolytic activity of phospholipase A_2. However, being interested in the lysoproduct for preparative purposes, all that has been added must be removed again. This may be well thought about considering the difficulty of lipid purification!

Generally, spectral features of NMR [Kat86, Ham92, Gun94, Hop65], mass spectrometry [Fen83, Eve94, Ryh60, Ham92, Kat86, Mur93] etc. corresponded perfectly with the typical features of lipids reported in literature.

2.2. Ligand molecules

Figure 2.2 depicts the synthesized ligand molecules, which are a compromise between structural requirements and synthetic accessibility. It consists of an anchoring and layer-forming fatty acid with an ω-standing thiol. As for the lipids, a C_{16} hydrocarbon chain has been chosen in order to reduce the danger of phase-segregation [Bai89b]. The trideca(ethylene glycol) spacer has a estimated length of about 47 Å.

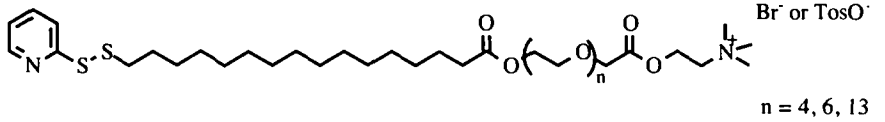

Fig. 2.2. Synthesized ligand molecules with three different spacer lengths.

Synthesis of a poly(ethylene glycol)-derivative of acetylcholine according to scheme 2.4 using bromoacetylcholine and the poly(ethylene glycol) alcoholate was not possible.

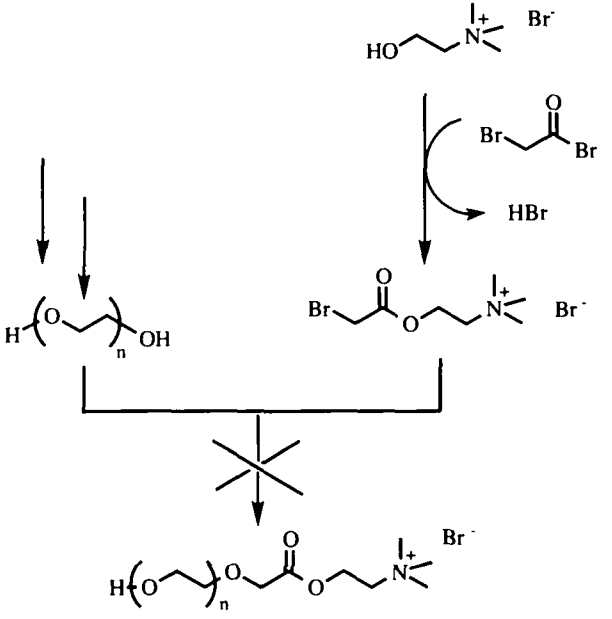

Scheme 2.4. Synthesis of poly(ethylene glycol)-acetylcholine using bromoacetylcholine bromide salt.

Scheme 2.5 shows the reaction pathway used for the synthesis of the ligand molecule with a hexa(ethylene glycol) spacer (PEG_6), which is the longest ethylene oxide polymer commercially available with a defined molecular weight. An excess of the homobifunctional hexa(ethylene oxide) was thereby reacted with sodium in dry di(ethylene glycol)dimethylether prior to addition

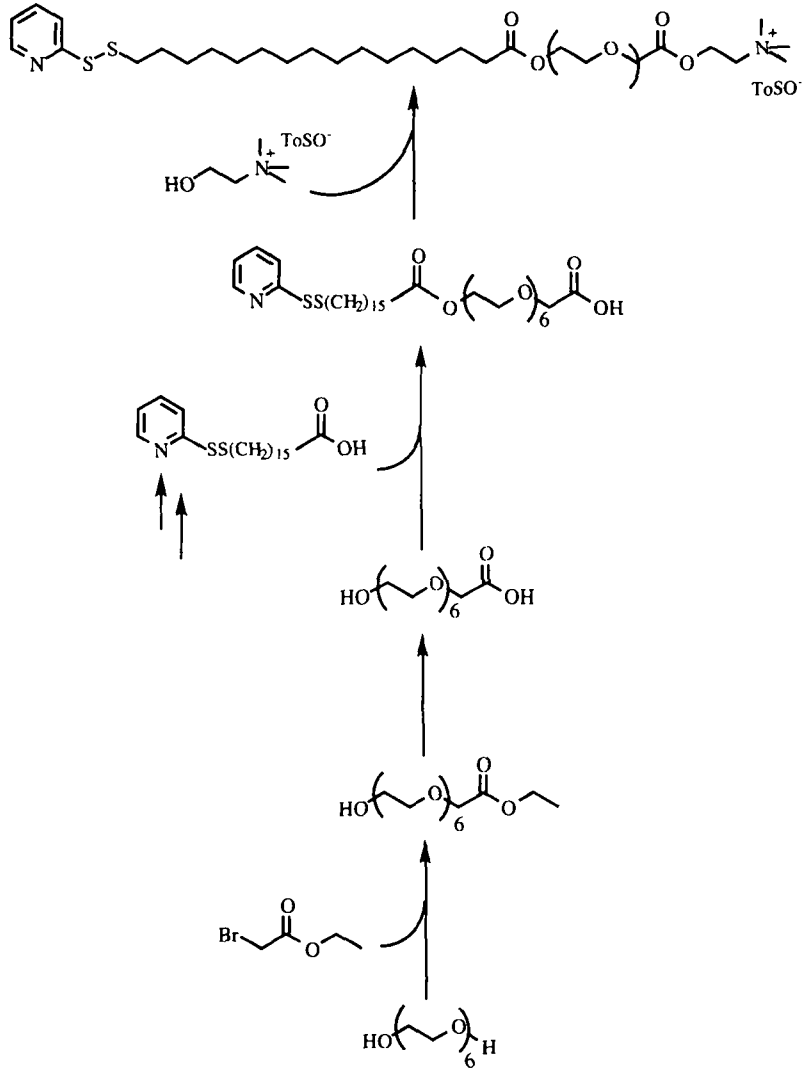

Scheme 2.5. Synthesis of the ligand molecule with a hexa(ethylene glycol) spacer.

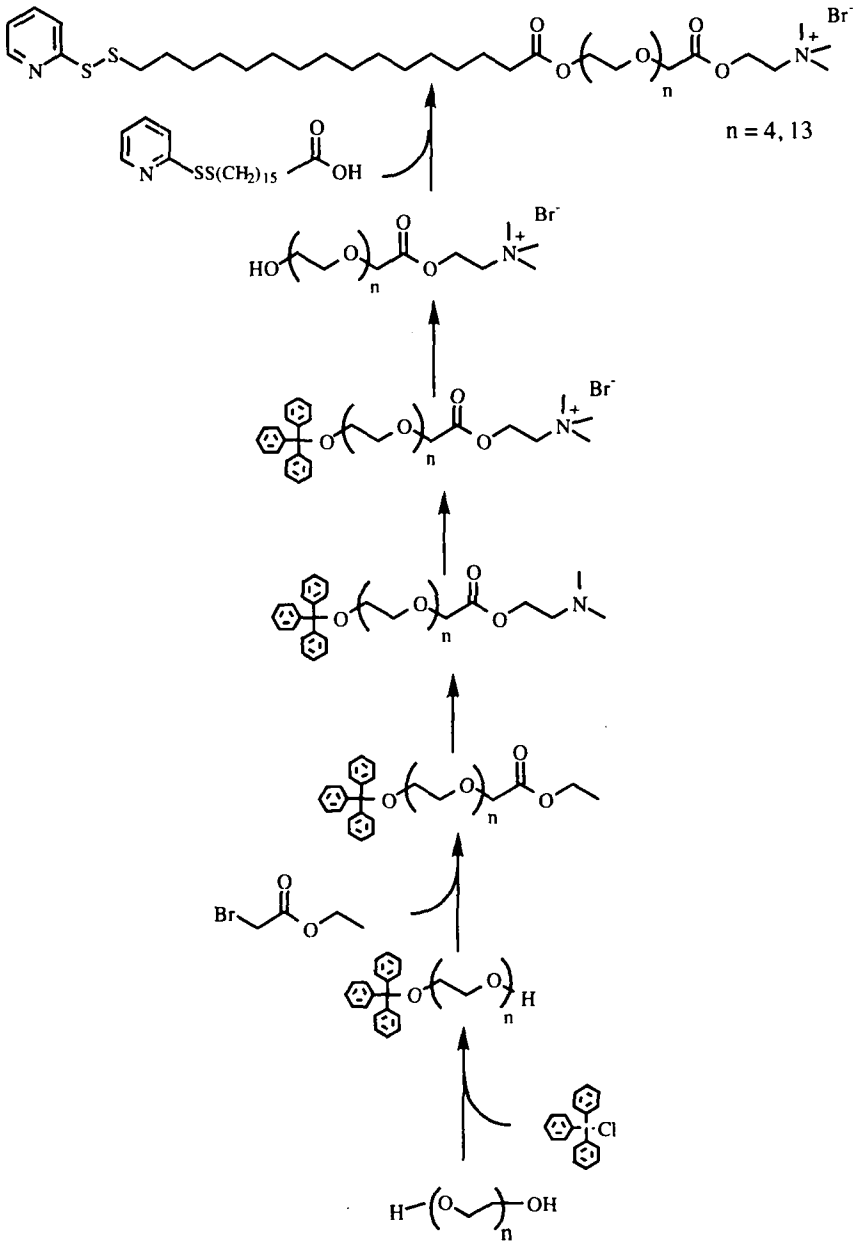

Scheme 2.6. Synthesis of ligand molecules with a tetra(ethyleneglycol) and a trideca(ethyleneglycol) spacer.

of bromoacetic acid ethyl ester. In contrast to the tetra(ethylene glycol) the sodium alcoholate of the hexa(ethylene glycol) is not soluble in THF. Choice of a polar, aprotic solvent was crucial for the success of the reaction. 16-(2-pyridyldithio)hexadecanoic acid was activated with a stoechiometric amount of carbonyldiimidazole prior to addition of the hexa(ethylene glycol)monocarboxylic acid. Use of the tosylate salt of choline allows dichloromethane as a solvent . The bromide salt is much more polar and soluble only up to isopropanol!

The ligand molecules with a tetra- and trideca(ethylene glycol) spacer ($PEG_{4/13}$) were synthesized according to scheme 2.6. Some NMR-spectra are shown in annex F. Here the homobifunctional ethylene glycols were first reacted with substoechiometric amounts of tritylchloride. Upon reductive deprotection of the choline esters their partial hydrolysis could not be avoided. The deprotected ester was therefore purified by chromatography using Sephadex LH-20 in acetone.

Both synthetic pathways have advantages and disadvantages. Scheme 2.5 shows a synthesis, which is more general than the one shown in scheme 2.6. Synthesis of a ligand molecule other than a derivative of acetylcholine is easily possible since the latter is introduced only in the last step. Generally, the choline esters seemed to be extremely susceptible to hydrolysis and reesterification in methanol during synthesis and purification. NMR studies testing the stability of bromoacetylcholine bromide salt and acetylcholine chloride salt in methanol, water, and phosphate buffer (pH 7.65), however, showed hydrolysis only upon prolonged standing at room temperature. Measurement of specific receptor-ligand interactions on self-assembled monolayers should therefore be possible.

Scheme 2.7 finally shows the reaction pathway for the trideca(ethylene glycol) spacer.

Varying chemical shifts of 0.1 to 0.2 ppm have been observed in the ^{1}H-NMR spectra for the protons next to the quarternary amine of the choline group, $-N^+(CH_3)_3$ and $CH_2-N^+(CH_3)_3$, meanwhile all other spectral features were unchanged for any analytical method! Various tests have suggested that the chemical shift of these protons is strongly dependent on the nature of the counterion!

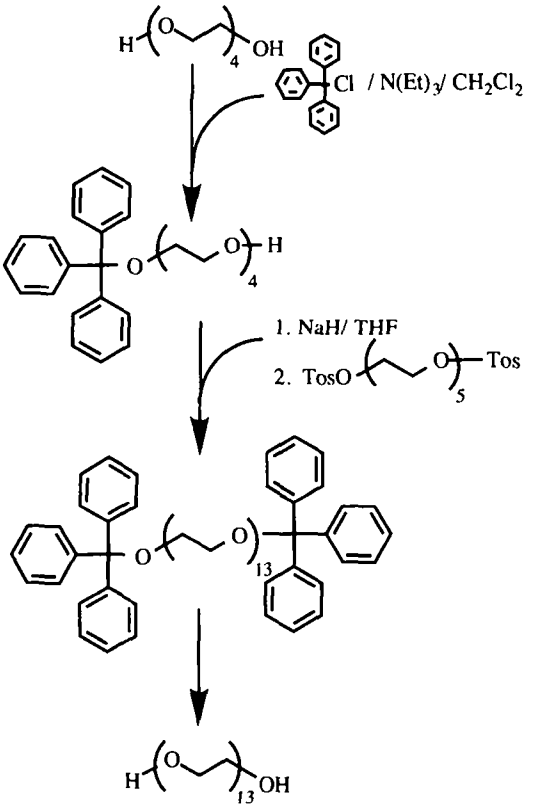

Scheme 2.7. Synthesis of trideca(ethylene glycol) in analogy to the method described by Jayasuriya [Jay90].

3. Characterization of Self-Assembled Thiolipid Monolayers

In this chapter, results from the investigation of the pure thiolipid monolayers self-assembled are discussed. **Surface plasmon resonance spectroscopy** has thereby been used to monitor in situ the self-assembly process and to determine the optical thickness of the layer. Polarity of the surface and thus orientation, packing and dynamics of the immobilized molecules have been probed by **contact angle measurements** with water. Electrical properties of the layers such as resistance and capacitance were investigated by **impedance spectroscopy**. **Infrared spectroscopy** finally was applied to determine conformation and packing properties of the adsorbed lipids. None of these methods requires molecular probes avoiding thus disturbance of the structural integrity of the layers. Experimental details are described in part III of this work.

3.1. Surface Plasmon Resonance Spectroscopy

3.1.1. Introduction

Surface plasmon resonance spectroscopy (SPR) was used to monitor the formation of thiolipid monolayers by self-assembly on planar gold surfaces. For this, the increase of the intensity of the reflected light at an angle of incidence slightly smaller than the resonance angle of bare gold was recorded as a function of time (time scan, fig. 3.1.a). Thicknesses of completed layers were determined by angle scans (fig. 3.1.b). In an angle scan the reflectivity is measured as a function of the angle of incidence of the light source. At the resonance angle, reflectivity is minimal due to excitation of surface plasmon waves in the thin metal film. The precise value of the resonance angle is calculated by fitting experimental angle scans with Fresnel equations. Upon adsorption of molecules to the metal film, the resonance angle is shifted. The angle shift is proportional to the optical thickness $\Delta n \cdot d$ of the adsorbed layer, where Δn is the difference of the refractive indices of the organic film and the adjacent medium, and where d is the geometrical thickness of the adsorbed layer. The optical thickness is a measure of the mass coverage per unit area. An appropriate refractive index for the adsorbed material has to be chosen. Bulk hydrocarbons have a refractive index of 1.50 [Wea73]. By using a lower refractive index of e.g. 1.45 for self-assembled alkylthiols [Lai95, Por87], reduced packing density and intercalation of water is taken into account. The tighter packed the hydrocarbon chains are in an adsorbed layer, the higher is the refractive index. Attribution of an appropriate refractive index to lipids with hydrated polar head groups is more delicate. It has been shown by electron spin resonance that

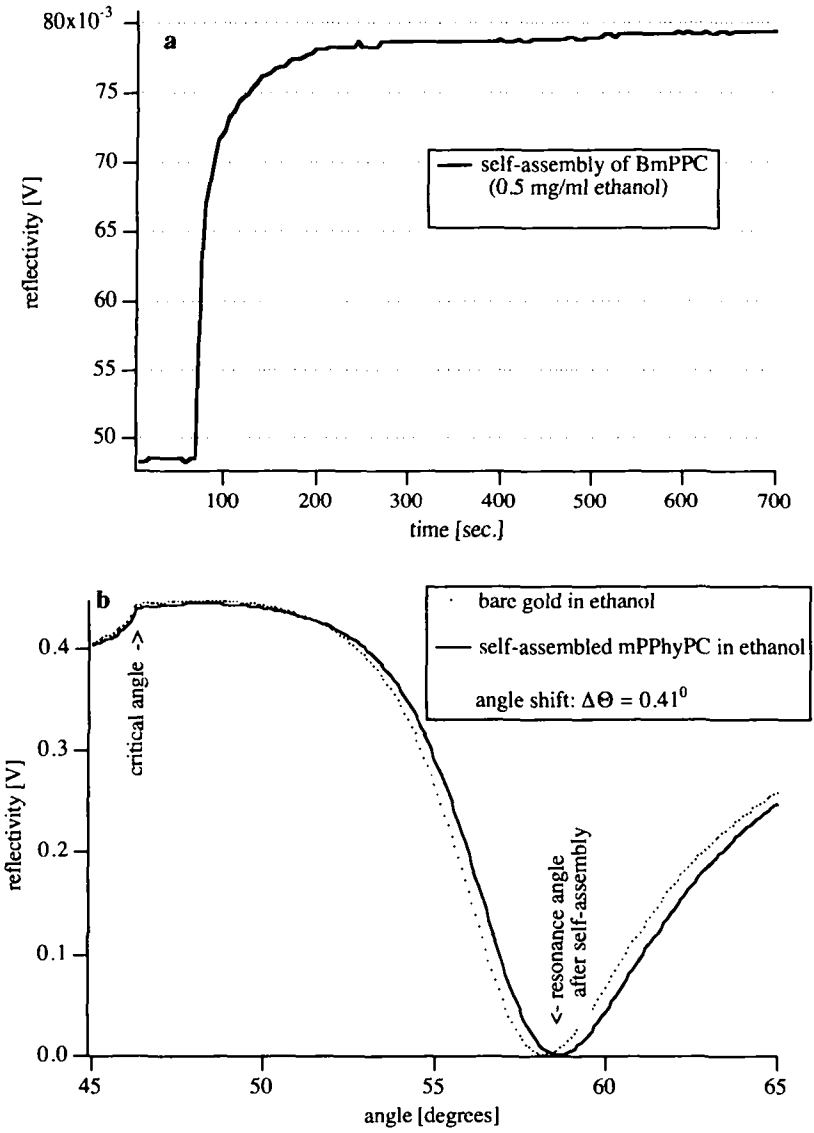

Fig. 3.1. a) Example of a time scan: The intensity of the reflected light at a constant angle of incidence Θ_i is recorded as a function of time for the self-assembly of BmPPC (0.5 mg/ml ethanol) on a thin gold film. b) Example of an angle scan: Self-assembled monolayer of mPPhyPC versus bare gold.

water partially penetrates the hydrocarbon core for lipids in the liquid crystalline state [Gri74] meanwhile it doesn't reach beyond the glycerol backbone in the gel phase [Wor76]. A refractive index of 1.45 is considered appropriate for lipids in the fluid state as well as for adsorbed proteins according to data published for well-defined model systems [Rei93, Spin92, Spin93, Ter93, Lan94]. FTIR showed that all of the synthesized thiolipids except BmPPC form very disordered layers by self-assembly on gold (see chapter 3.4.), which supports the use of a refractive index of 1.45 for these lipids. In water and ethanol, an angle shift $\Delta\Theta$ of 0.1^0 corresponds this refractive index and for the measurement set-up used to a geometrical thickness of 6.4 Å of the adsorbed layer [Dus96a].

3.1.2. Results and Discussion

Adsorption of the synthesized thiolipids to gold from an ethanolic solution was usually completed after six to seven hours. Shifts of the resonance angle as a consequence of thiolipid adsorption to planar gold surfaces were then determined by comparing angle scans of bare gold and self-assembled layer. The values are summarized in table 3.1 and figure 3.2. Layer thicknesses are calculated for two different refractive indices, 1.45 and 1.50. Although a value of 1.45 is generally used, Coyle et al. had determined the thickness of self-assembled BmPPC and PmPPC by ellipsometry using a refractive index of 1.50 [Coy89].

lipid	$\Delta\Theta$ (ethanol) [degrees]	d (n = 1.45) in ethanol	d (n = 1.50) in ethanol	$\Delta\Theta$ (water) [degrees]	d (n = 1.45) in water	d (n = 1.50) in water	ellipsometry (n = 1.50) [Coy89]
BmPPC	0.50 ± 0.13	32.0 ± 8.3	22.2 ± 5.8	0.43 ± 0.00	27.5 ± 0.0	19.1 ± 0.0	25 ± 2 Å
PmPPC	0.59 ± 0.05	37.8 ± 1.3	26.2 ± 2.2	0.65 ± 0.09	43.5 ± 5.1	28.9 ± 4.0	28 ± 1 Å
LmPPC	0.52 ± 0.05	33.3 ± 3.2	23.1 ± 2.2	0.56 ± 0.02	35.8 ± 1.3	24.9 ± 0.9	-
PhymPPC	0.38 ± 0.06	21.6 3.8	16.9 ± 2.7	0.48 ± 0.05	30.7 ± 3.2	21.3 ± 2.2	-
mPPhyPC	0.41 ± 0.01	26.2 ± 0.6	18.2 ± 0.4	0.43 ± 0.02	27.5 ± 1.2	19.1 ± 0.9	-

Tab. 3.1. Average shifts of SPR resonance angles $\Delta\Theta$ with standard deviations for completed monolayers of the five synthesized thiolipids self-assembled in ethanol. Values are means of three to four measurements. Layers were judged to be completed when no more change of reflectivity was visible (usually after six to seven hours). Ethanol was then exchanged against water. Geometrical thicknesses in ethanol and water are calculated for a refractive index of 1.45 (6.4 Å/ 0.1^0) and 1.50 (4.44 Å/0.1^0), respectively.

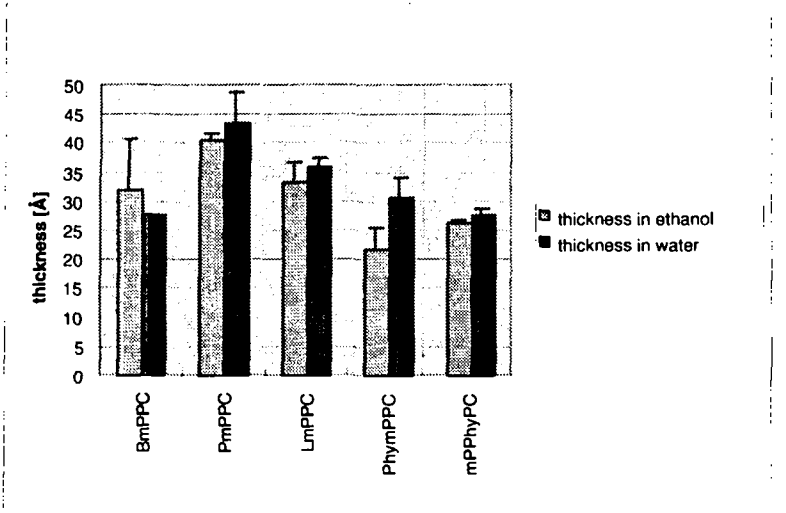

Fig. 3.2. Thicknesses of self-assembled thiolipid monolayers in ethanol and water calculated for a refractive index of 1.45. Values are means of three to five measurements.

Layer thicknesses of the self-assembled thiolipid monolayers in table 3.1 compare well with those reported in literature for lipid monolayers (tab. 3.2) even though monolayers on solid supports generally appear to be thicker than those of non-supported, conventional lipid bilayers. The latter are thicker in the gel phase than in the fluid phase. The thickness of BmPPC is very similar to that found for DPPC adsorbed on a layer of thiolipid 2 or 3 (fig. 3.3). Infrared measurements have shown that BmPPC forms very ordered layers (see chapter 3.4.), which could justify the use of a higher refractive index (1.50) for the thickness calculations. This leads

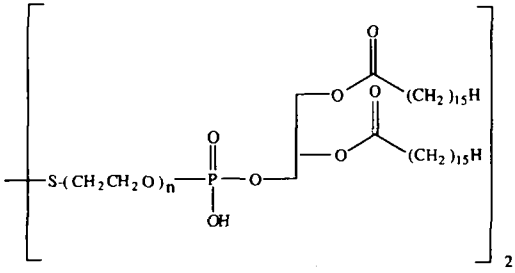

thiolipid 1: n = 1
thiolipid 2: n = 2
thiolipid 3: n = 3

Fig. 3.3. Synthetic thiolipids with thiol groups on the polar head group [Lan92b].

to an apparent reduction of the geometrical layer thickness, which then compares well also with thicknesses reported for DPPC layers in usual aggregates. In fact, great similarity of BmPPC and DPPC was also observed in the infrared. Spectra of both self-assembled BmPPC and its transferred LB-layer were very similar to that of a transferred LB-layer of DPPC (see annex D).

Like BmPPC PmPPC has two fatty acids of equal chain length. But the palmitic acid in the *sn-1* position of PmPPC is not attached to the surface. In order to accommodate this palmitic acid upon attachment of the lipid to the solid support, the hydrocarbon chains may be less tilted

Thicknesses of physisorbed lipid monolayers on hydrophobic surfaces								
substrate	**method**	**DMPC**		**DPPC**		**POPC**		**ref.**
		$\Delta\Theta$	d [Å]	$\Delta\Theta$	d [Å]	$\Delta\Theta$	d [Å]	
1-hexadecanethiol/ SA	OG micelles					0.30^0	19.2	[Lan94]
"	lipid liposomes					0.35^0	23.8	"
thiolipid 2/ SA	OG micelles	0.30^0	19.2	0.42^0	28.6	0.35 ± 0.03^0	23.8 ± 2.0	"
thiolipid 3/ SA	"	0.30^0	19.2	0.45^0	30.6	0.38 ± 0.03^0	25.8 ± 2.0	"
"	lipid liposomes	-	-	-	-	0.40^0		"
thicknesses [Å] of lipid monolayers in dispersions of lipid bilayers								
	method	DMPC		DPPC		POPC		ref.
L_α or $L_{\alpha'}$		17.1		19		-		[Cev93]
" hydrocarbon chains only	^{2}H-NMR	-		17.5		-		[See80]
"	calculated for all-trans conf. and no tilt	-		22.5		-		"
L_β or $L_{\beta'}$		21 ± 1		22.5 ± 0.5		-		"
"		-		24.9 ± 1.2		-		[Wie89]
L_c		-		25 ± 0.5		-		[Cev93]
crystal		27.5		-		-		[Pea79]

Tab 3.2. Monolayer thicknesses of various lipid monolayers. $\Delta\Theta$ is the shift of the resonance angle from SPR- measurements , where 1-hexadecanethiol, thiolipid 2 and 3 (fig. 3.3) were self-assembled on a gold substrate to yield a hydrophobic surface. A second lipid layer was formed on top either by fusion of lipid liposomes or from OG/ lipid micelles. Self-assembly of 1-hexadecanethiol yielded an angle shift of 0.26^0[Lan94]. Thicknesses are calculated for a refractive index of 1.45. Lamellar lipid phases: L_α or $L_{\alpha'}$ (liquid-crystalline), L_β or $L_{\beta'}$ (solid-analogous, gel), L_c (crystalline lamellar). Thicknesses of lipid monolayers in dispersions of lipid bilayers are calculated as half of the experimentally determined bilayer thickness. Note that the DMPC single-crystal contains only two water molecules per lipid molecule [Pea79]!

explaining the PmPPC layer being thicker than the BmPPC layer. If the *sn-1* chain is shortened by the four methylene units it extends further into the bilayer in the case of the DMPC single-crystal, the thickness measured is smaller (LmPPC). The thicknesses of PhymPPC and mPPhyPC are intermediate and very similar.

Generally, gold-supported, self-assembled layers of the thiolipids synthesized in this work appear to be thicker in water than in absolute ethanol. This may be explained by them expanding upon hydration and shows their flexibility despite covalent attachment to the surface. Several experimental findings support this interpretation: First, choline salts in general and phosphatidylcholine lipids in particular [Bül81] are known to be extremely hygroscopic. Second, infrared studies of the conformational behavior of choline showed strong frequency dependence of the symmetric N^+-$(CH_3)_3$ stretching vibration on its degree of hydration [Fri81]. Based on normal coordinate analysis this was attributed to strongly hydrated choline assuming gauche and trans conformation meanwhile loss of hydration was suggested to induce conversion of the trans to gauche conformation, exclusively (see [Fri81] and references therein). In addition, Wyckoff concluded from X-ray data of the choline crystal that the conformation is gauche [Wyc66] and also in the DMPC single crystal with only two water molecules per lipid molecule both DMPC conformations show the tendency of the nitrogen to fold back towards the phosphate group, so as to minimize the distance between the groups of opposite charge (see fig. 1.7b). Increase of thicknesses of the self-assembled thiolipid monolayers upon replacement of ethanol by water may therefore also induce a more extended trans-conformation of the phosphatidylcholine moiety (fig. 3.4).

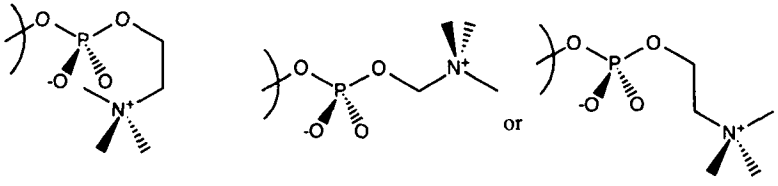

gauche conformation:
maximum interaction
between opposite charges
at low hydration

trans-conformation:
charges are screened by water at full hydration

Fig. 3.4. Proposed conformations of the phosphatidylcholine moiety at different degrees of hydration proposed in analogy to the findings for choline.

The geometrical thickness determined by SPR for the layer of PmPPC compares also very well to the value from literature determined by ellipsometry for a refractive index of 1.50 in air meanwhile the value for BmPPC is somewhat lower than the one from literature (tab. 1.2). The

BmPPC layer was found to be very ordered when self-assembled over night (see FTIR-measurements). An incomplete layer could therefore be responsible for the lower thickness measured by SPR. However, the layer thickness reported in literature could also be too large due to adsorption of contaminants during measurement in air.

3.2. Contact Angle Measurements

3.2.1. Introduction

Contact angle measurements (wetting) probe the polarity of a surface and thus orientation, packing density and dynamics of chemisorbed organic molecules by measuring the angle between a droplet of solvent and the surface [DeG85, Ulm91]. The advancing contact angle is measured applying a small droplet of solvent to the surface, the receding contact angle upon partial withdrawal of the solvent from the droplet. The difference between the two angles is attributed to the roughness of the surface, reorientation of the molecules at the interface upon interaction with the solvent, or even partial dissolution of molecules at the interface, which, of course, changes the nature of the probing droplet. The Young's equation describes the relation between interfacial free energies and the contact angles. The smaller the contact angle, the better the surface is wetted by the particular solvent. Typically, contact angles of 110 - 118^0 are measured for water on very hydrophobic surfaces such as polyethylene or monolayers of chemisorbed long-chain alkanethiols or fluorophores [Bai89a, Ulm91, Lai92a] and less than 10^0 on very hydrophilic surfaces. A strictly constant measurement protocol is crucial for the reproducibility of the contact angles.

3.2.2. Results and Discussion

Advancing and receding contact angles of water were determined for well dried thiolipid monolayers self-assembled over night (tab. 3.3 and fig. 3.5). Values are means of 15 to 20 measurements.

Generally, the contact angles are rather high. BmPPC, the lipid which is attached to the surface via both fatty acids, showed by far the lowest contact angle. PhymPPC showed the highest followed by mPPhyPC, thus the two lipids with the bulky phytanic acid. For all lipids, receding contact angles were smaller than advancing angles, but standard deviations were much smaller

for advancing than for receding contact angles. Both findings suggest restructuring of the surface upon exposure to water and thus flexibility of the layer despite covalent attachment of the thiolipids to the gold surface. Ruiz et al. had observed similar dynamic behavior for hydrophobic polymers functionalized with phosphatidylcholine [Rui97]. They exhibited different depth profiles of the choline distribution upon contact with air and water, respectively.

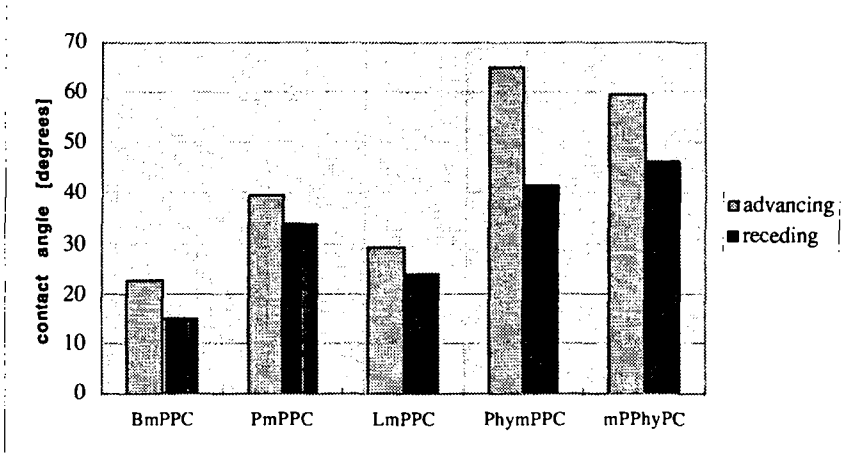

Fig. 3.5. Advancing and receding contact angles of water for thiolipid monolayers self-assembled on gold.

lipid	θ_a [^{0}]	standard deviation [%]	θ_r [^{0}]	standard deviation [%]
BmPPC	22.9 ± 2.5	10.8	14.9 ± 3.3	21
PmPPC	39.8 ± 3.2	8	33.9 ± 3.3	9.8
LmPPC	29.3 ± 0.8	2.6	24 ± 2.7	11.1
PhymPPC	65.2 ± 1.7	2.6	41.8 ± 4.1	9.9
mPPhyPC	59.5 ± 2.1	3.5	46.1 ± 3.8	8.3

Tab. 3.3. Advancing(θ_a) and receding (θ_r) contact angles of water for thiolipid monolayers self-assembled on gold.

Coyle et al. had determined a lower advancing contact angle for water on self-assembled BmPPC (19 ± 3^0 [Coy89] and < 10^0 [Fab89]!), but a higher one for PmPPC (46 ± 2^0) [Coy89]. However, their samples were measured at 59 - 70 % humidity after rinsing the self-assembled layers with methanol and drying them in air for 10 minutes. Different degrees of

hydration, rests of methanol and varying self-assembly times as well as contamination of the potentially very polar surfaces upon measurement in air may explain the differences observed.

3.3. Impedance Spectroscopy

3.3.1. Introduction

Impedance spectroscopy [Mac87] allows the investigation of electrical properties of the thiolipid monolayers self-assembled on a gold electrode [Lan94, Wei95]. For this investigation, the measurement set-up depicted in figure 10.1 has been used. An alternating tension with a sinusoidal frequency between 1 and 20 000 Hz is applied across the organic monolayer. The tension and its phase shift with respect to the applied voltage is recorded as a function of the frequency of the applied signal (frequency spectra). Comparison of measured and applied voltage allows to determine the equivalent circuit modeling the electrical properties of the self-assembled thiolipid monolayers. Thickness of the insulating fatty acid chains can be calculated from the capacitance of the adsorbed organic layer.

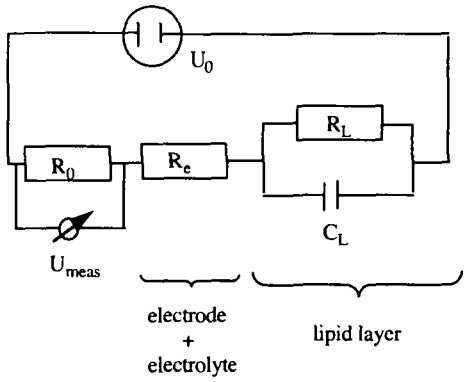

Fig. 3.6. Simplified equivalent circuit for the measurement cell depicted in figure 10.1. R_L represents the resistance of the lipid layer, C_L its capacitance. R_e is the resistance of the electrode together with the electrolyte , U_0 is the applied tension, U_{meas} the tension measured across the resistor R_0 [Lan94, Ste96].

Figure 3.6 shows the simplified equivalent circuit for the measurement set-up used (fig. 10.1). It includes the simplest equivalent circuit describing an insulating organic layer adsorbed on the gold electrode. For its detailed mathematical description see Lang et al. [Lan94].

The specific capacitance c (capacitance per unit area) of the layer can be estimated from the impedance spectra at the maximum phase shift:

$$c = \frac{U_{\theta max}}{U_0 \cdot 2\pi\nu_{\theta max} \cdot A \cdot S}$$

with	$U_{\theta max}$	: tension measured at maximum phase shift θ
	$\nu_{\theta max}$	: frequency at maximum phase shift θ
	U_0	: amplitude of the applied tension
	A	: amplification factor
	S	: surface area of the electrode.

This calculation is based on the assumption that the capacitance of the polar head groups is at least 100 x higher than that of the hydrocarbon chains and thus negligible [Lan94]. This is valid for supported lipid monolayers, which are not covalently bound to the surface and is applied here for the supported thiolipid monolayers investigated in this work. Impedance spectra have also been fitted with equivalent circuits modeling the adsorbed layer best.

The thiolipid layer adsorbed to the planar gold electrode can be described as a plate capacitor. The thickness d of the hydrocarbon chains can therefore be calculated from the specific capacitance determined experimentally:

$$d = \varepsilon_0 \varepsilon / c$$

with	ε_0	: dielectric constant of the vacuum ($8.85\ 10^{-12}$ As/Vm)
	ε	: dielectric constant of the adsorbed organic layer

The dielectric constant of the adsorbed organic layer is assumed to be 2.25 for densely packed hydrocarbon chains similar to bulk polyethylene [Wea73]. For fluid planar lipid bilayers a value of 2.0 to 2.2 may be used [Han64, Han65, Dil82, Ben75].

3.3.2. Results and Discussion

Table 3.4 summarizes values of the specific capacitances c of self-assembled thiolipid monolayers on gold estimated at maximum phase shift and calculated by fitting experimental data with equivalent circuits. Layer resistances were of the order of MΩ cm² for all layers.

lipid	c (estimated) [μF/cm²]	best fitting equivalent circuit	c (fit) [μF/cm²]	thickness [Å]
BmPPC	1.8	R_e(C[RQ])	1.5	13.3
PmPPC	1.5	R_e(CQ)	1.4	14.6
LmPPC	2.2	R_e(C[RQ])	1.9	10.6
PhymPPC	1.7	R_e(C[RQ])	1.5	13.3

Tab. 3.4. Specific capacitance c [μF/cm²] of self-assembled thiolipid monolayers estimated at maximum phase shifts and determined by fitting experimental data with equivalent circuits. Thicknesses are calculated for a dielectric constant ε of 2.25. Values are averages of at least three different electrodes. Q represents a constant phase element. R_e stands for the resistance of the electrolyte and the electrode together meanwhile elements in parenthesis model the supported lipid layer. Standard deviations for estimated specific capacitances are 0.1 μF/cm².

Values of the specific capacitances of the thiolipids used in this work (tab. 3.4) are generally above those expected for lipid monolayers (Tab. 3.5). This is not surprising considering the chemical structure of the thiolipids synthesized here. In fact, efforts had been made here to avoid formation of tightly packed, rigid layers since their nonspecific binding of proteins is supposedly higher than that of disordered, fluid-like layers (see chapter 1.1 and 4.). Use of a lower dielectric constant appropriate for low packing densities and disorder observed also with FTIR (chapter 3.4) would lead to even lower thicknesses of the hydrocarbon chains.

None of the lipid layers could be well described by an equivalent circuit modeling the lipid layer with a resistance in parallel with a capacitance, the simplest equivalent circuit usually describing lipid layers and physical interpretation of more complicated equivalent circuits is limited. The equivalent circuit R_e(C[RQ]) found to fit best most of the thiolipid monolayers self-assembled on gold (tab. 3.4) may describe an insulating layer with irregular defects.

Self-assembly was concluded to be completed over night as capacitance values didn't change upon further incubation with ethanolic lipid solution. Layers were found to be extremely stable. No change of capacitance could be observed upon incubation in electrolyte (0.1 M KCl) for up to ten days. This is a crucial property for such layers to be used in biosensors. Addition of

POPC vesicles did not change capacitance as would be expected for incomplete or defect layers [Dus96a]. No change of capacitance was observed, either, upon incubation of layers with 10 mg/ml BSA indicating no observable adsorption of the protein.

compound	c [μF/cm²]	reference
1-hexadecanethiol	1.13	[Lan94]
thiolipid 1	1.41	"
thiolipid 2	1.20	"
thiolipid 3	1.14	"
DOPSH	1.2	A. Schrader, personal communication.

Tab. 3.5. Capacitance values reported by others for monolayers of structurally different thiolipids self-assembled on gold. DOPSH: 1,2-dioctadecyl--sn-glycero-3-phosphothioethanol. For structures of thiolipid 1 - 3 see figure 3.3.

Immobilization of dipalmitoyl lipids via the head group (thiolipid 1 - 3, fig. 3.3 and tab. 3.5) have shown also increasingly ordered and tighter packed hydrocarbon chains with increasing spacer length decoupling them from the on a molecular scale rough solid support [Lan94]. The high capacitance values observed for the thiolipids of this work are therefore not surprising.

System investigated		thickness of hydrocarbon chains (monolayer)	thickness of entire monolayer	comments	reference
DPPC	gel phase	17.5 ± 0.5 Å	24.9 ± 1.2 Å		[Wie89]
	"		22.5 ± 0.5 Å		[Cev93]
	liquid-crystalline	17.5 Å	-	by ^{2}H-NMR	[Gen89]
	"	22.5 Å	19.0 Å	theoret. for all trans	[Cev93]
$HS(CH_2)_{15}CH_3$	by ellipsometry	22.5 Å	-	-> only $(CH_2)_{15}$	[Por87]
self-assembled on	calculated (25^0 tilt)	19.5 Å	-		
gold	" (no tilt)	16.5 Å	-		

Tab. 3.6. Reference values for thicknesses of the hydrophobic part in lipids determined by various methods.

Comparison of these findings with those from protein adsorption monitored by SPR (see chapter 4) suggests that poor insulation of a layer does not necessarily imply high nonspecific

binding of proteins. In fact, nonspecific protein binding was found to be extremely low for such layers (see chapter 4) and this was, of course, one of the major aims of this work!

3.4. FTIR

3.4.1. Introduction

Grazing incidence or reflection absorption FTIR spectroscopy has first been proposed by Greenler [Gre66]. Since then it has been extensively used for the characterization of thin organic films adsorbed to reflecting substrates [Gre69, All78, Deb82, Deb84, Swa85, All85b, Por87, Yen89, Mie93, Yam94]. For lipid aggregates, however, mostly ATR-FTIR has been used to provide information about the structure of the lipid molecules (orientation of the molecules at the surface, order and fluidity of the layer, coverage, tilt of hydrocarbon chains, conformation of the head group and fatty acids, etc.) [Fri77, Fri81, Men91, Hüb91, Lew96]. Such kind of information is aimed at by investigating supported, self-organized monolayers of the thiolipids synthesized in this work with grazing incidence FTIR. It is thereby of particular interest how the nature of the outermost surface relates to the amount of nonspecifically adsorbed protein and in what respect the choline moiety is responsible for low nonspecific protein adsorption, whether its effect can be enhanced by other adsorption reducing effects such as for instance repulsive entropic forces (see chapter 1.1). The degree of fluidity of the self-assembled layers is of particular interest (cf. chapter 1.1). Spectroscopic markers of lipid phases are band positions, intensities and half-height widths.

Characterization of self-assembled thiolipid monolayers was attempted on one side by comparing their infrared spectra with those of natural lipids (DPPC, DPhyPC, PLPC) and on the other side by comparing, to a limited extent, spectra acquired with different measurement configurations (transmission and GI-FTIR, cf. fig. 3.7). Comparison of grazing incidence and transmission spectra is limited due to systematic differences of absorption band positions, shapes, and intensities. The physical reasons are described in detail in [All78]. Briefly, peak maxima are shifted to higher wavenumbers in grazing incidence spectra as compared to transmission spectra. The magnitude of the shift thereby depends on the attenuation constant and the width of the absorption band. For the C=O stretching vibration of thin films of isotropic poly(methyl methacrylates), for example, the absorption maxima in the grazing incidence spectrum was at a 8 cm^{-1} higher position than in the transmission spectrum. Corrections of band positions for optical dispersion distortion effects in GI-FTIR spectrum of self-assembled $HS(CH_2)_nH$ (n = 4, 6, 8, 10, 12, 16, 18, 22) on gold were reported to be less than 1 cm^{-1} for

all peaks [Por87]. Intensity of absorption bands (of equally thick films) and band shape can also differ for the two measurement configurations. GI-FTIR bands have often distorted, asymmetric shapes exclusively for optical reasons such as major changes of the refractive index within an absorption band [All78].

All infrared spectra are shown in annex D. KBr-pellets have been prepared for transmission experiments. In a first set of GI-FTIR measurements, the five synthesized thiolipids were self-assembled on gold evaporated onto glass slides. A self-assembled layer of a completely deuterated hexadecanethiol, $HS(CD_2)_{16}D$, was thereby used as a reference (fig. 3.7). In a second set of GI-FTIR measurements, thiolipids as well as DPPC and DPhyPC were spread at the air-water interface and transferred onto a self-assembled layer of hydroxythiols, $HS(CH_2)_{11}OH$, which was also used as a reference. Behavior of zwitterionic and nonionic lipids is usually not perturbed upon contact with highly polar surfaces [Lew96]. Transfer of LB-lipid layers onto a hydrophobic layer of self-assembled C_{16}-alkylthiols was not possible as the first layer deposited upon dipping in of the slide was quantitatively removed during its withdrawal. Fringeli had also observed that in the case of phospholipids the first layer generally detaches upon redipping of the substrate [Fri79]. Yet, in the case of a hydrophobic substrate, deposition of a second lipid layer is necessary as the otherwise hydrophilic surface is easily contaminated.

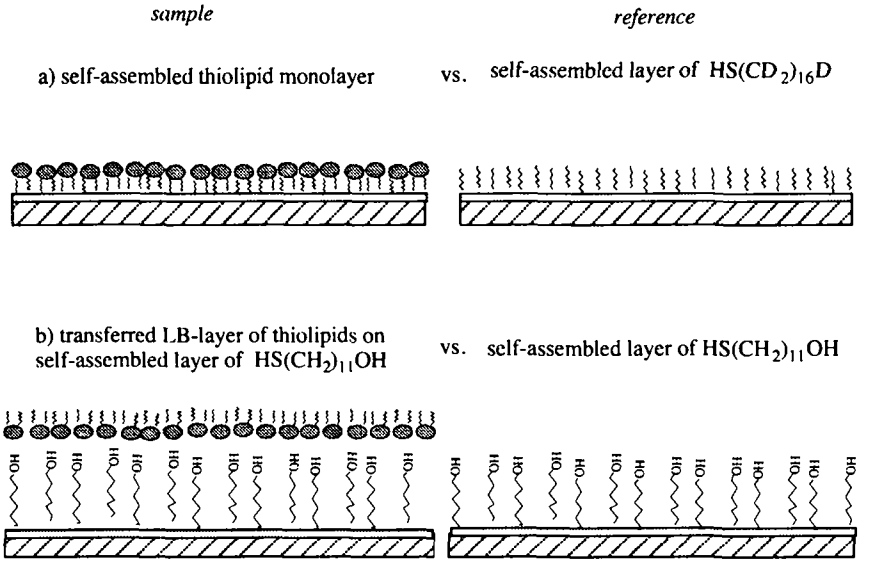

Fig. 3.7. GI-FTIR of synthesized thiolipids.

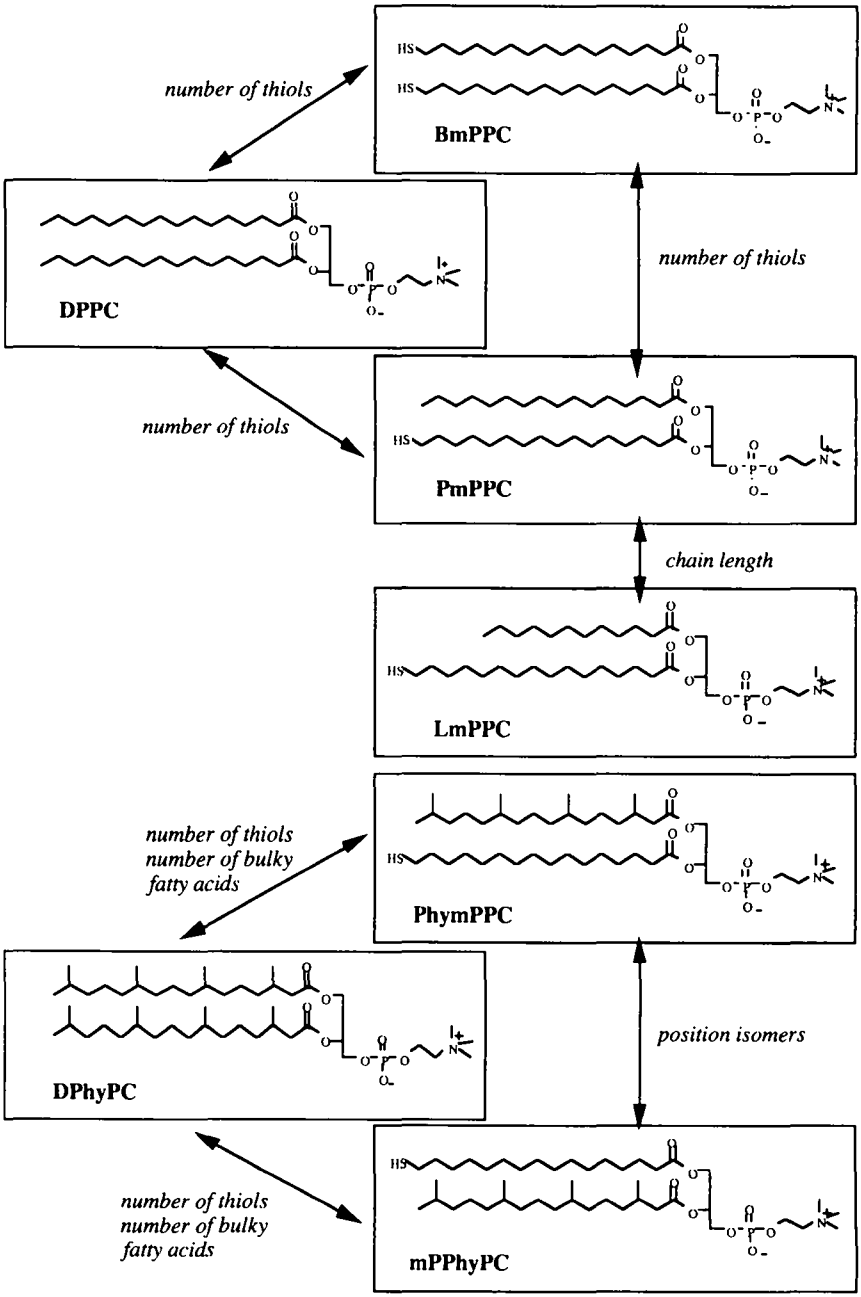

Fig. 3.8. Structural variation of the investigated lipids.

Most lipids contain IR-active groups in their hydrophobic, interfacial, and polar head group regions. Therefore, FTIR is suitable to distinguish between phenomena affecting the behavior of each of these regions. The five synthesized thiolipids have similar chemical structures differing only in the number of thiols, the chain length or the positions on the glycerol backbone where the fatty acids are attached to (fig. 3.8). Spectral differences are therefore expected to be small and mostly originating from the nature of the assembly rather than from the chemical structure.

vibration		wavenumber (cm^{-1})
C-H st	CH_3 st as	2962
	CH_2 st as	2936 - 2916
	CH_3 st sy	2872
	CH_2 st sy	2863 - 2843
C=O st	C=O st	1750 - 1720
C-H bend	N^+-$(CH3)_3$ bend as	1490 - 1470
	CH_2 bend	1469 - 1467
	CH_3 as	1450
	CH_2COOR bend	1422 - 1414
	N^+-$(CH_3)_3$ bend sy	1405 - 1395
	CH-$(CH_3)_2$	1385,1365
	CH_3 sy	1380 - 1370
CH_2 wagging	CH_2 wagging	1400 - 1300
		1330 - 1180
C-O st (ester)	C-O st (ester)	1278
PO_2^- st	PO_2^- st as	1260 - 1200
	PO_2^- st sy	1110 - 1085
P-O-C st	P-O-C st	-
$N^+(CH_3)_3$ bend	N^+-CH_3 bend as	970 - 950

Tab. 3.7.a. Assignment of absorption bands in lipids [Lew96]. st: stretch; as: asymmetric; sy: symmetric. The band position listed for the CH_2 bending mode is specific for rotationally disordered polymethylene chains.

vibration		wavenumber (cm^{-1})
C-H st	CH_3 st as ip	2965
	CH_3 st as op	ca. 2958 (sh)
	CH_3 st sy FR	2938
	CH_2 st as	2919
	CH_3 st sy FR	2878
	CH_2 st sy	2851

Tab. 3.7.b. Assignment of some infrared absorption bands found for $HS(CH_2)_{16}H$ self-assembled on gold [Nuz90]. Notation as for table 3.7.a. sh: shoulder; ip: in plane; op: out of plane; FR: band is split by Fermi resonance interactions with lower frequency CH_3 deformation modes.

In the following, FTIR spectra of the self-assembled thiolipid monolayers are analyzed with respect to the most important vibrational bands listed in tables 3.7.a and b. Analysis is based on three parameters, which characterize each absorption band:

1. its frequency
2. its intensity
3. the direction of its transition moment **M** with respect to a fixed axis (of the molecule or the molecular assembly).

Θ being the angle between the vector of the electric field **E** of the incident light and the direction of the transition moment **M** of the infrared transition, the intensity I of the absorption is proportional to the square of their dot product:

$$I \propto (\mathbf{M} \cdot \mathbf{E})^2 \propto \cos^2 \Theta \qquad (1)$$

Absorption is hence maximal for **M** and **E** being parallel and zero if they are perpendicular with respect to each other. Therefore, FTIR does not only yield information on the chemical structure of a molecule, but also on its orientation with respect to an external reference system. In the case of the grazing incidence FTIR measurement configuration, the exciting light interacts with a thin organic film adsorbed on a metallic support. Consequently, only the electric field normal to the support interacts with the IR transition dipole moments of the adsorbed molecules [Gre66]. Figure 3.9 shows the orientation of the electric field for different measurement configurations and figure 3.10 and 3.11 the orientation of some transition moments in self-assembled

thiolipids. Besides orientation and chemical structure of the adsorbed molecules, different conformations can be distinguished because they have often different force constants for a particular molecular vibration.

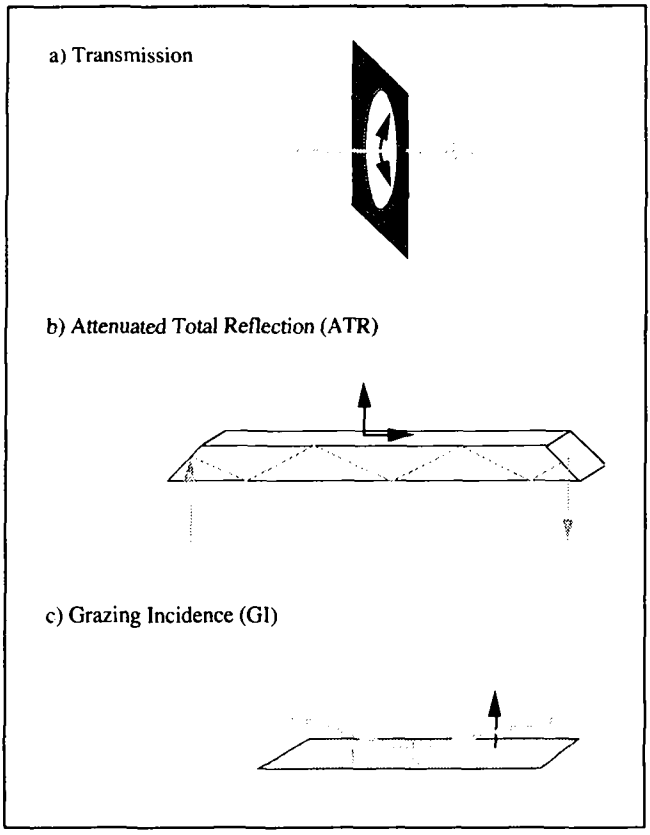

Fig. 3.9. Orientation of the probing electric field for different infrared measurement configurations (black arrows) [Swa85, Lew96]. Gray arrows indicate the light path.

For a selection of the vibrational transitions of the thiolipids synthesized in this work, the following three topics have been addressed:

1. effect of the *chemical structure* of lipids in *isotropic* samples (transmission spectra)
2. effect of the *chemical structure* of lipids in *anisotropic* samples (self-assembled and transferred LB-layers)
3. effect of *covalent attachment* of thiolipids to the surface

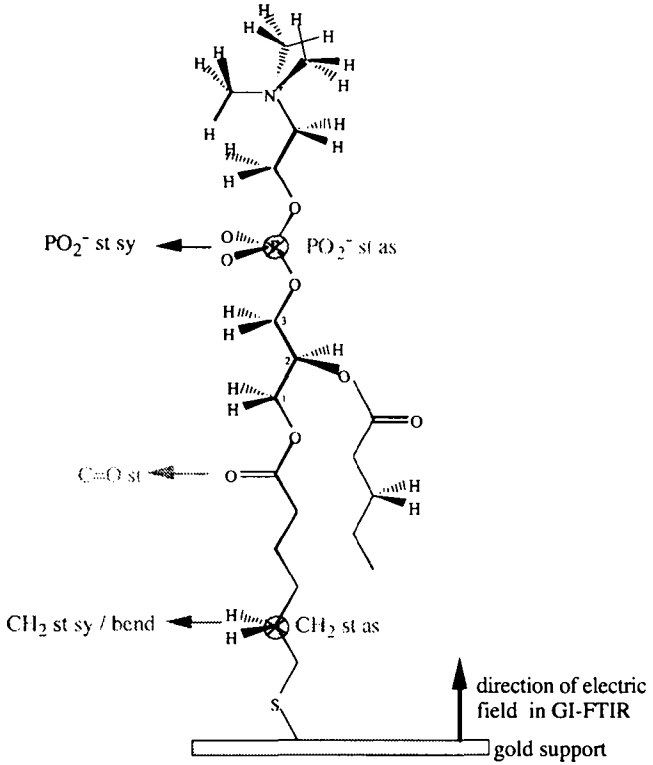

Fig. 3.10. Orientation of some infrared transition dipole moments indicated by the arrows [Lew96]. Orientation and conformation of the immobilized thiolipid has been chosen arbitrarily.

Comparison of spectra recorded with different measurement set-ups:

In GI-FTIR spectra of *isotropic* films, peak maxima were found to be systematically shifted to higher wavenumbers as compared to transmission spectra [All78]. This as well as asymmetry of absorption bands were attributed to the anomalous dispersion $n(\tilde{\nu})$ of absorption bands in GI-FTIR. Yet in more recent studies, comparison of transmission (KBr) and GI-FTIR spectra was attempted for long chain n-alkanoic acids adsorbed on oxidized aluminum oxide [All85b] and n-hexadecanethiol self-assembled on gold [Nuz90]. Using optical constants from bulk transmission spectra, GI-FTIR spectra were thereby calculated in order to obtain information about the molecular structure (order, tilt of hydrocarbon chains etc.) of the adsorbed layers. Three cases were distinguished for the comparison of GI-FTIR and transmission spectra:

1. The structure of the adsorbed layer is homogeneous and isotropic, thus structurally identical with the bulk material. In this case accurate calculation of the GI-spectrum of the adsorbed layer from the bulk transmission spectrum is possible (for an ideally flat substrate with known optical functions and for a known thickness of the adsorbed layer).

2. The adsorbed layer is anisotropic, but otherwise identical with the bulk structure. The calculated spectrum (I_{calc}) of the isotropic adsorption layer must be scaled accordingly (yielding $I_{observed}$):

$$I_{observed} = 3\cos^2\Theta \cdot I_{calc} \qquad (2)$$

with Θ being the angle between the transition dipole derivative M and the surface normal **z** (as in equation (1)).

3. Force constants, normal modes, and charge distributions of the adsorbed layer are different from the bulk material due to changed inter- and intramolecular interactions or interactions with the substrate leading for example to phenomena like ordering. In this case,

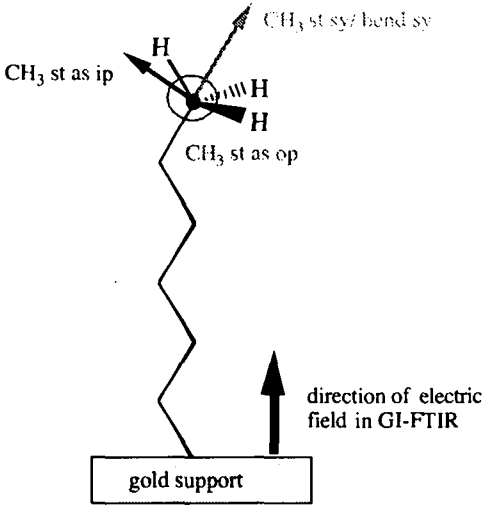

Fig. 3.11. Orientation of some infrared transition dipole moments found in lipids [Lew96, Nuz90].

spectra of adsorbed layers differ significantly from bulk spectra (band positions, intensities, shapes) and simple conclusions from comparison of transmission and GI-spectra are not possible!

Assuming the n-alkanoic acids adsorbed to aluminum oxide to belong to the second category, Allara et al. calculated tilt angles Θ of various bonds with respect to the surface normal by comparing integrated adsorption bands of calculated (I_{calc}) and measured ($I_{observed}$) GI-FTIR spectra (equation (2)).

3.4.2. Results: Analysis of IR-Absorption Bands

In order to investigate the effect of self-organization on spectral features, it would in principle be best to compare GI-spectra of anisotropic, self-assembled layers with a corresponding isotropic sample using the same measurement technique. However, samples prepared by drying down for example drops of a solution of BmPPC in dichloromethane onto a self-assembled layer of hydroxythiols ($HS(CH_2)_{11}OH$) showed formation of even more ordered lipid layers than the self-assembled one as judged from the position of the CH_2 st absorption bands. This may indicate a strong, substrate induced (?) ordering instead of homogeneous bulk structure. A similar method has in fact been described for the preparation of ordered multilayers of lipids using polar ATR-crystals as substrates [Fri79]. Lipid solutions were thereby dropped onto the latter and multilayers formed by striking slowly with a teflon bar over the crystal until all solvent had evaporated.

Therefore, grazing incidence FTIR-spectra of self-assembled monolayers (in the following abbreviated as SA/GI) and of transferred LB-layers (in the following abbreviated as LB/GI) of the five synthesized thiolipids as well as their transmission spectra (in the following abbreviated as KBr) are compared in this chapter by analyzing position and intensity of each absorption band separately and concluding from this on the effects, variations of the chemical thiolipid structure (fig. 3.8) have on structural features of the supported thiolipid monolayers. All spectra are shown in annex D (no baseline correction).

The notation of table 3.7.a is used to designate the type of vibration.

a) C-H stretching vibrations

- Comparison of band positions

The C-H stretching vibrations can provide information about conformation and orientation of hydrocarbon chains. Studies of bulk and self-organized hydrocarbons by various groups have shown that the location of the asymmetric and the symmetric CH_2 stretching bands are sensitive indicators for the extent of the lateral interactions between long n-alkyl chains [Sny82, Sny86, Por87]. Their precise positions can be used to distinguish between all-trans (crystalline-like) and disordered (liquid-like) conformations of the alkyl chains. From this it was concluded that in the case of alkanethiols $HS(CH_2)_nH$ with a chain length n of $16 \leq n \leq 22$ self-assembled on gold, the average local environment for an individual hydrocarbon chain is very similar to that in the bulk crystalline phase [Por87].

$HS(CH_2)_nH$	type of sample	CH_2 st as	CH_2 st sy	Ref.
n = 6	self-assembled on gold	2921	2852	[Por87]
n = 8		2921	2852	"
n = 10		2920	2851	"
n = 12		2919	2851	"
		2922	2851	[Ber93]
n = 14		2921	2851	"
n = 15		2919	2851	"
n = 16		2918	2850	[Por87]
		2920	2851	[Ber93]
n = 18		2917	2850	[Por87]
n = 22		2918	2850	"
$HS(CH_2)_{22}H$	crystalline, in KBr	2918	2851	[Por87]
$HS(CH_2)_7H$	liquid, in liquid prism cell	2924	2855	[Por87]
$HS(CH_2)_{16}OH$		2818	2851	[Ber93]

Tab. 3.8. Infrared absorption band positions (cm^{-1}) of the symmetric (CH_2 st sy) and asymmetric CH_2 stretching (CH_2 st as) modes of various alkylthiols.

Table 3.8 lists values from literature for the band positions of the symmetric and asymmetric CH_2 stretching vibrations of various alkylthiols self-assembled on gold. It can be seen that the wavenumber decreases with increasing length of the hydrocarbon chain. Comparing band

positions of bulk crystalline and liquid alkylthiols (tab. 3.8), it was concluded that the decrease of the wavenumber correlates with the degree of order of the hydrocarbon chains: Very ordered, crystalline-like layers show absorption maxima between 2917 and 2920 cm^{-1} for the asymmetric and between 2849 and 2851 cm^{-1} for the symmetric CH_2 vibrations whereas very disordered layers show band positions of up to 2928 cm^{-1} for the asymmetric and 2856 cm^{-1} for the symmetric CH_2 vibrations. Both, the asymmetric and the symmetric CH_2 stretching vibration, show thus a similar trend, but in the case of the symmetric mode it is usually less pronounced .

Table 3.9 lists the positions of the absorption maxima of the symmetric and the asymmetric CH_2 stretching vibration for the three measurement configurations used for the five synthesized thiolipids and the two structurally closely related lipids without thiols (fig. 3.8).

Generally, self-assembled layers and transferred LB-layers have similar positions meanwhile transmission spectra show mostly lower wavenumbers (fig. 3.12 a and b).

lipid	CH_2 st as			CH_2 st sy		
	SA/GI [a]	LB/GI [b]	KBr [c]	SA/GI	LB/GI	KBr
DPPC	-	2918.8	2917.6	-	2850.4	2850.1
BmPPC	2918.7	2919.1	2917.4	2850.6	2850.4	2850.0
PmPPC	2926.5	2927.3	2917.3	2855.0	2854.1	2850.0
LmPPC	2926.6	2929.4	2918.6	2854.3	2856.6	2850.4
PhymPPC	2926.7	2928.4	2924.4	2852.7	2855.4	2853.2
mPPhyPC	2927.3	2928.3	2924.2	2853.8	2853.6	2852.8
DPhyPC	-	2928.8	2926.4	-	2851.1	2858.0
PLPC	-	-	2920.5	-	-	2851.6

Tab. 3.9. Infrared absorption band positions (cm^{-1}) of the symmetric (CH_2 st sy) and asymmetric CH_2 (CH_2 st as) stretching modes of the synthesized thiolipids and the reference lipids. a) GI-FTIR spectra of self-assembled layer. b) GI-FTIR spectra of transferred Langmuir-Blodgett layer. c) Transmission spectra of KBr pellet.

From the experimental data in table 3.9 and figure 3.12, it can be concluded that only BmPPC forms very ordered monolayers by self-assembly meanwhile all other thiolipids form very disordered layers. As expected the differences of the band positions of the symmetric CH_2 stretching vibration are less pronounced than that of the asymmetric one. Lewis et al. recommended to use the symmetric mode as an indicator of order as it overlaps less with the methyl stretch vibrations [Lew96]. In fact, comparing the band positions of the symmetric and

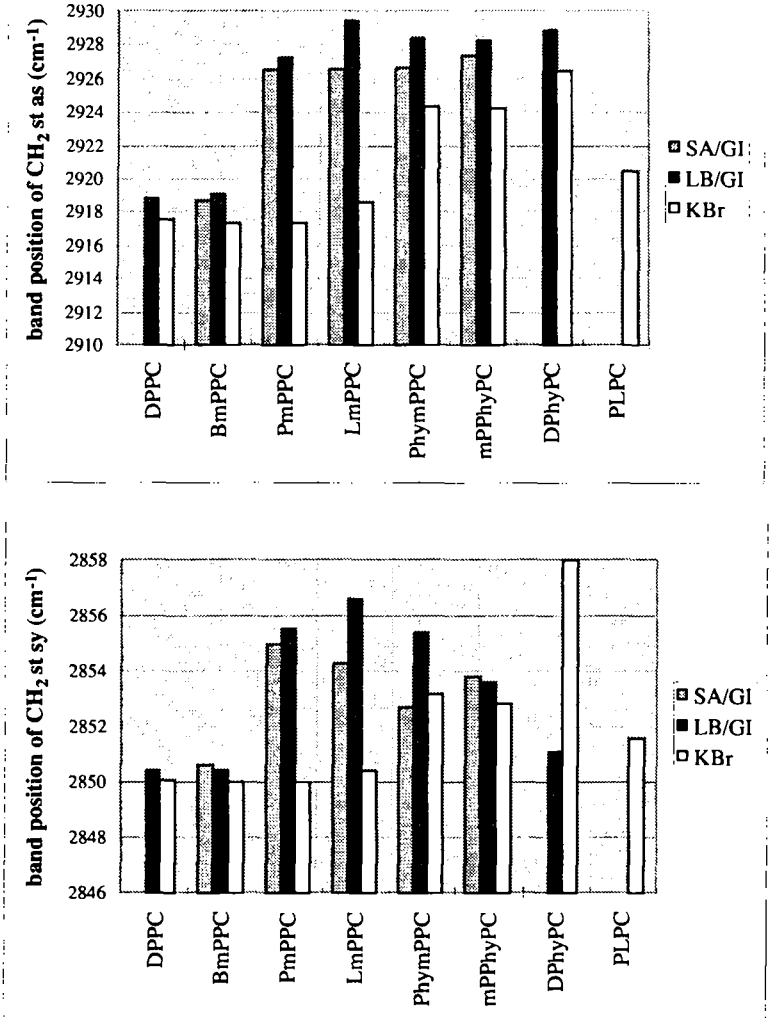

Fig. 3.12. Band position of CH_2 st vibrations for three different measurement configurations. SA/GI: GI-FTIR of self-assembled monolayer; LB/GI: GI-FTIR of transferred LB-layer; KBr: transmission spectra of KBr pellets.

the asymmetric CH_2 stretching vibrations of the lipids containing phytanic acid, contribution of the asymmetric CH_3 stretching vibration might be the reason why on a relative scale these lipids

appear more disordered when judging from the band position of the asymmetric CH_2 stretching mode than from the symmetric one.

Among the structural differences between the investigated lipids (fig. 3.8), the number of thiols has obviously the largest impact on the order of the hydrocarbon chains. Their length as well as position of attachment on the glycerol backbone seem to affect order to a much lesser extent. Immobilization of the thiolipid via the fatty acid in the 1-position seems to slightly increase disorder in the self-assembled layer, which would agree with the greater mechanical freedom predicted for the lipid immobilized via the fatty acid in the *sn-1* position. Reduction of the chain length by four methylene units seems to lead to a slight increase of order. This as well confirms expectations from structural reflections based on the crystal structure of the DMPC bilayer (fig. 1.7), where the fatty acids in the *sn-1* positions of one lipid monolayer protrude further into the adjacent monolayer. It suggests also an ordering effect of the gold substrate as the gel-liquid phase transition temperature of LPPC bilayers in water is about 20^0 lower than that of DPPC bilayers (cf. tab. 9.1).

Disorder of the hydrocarbon chains encountered in most self-assembled thiolipid monolayers could at least partially also be due to the fact that well dried layers are measured in air. As already indicated by SPR and contact angle measurements, the self-assembled thiolipid monolayers have a certain flexibility despite their covalent-like attachment to the gold surface. This flexibility is larger for the thiolipids being attached via only one fatty acid. Thus, although not in contact with the surrounding fluid phase (water and polar organic solvents), the fatty acid chains which are not bound to the gold surface may partially flip out of the layer upon exposure to an apolar environment like dry nitrogen burying the polar head groups. Ruiz et al. have reported a similar phenomenon when investigating hydrophobic polymers functionalized with phosphorylcholine by ToF-SIMS and XPS [Rui97]. They could show that choline groups were found at different depths in the apolar polymer and at the very surface, respectively, depending on the polarity of the solvent in contact with the polymer. The significance of structural characterizations of dry self-assembled lipid monolayers by GI-FTIR is thus limited since only their fully hydrated structure in water is relevant with respect to nonspecific protein adsorption.

From figure 3.12, it can be seen that even though transferred LB-layers clearly show the same tendencies for all lipids with BmPPC being the only well ordered thiolipid layer, the hydrocarbon chains of transferred LB-layers seem to be slightly more disordered than the corresponding self-assembled layers. This agrees with the results of Duschl et al., who investigated the order of hydrocarbon chains of thiolipids 1 - 3 (fig. 3.3) by surface plasmon enhanced Raman spectroscopy [Dus96a]. By comparing the spectra of LB-layers transferred below and above the phase transition temperature with those of the corresponding self-assembled layers, they found that the self-assembled layers are the most ordered. All LB-layers

of the thiolipids synthesized in this work (fig. 2.1) were transferred at a surface pressure of around 30 mN/m with exception of BmPPC, which was transferred at about 18 mN/m, but only DPPC had clearly shown a phase transition until then. Band positions of the LB-layers of BmPPC and DPPC are almost identical (fig. 3.12) whereas substitution of only one methyl group by a thiol (PmPPC) seems to have a great impact on order also in transferred LB-layers. All other differences of the lipid structures show a much smaller impact on the band positions. However, interpretation of the small differences observed suggests the following tendencies: Shortening of one hydrocarbonchain (-> LmPPC) leads to more disorder in transferred LB-layers (fig. 3.12) whereas it seems to lead to slightly more order in self-assembled layers. The position isomer where the bulky phytanic acid is attached in the 1-position of the glycerol backbone (PhymPPC, fig. 3.8) shows less order in the transferred LB-layer than mPPhyPC, where the bulky phytanic acid is attached in the 2-position of the glycerol backbone, whereas the opposite was the case for self-assembled layers. The latter can only be concluded from comparison of the position of the symmetric CH_2 stretching vibration since the asymmetric ones are almost the same for transferred LB-layers as well as for the self-assembled layers, probably again due to overlapping with the asymmetric CH_3 stretching vibration.

In general, it seems to be crucial for a thiolipid layer to be ordered that the fatty acids both in the *sn1*- and the *sn2*-position of the glycerol backbone are identical. However, it can not be excluded that disorder is also introduced upon transfer of the LB-layer as transfer ratios have not been determined.

The asymmetric and symmetric CH_2 stretching vibration in the KBr spectra appear for all lipids at lower wavenumbers than in the corresponding GI-spectra of the self-assembled and the transferred LB-layers. This might be attributed to the systematic shift of absorption maxima to higher wavenumbers in grazing incidence as opposed to transmission spectra [All78]. But a truly increased order of the lipids in the KBr samples may be responsible as well for the lowering of the band positions and it might be explained by the way samples have been prepared: DPPC and PLPC were added as powders to the KBr crystals, whereas the thiolipids were sticky films rather than powders and therefore they have been dissolved in dichloromethane and dropped onto the KBr crystals. After evaporation of the solvent, the samples were dried over phosphorpentoxide at reduced pressure, molded and pressed. As mentioned above, ordered lipid multilayers can be prepared from an organic solution by dropping it onto a polar ATR support and striking over the lipid solution with a teflon bar until complete evaporation of the solvent [Fri81, Hüb91, Man91]. Formation of ordered multilayers might have also occurred here with the polar KBr grains as substrates. Transmission spectra may therefore not be the spectra of bulk lipids, but those of ordered assemblies. This interpretation is supported by the fact that both, the symmetric and the asymmetric absorption

maxima of DPPC and BmPPC, which both showed very ordered monolayers, occur at only slightly lower wavenumbers for the KBr pellets than for the GI-spectra of the monolayers.

These findings also correlate with phase transition temperatures determined by calorimetry for liposomes of the synthesized lipids: They are similar for DPPC, BmPPC (and PmPPC) whereas no phase transition was observed between 11^0 and 60^0 for PhymPPC and mPPhyPC. No phase transition between -120^0 and 80^0 for DPhyPC is also reported in literature [Ava94]. The latter as well as PhymPPC and mPPhyPC show elevated wavenumbers also in KBr pellets, indicating that no ordered multilayers can be formed even by the method for the preparation of multilayers described above.

- *Comparison of band intensities*

In GI-FTIR spectra of lipid monolayers, intensities of absorption bands of the hydrocarbon chains give information about their orientation with respect to the surface normal. Tilt angles for various alkylthiols self-assembled on gold and other metals have been calculated, either by fitting GI-FTIR intensities of a homologous series of alkylthiols with different chain lengths assuming similar packing densities and order as for example described by Porter et al. [Por87] or from dichroic ratios using different polarizations for ATR-FTIR. The latter method was used to determine also orientation of hydrocarbon chains in lipid multilayers [Fri79, Fri81]. A tilt angle of 29^0 - 33^0 with respect to the bilayer normal was found for the hydrocarbon chains of microcrystalline DPPC at 0 % relative humidity [Fri79]. However, so far self-assembly technology on metal films and ATR-FTIR are not compatible.

Variation of intensity of a CH_2 stretching band in a GI-FTIR spectrum of alkylthiols self-assembled on gold can have at least three reasons [Por87]:

1. different coverage (less coverage, less intensity)
2. different chain orientation (decreasing intensity for increasingly perpendicular hydrocarbon chains)
3. different order of the hydrocarbon chains.

The contribution from the last point is the most difficult to evaluate as it can result in two opposing contributions. On one side, decreased order leads to *decreased* intensity of the CH_2 stretching bands for a *bulk* sample with *isotropic* distribution of the transition dipole moments. On the other side, for a *monolayer* at a surface, disordering leads to an isotropic distribution of

the CH_2 stretching transition moments and thus to an *increase* of intensity of the absorption bands (for details see [Por87]).

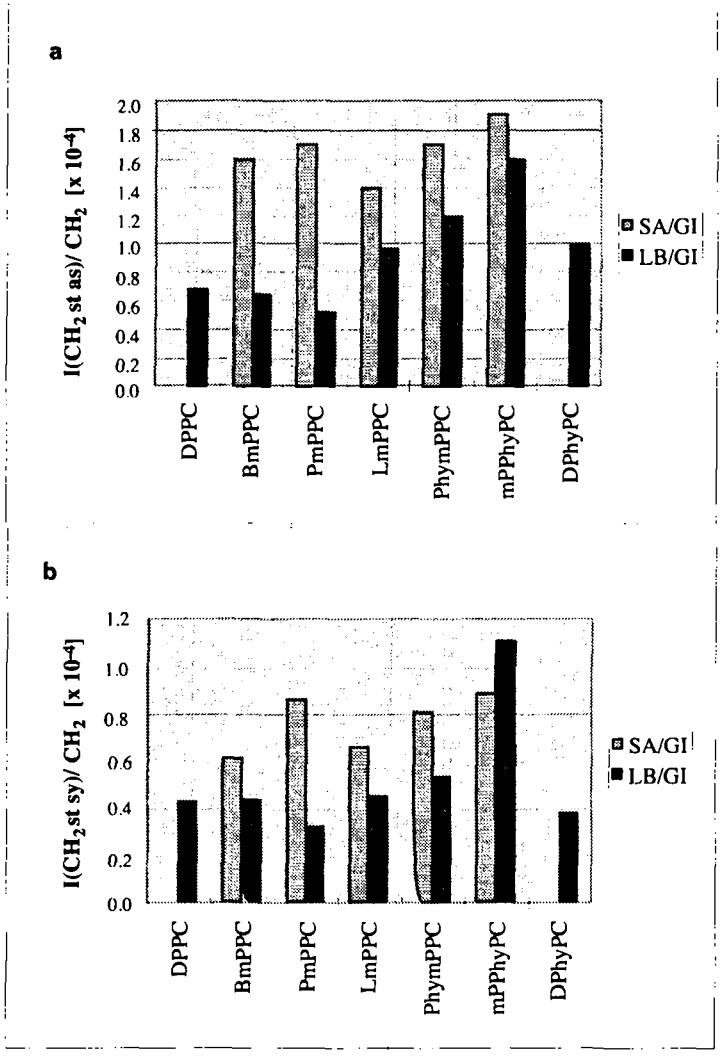

*Fig. 3.13. GI-FTIR intensity of the CH_2 stretching bands of self-assembled (SA/GI) and transferred LB-layers (LB/GI) normalized by the number of methylene units in the lipid. **a**: asymmetric CH_2 stretch; **b**: symmetric CH_2 stretch.*

Figures 3.13 a and b show the intensities of the symmetric and the asymmetric CH_2 stretching bands normalized by the number of methylene groups in the lipid ("specific intensity") for self-assembled monolayers and transferred LB-layers. Even though the absolute values may not be very precise, there is clearly a tendency that lipids have lower specific intensities in transferred LB-layers than in self-assembled layers. Assuming similar coverage and order for both layer types, which is well justified by the similar positions of these absorption bands for self-assembled as well as for transferred LB-layers, the differences observed suggest that hydrocarbon chains in the transferred LB-layers are generally less tilted from the surface normal than in self-assembled layers (see also figure 3.10). For the lipids containing phytanic acid, uncertainties are larger due to overestimation of the asymmetric (overlapping bands) and underestimation (several bands difficult to assign) of the symmetric band.

b) The C=O stretch vibration

Literature:

The carbonyl stretch vibration (C=O st) of the glycerol esters in lipids is diagnostic for the polar-apolar interface. Its features depend on the chemical structure of the polar head group as well as on the nature of the hydrocarbon chains (length, structure, number of methylene groups being odd or even, etc.), but also for example on the degree of hydration (hydrogen bonding) and the physical state of the lipid membrane. It can be affected by structural changes located far from the carbonyl group [Lew90, Lew96]. Mantsch et al. observed hardly any difference in the C=O st band position of the *sn-1* carbonyl group in going from a dry film of DMPC (C=O st at 1740 cm^{-1}) to a hydrated film in the gel phase (C=O st at 1739 cm^{-1}), but a decrease of 5 cm^{-1} in going from the gel to the liquid-crystalline state (C=O st at 1734 cm^{-1}) [Man91]. The band position of the ^{13}C-labeled carbonyl group in the *sn-2* position, however, did thereby change but very little (decrease of 1 cm^{-1} in going from the gel to the liquid-crystalline state). Crystalline or quasi-crystalline lipid assemblies often show splitting of the C=O band [Lew90, Lew96]. For stable L_c phases of phosphatidylcholines a tremendous change of the C=O stretching band could be shown as a function of the chain length of the fatty acids [Lew90], but structurally similar lipids do not necessarily show the same behavior [Lew96]. Hübner and Mantsch have investigated the orientation of the ester carbonyl groups in dry and hydrated bilayers of DMPC and DPPC below and above the respective gel to fluid phase transitions by selective ^{13}C-labeling of the *sn-2* carbonyl group [Hüb91]. From polarized ATR-FTIR spectra it was concluded that the *sn-1* and *sn-2* carbonyl groups were similarly oriented with respect to the bilayer normal, in contrast to their very different orientation in the 3D-crystal of DMPC ([Pea79], fig. 1.7.a and b).

Discussion of spectra of the synthesized thiolipids:

- *Band position*

Table 3.10 summarizes band positions of the C=O stretching (C=O st) vibration of synthesized thiolipids and reference lipids for the different measurement configurations (SA/GI, LB/GI, KBr). In principle, all monolayers should contain equal amounts of water, but it is very probable that transferred LB-layers are still more hydrated than self-assembled layers as they have only been dried by flushing the infrared measurement chamber with dry nitrogen. This could explain why transferred LB-layers show generally lower wavenumbers than the corresponding self-assembled layers, but the band positions of the self-assembled layers could also be more like for lipids in the gel state ([Man91], see also increased order of self-assembled layers as opposed to transferred layers in [Dus96a]). The low signal-to-noise ratio between 1800 and 1600 cm^{-1} is due to baseline correction by subtraction of water bands. For the transferred LmPPC layer the band position of the C=O st band could not be determined since water subtraction was not well enough possible. Comparing the band locations of the C=O stretching bands (tab. 3.10), the one of the self-assembled BmPPC layer showed by far the highest wavenumber. In analogy to the higher wavenumbers found for DMPC in the gel state compared to the liquid crystalline state [Man91] this would agree well with the self-assembled BmPPC layer being the most crystalline-like layer, which has also been concluded above from the band position of the CH_2 stretching modes.

lipid	SA/ GI	LB/ GI	KBr
DPPC	-	1741.8	1740.7
BmPPC	1743.5	1740.8	1738.1
PmPPC	1737.9	1734.4	1738.3
LmPPC	1739.5	-	1738.5
PhymPPC	1741.7	ca. 1735.1	1736.7
mPPhyPC	1740.8	ca. 1740.9	1737.6
DPhyPC	-	1735.4	1736.5
PLPC	-	-	1750/1729.9

Tab. 3.10. Positions of absorption maxima of the C=O stretch bands.

No splitting of the bands was observed, but most bands weren't completely symmetric indicating populations of differently hydrated carbonyls [Lew96] or simply systematic distortion of absorption bands generally observed in grazing incidence spectra for optical reasons as described in 3.4.1. (for details see [All78]. None of the recorded DPPC spectra exhibits the

features reported by Lewis et al. for its stable L_c phase [Lew96], from which one may conclude that the transferred LB-layers aren't as crystalline as theirs. And none of the synthesized thiolipids exhibits any substructuring and asymmetry of the C=O stretch absorption band comparable to those observed for varied chain lengths of crystalline DPPC or other crystalline lipids (see [Lew96]).

- Band intensity

In the DMPC crystal and in hydrated bilayers of PC-lipids the carbonyl groups of the *sn-1* and the *sn-2* fatty acids are oriented very differently with respect to the surface normal due to the glycerol backbone being almost perpendicular to the surface (fig. 1.7a, [Bül81]). The absorption bands of the two carbonyl groups, however, have generally very similar wavenumbers. Unless the carbonyl groups are labeled with isotopes, GI-FTIR intensities of the C=O stretching band therefore can only provide information about their average orientation.

Mantsch et al. observed variation of C=O st band intensity for DMPC upon variation of the degree of hydration and as a function of temperature using polarized ATR-FTIR and ^{13}C-labeling of the ester carbonyl groups [Man91]. Calculated changes of the angle θ between the bilayer normal and the carbonyl group in the *sn-1* and the *sn-2* position are listed in table 3.11.

For the grazing incidence set-up, the intensity of the absorption band decreases with increasing tilt of the carbonyl group from the surface normal (see fig. 3.10).

sample	θ (*sn-1* C=O)	θ (*sn-2* C=O)
dry film	64^0	65.5^0
gel	64^0	66^0
liquid-crystalline	62^0	66^0

Tab. 3.11. Angles between the bilayer normal of ^{13}C-labeled DMPC and its carbonyl groups calculated from the dichroic ratios of the C=O st absorption bands [Man91].

Comparison of the intensities of the C=O st bands of the self-assembled thiolipids (fig. 3.14) yields the most perpendicular, average orientation of the carbonyl groups for BmPPC and the most parallel orientation for LmPPC (fig. 3.15), assuming all lipids to be equally hydrated.

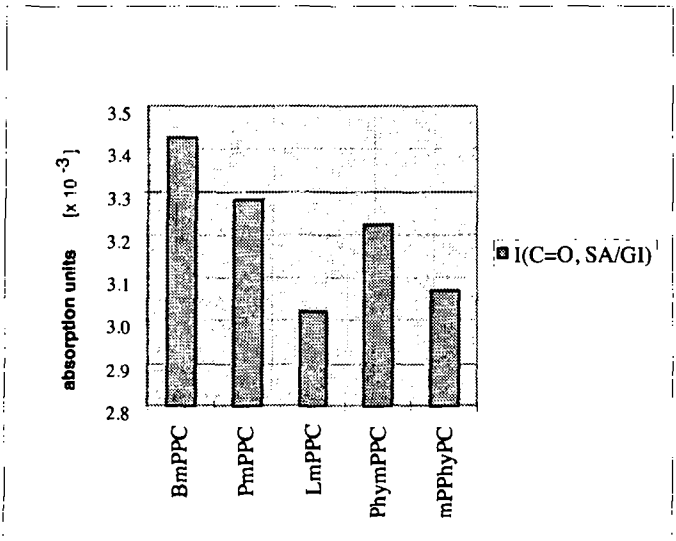

Fig. 3.14. Intensities of C=O stretching bands in GI-FTIR spectra of self-assembled thiolipid monolayers.

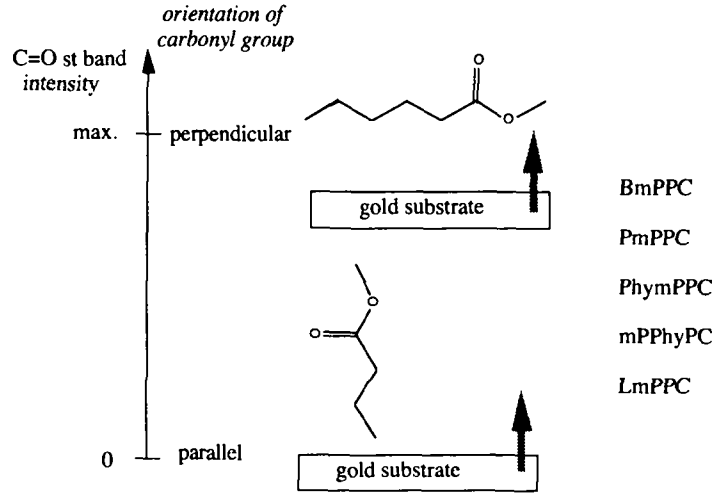

Fig. 3.15. Average orientation of carbonyl groups in self-assembled thiolipid monolayers. The bold gray arrow indicates the direction of the probing electric field in the GI-FTIR experiment.

c) CH bending

The region between 1490 and 1370 cm^{-1} comprises various bending modes listed in detail in table 3.7.a. The CH_2 bending mode is sensitive to the conformation of the hydrocarbon chains. For rotationally disordered polymethylene chains it is located between 1469 and 1467 cm^{-1}. All self-assembled thiolipid monolayers show absorption maxima within this range. In the transmission spectra of the lipids containing phytanic acid maxima are shifted to lower wavenumbers due to overlapping with the asymmetric CH_3 bending mode. The transition dipole moment of the latter must be oriented almost parallel to the surface in the case of the self-assembled layers since less band shifting was observed there.

The CH_2 bending mode of the α-methylene group is presumed to be conformationally sensitive. For the self-assembled thiolipid monolayers, the corresponding band positions vary slightly (table 3.12) with BmPPC being at the upper and mPPhyPC at the lower edge.

Different intensities in this region for the GI-FTIR spectra of self-assembled and transferred LB-layers indicate different orientations of the hydrocarbon chains in the chemisorbed and the corresponding physisorbed lipid layer.

lipid	CH_2COOR (cm^{-1})
BmPPC	1422
PmPPC	1418
LmPPC	1418
PhymPPC	-
mPPhyPC	1415

Tab. 3.12. Position of infrared absorption maxima of the α-methylene CH_2 bending mode (CH_2COOR) in GI-FTIR spectra of self-assembled thiolipid monolayers. According to Lewis et al. it is located between 1422 and 1414 cm^{-1} [Lew96]. PhymPPC showed no absorption at this position.

d) CH_2 wagging modes

Information on the conformation of the hydrocarbon chains of lipids may also be gained from the conformationally sensitive CH_2 wagging bands between 1180 and 1400 cm^{-1}. Interpretation of their spectral features, however, is strongly limited to molecular classes (e.g. n-alkanes, where they depend on the number of methylene units, or hydrated, liquid-crystalline assemblies)

[Lew96]. Fringeli reported marked alterations of wagging progression such as loss of intensity, band broadening, and finally disappearance of the progression with decreasing all-trans conformation of the hydrocarbon chains [Fri79]. He claimed that CH_2 wagging band progression can also be observed for phospholipids, the head groups of which absorb strongly in this region (PO_2^- st as ca. 1250 cm^{-1}), and that band structuring between 1320 and 1180 cm^{-1} decreases with increasing temperature for hydrated DL-α-DPPC (DPPC : water 1:1).

In table 3.13 the bands between 1320 and 1400 cm^{-1} of the transmission spectrum of DPPC (KBr pellet; annex D) can be clearly attributed to distinct conformational segments in the lipid hydrocarbon chains [Lew94, Men91].

conformational unit	wavenumber	reference
gtg + gtg' (kink)	1368 cm^{-1}	[Men91]
double gauche	1353 cm^{-1}	"
end gauche	1341 cm^{-1}	"

Tab. 3.13. Assignment of conformational units to CH_2 wagging modes.

The relative absorption band intensities of the LB-layer of DPPC transferred onto a germanium ATR-crystal are very different in this region compared to those of the bulk transmission spectrum, which indicates different chain structure (orientation or conformation).

Most structuring of the absorption bands in this region of the grazing incidence spectra of the self-assembled thiolipids is observed for PmPPC, but it is still much less than what Fringeli observed for his hydrated DPPC multilayers. This could not only have structural reasons, but also for instance be due to the lower signal-to-noise ratio in the case of the investigated monolayers or the orientation of the transition dipole moments. In fact, Fringeli's spectra show also much less band structuring for the perpendicular than for the parallel polarized ATR-spectra of hydrated DPPC multilayers [Fri79].

The end gauche band seems to be stronger for BmPPC and PmPPC than for LmPPC, which is reasonable (fig. 1.8) taking into account the fact that lauric acid is four methylene units shorter than palmitic acid. As discussed earlier, the fatty acids in the *sn-1* position of the DMPC crystal protrudes further into the bilayer (fig. 1.7.a), and it is therefore to be expected that the *sn-1* palmitic acid chain in BmPPC and PmPPC is jolt upon attachment to a solid surface (cf. fig. 1.7). And in fact, the corresponding LB-layers show less absorption due to end gauche conformation.

Branched hydrocarbon chains such as phytanic acid, however, show in this region additionally a strong doublet assigned to the CH bending mode of the isopropyl unit (DPhyPC/ transmission: 1378.3/ 1366.7 cm^{-1}) and a CH bending mode of the tertiary carbons at about 1337 cm^{-1}. No information about hydrocarbon chain conformation can thus be obtained from this region for such lipids.

e) asymmetric PO_2^- stretching

The orientation of the PC-head group both in the solid and in the liquid-crystalline phase is almost parallel to the layer surface as shown by X-ray and neutron diffraction [Gen89].

The position of the infrared absorption maximum of the asymmetric PO_2^- stretching vibration (PO_2^- st as) and the orientation of its transition dipole moment are strongly affected by the degree of hydration of the lipid assembly. The wavenumber decreases by about 25 cm^{-1} upon hydration (tab. 3.14).

lipid		phase	PO_2^- st as (cm^{-1})		θ	reference
DMPC	dry film		1255		72^0	[Man91]
	hydrated film	gel	1229		72^0	"
	"	liquid-crystalline	"		66^0	"
			for ATR polarization			
			parallel	*perpendicular*		
DPPC	0 % rel. humidity		1260	1250		[Fri79]
	60 %		1235 ± 5			"
	90 %		"	1225		"

Tab. 3.14. Position of the absorption maximum of the asymmetric PO_2^- stretching vibration (PO_2^- st as) as a function of hydration. θ is the angle between the bilayer normal and the transition dipole moment of the PO_2^- st as vibration (see fig. 3.8).

Band positions of the self-assembled layers (tab. 3.15) correspond well with those reported for dry layers of DPPC and DMPC. PmPPC shows a very structured band with three distinct absorption maxima, which may indicate different populations of phosphate groups with different degrees of hydration and/ or conformation. BmPPC shows nearly the same intensity both for the self-assembled and the transferred LB-layer. For all other lipids the signal-to-noise ratio of the corresponding absorption bands in the transferred LB-layers are generally too low to allow accurate determination of maxima. This suggests a different orientation of the phosphate group

in the LB- layer as opposed to the self-assembled layer with the transition dipole moment being much more parallel to the surface in the case of the LB-layers. Transmission spectra show slightly lower band positions suggesting wetter samples.

lipid	PO_2^- st as (cm^{-1})		
	SA/ GI	LB/ GI	KBr
DPPC	-	1247.4	1244.6
BmPPC	1250.2	1253.0	1244.6
PmPPC	1264.5/ 1249/ 1226	1246.8	1244.8
LmPPC	1244.6 (flat)	(1242.0)	1251.2
PhymPPC	1250.1	(1263.2)	1250.7
mPPhyPC	1254.0	(1262.6)	1250.8
DPhyPC	-	(1247.1)	1251.0

Tab. 3.15. Band positions of the asymmetric PO_2^- stretching vibration for the synthesized thiolipids and commercial reference lipids. Values in brackets have a greater uncertainty due to low signal-to-noise ratio.

In the case of DMPC, the transition dipole moment of the asymmetric PO_2^- stretching vibration is equally close to parallel to the surface in the dry and in the gel state ($\Theta = 72^0$) and more parallel to the surface than in the liquid-crystalline phase ($\Theta = 66^0$) [Man91]. Low intensity should be observed by grazing incidence FTIR for a phosphate group oriented like DMPC. The self-assembled monolayers of BmPPC and PmPPC show equally strong PO_2^- st as bands whereas LmPPC absorbs much less. Again this corresponds well to the concept that by shortening of the fatty acid in the *sn-1* position (LmPPC vs. PmPPC) the orientation of the PC-head group is less disturbed upon covalent attachment to a surface (fig. 1.8) as compared to its orientation and conformation in a unsupported membrane.

Introduction of bulky, branched fatty acids on the other side increases the cross-section of the hydrocarbon chains, so that conformational changes of the head group are to be expected. In fact, the intensities of the asymmetric PO_2^- stretching bands of self-assembled PhymPPC and mPPhyPC are almost identical and intermediate between LmPPC and BmPPC/ PmPPC. Orientation of the transition dipole moment is therefore more perpendicular than in hydrated DMPC multilayers.

In general intensities are much lower for transferred LB-layers than for self-assembled layers indicating that without "conformational stress" induced by covalent attachment of the thiolipids to a flat surface the head groups assume again a more natural, DMPC-like orientation.

f) symmetric PO_2^- stretching

In table 3.16 and figure 3.16 positions of the absorption maxima of the symmetric PO_2^- stretching mode are listed.

lipid	PO_2^- st sy (cm^{-1})		
	SA/ GI	LB/ GI	KBr
DPPC	-	1099.1	1091.6
BmPPC	1097.9	1101.1	1094.5
PmPPC	1102.1	1099.8	1094.8
LmPPC	1098.0	1099.5	1095.7
PhymPPC	1096.0	1098.2	1092.3
mPPhyPC	1098.0	1094.7	1093.1
DPhyPC	-	1093.1	1092.9

Tab. 3.16. Positions of the absorption maxima of the symmetric PO_2^- stretching mode for the different measurement configurations.

The transition dipole moment of the symmetric PO_2^- stretching vibration for the two conformations of DMPC single-crystal has a tilt angle from the surface normal of 53^0 and 57^0, respectively [Hau81] and of $50^0 \pm 5^0$ in oriented, crystalline DPPC monohydrate as determined

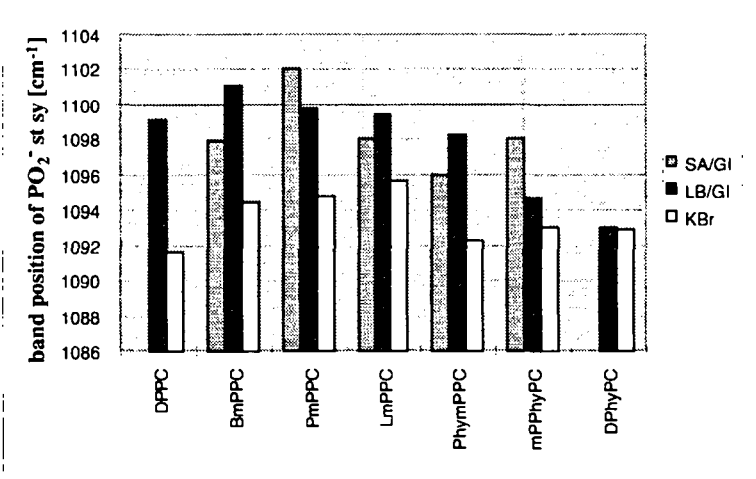

Fig. 3.16. Position of absorption maxima of symmetric PO_2^- stretching (cm^{-1}) for different measurement configurations.

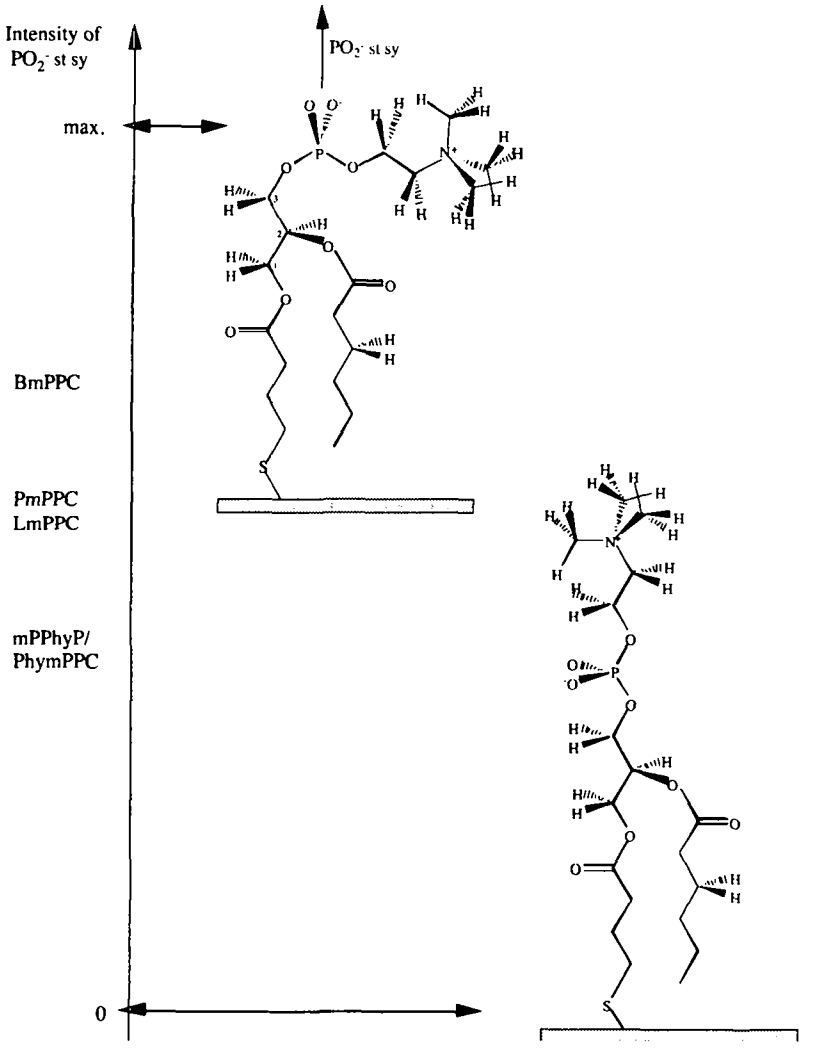

Fig. 3.17. Schematic representation of the different orientations of the phosphate group with maximal and minimal intensity of the symmetric PO_2^- stretching band in GI-FTIR and tendency of the phosphate orientation in self-assembled monolayers of the synthesized thiolipids. In the DMPC single-crystal the transition dipole moment of the symmetric PO_2^- stretching vibration is tilted 53^0 and 57^0 from the surface normal for the two conformations [Hau81].

by ^{31}P-NMR [Pow77]. In general, the conformation and orientation of the phosphodiester part in lipids changes as a function of the degree of hydration and temperature (phase), but depends little on the length and degree of unsaturation of the fatty acid chains [Bül81].

Self-assembled and transferred LB-layers of BmPPC show by far the strongest PO_2^- st sy as well as P-O-C st absorption bands with the lowest half-height width, which suggests also the most crystalline head group region as compared to the other thiolipids.
Unlike for the asymmetric PO_2^- stretching vibration intensities of the symmetric PO_2^- st are similar both in self-assembled and LB-layers suggesting similar orientation of the transition dipole moment in both layers!

Figure 3.17 summarizes tendencies of orientations of the phosphate groups in self-assembled thiolipid monolayers suggested by comparison of the absolute intensities of the GI-FTIR spectra. Both symmetric and asymmetric phosphate absorption is strongest for BmPPC.

g) C-O stretching (ester)

The absorption band position of the C-O stretching mode of the ester group has been reported to depend on the conformation of the -C-(C=O)-O-C- moiety. It is located at 1180 cm^{-1} for a planar conformation and at 1160 cm^{-1} for a non-planar conformation [Fri81]. Its position and intensity has been investigated for DMPC by polarized ATR-FTIR as a function of hydration and temperature (table 3.17).

DMPC	phase	C-O st (*sn-1*)	-> θ	C-O st (*sn-2*)	-> θ
dry film	gel	1179 cm^{-1}	ca. 30^0	1153 cm^{-1}	62^0
fully hydrated film	"	1178 cm^{-1}	"	1153 cm^{-1}	"
"	liquid-crystalline	1176 cm^{-1}	ca. 40^0	1148 cm^{-1}	"

Tab. 3.17. Positions of absorption maxima of the C-O st (ester) vibration of DMPC as a function of hydration and temperature (polarized ATR-FTIR). θ is the angle between the transition dipole moment and the surface normal [Man91].

Obviously the band position is lowered by 1 cm^{-1} upon hydration and by 2 cm^{-1} when going from the gel to the liquid-crystalline phase. Table 3.18 shows the band positions found for the synthesized thiolipids. Again BmPPC and DPPC have the highest and thus most crystalline-like band positions, which correlates well with the findings from the position of the CH_2 stretching modes.

Whereas absorption bands in the GI-spectra of the self-assembled layers were sharp and narrow, they were broad in the transmission spectra and hardly existent in the GI-spectra of the transferred LB-layers. The population of absorbing esters is thus probably much more uniform in the self-assembled layers than in the KBr pellets. Orientation of the transition dipole moment must be nearly parallel to the surface for all lipids except BmPPC and DPPC, which once more shows an exceptional behavior. The two thiolipids containing the branched fatty acid have thereby by far the lowest wavenumbers and resemble thus highly disordered layers.

lipid	band position of the C-O st (ester) (cm^{-1})		
	SA/GI	LB/GI	KBr
DPPC	-	ca. 1184	ca. 1182.6
BmPPC	1182.7	1178.5	ca. 1175
PmPPC	1178.3	not visible	ca. 1179.8
LmPPC	1181.6	"	1180.3
PhymPPC	1170.0	"	≤ 1170.0
mPPhyPC	1169.4	"	ca. 1169.4
DPhyPC	-	"	1168.3

Tab. 3.18. Position of the absorption maxima of the C-O st (ester) mode for the different measurement configurations.

3.4.3. Are self-assembled thiolipid monolayers "fluid"?

Force profile measurements using the Surface Forces Apparatus have shown that approaching liquid-crystalline bilayers are subjected to a repulsive force at greater distance than bilayers in the gel state [Isr92a].

The aim of the project being the design of surfaces with low nonspecific binding of proteins the following questions were addressed:

Is a protein approaching a liquid-crystalline bilayer as well subjected to a repulsive force at a greater distance than upon approaching a crystalline layer?

Can self-assembled thiolipid monolayers be "fluid"?

How can this be determined? -> Is a phase transition observable?

Thermally induced melting of monolayers of long-chain amphiphiles on solid supports has been observed by FTIR spectroscopy [Coh86]. Sharp thermal phase transitions of a supported DPPC bilayer formed by transfer of two LB-layers to a solid hydrophilic support can be observed. They correspond to the main and pre-transitions observed in lamellar lipid dispersions [Gen89].

In a fluid lipid bilayer, lipids can rotate, diffuse laterally, and fluctuate vertically. In a supported thiolipid monolayer, mobility of the lipids is, of course, greatly restricted. Maximum mobility and flexibility of the adsorbed molecules may therefore be more realistic to aim at rather than true fluidity. The thiolipids should hence be attached to the gold substrate as little as necessary for the formation of a stable and well defined layer in order to preserve as much as possible of the mobility a lipid molecule has in a fluid bilayer.

Spectroscopic markers of crystallinity are low half-widths of absorption bands and strong polarization effects (i.e. strongly different absorptions for parallel and perpendicular polarized light in ATR-FTIR) [Fri79]. Certain phase transitions are accompanied by melting of the hydrocarbon chains. Chain melting is accompanied by discontinuous increases of both absorption maxima and band widths due to increased conformational disorder (gauche conformers) and mobility of the hydrocarbon chains. Virtually all infrared absorption bands of the CH_2 group can be used to detect such a transition. Yet, the symmetric CH_2 stretching mode is most suitable if fatty acids chains are the predominant source of methylenes in a lipid as the asymmetric CH_2 stretching band often contains overlapping contributions from the asymmetric CH_3 stretching mode and can also be perturbed by Fermi resonance interaction with the first overtones of the methylene scissoring vibration [Lew96]. The magnitude of the increase of the band position of the symmetric CH_2 stretching mode is usually between 1.5 and 2.5 cm^{-1}, depending on the length and chemical structure of the hydrocarbon chains, the nature of the polar head group, and the type of phase transition [Lew96]. Casal et al. for example reported for an L_{β} - L_{α} phase transition of DPPC an increase of 2.5 cm^{-1} from 2851 to 2853 cm^{-1} for the absorption maximum of the symmetric CH_2 stretching mode at about 42^0 C [Cas83].

From the positions of the symmetric and the asymmetric CH_2 stretching bands, it has been concluded above that all the synthesized thiolipids attached by only one fatty acid to the gold substrate form very disordered layers by self-assembly. However, an absorption band position corresponding to disordered hydrocarbon chains does not necessarily imply "fluidity" of the investigated layer whereas a fluid lipid layer certainly has disordered fatty acids. The question whether disorder of the hydrocarbon chains of the supported thiolipid monolayers and "fluid-like" behavior correlates was thus addressed by attempting to observe a phase transition in the self-assembled layers. Two lipids, BmPPC and PmPPC, were chosen. They have similar phase transition temperatures in vesicles (see chapter 9), but the self-assembled monolayers show very different spectral features in the infrared: BmPPC forms very ordered and PmPPC very

disordered layers by self-assembly. LB- layers and self-assembled layers of both lipids were heated using the set-up described in section 10.2.5. and their GI-FTIR spectra recorded as a function of temperature.

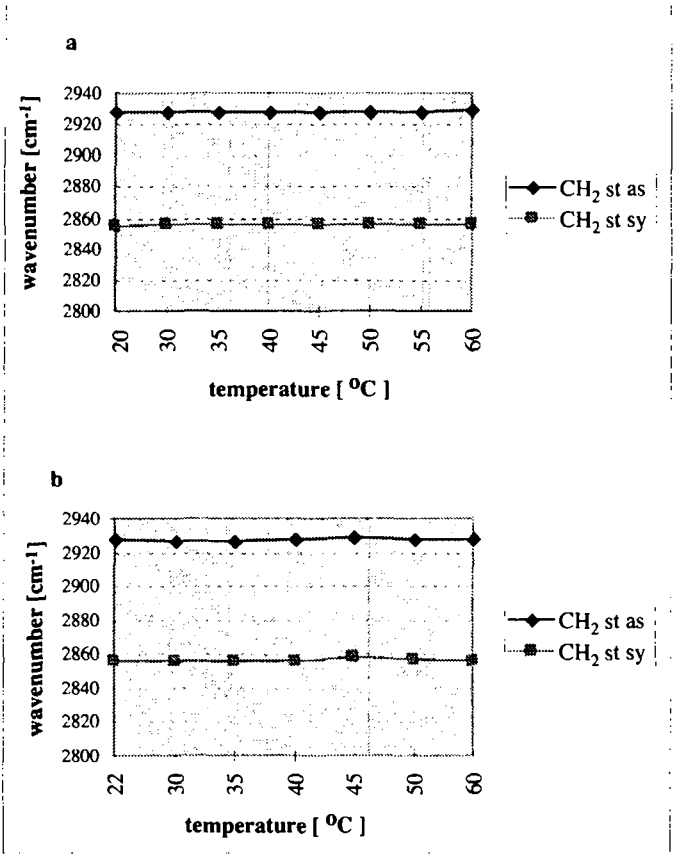

Fig. 3.18. Temperature dependence of CH_2 stretching modes in GI-FTIR spectra of a self-assembled monolayer (a) and a transferred LB-layer (b) of PmPPC.

Both, the self-assembled and the transferred LB-layer of PmPPC (fig. 3.18) as well as the self-assembled layer of BmPPC showed no chain melting between 0^0 and 60^0 C as judged from the temperature independence of the methylene stretching modes, suggesting very heat stable layers. The transferred LB-layer of BmPPC, however, clearly showed a discontinuous increase of the band positions of the symmetric and asymmetric CH_2 stretching vibrations at about 48.0^0 C, suggesting melting of the hydrocarbon chains (fig. 3.19). This corresponds well to the phase

transition temperature found for the vesicles in phosphate buffer ($T_c = 48.0^0$ C, see chapter 9). Locations of the absorption maxima of the CH_2 stretching vibrations increased by 2.8 cm^{-1} for the symmetric and by 9 cm^{-1} for the asymmetric CH_2 stretching mode, reaching the values typically observed for the other thiolipid layers (see table 3.9). Frequency shifts associated with chain melting are reported to be generally much larger for the asymmetric than for the symmetric CH_2 stretching vibration [Lai95], which agrees well with the observations made here. Since both methyl groups on the fatty acid chains of BmPPC are replaced by thiols, there is no contribution of the asymmetric CH_3 stretching band to the asymmetric CH_2 stretching so that the transition temperature found is reliable.

A self-assembled BmPPC layer, however, seems to be greatly stabilized by its interaction with the gold substrate. This agrees well with the finding that melting of supported monolayers depends on the nature of substrate-monolayer interactions (covalent, ionic, or physical bonds): Only the covalently bound octadecyltrichlorosilane monolayer did not undergo a large, irreversible randomization upon heating [Coh86].

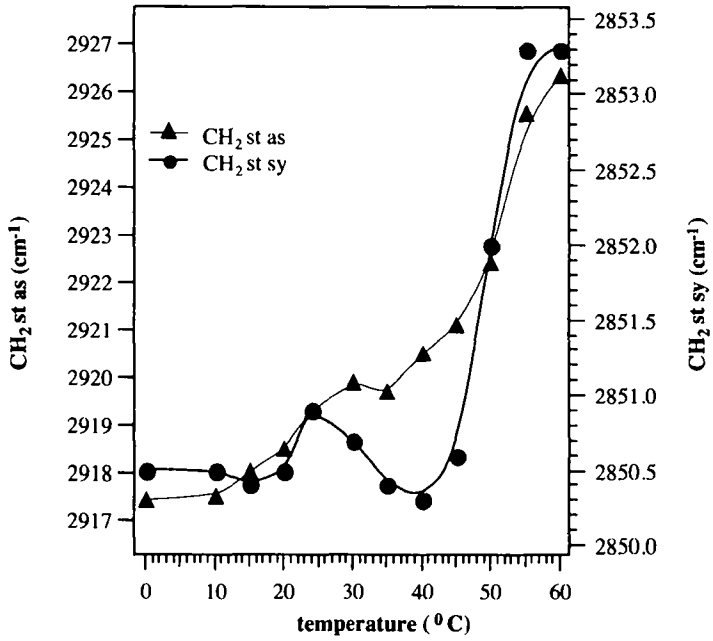

Fig. 3.19. Maxima of the symmetric and the asymmetric CH_2 stretching vibrations of a transferred LB-layer of BmPPC as a function of temperature.

Laibinis et al. had observed a similar phenomenon of "forced order" by self-assembly when comparing GI-FTIR spectra of long-chain alkanethiols ($HS(CH_2)_{16}(CH_2)_nH$, n = 0 -6) with related compounds where one methylene unit had been replaced by an oxygen atom [Lai95]. The conformational perturbation induced by the oxygen atom was much lower in self-assembled monolayers than in the corresponding bulk samples. They concluded that in self-assembled monolayers the lattice is fixed and the increased flexibility of a segment cannot induce a structural phase transition in the same way as in a bulk phase.

In summary, in supported thiolipid monolayers with disordered fatty acids, disorder of the hydrocarbon chains can not be further increased by heating nor can any disordering of the highly ordered, but immobilized fatty acids of BmPPC be induced in the self-assembled layer. Yet, a highly ordered, transferred LB-layer of BmPPC shows chain melting at the phase transition temperature found in the corresponding vesicles. The fatty acids in the disordered, self-assembled thiolipid monolayers may thus have an average local environment similar to that found in a fluid lipid layer possibly including a certain conformational mobility of the chains. In analogy to PEG, their potentially increased protein repellence may be attributed to the entropically unfavorable reduction of conformations accessible to the hydrocarbon chains upon approaching of a protein (see chapter 4).

3.4.4. Summary and outlook

Even though it is difficult to obtain absolute information from infrared spectroscopy, relative information about monomolecular films of the thiolipids synthesized in this work can be obtained by comparing spectra of the different lipids and "calibrating" thus spectral features. Under almost every aspect considered, BmPPC shows exceptional spectral features, which often resemble closely the ones of the corresponding DPPC sample. For all the spectroscopic markers of lipid phases (positions of absorption maxima of symmetric and asymmetric CH_2 stretching, C=O stretching, C-O stretching (ester), half-height widths of absorption bands), self-assembled BmPPC shows always the most crystalline-like features as compared to the other thiolipids.

A thiol group at the end of both fatty acids of a PC-lipid is therefore the feature of the chemical structure, which has the largest impact on spectral features and thus layer properties. All other variations of the chemical structures of the fatty acids such as differences of chain lengths and position of attachment to the glycerol backbone etc. (cf. fig. 3.6) influence the spectral features

and thus the nature of the layer to a much lesser extent. They are responsible for the "fine tuning" of the layer properties.

Results from contact angle measurements (chapter 3.2) and SPR (chapter 3.1) suggest, however, that the structure of such covalently adsorbed thiolipid monolayers in air or apolar solvents is different from the one in contact with water. The significance of these infrared investigations presented with respect to structural features of the layers in water should therefore not be overestimated. Investigation of the structure of self-assembled thiolipid monolayers under water by ATR-FTIR as described in [Lil97] would therefore be desirable.

4. Nonspecific Binding of Proteins to Self-Assembled Lipid Monolayers

4.1. Introduction

The design of a surface with low nonspecific binding of proteins was one of the main goals of this work. The chemical structure of its constituents is therefore mainly the result from these considerations.

There is a long list of protein properties which are thought to be responsible for the tendency of a protein to adsorb to a surface [And86, Pri91, Pri95]:

- size
- concentration
- diffusion coefficient
- structure and function
- conformational lability
- denaturability at a surface
- carbohydrate moieties
- charge (pI) etc.

Three representative proteins have been chosen for the investigation of nonspecific binding to the self-assembled layers: immunoglobulin G (IgG, from rabbit serum), fibrinogen (from bovine plasma), and bovine serum albumin (BSA). They are among the proteins with the highest physiological concentrations. They have been adsorbed at a concentration of 1.0 mg/ml, which is the highest concentration usually tested in literature. In order to differentiate further between the five synthesized thiolipids, self-assembled layers were also exposed to physiological protein concentrations as well as a mixture of proteins (rabbit serum). On Andrade's "protein complexity scale" fibrinogen, IgG, and albumin belong to the class of large complex proteins, the approximate structures of which are known [And92].

Table 4.1 summarizes some important properties of the chosen proteins. Fibrinogen is a water soluble protein of about 3000 amino acids, which is converted to the insoluble fibrin by thrombin and factor XIIIa in a multistep process involving partial proteolysis and aggregation [Sha88]. Fibrin forms the matrix of the blood clots. Fibrinogen is a heterohexamer $(\alpha\beta\gamma)_2$ with a two-fold rotational symmetry [Kyt95]. It contains long α-helical segments, which are twisted around each other forming a triple coiled coil. Fibrinogen was found to be an important promoter for the aggregation of activated blood platelets, which is an early event in the blood clotting cascade. The process is initiated by the binding of fibrinogen to its receptor on the

surface of activated platelets. Little fibrinogen binds to non-activated platelets. However, surface-adsorbed fibrinogen was found to induce platelet aggregation [Col80, And86]. It is thought to work as in the case of polymeric fibrinogen, which can induce the clustering of fibrinogen receptors on the platelet surface typical for activated platelets by multifold low-affinity binding [Sha88]. This is supported by the fact that fibrinogen oligomerizes at high concentrations and is therefore thought to be polymeric when adsorbed to a surface. Fibrinogen is therefore a crucial protein in context with the development of non-thrombogenic materials and has therefore been often chosen for the study of nonspecific adsorption of proteins to surfaces [Pri91, Gom91, Woj93, Mal96, Thi97].

	fibrinogen	immunoglobulin G (IgG)	serum albumin
mole. weight [g/mole]	341 000	150 000	66 500
conc. in blood [mg/ml]	2.0 - 4.5	≤ 24 [1)]	35 - 55
diffusion coefficient [$cm^2\ s^{-1}$]	$2.0 \cdot 10^{-7}$	$4.0 \cdot 10^{-7}$	$6.1 \cdot 10^{-7}$
isoelectric point (pI)	5.54	5.8 - 7.3	4.92
specific partial volume [cm^3/g]	0.723	0.729	0.733
weight % of carbohydrates with respect to entire protein	2.52	2.95	0.2

Tab. 4.1. Properties of immunoglobulin G, fibrinogen, and serum albumin in human blood plasma [Cib79]. [1)] all different species together.

Immunoglobulins are late antibodies in primary and secondary immunization. They are water soluble, Y-shaped molecules consisting of two light and two heavy chains with various domains. The domains consist of layers of antiparallel β-sheets, which are linked by disulfide bonds.

Albumin binds and transports water, ions, fatty acids, pigments, acetylcholine, vitamins, hormones, drugs, etc. [Cib79]. It consists of one peptide chain with 585 amino acids in the case of human serum albumin, which is divided in three domains of about 20 kDa, and is thus the simplest multi-domain protein. It is a highly hydrophobic protein, which is expected to adsorb irreversibly to hydrophobic surfaces meanwhile it adsorbs highly reversibly on highly hydrophilic surfaces such as clean quartz [Mor77]. In this case the major adsorptive interaction is probably ionic rather than hydrophobic.

4.2. Discussion of Results from SPR Investigations

Results from nonspecific adsorption of BSA, fibrinogen, and IgG to self-assembled thiolipid monolayers are summarized in table 4.2 and figure 4.1. Absolute amounts of adsorbed proteins may not be reliably comparable as refractive indices for the studied proteins can vary slightly depending on the ratio of protein to water in the adsorbed film. However, in the case of the three proteins chosen refractive indices should be very similar since their specific partial volumes vary but very little assuming similar properties of the proteins from different species (tab. 4.1). Refractive indices of proteins adsorbed at interfaces usually fall between 1.35 and 1.55 [Arn85, Cuy78, Pri93]. For the SPR experiments performed in this work (tab. 4.2), a refractive index of 1.45 is used to calculate the geometrical thickness of the adsorbed protein layer.

Generally, very little protein is adsorbed to the self-assembled thiolipid monolayers as compared to the amount adsorbed to self-assembled layers of hydroxythiols and values reported in literature (tab. 4.3)! Even at physiological protein concentration adsorption is very low.

protein ->	BSA				IgG		fibrinogen						rabbit serum	
concentration	1.0 mg/ml		100 mg/ml		1.0 mg/ml		1.0 mg/ml		25 mg/ml		50 mg/ml			
	ΔΘ	Å	ΔΘ	Å	ΔΘ	Å	ΔΘ	Å	ΔΘ	Å	ΔΘ	Å	ΔΘ	Å
BmPPC	0	0	-	-	0.03	1.9	0.1	6.4	-	-	-	-	0.34	21.8
PmPPC	0.05	3.2	-	-	0.03	1.9	0.05	3.2	0.16	10.2	-	-	0.11	7.0
LmPPC	0.1	6.4	-	-	0.09	5.8	0.01	0.6	0.19	12.2	-	-	0.18	11.5
PhymPPC	0.01	0.6	0.01[1)]	0.6	0.02	1.3	0.05	3.2	0.6	38.4	0.04[1)]	2.6	0.18	11.5
mPPhyPC	0	0	-	-	0.03	1.9	0	0	-	-	-	-	0	0
$HS(CH_2)_{11}OH$	-	-	-	-	-	-	-	-	0.86	55.0	-	-	0.36	23.0
$HS(CH_2)_{16}OH$	-	-	-	-	0.35	22.4	-	-	-	-	-	-	-	-

Tab. 4.2. Nonspecific adsorption of proteins to self-assembled thiolipid monolayers monitored by SPR. Layer thicknesses given in A are calculated from shifts of the SPR resonance angle ΔΘ assuming a refractive index of 1.45 for the adsorbed protein layers (6.4 A per 0.1^0 of angle shift for the measurement configuration used).

[1)] In this experiment the layer was first incubated with 1.0 mg/ml BSA followed by 100 mg/ml BSA and 50 mg/ml fibrinogen washing with buffer between the different protein adsorption steps.

For most thiolipids, there is much less BSA adsorbed than fibrinogen and IgG. This agrees well with the low and highly reversible adsorption of BSA to highly hydrophilic surfaces reported inliterature [Mor77, And86]. Tendencies seem to indicate that BmPPC adsorbs most protein

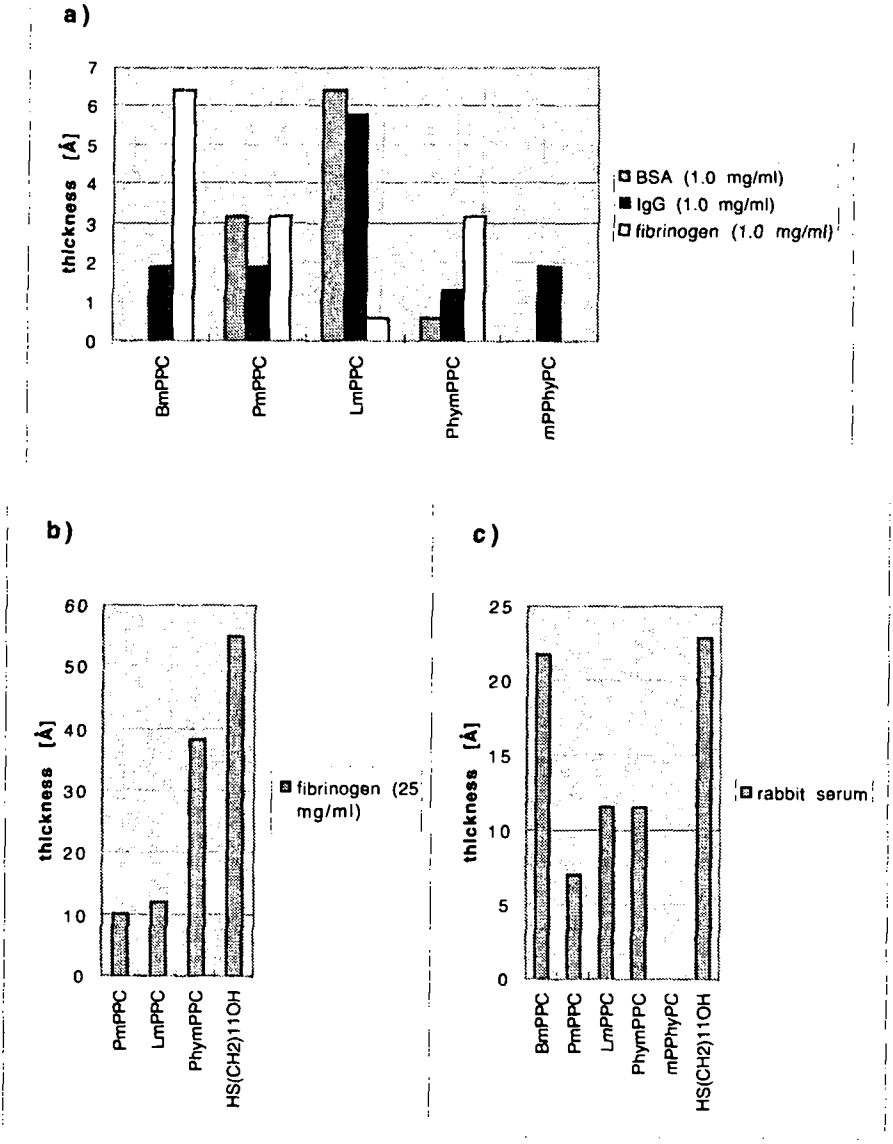

Fig. 4.1 a - c. Thicknesses of protein layers adsorbed to self-assembled thiolipid monolayers calculated from the angle shifts of SPR measurements (cf. legend table 4.2). Protein concentrations are indicated in the legends.

whereas the lipids conatining the branched phytanic acid seem to adsorb least with mPPhyPC forming the most protein repellent layer. Such findings would agree well with expectations from theoretical reflections described in chapter 2.2 and confirm the importance of the structural aspects considered. However, the observed tendencies should be confirmed for a statistically more relevant number of experiments, which was not possible to perform within the time allowed for this work. Self-assembly times should be extended to 12 to 24 hours to ensure completeness of the layer.

substrate	method of investigation	protein	concentration [mg/ml]	thickness of adsorbed amount [Å]	reference
$HS(CH_2)_{11}OH$/ SA	SPR	IgG	0.18	14.7	[Dus96b]
$HS(CH_2)_{11}OH$/ $HS(CH_2)_{11}(NANP)_6Y$/SA	"	"	"	3.2	"
$HS(CH_2)_{11}H$/ $HS(CH_2)_{11}(OCH_2CH_2)_nOR$ (with n = 0 - 17 and R = H or CH_3)	ellipsometry	fibrinogen	1.0	0 - 60	[Pri91], [Pri93]
PEG-containing polysiloxanes/ SA	SPR	fibrinogen	0.6[1)]	3.0	[Thi97]

Tab. 4.3. Nonspecific adsorption of proteins to various surfaces reported in literature. Thicknesses were calculated using a refractive index of 1.45. SA: layer formed by self-assembly.

1) Concentrations indicated in reference do not take into account the salt present (J. Thiele, personal communication).

4.3. Conclusions and Outlook

Self-assembled thiolipid monolayers show very low nonspecific adsorption of proteins compared to values reported in literature (tab. 4.3). It can thus be concluded that the strategies applied for the design of surfaces with low nonspecific protein binding have been successful. As in the case of poly(ethylene glycol) chains attached to a surface [Jeo91] **steric repulsion** may also be an important factor for the protein repellent character of supported lipid monolayers since

increasing disorder and possibly flexibility of the fatty acid chains correlates well with decreasing protein adsorption of the lipid layers.

Such surfaces can be considered well suited for functionalization in order to investigate specific protein interactions, but other applications such as their use for the coating of implant materials could be very promising. Currently, the impact of such surfaces on cell adhesion and metabolism are investigated. Further optimization of the chemical structure of the thiolipids may be worthwhile in order to use them in the future as matrices for biosensors.

No protein adsorption could be detected by impedance spectroscopy upon incubation of a self-assembled layer of BmPPC with 10 mg/ml BSA (no detectable change of capacitance).

Investigation of protein adsorption to such self-assembled thiolipid monolayers by FTIR would be very interesting as it is believed that not necessarily the type and amount of protein adsorbed to the surface is important for the biocompatibility of a surface, but rather the orientation and conformational state of those proteins [And86]. Changes of protein conformation upon adsorption to a surface have been reported in literature. Systematic investigations may also allow in the future to substitute some of the tests for the evaluation of the biocompatibility of a medical device using life animals. Application of a modified ATR-FTIR technique allowing to investigate under water adsorption processes of proteins to solid surfaces using well established gold/sulfur chemistry would also for such investigations be very useful [Lil97].

5. Specific Interaction of the Acetylcholine Receptor with Functionalized Thiolipid Monolayers

5.1. Introduction

For the specific binding of the nicotinic acetylcholine receptor to the functionalized supported thiolipid monolayers (fig. 1.6), the number of parameters, which can be varied and have thus to be optimized, is very large: Five thiolipids may were available as matrix molecules, which could be mixed with various concentrations of three ligand molecules differing in the length of the oligo(ethylene glycol) spacer. The choice of the buffer depends largely on the kind of receptor preparation used. Enriched membranes from the electric organ of *Torpedo Californica* and purified receptor solubilized in detergent or reconstituted in lipid vesicles were available. The protein concentration can be varied as well. This work is therefore only the first step towards the use of a membrane receptor in biosensors. The thiolipid which presumably has the lowest nonspecific protein binding (chapter 4) was chosen to start with. For all binding experiments described below, the same type of layer was formed by self-assembly on gold using a solution of mPPhyPC and PyP-PEG_{13}-ACh with a molar ratio of 2.9:1. On Andrade's "protein complexity scale" the nicotinic acetylcholine receptor belongs to the more complicated multicomponent systems containing competing proteins and other components [And92].

Membrane receptor proteins are a class of proteins which is extremely delicate and very susceptible to denaturing and loss of activity. Due to their amphiphilic nature with polar extramembranous parts and apolar domains within the lipid membrane, their structural integrity and activity throughout purification is only preserved in aggregates such as detergent micelles ("solubilized") or upon reconstitution into liposomes. Analytes entering in contact with the functionalized surface are thus additionally complicated by the presence of surface active tensides, ions etc..

5.2. Results from SPR Investigations

a) Behavior of the self-assembled layer was first tested in the different buffers used for the solubilization of the acetylcholine receptor. The purified receptor preparations from T. Schürholz were supplied in a CHAPS containing HEPES-buffer (10 mM HEPES (pH 7.4), 16 mM CHAPS, 5 mg/ ml soya lecithin (type IV-S, Sigma), 1 mM EDTA, and 3 mM NaN_3) [Sch92]. The thickness of the mixed self-assembly layers decreased continuously upon incubation and

washing with this buffer. It is not clear, however, whether CHAPS, the soya bean lipids or even HEPES is responsible for this behavior.

Substitution of CHAPS by n-octyl-β-D-glucopyranoside (octylglucoside, OG) was tested first. Use of octylglucoside for the solubilization of the nAChR is described in [Her90]. Self-assembled monolayers of alkylthiols and hydroxythiols are reported to be stable in 40 mM OG. The mixed self-assembled layers investigated in this work proved also to be stable in OG-buffer (10 mM potassium phosphate (pH 7.4), 50 mM OG).

The presence of negatively charged lipids was shown to be important for the nAChR to preserve its channel activity. Such lipids have therefore to be included in the receptor buffer. However, lipid vesicles can have an impact on self-assembled layers. Lang et al. reported multilayer formation upon incubation of hydrophobic self-assembly layers on gold with aqueous dispersions of DMPC vesicles whereas only a monolayer was formed upon incubation of the same hydrophobic substrates with POPC vesicles [Lan94]. Yet, this process of thickness increase being monitored by SPR, adsorption of entire vesicles could not be distinguished from real multilayer formation. It is well possible that DMPC and DPPC do not form multilayers. Lang et al. reported further that the adsorbed lipids could not be completely removed with detergent (OG) when adsorbed onto a layer of his thiolipid 1 (fig. 3.2). Upon incubation of such a substrate with DMPC and DPPC vesicles or OG-micelles in presence of 100 mM KCl multilayer formation was always observed meanwhile only a monolayer was formed using POPC. Using a buffer which contained only a mixture of soybean lipids (asolectin, Fluka) and cholesterol (10 mM phosphate (pH 7.4)/ 0.5 mg/ml lipids mixed with cholesterol (9:1)/ 0.02 % NaN_3) essential for the preservation of the activity of the receptor [Sch92], both without and in presence of 100 mM NaCl significant irreversible adsorption ($\Delta\Theta = 0.28 - 0.40^0$) was observed even in absence of protein. The adsorbed layer could only be removed by washing with organic solvents.

b) An enriched membrane preparation from the electric organ of *Torpedo Californica* from F. Hucho was solubilized in the same OG-buffer (10 mM potassium phosphate (pH 7.4)/ 50 mM OG) for which the supported layer has been found to be stable, by slowly shaking 100 µl of receptor preparation in water and 900 µl buffer for 20 hours at 4^0 C. After centrifugation for 1 hour at 45 000 g and 4^0 C 100 µl fractions of the supernatant were rapidly frozen in liquid nitrogen and thawed just before use. The protein concentration was at most 0.2 mg/ml, which is 5 times lower than the protein concentration used to determine the amount of nonspecifically adsorbed proteins. A binding assay using radioactive α-bungarotoxin was performed to determine the concentration of active receptor before the solubilization step. It was found to be about a tenth of the total protein concentration. The final concentration of active receptor was thus no more than 0.02 mg/ml in 9 mM potassium phosphate (pH 7.4)/ 45 mM OG.

Upon incubation of the mixed layer with the solubilized receptor the signal decreased slowly and continuously after an initial strong increase. Such adsorption behavior has often been reported in literature and the kinetic model of Sevastianov et al. fits well such data [Sev83, Sev84]. The model takes into account the effect of surface heterogeneity on the adsorption process by arguing that adsorption, but also desorption can be irreversible due to conformational changes of the protein.

In the receptor preparation used for the binding experiment above acetylcholine esterase had not been previously removed nor blocked. It may therefore be possible that the continuous decrease of the signal is due to hydrolytic activity of the acetylcholine esterase, which binds itself to the immobilized ligand and hydrolyses it. This is supported by the observation that upon addition of fresh receptor to the same surface no further adsorption was monitored.

After partial desorption, the layer was washed with buffer and incubated with 10^{-4} M acetylcholine followed by 10^{-3} M acetylcholine. A short period of steep signal decrease may thereby be attributed to competitive displacement of bound receptor. Intensity decreased then much less rapidly and finally almost stabilized. After rinsing with buffer an angle shift of 0.31^0 was measured.

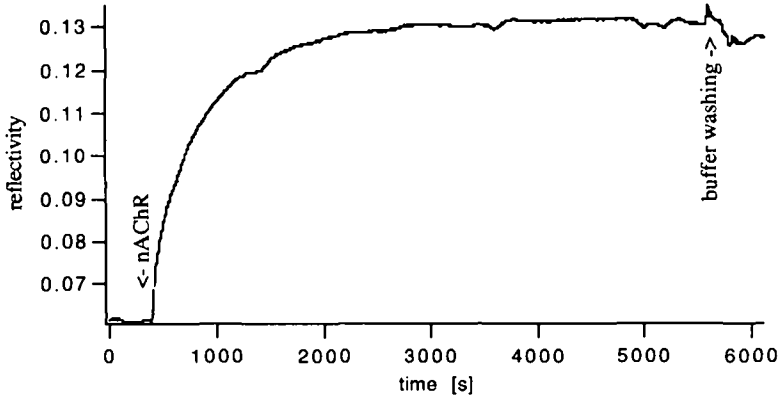

Fig. 5.1. Adsorption of nicotinic acetylcholine receptor (nAChR), enriched membrane preparation solubilized in 10 mM potassium phosphate/ 50 mM OG) to a self-assembled monolayer of mPPhyPC/ PyP-PEG$_{13}$-ACh. Protein concentration 0.02 mg/ml; concentration of active receptor: ≤ 2 μg/ml.

The experiment was repeated with a 10-fold lower protein concentration and yielded the saturating binding curve shown in figure 5.1. An angle shift of 0.47^0 was measured after washing with buffer.

Using a refractive index of 1.45 for a protein layer with an average water content, this angle shift corresponds to a thickness of 30.1 Å for the adsorbed layer, which is about 20 % of the maximum extension of the channel (140 Å). A monolayer of tightly packed receptor would yield a maximal angle shift of 2.2^0 for the same refractive index. However, the geometry of the receptor protein suggests that perfectly tight packing is not possible (fig. 5.2). This would imply the use of a lower refractive index due to the higher water content of the adsorbed layer and would thus result in an increased geometrical thickness.

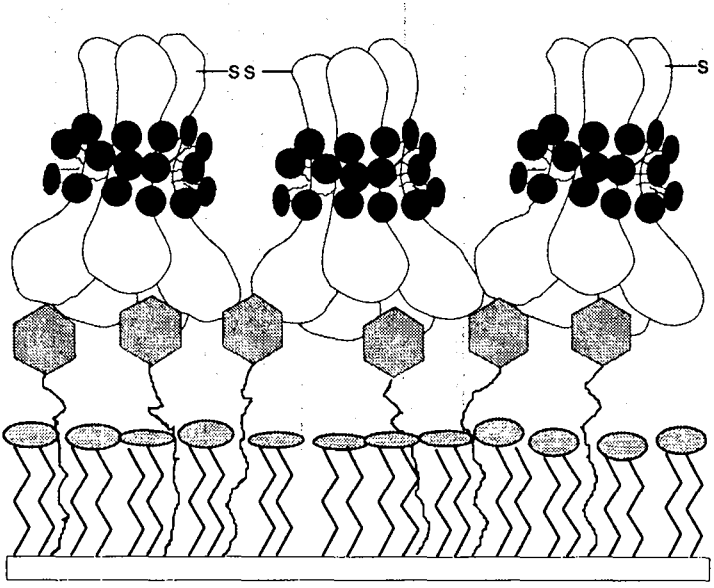

Fig. 5.2. Interaction of solubilized acetylcholine receptor with immobilized ligand.

Continuous monitoring of the reflectivity showed during the following hour a slight, continuous decrease of the signal. Washing of the adsorbed layer with buffer containing 50 mM NaCl removed part of the bound material with a remaining angle shift of 0.27^0 (57 % of the initial signal) whereas washing with buffer containing 100 mM NaCl removed almost all of the adsorbed material. Hardly any receptor could be displaced by incubation with up to 0.1 M acetylcholine both in presence and absence of salt nor by incubating with 0.4 mg/ml α-

bungarotoxin. The binding activity of the latter is, of course, questionable since it has to be dissolved in a buffer containing detergent, which may denature the protein.

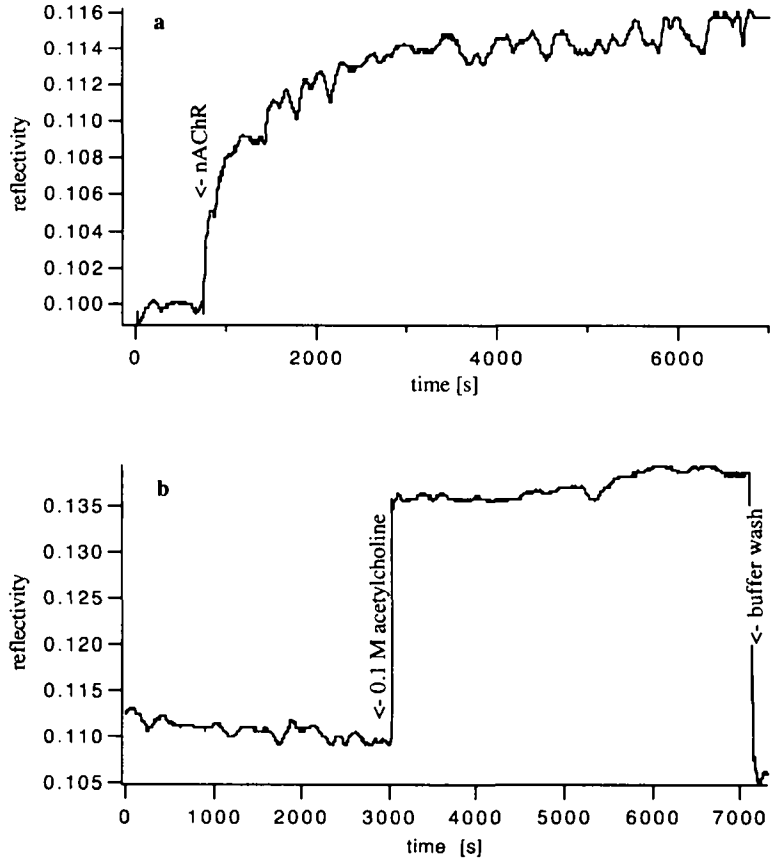

Fig. 5.3. a) Adsorption of nicotinic acetylcholine receptor (nAChR), enriched membrane preparation solubilized in 10 mM potassium phosphate/ 50 mM OG/ 25 mM NaCl) to a self-assembled monolayer of mPPhyPC/ PyP-PEG$_{13}$-ACh. Protein concentration 0.02 mg/ml; concentration of active receptor: ≤ 2 µg/ml. b) desorption of receptor by incubation with 100 mM acetylcholine/ 10 mM potassium phosphate/ 50 mM OG/ 25 mM NaCl after washing of layer with 10 mM potassium phosphate/ 50 mM OG/ 25 mM NaCl. The strong increase and decrease of the signal, respectively, is due to the change of refractive index between the buffers with and without acetylcholine.

When incubating the layer with the same preparation of the receptor in presence of 90 mM NaCl, no adsorption was observed. In presence of 25 mM salt, adsorption of about 20 % of the material adsorbed in absence of salt was observed (fig. 5.3a), and almost 50 % of that adsorbed material could be removed by incubation with 100 mM acetylcholine in presence of 25 mM NaCl after washing previously with 25 mM salt alone (fig. 5.3b). This may indicate specific binding. It is unlikely that displacement of these 50 % of adsorb material is simply due to a salt-effect of the 100 mM acetylcholine in analogy to the incubation with 100 mM NaCl described above, where almost all adsorbed material could be removed, since in that case no receptor could be removed by incubation with 100 mM acetylcholine (both in presence and absence of salt). The presence of salt during adsorption of the receptor seems therefore important for its reversible binding to the immobilized ligand. The remaining adsorbed material could be quantitatively removed with water. This suggests nonspecifically adsorbed material, which could for example be negatively charged lipids interacting with the positively charged acetylcholine immobilized on the surface. High salt content also prevents this kind of interactions.

The balance between inhibition of specific and/ or nonspecific receptor binding as a function of salt content is delicate. Too high salt concentrations are also known to inhibit receptor binding to affinity resins or desorb bound receptor, whereas too low concentrations lead to nonspecific binding. Optimizing the salt concentration in order to obtain high yields of highly pure receptor is thus a contradictory task. Schürholz et al. applied the solubilized receptor in absence of salt to the affinity column and washed with a maximal salt concentration of 80 mM [Sch92]. The receptor protein was eluted with 150 mM Flaxedil in presence of 60 mM salt. In [Her90] the solubilized receptor is applied to an acetylcholine agarose column in Ringer's solution, washed with maximal 50 mM NaCl and eluted with 50 mM carbamoylcholine in presence of 50 mM NaCl.

When layer and receptor were preincubated with 10 mM acetylcholine, almost no adsorption was detected ($\Delta\Theta = 0.03^0$). When a second sample of the same receptor preparation was preincubated with 10 mM acetylcholine for about five hours at ambient temperature, approximately 80 % of the amount of material adsorbed without preincubation with acetylcholine was adsorbed again. This indicates the presence of active acetylcholine esterase, but also that the latter could be the protein binding to the surface. It would therefore be better not to immobilize the ligand which is the substrate of two proteins present in the same sample if crude receptor preparations are to be used.

c) To exclude binding and hydrolytic activity of acetylcholine esterase purified nAChR of confirmed activity, solubilized in 10 mM HEPES (pH 7.4)/ 0.5 % CHAPS/ 2 mg/ml soya bean lipids mixed with cholesterol (9:1), was used for adsorption experiments. After a 10-fold dilution with 10 mM phosphate/ 50 mM OG the protein concentration was 0.12 mg/ml. Upon

addition to the functionalized surface the reflectivity increased fast, but decreased then continuously as had been observed for experiments using high protein concentrations (0.2 mg/ml) as well as for CHAPS (1 %) and lipid containing buffers. In this experiment the CHAPS concentration was 0.05 % after dilution. An initial angle shift of 0.21^0 was measured after 45 minutes of incubation when the layer was washed with buffer. The angle shift decreased to zero upon washing with buffer containing 50 mM NaCl.

These findings suggest nonspecific adsorption or too high salt concentration during washing steps. It is also possible that the receptor has been denatured upon dilution with a different buffer or during washing cycles. Activity of the receptor should therefore be checked after diluting the sample with a layer compatible buffer.

5.3. Conclusion

Specific binding of the nicotinic acetylcholine receptor to self-assembled layers of thiolipids and ligand molecules is not easy to show. Measurement of specific protein-ligand interactions for membrane proteins is obviously additionally complicated by the presence of detergents in the buffer, which can affect the layer. The receptor risks to be denatured already by simple dilution or during washing cycles with buffer.

Saturating binding curves and continuously decreasing intensity after an initially strong adsorption as described by kinetic models taking into account irreversible ad- and desorption have been observed. Adsorbed material was generally difficult to remove from the surface. The following list suggests a few possible reasons for this phenomenon.

a) The nicotinic acetylcholine receptor has two acetylcholine binding sites per channel. The nAChR from *Torpedo californica* is a dimer, having thus four binding sites per two channels, which are linked via a disulfide bridge (fig. 5.2). It is obvious that statistically it is a much rarer case that four immobilized ligands occupying the four binding sites of the receptor dimer are simultaneously displaced by free ligands than in the case of just one binding site per molecule. The probability of all four binding sites being occupied by a free ligand is in fact only 7 %! In the case of two binding sites per molecule as for instance in the case of antibodies this probability rises to 25 %. Dissociation from the surface is thus 3.5 times more likely. The molecule cannot diffuse away unless it is no more bound to the surface. It is therefore possible that one binding site reassociates with the surface meanwhile another site dissociates. High flexibility of the immobilized ligands due to the long poly(ethylene glycol) spacer favors

reassociation of the receptor. The planar surface may additionally favor binding via all four binding sites as compared to affinity resins, which are highly porous and have rough surfaces. The latter's structure as well as low ligand concentrations prevent proteins from binding too strongly to a chromatography matrix. In affinity chromatography it is a well known phenomenon that the protein to be purified cannot be eluted anymore. There are various reasons for this, the concentration of immobilized ligand is surely a crucial one. The ligand concentration on the surface might simply be too high in the case of the self-assembled layer used. The ratio of bulk concentrations does not necessarily correspond to the one in the self-assembled layer since less soluble molecules tend to adsorb preferentially to the surface. Many protein-surface interactions lead to irreversible adsorption of the protein to the surface due to a too high density of binding sites on the surface [And85b]. On highly polar surfaces reversible protein adsorption has been reported. Chromatography gels used for the purification of (non-denatured) proteins are polar. Variation of the nature of the aqueous eluent (ionic strength, pH, etc.) is often limited due to the risk of denaturing of the protein. At the interface between a solid and a liquid there is always a layer of undisturbed solution, within which mass is only transported by diffusion [And86]. The thickness of the boundary layer depends on temperature, stirring, and the interface itself. In unstirred solutions it has a thickness of up to 1000 μm whereas in vigorously stirred solutions it approaches 10 μm. Increased stirring in SPR experiments is thus of limited use since the depth of penetration of the evanescent field is only in the order of the wavelength of the exciting light, thus about 650 nm for the set-up used here. Partially irreversible binding of antibodies to planar surfaces functionalized with antigens was also reported by Duschl et al. [Dus96b]. Addition of excess free antigen could not displace a protein layer corresponding to an SPR angle shift of 0.1 to 0.2^0.

Monomeric acetylcholine receptors may be used, the preparation of which has been described [Sch92]. In general, measurement of specific reversible protein binding should be easier for receptors having only one binding site per molecule!

b) A second reason for the irreversible binding of the receptor to the surface could be that the free ligand does not have access to the binding sites for steric reasons. The large receptor bound to the surface may screen the binding sites such that the effective concentration of the ligand near the binding site is much lower than in the bulk (fig. 5.2). This problem may be less pronounced for porous chromatography resins. Lower protein concentrations may solve this problem. Analogies between planar surfaces and chromatography resins are therefore limited.

c) Too high protein concentrations in the bulk are reported to induce denaturing of the receptor [Her90, T. Schürholz, personal communication]. Adsorption of the receptor protein to the surface increases its local concentration and may induce aggregation, denaturing, and irreversible binding. Lower protein concentrations may solve this problem.

d) In the case of the enriched membrane preparations the acetylcholine esterase may bind irreversibly or additionally to the surface or continuously hydrolyzes approaching free ligands. Use of other ligands than acetylcholine, blocking of the esterase with inhibitors like eserine may solve this problem. Protein ligands such as toxins should be checked for stability and binding activity in detergent buffers.

e) Negatively charged lipids essential for the reconstitution of the nAChR, which are also present in the natural membranes, may interact with the positively charged acetylcholine immobilized on the surface at low salt concentrations. Desorption of the receptor from the surface may therefore be additionally hindered. Use of high salt concentrations could solve this problem.

For future experiments purified receptor protein, if possible a monomer, should be solubilized in a phosphate/octylglucoside buffer. Activity of the preparation should be checked with a classical binding assay. The protein concentration should be lower than 0.1 mg/ml. Adsorption experiments should be performed using a flow-through cell as washing of the surface by means of a syringe may risk denaturing of the protein due to foaming. Lower concentrations of immobilized ligand molecule should be used.

6. Conclusion and Outlook

Specific and nonspecific interactions between proteins and surfaces have been investigated in this work. Five different thiolipids with ω-standing thiols on their fatty acid have therefore been synthesized and supported lipid monolayers have been formed by self-assembly on planar gold substrates. All thiolipids have phosphatidylcholine head groups since the phosphatidylcholine moiety has been reported to show very low nonspecific binding of proteins. An interfacial free energy of zero between a surface and a solution containing proteins is the concept proposed by Andrade [And76] for the absence of nonspecific protein adsorption to a surface. Phosphatidylcholine layers show low nonspecific protein adsorption. Preservation of the conformation of the PC-head group region in thiolipids attached to a planar surface was therefore attempted by optimizing the structure of their fatty acids. Nonspecific adsorption of fibrinogen, IgG, and BSA at a concentration of 1.0 mg/ml and higher as well as protein adsorption upon incubation with blood serum showed exceptionally low protein binding and thus proved the concepts applied for the design of their structures to be successful. The results also showed that the protein repellent character of the phosphatidylcholine moiety could be modulated and enhanced by the appropriate choice of the fatty acids. The layers formed by self-assembly have been characterized by GI-FTIR, SPR, wetting, and impedance spectroscopy. It could be shown that very stable hydrophilic monolayers are formed. The results all indicated that the number of thiols attaching the lipid molecule to the surface is the structural feature, which has the greatest impact on the layer properties. All other variations are responsible for the "fine tuning" of the structural properties of the layer. The level of nonspecific binding was judged to be sufficiently low as to be able to measure a specific signal.

Acetylcholine was immobilized on the surface by synthesizing three ligand molecules consisting of a layer-forming and anchoring part, a oligo(ethylene glycol) spacer, and the acetylcholine ligand attached to it. The oligo(ethylene glycol) spacer of maximal thirteen ethylene oxide units thereby unites water solubility and flexibility with a protein repellent character attributed to the entropic force (see chapter 1.1.1). Mixed monolayers have been formed by self-assembly. Specific interactions between enriched membranes of the electric organ of *Torpedo Californica* and purified acetylcholine receptor solubilized in detergent have been investigated. The results suggest the ionic strength during adsorption and washing steps to be a critical parameter for reversible adsorption. Adsorption was often irreversible, which is attributed to the too high concentration of binding sites on the surface on one side and the low probability of the simultaneous displacement of four immobilized ligands on the receptor dimer by free ligands.

In future experiments the ligand concentration on the surface should definitely be lowered and receptor monomers should be used. Salt conditions should be optimized. Hand mixing and

exchange of solutions should eventually be substituted by a flow system in order to avoid denaturing of the receptor protein and increase reproducibility of the system. The layers may be optimized further with respect to nonspecific protein binding by synthesizing structurally more adapted fatty acids. As increasing times of interaction between proteins and surfaces lead to decreasing reversibility, kinetic rather than equilibrium measurements may be applied [Spi95]. However, this requires high reproducibility of the system and constant flow in flow-through systems.

Part III. Experimental Part

7. Materials and Methods

7.1. Chemicals

Reagents were purchased from the following companies and used without further purification if not indicated otherwise:

Sigma: 1,16-hexadecanolide, phospholipase A_2 from crotalus adamanteus venom (400 units/ mg protein), palmitoyl-L-α-lysophosphatidylcholine (~ 99 %), lauroyl-L-α-lysophosphatidylcholine (~ 99 %), soya lecithin (Type IV-S), α-bungarotoxin (from Bungarus multicinctus), cholesterol

Fluka: hydrobromic acid (48 %), thiourea (puriss p.a.), 2,2'-dipyridyldisulfide (> 99 %), boron trifluoride ethyletherate (purum), phytol (pract., mixture of isomers), *sn*-glycero-3-phosphorylcholine $(CdCl_2)_x$ (BioChemica), 4-(dimethylamino)pyridine (purum, twice recrystallized from toluene), dicyclohexylcarbodiimide (puriss.), 1,4- dithio-DL-threitol (BioChemica), tris(hydroxymethyl)aminomethane (BioChemica), $CaCl_2 \cdot 2\ H_2O$ (microselect), phospholipase A_2 from honey bee venom (BioChemika, 1020 u/mg), phospholipase A_2 from hog pankreas (BioChemika, 1091 u/mg), tetra(ethylene glycol) (puriss.), triphenylchlormethane (purum), triethylamine (purum, distilled), sodium hydride (55 - 65 % in oil), penta(ethylene glycol)-di-p-toluenesulfonate (pract.), triethylsilane (purum), trifluoroacetic acid (puriss.), diethyleneglycoldimethylether (puriss. abs.), hexa(ethylene glycol) (purum), bromoacetic acid ethylester (pract.), Silicagel 60 (35 - 70 μm and 63 - 200 μm), various solvents (for preparative HPLC), KH_2PO_4 (microselect), K_2HPO_4 (microselect), NaCl (microselect), KCl (microselect), asolectin, acetylcholine chloride, N-(3-dimethylaminopropyl)-N'-ethyl-carbodiimid (EDC; puriss.), 4-(2-hydroxyethyl)piperazine-1-ethanesulfonic acid (HEPES; BioChemika), 3-[(3-cholamidopropyl)dimethylammonio]-1-propane sulfonate (CHAPS; BioChemika), ethylenediaminetetraacetic acid (EDTA; BioChemika), methylbromide (purum), triethylsilane (purum)

E. Merck:	glacial acetic acid, TFA (Uvasol)
Avanti Polar Lipids Inc.:	1,2-*sn*-diphytanoyl-3-phosphatidylcholine
ROMIL:	solvents (SPS quality), non-volatile residue < 0.0001 %, used for optical measurements
water:	ultrafiltered type I water of a NANOpure ultrapure water system from Barnstead

7.2. Instruments and Analytical Procedures

If not indicated otherwise, analytical **thin layer chromatography** was carried out on aluminum plates precoated with silica 60 or silica 60 F_{254} (E. Merck). Products were visualized using UV-light (254 nm) or one of the reagents described in annex F.

Melting points were measured on a Büchi 530 apparatus using open capillaries and were not corrected.

NMR-spectra were measured on a Bruker AC-P200 spectrometer (^{1}H- NMR: 200 MHz, ^{13}C-NMR: 50 MHz; 4.7 Tesla). Chemical shifts are given in ppm relative to the internal standard TMS (^{1}H- and ^{13}C-NMR) and to the external standard 85 % phosphoric acid (^{31}P-NMR). Coupling constants J are given in Hertz. Multiplicity of the signals is abbreviated as follows: s (singlet), d (doublet), t (triplet), q (quadrublet), quin (quintet), h *(septet)*, n (nonet), m (multiplet), br (broad signal) and combinations thereof. ^{13}C-NMR are broadband decoupled.

Chemical ionization-mass spectra (CI) were measured on a Nermag R10-10C mass spectrometer (resolution: 1500) ionizing with NH_3, **FAB$^+$-mass spectra** on a *VG ZAB-2 SEQ* using 3-NOBA (m-nitrobenzyl alcohol) as a matrix. For **EI- mass spectra** an ionization energy of 70 eV was used. Values are given in m/z units. Only the major peaks are listed with their relative intensities in brackets.

Infrared spectra (FTIR) were measured on a Bruker IFS 28 spectrometer. For transmission measurements a DTGS detector was used, whereas for attenuated total reflection (ATR) and

grazing incidence (GI) measurements a MCT (mercury- cadmium- telluride) detector cooled with liquid nitrogen was used. Grazing incidence spectra were taken by reflection of the incident non-polarized radiation at an angle of incidence of 85^0. Spectra are the average of 1000 scans (300 scans for transmission spectra) recorded at a resolution of 1 cm^{-1} with a scanner velocity of 60 kHz. All other acquisition parameters are listed in annex C. Interferometer and sample chamber were purged with dried boil-off from liquid nitrogen. Spectra are reported as $-\log(I/I_0)$, where I is the reflected intensity of the sample and I_0 the reflected intensity of the reference. After water subtraction spectra were smoothed by reducing the resolution to 4 cm^{-1} (annex D). Positions of the absorption bands are given in cm^{-1}. Synthesized products were analyzed by ATR-FTIR using a germanium crystal as substrate. Positions of absorption bands are given in cm^{-1} and relative intensities are shown in brackets and are abbreviated as follows: vs. (very strong), s (strong), m (middle), w (weak), br (broad).

Evaporator: An Edwards Auto 306 Turbo evaporator was used for resistive evaporation of gold (Metalor, 999.9) and chromium (Balzers, 99,98 %) onto glass substrates, which had been cleaned previously according to the procedure described in annex B. Pressure during evaporation was less than $4 \cdot 10^{-6}$ mbar.

8. Synthesis

8.1. Synthesis of Thiolipids

16-Bromohexadecanoic acid, 16-mercaptohexadecanoic acid, and 16-(2-pyridyldithio)hexadecanoic acid were synthesized according to [Coy89].

16-(2-Pyridyldithio)hexadecanoic acid [Coy89]

2.22 g (10.1 mmol) of 2,2'-dipyridyldisulfide and 5.2 µl (0.04 mmol) of boron trifluoride ethyletherate in 40 ml ethylacetate were added to 2.91 g (10.1 mmol) of 16-mercaptohexadecanoic acid dissolved in 40 ml of ethyl acetate. After stirring for 20 hours at room temperature under nitrogen the reaction mix was filtered, the solvent evaporated, and the product purified by recrystallization from methanol (yield: 73 %).

Molecular weight:	397.64 ($C_{21}H_{35}O_2S_2N$)
^{1}H-NMR ($CDCl_3$):	1.3 (m, 22 H), 1.7 (m, 4 H), 2.4 (t, J = 6.7 Hz, 2 H), 2.8 (t, J = 6.7 Hz, 2 H), 7.1 (m, 1 H), 7.7 (m, 2 H), 8.5 (m, 1 H)
^{13}C-NMR ($CDCl_3$):	24.71, 28.47, 28.93, 29.06, 29.15, 29.23, 29.40, 29.43, 29.53, 29.58, 33.97, 39.05, 119.63, 120.49, 137.02, 149.48, 179.12
IR (ATR-FTIR):	2920 (s), 2850 (m), 1698 (s), 1578(m), 1540 (m), 1435(m), 1413 (s)
MS (CI):	398 (100), 306 (1.0), 221 (4.5), 114 (5.4), 113 (9.1), 112 (94.2), 111 (25.2), 78 (2.1)
m.p.:	69 ^{0}C
TLC- system (R_f):	$CHCl_3$/ MetOH 20:1 (0.34) toluene/ MetOH 96: 4 (0.29)

16-(2-Pyridyldithio)hexadecanoic acid N-hydroxy succinimide ester

5.04 g (12.7 mmol) of 16-(2-pyridyldithio)hexadecanoic acid were dissolved in 750 ml of dry dichloromethane. 2.31 g (20.1 mmol) of N-hydroxysuccinimide, 3.05 g (14.8 mmol) of DCC and 0.77 g (6.3 mmol) of DMAP were added and the solution stirred over night under nitrogen at room temperature. After filtration and evaporation of the solvent the residue was suspended in hot petroleum ether and filtered. The precipitate formed upon cooling was filtered off and again recrystallized from petroleum ether yielding 2.35 g (37 %) of 16-(2-Pyridyldithio)hexadecanoic acid N-hydroxy succinimide ester.

Molecular weight: 494.72 ($C_{25}H_{38}N_2O_4S_2$)

^{1}H-NMR ($CDCl_3$): 1.3 (m, 22 H), 1.7 (m, 4 H), 2.6 (t, J = 6.7 Hz, 2 H), 2.8 (t, J = 6.7 Hz, 2 H), 2.9 (s, 4 H), 7.1 (m,1 H), 7.7 (m, 2 H), 8.5 (m, 1 H)

^{13}C-NMR ($CDCl_3$): 24.6, 25.6, 29.6- 28.5, 31.0, 39.1, 119.6, 120.4, 136.9, 149.6, 160.0, 168.7, 169.15

IR (ATR-FTIR): 2920 (s), 2850 (m), 1824 (m), 1794 (m), 1738 (s), 1721 (vs.), 1647 (w), 1566 (m), 1456 (m), 1412 (m), 1376 (m), 1206 (s), 1068(s), 860 (m), 762 (m)

MS (CI): 498 (8.1), 497 (28.6), 496 (52.8), 495 (87), 461 (4.3), 382 (5.3), 381 (13.2), 380 (26), 225 (7.6), 221 (15.0), 220 (7.7), 144 (6.9), 143 (11.0), 124 (8.9), 123 (21), 122 (9.5), 121 (5.5), 114 (15.9), 113 (54), 112 (94), 111 (100), 110 (8.8), 97 (11), 95 (6.8), 87 (8.7), 83 (9.4), 78 (10), 70 (6.0)

m.p.: 58 ^{0}C

Elemental analysis:

	C	H	N	O	S
% calculated:	60.70	7.74	5.66	12.94	12.96
% found:	60.71	7.71	5.63	12.86	12.87

TLC- system (R_f): $CHCl_3$/MetOH 20:1 (0.34)

3,7,11,15-Tetramethylhexadecanoic Acid (Phytanic acid) [Red71]

12.9 g (44 mmol) of phytol were dissolve in 150 ml of methanol. 320 mg (1.4 mmol) of PtO_2 were added as a catalyst. Phytol was then reduced with hydrogen (34 mbar) using the set-up depicted in figure 8.1. After stirring over night at room temperature the theoretical amount of gas had been consumed and the starting material was no more visible on TLC. The catalyst was removed by filtration and the solvent evaporated. 34 ml of a solution of 26.7 g (0.27 mol) chromic trioxide and 23 ml (ca. 0.23 mol) of concentrated sulfuric acid diluted to 100 ml with water ("Jones reagent") were dropwise added to the residue dissolved in 130 ml of acetone and cooled to 0^0 C. The mixture was stirred for one hour at 0^0 C. After addition of 11 ml of isopropanol and 260 ml of ice water the solution was extracted with five times 100 ml of ether. The united ether fractions were washed with water, dried form anhydrous Na_2SO_4 and evaporated to dryness. The product was purified by two subsequent chromatographies (silicagel 60, 35 - 70 µm) eluting with petroleum ether-ether 9:1 and dichloromethane yielding phytanic acid as a mixture of isomers (eight diastereomeric pairs of enantiomers).

Molecular weight: 312.54 ($C_{20}H_{40}O_2$)

^{1}H-NMR ($CDCl_3$): 0.86 (d, J = 6.5 Hz, 6 H), 0.89 (d, J = 6.5 Hz, 6 H), 0.99 (d, J = 6.5 Hz, 3 H), 1.0 - 1.4 (br m, 20 H), 1.54 (n, J = 6.5 Hz, 1 H), 1.9 (m, 1 H), 2.15 (dd, J_1 = 16.0, J_2 = 7.4 Hz, 1 H), 2.38 (d, J_1 = 14.3 Hz, J_2 = 5.7 Hz, 1 H)

^{13}C-NMR ($CDCl_3$): 19.59, 19.65, 19.67, 19.71, 19.74, 22.61, 22.70, 24.32, 24.45, 24.80, 27.97, 30.16, 32.73, 32.77, 36.99, 37.03, 37.06, 37.30, 37.37, 37.39, 37.45, 39.37, 41.60, 41.67, 179.77

IR (ATR-FTIR): 3100 (s), 3033 (sh), 2965 (vs.), 2845 (vs.), 2710 (m), 2680 (m), 1705 (vs.), 1465 (s), 1405 (m), 1368 (m), 1285 (m), 1210 (w)

MS (CI): 312 (12.1), 250 (19.5), 157 (34.7), 150 (10.7), 149 (20.3), 140 (13.3), 139 (23.9), 129 (12.5), 113 (14.0), 112 (11.4), 111 (24.1), 99 (13.5), 98 (10.5), 97 (34.9), 87 (10.1), 85 (31.6), 83 (20.2), 71 (60.2), 70 (12.1), 69 (35.3), 57 (70.8), 56 (17.1), 55 (39.9)

TLC- system (R_f): CH_2Cl_2/MetOH/NH_4OH conc. 65 :10 :1 (0.58)

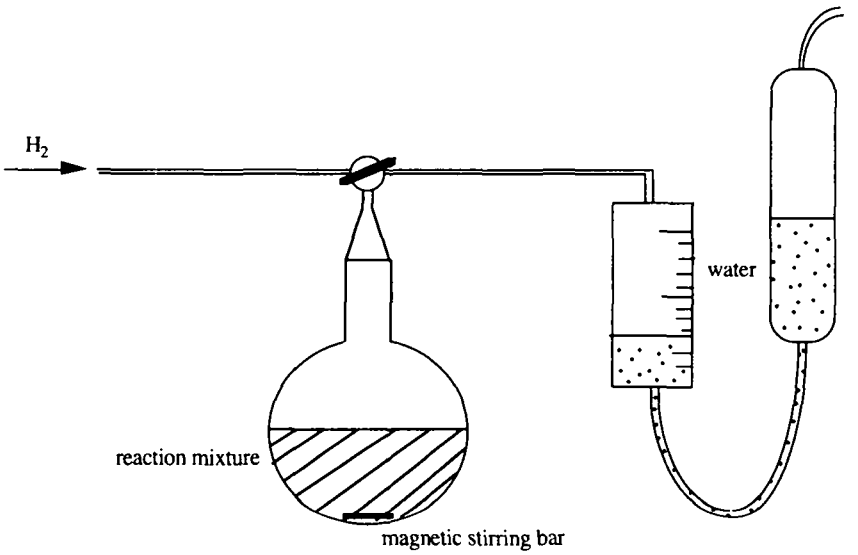

Fig. 8.1. Hydration apparatus used for the reduction of phytol.

1,2-Bis[16-(2-pyridyldithio)hexadecanoyl]-*sn*-glycero-3-phosphatidylcholine [Coy89]

1.00 g (2.5 mmol) of 16-(2-pyridyldithio)-hexadecanoic acid was dissolved in 10 ml of dry dichloromethane. 0.72 g (3.5 mmol) of dicyclohexylcarbodiimide, 0.37 g (3 mmol) of 4-(dimethylamino)pyridine, and 0.44 g (1 mmol) of *sn*-glycero-3-phosphorylcholine $(CdCl_2)_x$ were added to the suspension and stirred for 24 hours under argon in the dark. Another 0.206 g (10 mmol) of dicyclohexylcarbodiimide were added and stirring continued for additional 24 hours. The suspension was then filtered and the solvent completely evaporated. The residue was washed seven times with 5 ml of ether, then twice dissolved in 2 ml of dichloromethane and precipitated in the cold with 10 ml of ether, which were decanted. Purification by chromatography (silica gel 60) using CH_2Cl_2/MetOH 65:25 to 1:2 yielded 0.46 g (45 %) of 1,2-bis[16-(2-pyridyldithio)hexadecanoyl]-*sn*-glycero-3-phosphatidylcholine.

Molecular weight: 1016.49 ($C_{50}H_{86}O_8N_3S_4P$)

^{1}H-NMR ($CDCl_3$): δ = 1.1 - 1.3 (br m, 44 H), 1.6 (m, 8 H), 2.3 (m, 4 H), 2.8 (t, J=6.8 Hz, 4 H), 3.3 (s, 9 H), 3.75, 3.85, 4.05, 4.25 (several m, 8 H), 5.1 (m, 1 H), 7.1 (m, 2 H), 7.6 (m, 4 H), 8.4 (m, 2 H)

^{13}C-NMR ($CDCl_3$): 24.89, 24.97, 28.49, 28.93, 29.18, 29.34, 29.36, 29.48, 29.58, 29.68, 34.14, 34.33, 39.05, 54.44, 59.68, 62.97, 63.59, 66.52, 70.63, 119.53, 120.45, 136.90, 148.55, 160.73, 173.53

^{31}P-NMR ($CDCl_3$): - 0.41

IR (ATR-FTIR): 2915(vs), 2840 (s), 1735 (s),1645 (w), 1578 (m), 1464 (m), 1437 (m), 1405 (m), 1244 (s), 1150 (m), 1090 (s), 1045 (s), 940 (m)

MS (FAB^+): 1016.3 (49.7), 905.3 (16.9), 796.3 (16.7), 737.3 (5.0)532.2 (17.3), 483.2 (10.1), 380.1 (4.8), 184.0 (100), 166.0 (13.49, 154.0 (9.0), 137.0 (5.8), 136.0 (11.0), 124.9 (6.9), 123.0 (15.5), 111.9 (12.7), 110.9 (16.5), 104.0 (12.6)

TLC- system (R_f): CH_2Cl_2/MetOH/NH_4OH conc. 65:25:4 (0.34)

1,2-Bis(16-mercaptohexadecanoyl)-*sn*-glycero-3-phosphatidylcholine [Coy89]

A solution of 0.208 g (0.2 mmol) of 1,2-bis[16-(2-pyridyldithio)hexadecanoyl]-*sn*-glycero-3-phosphatidylcholine and 1.23 g (8.0 mmol) of 1,4- dithio-DL-threitol in 15 ml of absolute ethanol was stirred under argon for 23 hours at 20 °C. After complete evaporation of the solvent the residue was dissolved in 15 ml of chloroform, which was extracted with five times 4 ml of water. The chloroform phase was dried from anhydrous sodium sulfate, filtered and evaporated. Chromatographic purification (silicagel 60, 35 - 70 µm) using CH_2Cl_2/MetOH/acetic acid 65:25:4 until all DTT and derivatives were eluted followed by CH_2Cl_2/MetOH/H_2O 65:30:5 yielded 142 mg (89 %) of 1,2-bis(16-mercaptohexadecanoyl)-*sn*-glycero-3-phosphatidylcholine.

Molecular weight: 798.19 ($C_{40}H_{80}O_8NS_2P$)

^{1}H-NMR ($CDCl_3$): 1.1 -1.3 (br m, 44 H), 1.6 (m, 8 H), 2.3 (m, 4 H), 2.54 (q, J = 7.6 Hz, 4 H), 3.3 (s, 9 H), 3.75, 3.85, 4.05, 4.25 (several m, 8 H), 5.1 (m, 1 H), 7.0 (m, 2 H), 7.6 (m, 4 H), 8.4 (m, 2 H)

^{13}C-NMR ($CDCl_3$): 24.61, 24.87, 24.96, 28.36, 29.07, 29.14, 29.18, 29.32, 29.36, 29.51, 29.55, 29.59, 29.65, 29.67, 34.02, 34.11, 34.30, 54.28, 59.43, 62.98, 63.42, 66.27, 70.44, 173.11, 173.46

^{31}P-NMR ($CDCl_3$): - 0.45

IR (ATR-FTIR): 2917.6 (vs), 2849.6 (s), 1737.0 (m), 1468.7 (w), 1240.5 (m), 1170.9 (w), 1090.2 (m), 969.4 (w)

MS (FAB^+): 798.5 (60.2), 796.5 (7.3), 185.1 (11.2), 184.1 (100), 166.1 (22.6), 154.1 (10.0), 137.1 (7.0), 136.1 (9.9), 125.0 (13.4), 104.1 (17.4), 102.1 (7.3)

Elemental analysis:

	C	H	N	O	S
% calculated:	60.19	10.10	1.75	16.03	8.03
% found:	57.88	10.09	1.87	15.65	7.67

TLC- system (R_f): CH_2Cl_2/MetOH/NH_4OH conc. 65:25:4 (0.40)

Note: 1,2-Bis(16-mercaptohexadecanoyl)-sn-glycero-3-phosphatidylcholine polymerizes very easily upon exposure to air as indicated by the triplet at 2.65 ppm (^{1}H-NMR, $CDCl_3$) and spots on TLC with $R_f < 0.40$ (CH_2Cl_2/MetOH/NH_4OH conc. 65:25:4).

1-Palmitoyl-2-[16-(2-pyridyldithio)hexadecanoyl]-*sn*-glycero-3-phosphatidylcholine

50 mg (0.1 mmol) of palmitoyl-L-α-lysophosphatidylcholine were dissolved in 2 ml of dry chloroform. 50 mg (0.125 mmol) of 16-(2-pyridyldithio)hexadecanoic acid, 60 mg (0.28 mmol) of DCC and 18 mg (0.15 mmol) of DMAP were added and the suspension stirred under argon for 90 hours at room temperature in the dark. Additional 25 mg (0.06 mmol) of 16-(2-pyridyldithio)hexadecanoic acid and 20 mg (0.1 mmol) of DCC were added and stirring continued. After 117 hours almost no lysophosphatidylcholine was visible any more on TLC. The suspension was filtered and the solvent evaporated. The residue was redissolved in 1.5 ml

of chloroform, dropped onto 4 ml of absolute ether and filtered. The ether insoluble precipitate was washed with chloroform, which contains the product. The ether phase was evaporated and the precipitation procedure repeated. The united chloroform phases were dried, resuspended in chloroform and again filtered yielding 82 mg (94 %) of 1-palmitoyl-2-[16-(2-pyridyldithio)hexadecanoyl]-*sn*-glycero-3-phosphatidylcholine.

Molecular weight: 875.2 ($C_{45}H_{83}O_8N_2S_2P$)

^{1}H-NMR ($CDCl_3$): 0.9 (m, 3 H), 1.1 - 1.3 (br m, 46 H), 1.6 (m, 6 H), 2.2 (m, 4 H), 2.8 (t, (6.9 Hz, 2H), 3.3 (s, 9 H), 3.75, 3.85, 4.05, 4.25 (several m, 8 H), 5.1 (m, 1 H), 7.0 (m, 1 H), 7.6 (m, 2 H), 8.4 (m, 1 H)

^{13}C-NMR ($CDCl_3$): 14.10, 22.67, 24.89, 24.97, 25.64, 28.49, 28.93, 29.17, 29.32, 29.35, 29.47, 29.53, 29.58, 29.70, 31.91, 33.79, 34.14, 34.33, 39.05, 49.05, 54.45, 59.56, 63.20, 63.56, 66.71, 70.71, 119.53, 120.43, 136.89, 149.54, 160.73, 173.11, 173.46

MS (FAB^+): 875.5 (67.7), 766.5 (6.4), 765.5 (6.7),764.5 (12.4), 224.1 (9.7), 185.1 (8.5), 184.1 (100.0), 166.1 (18.2), 154.1 (8.1), 136.0 (8.3), 125.0 (8.4), 111.0 (5.4), 104.1 (12.8), 102.0 (5.5)

TLC- system (R_f): CH_2Cl_2/MetOH/NH_4OH conc. 65:25:4 (0.58)

1-Palmitoyl-2-[16-mercaptohexadecanoyl]-*sn*-glycero-3-phosphatidylcholine

82 mg (0.094 mmol) of 1-palmitoyl-2-[16-(2-pyridyldithio)hexadecanoyl]-*sn*-glycero-3-phosphatidylcholine and 310 mg (2 mmol) of 1,4-dithio-DL-threitol were dissolved in 4 ml of absolute ethanol and stirred for 23 hours under argon at room temperature in the dark. After evaporation of the solvent the residue was dissolved in 5 ml of chloroform and extracted with four times 2 ml of water, whereby the phases were separated by centrifugation. The united water phases were back extracted with chloroform and the united chloroform phases dried from $NaSO_4$, filtered, and evaporated to dryness. The residue (91 mg) was purified by chromatography (silicagel 60, 35 - 70 µm) using CH_2Cl_2/MetOH/acetic acid 65:25:4 until all DTT and derivatives were eluted followed by CH_2Cl_2/MetOH 65: 25 and CH_2Cl_2/MetOH/H_2O 65:30:5 yielding 54 mg (75 %) of 1-palmitoyl-2-[16-mercaptohexadecanoyl]-*sn*-glycero-3-phosphatidylcholine.

Molecular weight:	766.2 ($C_{40}H_{80}O_8NSP$)
^{1}H-NMR ($CDCl_3$):	0.9 (m, 3 H), 1.1 - 1.3 (br s m, 46 H), 1.6 (m, 6 H), 2.2 (m, 4 H), 2.5 (q, J = 6.8 Hz, 2 H), 3.3 (s, 9 H), 3.75, 3.85, 4.05, 4.25 (several m, 8 H), 5.1 (m, 1 H)
^{13}C-NMR ($CDCl_3$):	14.10, 22.65, 24.61, 24.87, 24.95, 28.36, 29.06, 29.14, 29.17, 29.31, 29.34, 29.52, 29.58, 29.68, 31.89, 34.03, 34.12, 34.31, 54.33, 59.51, 63.17, 63.52, 66.55, 70.63, 173.11, 173.48
IR (KBr):	2917.3 (vs), 2850.0 (s), 1738.9 (m), 1467.4 (w), 1244.8 (w), 1094.8 (w), 1073.6 (w), 973.5 (w)
MS (FAB^+):	766.4 (74.6), 765.4 (5.5), 764.4 (9.6), 732.4 (6.1), 550.2 (7.6), 478.2 (5.1), 185.0 (10.1), 184.0 (100.0), 166.0 (14.6), 124.9 (8.9), 104.0 (16.0)
TLC- system (R_f):	CH_2Cl_2/MetOH/NH_4OH conc. 65:25:4 (0.31)

1-Lauroyl-2-[16-(2-pyridyldithio)hexadecanoyl]-*sn*-glycero-3-phosphatidylcholine

48 mg (0.11 mmol) of lauroyl-L-α-lysophosphatidylcholine, 50 mg (0.13 mmol) of 16-(2-pyridyldithio)hexadecanoic acid, 50 mg (0.25 mmol) of DCC, and 18 mg (0.15 mmol) of DTT were suspended in 2 ml of absolute chloroform and stirred at room temperature under argon for 71 hours. Further 50 mg (0.13 mmol) of 16-(2-pyridyldithio)hexadecanoic acid and 20 mg (0.1 mmol) of DCC were added and the same again after additional 46 hours of stirring. After totally 125 hours of stirring the reaction was completed as determined by TLC. The solvent was evaporated, the residue redissolved in 1 ml of chloroform, dropped onto 4 ml of absolute ether, the precipitate filtered off and washed with ether. The ether insoluble residue in the filter was then washed with chloroform, which contains the product. The ether phase was evaporated, the residue resuspended in little ether, the insoluble precipitate filtered off and washed with ether. The ether insoluble residue in the filter was again washed with chloroform. Extraction of the ether phase was repeated several times until it contained no more product as judged by TLC. Chloroform phases were finally united and dried yielding 89 mg (99 %) of 1-lauroyl-2-[16-(2-pyridyldithio)hexadecanoyl]-*sn*-glycero-3-phosphatidylcholine.

Molecular weight:	819.1 ($C_{41}H_{75}O_8N_2S_2P$)
^{1}H-NMR ($CDCl_3$):	0.9 (m, 3 H), 1.1 - 1.3 (br m, 38 H), 1.6 (m, 6 H), 2.2 (m, 4 H), 2.8 (t, J = 6.96, 2H), 3.3 (s, 9 H), 3.75, 3.85, 4.05, 4.25 (several m, 8 H), 5.1 (m, 1 H), 7.0 (m, 1 H), 7.6 (m, 2 H), 8.4 (m, 1 H)
^{13}C-NMR ($CDCl_3$):	14.09, 22.65, 24.60, 24.87, 24.97, 25.64, 28.47, 28.92, 29.16, 29.30, 29.32, 29.35, 29.46, 29.50, 29.54, 29.56, 29.61, 29.63, 29.67, 31.89, 33.96, 34.12, 34.32,39.04, 49.01, 54.38, 59.52, 62.98, 63.76, 66.67, 70.62, 119.52, 120.42, 136.89, 149.53, 160.73, 173.14, 173.50
MS (FAB^+):	819.5 (83.0), 710.5 (6.6), 709.5 (7.5), 708.5 (14.8), 224.1 (7.4), 185.1 (8.4), 184.1 (100.0), 166.1 (16.7), 125.0 (9.2), 111.0 (5.6), 104.1 (12.4), 102.1 (5.0)
TLC- system (R_f):	CH_2Cl_2/MetOH/NH_4OH conc. 65:25:4 (0.34)

1-Lauroyl-2-[16-mercaptohexadecanoyl]-*sn*-glycero-3-phosphatidyl-choline

89 mg (0.11 mmol) of 1-lauroyl-2-[16-(2-pyridyldithio)hexadecanoyl]-*sn*-glycero-3-phosphatidyl-choline and 310 mg (2 mmol) of 1,4-dithio-DL-threitol were dissolved in 4 ml of absolute ethanol and stirred for 22 hours under argon at room temperature in the dark. After evaporation of the solvent the residue was dissolved in 5 ml of chloroform and extracted with four times 2 ml of water, separating the phases by centrifugation. The united water extracts were back extracted with chloroform. United chloroform phases were then dried from $NaSO_4$, filtered, and evaporated to dryness. Purification by chromatography (silicagel 60, 35 - 70 µm) using CH_2Cl_2/MetOH/acetic acid 65:25:4 till all DTT and derivatives were eluted followed by CH_2Cl_2/MetOH 65: 25 and CH_2Cl_2/MetOH/H_2O 65:30:5 yielded 59 mg (76 %) of 1-lauroyl-2-[16-mercaptohexadecanoyl]-*sn*-glycero-3-phosphatidylcholine.

Molecular weight:	710.0 ($C_{36}H_{72}O_8NSP$)
^{1}H-NMR ($CDCl_3$):	0.9 (m, 3 H), 1.1 - 1.3 (br m, 38 H), 1.6 (m, 6 H), 2.2 (m, 4 H), 2.8 (q, J = 6.7 Hz, 2H), 3.3 (s, 9 H), 3.75, 3.85, 4.05, 4.25 (several m, 8 H), 5.1 (m, 1 H)

^{13}C-NMR ($CDCl_3$):	14.08, 22.65, 24.60, 24.87, 24.97, 28.37, 29.07, 29.16, 29.30, 29.32, 29.35, 29.51, 29.54, 29.60, 29.64, 29.70, 31.89, 34.02, 34.12, 34.32, 54.36, 59.66, 62.98, 63.59, 66.55, 70.61, 173.14, 173.49
^{31}P-NMR ($CDCl_3$):	- 0.59
IR (KBr):	2918.6 (vs), 2850.4 (s), 1738.5 (s), 1467.4 (w), 1251.2 (m), 1180.3 (w), 1095.7 (m), 970.2 (w)
MS (FAB^+):	710.3 (100.0), 709.3 (5.7), 708.3 (7.8), 224.0 (6.0), 185.0 (8.6), 184.0 (86.2), 166.0 (13.5), 1004.0 (12.0)
TLC- system (R_f):	CH_2Cl_2/MetOH/NH_4OH conc. 65:25:4 (0.64)

1-Phytanoyl-*sn*-glycero-3-phosphatidylcholine

380 mg (0.45 mmol) of 1,2-*sn*-diphytanoyl-3-phosphatidylcholine were suspended in 80 ml buffer (100 mM Tris, 10 mM $CaCl_2$, pH 8.0) by ultrasonication (Branson sonifier) leading to a very opaque solution, which was heavily stirred at 37 ^{0}C. The suspension was periodically sonified followed by the addition of a fresh portion of about 1000 units (total 4093 units) of phospholipase A_2 from bee venom, crotalus adamanteus venom or hog pankreas. Hydrolysis was monitored by TLC. After 6 days stirring was stopped, the water evaporated, and the reaction mixture purified by flash chromatography (silicagel 60, 35 - 70 µm) eluting with CH_2Cl_2/MetOH/H_2O 65:25:4. United dried product fractions were extracted with chloroform in order to remove remaining Tris-salt. The chloroform phase was extracted with little 1 M HCl followed by 1 M NaOH, dried from sodium sulfate, filtered and evaporated yielding 116 mg (47 %) of 1- phytanoyl-*sn*-glycero-3-phosphatidylcholine.

Molecular weight: 551.75 ($C_{28}H_{58}O_7NP$)

^{1}H-NMR ($CDCl_3$):	0.86 (d, J = 6.5 Hz, 6 H), 0.89 (d, J = 6.5 Hz, 6 H), 0.99 (d, J = 6.5 Hz, 3 H), 1.0 - 1.4 (br m, 20 H), 1.54 (n, J = 6.5 Hz, 1 H), 1.9 (m, 1 H), 2.20 (dd, J_1 = 15.1 Hz, J_2 = 8.1 Hz, 1 H), 2.42 (dd, J_1 = 14.6 Hz, J_2 = 5.4 Hz, 1 H), 3.3 (s, 9 H), 3.75, 3.9, 4.1, 4.3 (several br m, 9 H)
IR (ATR-FTIR):	2950 (m), 2920 (m), 2875 (w), 2860 (w), 1720 (m), 1450 (m), 1374 (w), 1255 (s), 1120 (s), 1105 (s), 1075 (s), 978 (s)
MS (FAB^+):	552. 3 (29.6), 534.3 (25.0), 508.8 (5.1), 184.0 (5.3), 132.9 (9.9), 104.0 (100.0)
TLC- system (R_f):	CH_2Cl_2/ MetOH/ NH_4OH conc. 65:25:5 (0.17)

1-Phytanoyl-2-[16-(2-pyridyldithio)hexadecanoyl]-*sn*-glycero-3-phosphatidyl-choline

116 mg (0.21 mmol) of 1- phytanoyl-*sn*-glycero-3-phosphatidylcholine, 160 mg (0.4 mmol) of 16-(2-pyridyldithio)hexadecanoic acid, 124 mg (0.6 mmol) of DCC, and 50 mg (0.4 mmol) of DMAP were dissolved in 3 ml of chloroform and stirred for 17 hours at room temperature under argon. Little more DCC was added and stirring continued for additional 16 hours. The suspension was filtered, the filtrate evaporated to dryness. Purification of the residue by chromatography (silicagel 60, 0.063 - 0.2 mm) eluting first with acetone, then with CH_2Cl_2 containing increasing percentages of methanol and water yielded 131 mg (71 %) of 1-phytanoyl-2-[16-(2-pyridyldithio)hexadecanoyl]-*sn*-glycero-3-phosphatidyl-choline.

Molecular weight:	931.4 ($C_{49}H_{91}O_8N_2S_2P$)
^{1}H-NMR ($CDCl_3$):	0.86 (d, J = 6.5 Hz, 6 H), 0.89 (d, J = 6.5 Hz, 6 H), 0.99 (d, J = 6.5 Hz, 3 H), 1.0 - 1.4 (br m, 42 H), 1.4 - 1.6 (br m, 5 H), 1.9 (m, 1 H), 2.1 (m, 1 H), 2.28 (m, 3 H), 2.8 (t, J = 6.7 Hz, 2 H), 3.3 (s, 9 H), 3.7 - 4.4 (several m, 8 H), 5.2 (m, 1 H), 7.0 (m, 1 H), 7.6 (m, 2 H), 8.4 (m, 1 H)

^{13}C-NMR ($CDCl_3$): 19.54, 19.61, 19.66, 19.73, 22.61, 22.71, 24.77, 2.95, 27.93, 28.48, 28.92, 29.17, 29.38, 29.48, 29.58, 29.66, 29.70, 32.77, 32.80, 37.27, 37.38, 37.42, 37.45, 39.02, 39.35, 41.69, 54.31, 59.27, 62.89,63.74, 66.35, 70.87, 119.49, 120.41, 136.86, 149.52, 160.73, 172.98, 173.12

^{31}P-NMR ($CDCl_3$): - 0.68 ppm

MS (FAB^+): 931.5 (86.2), 929.5 (6.3), 820.5 (13.3), 224.0 (9.0), 185.0 (10.0), 184.0 (100.0), 166.0 (15.4), 124.9 (7.8), 110.9 (5.8), 104.0 (11.5)

TLC- system (R_f): CH_2Cl_2/MetOH/NH_4OH conc. 65:25:4 (0.63)

1-Phytanoyl-2-[16-mercaptohexadecanoyl]-*sn*-glycero-3-phosphatidylcholine

131 mg (0.14 mmol) of 1-phytanoyl-2-[16-(2-pyridyldithio)hexadecanoyl]-*sn*-glycero-3-phosphatidylcholine and 430 mg (2.8 mmol) of 1,4-dithio-DL-threitol dissolved in 5 ml of absolute ethanol were stirred for 50 hours at room temperature in the dark in a closed flask. After evaporation of the solvent the reaction mixture was purified by chromatography (silicagel 60, 35 - 70 µm) using CH_2Cl_2/MetOH/acetic acid 65:25:2 until all DTT and derivatives were eluted followed by CH_2Cl_2/MetOH/H_2O 65:30:3 yielding 96 mg (83 %) of 1-phytanoyl-2-[16-mercaptohexadecanoyl]-*sn*-glycero-3-phosphatidyl-choline.

Molecular weight: 822.4 ($C_{44}H_{88}O_8NSP$)

^{1}H-NMR ($CDCl_3$): 0.86 (d, J = 6.5 Hz, 6 H), 0.89 (d, J = 6.5 Hz, 6 H), 0.99 (d, J = 6.5 Hz, 3 H), 1.0 - 1.4 (br m, 42 H), 1.4 - 1.6 (br m, 5 H), 1.9 (m, 1 H), 2.1 (m, 1 H), 2.3 (m, 2 H), 2.5 (q, J = 6.7 Hz, 2 H), 3.3 (s, 9 H), 3.7 - 4.4 (several m, 8 H), 5.2 (m, 1 H)

^{13}C-NMR ($CDCl_3$): 19.54, 19.61, 19.66, 19.73, 22.60, 22.69, 24.60, 24.77, 29.06, 29.15, 29.35, 29.51, 29.54, 29.58, 29.67, 32.77, 34.02, 37.27, 37.38, 37.42, 37.45, 39.35, 41.69, 54.34, 59.56, 62.88, 63.52, 66.42, 70.46, 172.98, 173.11

^{31}P-NMR ($CDCl_3$): - 0.65

IR (KBr): 2953.6 (s), 2924.4 (vs), 2853.2 (s), 1736.7 (s), 1466.6 (m), 1384.0 (w), 1250.7 (m), 1170.0 (w), 1092.3 (m), 1069.7 (m), 969.8 (w)

MS (FAB^+): 822.5 (78.3), 820.4 (8.4), 224.0, (8.6), 185.0 (11.5), 184.0 (100.0), 166.0 (15.3), 124.9 (8.5), 104.0 (15.4)

TLC- system (R_f): CH_2Cl_2/MetOH/NH_4OH conc. 65:25:2 (0.22)

1-[16-(2-pyridyldithio)hexadecanoyl]-*sn*-glycero-3-phosphatidylcholine

576 mg (0.57 mmol) of 1,2-bis[16-(2-pyridyldithio)hexadecanoyl]-*sn*-glycero-3-phosphatidylcholine were suspended in 100 ml of buffer (100 mM Tris, 10 mM $CaCl_2$, pH 8.0) by ultrasound, repeatedly frozen in liquid nitrogen and again thawed in the ultrasound bath. 1000 units of phospholipase A_2 (from hog pankreas) were added and the suspension stirred at 45 ^{0}C for 57 hours until no more starting material could be seen on TLC. Water was evaporated after addition of some ethanol, the residue suspended in 100 ml of ethanol/ $CHCl_3$ 9:1, stirred for 30 minutes at 70 ^{0}C, filtered and the solvent evaporated. The residue (1.56 g) was washed with five times 10 ml of chloroform and filtered. United chloroform phases were evaporated. The residue (380 mg) was dissolved in 5 ml of chloroform, 2 ml of water were added, the pH of which was adjusted to about 7 with 1 M HCl. The aqueous phase was back extracted with chloroform and the united chloroform phases extracted with a saturated solution of $NaHCO_3$, which was again back extracted with chloroform. The united organic phases were dried from Na_2SO_4, filtered and evaporated. Purification by chromatography (silicagel 60, 35 - 70 µm) using CH_2Cl_2/MetOH 65:25 followed by CH_2Cl_2/MetOH/H_2O yielded 120 mg (31 %) of 1-[16-(2-pyridyldithio)hexadecanoyl]-*sn*-glycero-3-phosphatidylcholine.

Molecular weight: 636.9 ($C_{29}H_{53}O_7N_2S_2P$)

^{1}H-NMR ($CDCl_3$): 1.1 - 1.3 (br s and m, 22H), 1.6 (m, 4 H), 2.3 (m, 2 H), 2.8 (t, J = 7.1 Hz, 2 H), 3.3 (s, 9 H), 3.8, 3.9, 4.1, 4.3 (several br m, 9 H) 7.0 (m, 1 H), 7.6 (m, 2 H), 8.4 (m, 1H)

^{13}C-NMR ($CDCl_3$): 24.94, 28.49, 28.93, 29.17, 29.26, 29.40, 29.48, 29.58, 29.66, 29.69, 34.17, 39.05, 54.27, 65.25, 66.10, 119.52, 120.45, 136.92, 149.54, 160.71, 173.81

^{31}P-NMR ($CDCl_3$): 0.26

MS (FAB^+): 637.3 (100.0), 528.3 (5.8), 527.3 (5.7), 526.3 (15.5), 412.2 (10.8), 308.1 (6.7), 307.1 (25.2), 289.1 (12.2), 226.1 (7.8), 184.1 (43.9), 176.0 (7.1), 167.1 (6.6), 166.1 (15.2), 165.1 (5.2)

TLC- system (R_f): CH_2Cl_2/MetOH/NH_4OH conc. 65:25:4 (0.25)

1-[16-(2-Pyridyldithio)hexadecanoyl]-2-phytanoyl-*sn*-glycero-3-phosphatidylcholine

120 mg (0.17 mmol) of 1-[16-(2-pyridyldithio)hexadecanoyl]-*sn*-glycero-3-phosphatidylcholine, 94 mg (0.3 mmol) of phytanic acid, 130 mg (0.6 mmol) of DCC and 50 mg (0.4 mmol) of DMAP were dissolved in 3 ml of absolute chloroform and stirred for 22 hours at room temperature in the dark in a closed flask. More phytanic acid (2 x 36 mg) was added and stirring continued for several hours until no more lysophosphatidylcholine was visible. The suspension was filtered, the solvent evaporated and the dried residue (464 mg) extracted three times with pentane. The extracted residue was again suspended in chloroform, filtered and the solvent evaporated. The 185 mg crude product were purified by chromatography (silicagel 60, 63 - 200 µm) eluting with acetone, then with CH_2Cl_2 containing increasing amounts of methanol and water (until CH_2Cl_2/MetOH/H_2O 50:46:4). 151 mg (95 %) of pure 1-[16-(2-pyridyldithio)hexadecanoyl]-2-phytanoyl-*sn*-glycero-3-phosphatidylcholine were isolated.

Molecular weight: 931.4 ($C_{49}H_{91}O_8N_2S_2P$)

^{1}H-NMR ($CDCl_3$):	0.86 (d, J = 6.5 Hz, 6 H), 0.89 (d, J = 6.5 Hz, 6 H), 0.99 (d, J = 6.5 Hz, 3 H), 1.0 - 1.4 (br m, 42 H), 1.4 - 1.6 (br m, 5 H), 1.9 (m, 1 H), 2.1 (m, 1 H), 2.28 (m, 3 H), 2.8 (t, J = 7.1 Hz, 2 H), 3.3 (s, 9 H), 3.7 - 4.4 (several m, 8 H), 5.2 (m, 1 H), 7.0 (m, 1 H), 7.6 (m, 2 H), 8.4 (m, 1 H)
^{13}C-NMR ($CDCl_3$):	19.62, 19.66, 22.61, 22.71, 24.50, 24.78, 24.86, 27.95, 28.48, 28.92, 29.17, 29.32, 29.47, 29.53, 29.57, 29.67, 32.78, 34.12, 37.28, 37.39, 37.42, 37.46, 39.04, 39.35, 41.85, 54.36, 59.36, 63.36, 63.42, 66.17, 70.67, 119.50, 120.42, 136.88, 149.53, 160.73, 172.60, 173.49
^{31}P-NMR ($CDCl_3$):	- 0.53
MS (FAB^+):	931.4 (100.0), 822.4 (7.1), 821.3 (7.7), 820.3 (13.1), 184.0 (56.4), 166.0 (6.9),
TLC- system (R_f):	CH_2Cl_2/MetOH/NH_4OH conc. 65:25:2 (0.26)

1-[16-Mercaptohexadecanoyl]-2-phytanoyl-*sn*-glycero-3-phosphatidylcholine (mPPhyPC)

151 mg (0.16 mmol) 1-[16-(2-pyridyldithio)hexadecanoyl]-2-phytanoyl-*sn*-glycero-3-phosphatidyl-choline and 495 mg (3.2 mmol) 1,4-dithio-DL-threitol were dissolved in 5 ml of ethanol and stirred for 46 hours in the dark under argon until no more starting material was visible on TLC. The solvent was evaporated and the residue purified by chromatography (silicagel 60, 35 - 70 µm) using CH_2Cl_2/MetOH/acetic acid 65:25:2 until all DTT and derivatives were eluted followed by CH_2Cl_2/MetOH/H_2O 65:25:3 yielding 124 mg (94 %) of 1-[16-Mercaptohexadecanoyl]-2-phytanoyl-*sn*-glycero-3-phosphatidylcholine.

Molecular weight:	822.4 ($C_{44}H_{88}O_8NSP$)
^{1}H-NMR ($CDCl_3$):	0.86 (d, J = 6.5 Hz, 6 H), 0.89 (d, J = 6.5 Hz, 6 H), 0.99 (d, J = 6.5 Hz, 3 H), 1.0 - 1.4 (br m, 42 H), 1.4 - 1.6 (br m, 5 H), 1.9 (m, 1 H), 2.1 (m, 1 H), 2.28 (m, 3 H), 2.5 (q, J = 6.9, 2 H), 3.3 (s, 9 H), 3.7 - 4.4 (several m, 8 H), 5.2 (m, 1 H)

^{13}C-NMR ($CDCl_3$): 19.61, 22.60, 24.47, 24.61, 24.77, 24.86, 27.95, 28.36, 29.05, 29.17, 29.30, 29.51, 29.58, 29.63, 29.66, 32.78, 34.02, 34.11, 37.29, 37.39, 37.42, 37.46, 39.36, 41.90, 54.38, 59.42, 63.09, 63.53, 66.47, 70.65, 172.58, 173.47

^{31}P-NMR ($CDCl_3$): - 0.46

IR (KBr): 29.50.7 (m, sh), 2924.2 (vs), 2852.8 (s), 1737.6 (s), 1465.9 (m), 1380.1 (w), 1250.8 (m), 1093.1 (s), 968.7 (m)

MS (FAB^+): 822.6 (51.1), 224.1 (9.4), 18.1 (8.5), 184.0 (100.0), 166.0 (15.4), 125.0 (9.1), 104.0 (12.2)

TLC- system (R_f): CH_2Cl_2/MetOH/H_2O 65:25:4 (0.84)

8.2. Ligand molecules

Tetra(ethylene glycol)mono(triphenylmethyl)ether [Jay90]

A solution of 33.5 g (120 mmol) of triphenylchlormethane in 100 ml of dry dichloromethane was dropwise added over one hour to 92 g (475 mmol) of tetra(ethylene glycol) (dried by repeatedly distilling off toluene) and 14.2 g (140 mmol) of triethylamine (distilled from KOH) in 100 ml of absolute dichloromethane. The reaction mixture was stirred for 20 hours at ambient temperature under nitrogen in the dark. Unreacted tetra(ethylene glycol) was removed by extracting the yellow suspension with three times 200 ml of cold water. The organic phase was dried from K_2CO_3, filtered and evaporated. Chromatographic purification (silicagel 60) of the crude product eluting with CH_2Cl_2, CH_2Cl_2/ether 2:1, 1:1, 1:3 and finally with ether yielded 36.7 g (70 %) of tetra(ethylene glycol)mono(triphenylmethyl)ether.

Molecular weight: 436.6 ($C_{27}H_{32}O_5$)

^{1}H-NMR ($CDCl_3$): 2.7 (br s, 1 H), 3.2 (t, J = 5.1 Hz, 2 H), 3.58 (m, 2 H), 3.65 (m, 12 H), 7.25 (m, 9 H), 7.45 (m, 6 H)

IR (ATR-FTIR): 3082.6 (w), 3057.9 (w), 3022.7 (w), 2931.8 (m), 2874.0 (m), 1613.4 (w), 1497.9 (m), 1440.1 (s), 1343.0 (m), 1289.3 (w), 1229.3 (m), 1080.6 (vs), 925.6 (m)

MS (CI, NH_3): 454 (35.9), 259 (9.8), 256 (15.0), 245 (20.2), 244 (73.4), 243 (100.0), 242 (9.3), 241 (9.1), 240 (5.2), 195 (11.3), 166 (8.2), 165 (33.1), 163 (12.6), 149 (5.4), 133 (6.3), 105 (13.5)

TLC- system (R_f): ether (0.22)

Trideca(ethylene glycol)di(triphenylmethyl)ether [Jay90]

0.40 g (10 mmol) of sodium hydride (55 - 65 % in oil, washed with pentane) were suspended in 5 ml of dry tetrahydrofurane. A solution of 4.37 g (10 mmol) of tetra(ethylene glycol)mono(triphenylmethyl)ether in 5 ml of absolute THF was dropwise added under argon at ambient temperature. Additional 0.20 g (5 mmol) of sodium hydride were added and the solution stirred for 1 hour at room temperature followed by refluxing for 30 minutes. After cooling to 20^0 C a solution of 2.19 g (4 mmol) of penta(ethylene glycol)-di-p-toluenesulfonate in 5 ml of absolute tetrahydrofurane was dropwise added. The solution was stirred for 24 hours at ambient temperature and then refluxed for 2 hours. After cooling to 20^0 C 0.5 ml of methanol were added and the solvent was evaporated. The residue was suspended in 30 ml of dichloromethane and extracted with twice 30 ml of water. The united organic phases were dried from Na_2SO_4, filtered and the solvent evaporated. Purification by chromatography (silicagel 60) eluting first with ether, then with ether/methanol 3:1 yielded 3.32 g (77 %) of trideca(ethylene glycol)di(triphenylmethyl)ether.

Molecular weight: 1075.4 ($C_{64}H_{82}O_{14}$)

^{1}H-NMR ($CDCl_3$): 3.2 (t, J = 5.1 Hz, 4 H), 3.6 (m, 48 H), 7.2 (m, 18 H), 7.4 (m, 12 H)

^{13}C-NMR ($CDCl_3$): 63.35, 70.59, 70.69, 70.73, 70.80, 86.83, 126.92, 127.76, 128.74, 144.15

MS (NH_3): 1092 (0.2), 245 (11.2), 244 (54.1), 243 (100.0), 166 (5.1), 105 (5.6), 89 (5.3), 87 (5.2)

TLC- system (R_f): toluene/ MetOH 85:15 (0.35)

Trideca(ethylene glycol)

0.74 g (6.3 mmol) of triethylsilane and 5 ml of trifluoroacetic acid were added to 3.3 g (3.1 mmol) of trideca(ethylene glycol)di(triphenylmethyl)ether in 10 ml of dichloromethane and stirred for 30 minutes at room temperature. The solvent was then evaporated, the residue dissolved in 10 ml of toluene and the latter evaporated again. This was repeated three times. The dried brown solid was then extracted repeatedly with pentane and then dissolved in little water. Activated charcoal was added, the suspension stirred, filtered and the water evaporated. The residue was again dissolved in water, $NaHCO_3$ was added, the water again evaporated, the residue suspended in chloroform, and filtered and evaporated. 1.84 g (100 %) of trideca(ethylene glycol) were isolated after evaporation of the solvent.

Molecular weight: 590.7 ($C_{26}H_{54}O_{14}$)

^{1}H-NMR ($CDCl_3$): 3.62 (m, 4 H), 3.7 (m, 48 H)

^{13}C-NMR ($CDCl_3$): 62.08, 71.20, 71.34, 71.37, 73.50

IR (ATR-FTIR) 2929.4 (sh, m), 2877.9 (m), 1645.6 (w), 1454.4 (w), 1354.4 (m), 1292.7 (w), 1250 (m), 1098.5 (vs), 1069.1 (vs), 950.0 (m), 895. (m)

MS (NH_3): 591 (0.4), 177 (8.4), 141 (12.4), 134 (8.8), 133 (59.6), 131 (16.6),117 (14.6), 115 (5.2), 103 (15.1), 101 (15.1), 100 (7.6), 90 (19.2), 89 (100.0), 88 (24.7), 87 (76.1), 86 (9.1),73 (47.0), 72 (27.5), 71 (9.5), 70 (6.4)

TLC- system (R_f): CH_2Cl_2/ MetOH 65: 10 (0.66)

Trideca(ethylene glycol)mono(triphenylmethyl)ether

9.0 g (15 mmol) of trideca(ethylene glycol) and 0.51 g (5 mmol) of triethylamine distilled from KOH were dissolved in 10 ml of dichloromethane. 1.12 g (4 mmol) of tritylchloride in 10 ml of

dichloromethane were dropwise added during one hour at room temperature, whereby the solution turned turbid. Stirring at ambient temperature was continued for additional seven hours, the suspension cooled to 4^0 C and filtered. The organic phase was extracted with two times 50 ml and three times 20 ml of water, dried from anhydrous Na_2SO_4, filtered and evaporated yielding 2.72 g (82 %) of trideca(ethylene glycol)mono(triphenylmethyl)ether.

Molecular weight: 833.0 ($C_{45}H_{68}O_{14}$)

^{1}H-NMR ($CDCl_3$): 2.7 (br s, 1 H), 3.2 (t, J = 5.1 Hz, 2 H), 3.65 (m, 50 H), 7.25 (m, 9 H), 7.45 (m, 6 H)

^{13}C-NMR ($CDCl_3$): 61.71, 63.35, 70.37, 70.58, 70.62, 79.68, 70.71, 70.79, 72.54, 86.43, 126.91, 127.75, 128.72, 144.11

IR (ATR-FTIR) 3082.6 (w), 3057.9 (w), 3022.7 (w), 2931.8 (m), 2874.0 (m), 1613.4 (w), 1497.9 (m), 1440.1 (s), 1343.0 (m), 1289.3 (w), 1229.3 (m), 1080.6 (vs), 925.6 (m)

TLC- system (R_f): toluene/MetOH 85:15 (0.23)

Monotrityltetra(ethylene glycol)acetic acid ethylester

0.6 g (ca. 15 mmol) of NaH (55 - 65 % in oil) were carefully added to 10 ml of dry THF. 4.4 g (10 mmol) of tetra(ethylene glycol)mono(triphenylmethyl)ether in 8 ml of absolute THF were portionwise added to the gray suspension. The mixture was stirred for two hours at room temperature and then dropwise added during 24 hours to a solution of bromoacetic acid ethylester in 5 ml of absolute THF. After filtration solvent and excess bromoacetic acid ethylester were evaporated. The residue was dissolved in 25 ml of chloroform and extracted with 10 ml of water. The organic phase was dried from anhydrous sodium sulfate and evaporated. Chromatographic purification (silicagel 60) using toluene/ether 3:1 yielded monotrityltetra(ethylene glycol)acetic acid ethylester (13 %) as a slightly yellow oil.

Molecular weight: 522.6 ($C_{31}H_{38}O_7$)

^{1}H-NMR (CD_3OD): 1.3 (t, J = 7.5 Hz, 3 H), 3.3 (t, J = 5.1 Hz, 2 H), 3.7 (m, 14 H), 4.13 (s, 2 H), 4.2 (q, J = 7.5 Hz, 2 H), 7.3 (m, 9 H), 7.5 (m, 6 H)

^{13}C-NMR (CD_3OD): 14.55, 47.76, 61.83, 64.58, 67.38, 69.32, 87.85, 128.09, 128.82, 129.91, 145.53, 172.25

TLC- system (R_f): toluene/ether 1:1 (0.47)
ether (0.87)

Monotrityltrideca(ethylene glycol)acetic acid ethylester

0.25 g (ca. 6 mmol) of NaH (55 - 65 % in oil) were suspended in 5 ml of absolute THF. 2.7 g (3.2 mmol) of trideca(ethylene glycol)mono(triphenylmethyl)ether in 3 ml of absolute THF were added dropwise under argon during 15 minutes at room temperature. The suspension was then refluxed and 1.22 g (7 mmol) of bromoacetic acid ethylester in 3 ml of absolute THF were added dropwise within 20 minutes. The mixture was refluxed for one hour and then stirred over night at room temperature. Solvent and excess bromoacetic acid ethylester were evaporated, the residue dissolved in 20 ml of chloroform and little water, filtered and evaporated to dryness yielding 3.26 g (100 %) of monotrityltrideca(ethylene glycol)acetic acid ethylester.

Molecular weight: 919.1 ($C_{49}H_{74}O_{16}$)

^{1}H-NMR ($CDCl_3$): 1.3 (t, J = 7.5 Hz, 3 H), 3.3 (t, J = 5.1 Hz, 2 H), 3.7 (m, 50 H), 4.13 (s, 2 H), 4.2 (q, J = 7.5 Hz, 2 H), 7.3 (m, 9 H), 7.5 (m, 6 H)

^{13}C-NMR ($CDCl_3$): 14.19, 60.74, 63.32, 68.78, 70.51, 70.64, 70.66, 70.76, 70.83, 86.69, 126.89, 127.73, 128.70, 144.13, 170.68

MS (FAB^+): 941.5 (87.7, M + Na), 897.5 (14.7), 855.5 (11.3), 854.5 (11.3), 853.4 (24.1), 765.4 (7.1), 721.4 (6.7), 245.1 (6.5), 244.1 (33.7), 243.1 (100.0), 183.1 (5.5), 167.1 (6.6), 166.1(6.3), 165.1 (20.0), 154.1 (8.8), 149.1 (6.0), 139.1 (5.6), 138.1 (55.6), 137.1 (12.7), 136.0 (9.1), 135.1 (5.6), 133.1 (7.6), 131.1 (12.9), 123.1 (10.7), 121.1 (8.6), 119.1 (6.5), 117.0 (5.7), 115.0 (6.2), 111.1 (10.9), 109.1 (17.2), 107.0 (12.8), 106.0 (5.3), 105.0 (21.4), 103.0 (8.7)

TLC- system (R_f): CH_2Cl_2/ MetOH 65: 5 (0.46)

Monotrityltetra(ethylene glycol)acetic acid N,N-dimethylaminoethanol ester

Little sodium was added to 2 ml (20 mmol) of freshly distilled N,N-dimethylaminoethanol. 0.36 g (0.68 mmol) of monotrityltetra(ethylene glycol) acetic acid ethylester in 0.9 g (10 mmol) of freshly distilled N,N-dimethylaminoethanol were added and the mixture stirred at 100^0 C for one hour. The residue was extracted with ether, the united ether phases evaporated and extracted with pentane. The united pentane extracts were evaporated to dryness yielding monotrityltetra(ethylene glycol)acetic acid N,N-dimethylaminoethanol ester (77 %) as a highly viscous oil.

Molecular weight: 565.7 ($C_{33}H_{43}O_7N$)

^{1}H-NMR ($CDCl_3$): 2.3 (s, 6 H), 2.6 (m, 2 H), 3.3 (m, 2 H), 3.7 (m, 14 H), 4.18 (s, 2 H), 4.25 (m, 2 H), 7.3 (m, 9 H), 7.5 (m, 6 H)

^{13}C-NMR ($CDCl_3$): 45.67, 57.5, 62.39, 63.35, 68.5, 70.61, 70.66, 70.72, 70.80, 70.90, 86.5, 126.92, 127.75, 128.74, 144.15, 170.8

MS (FAB^+): 566.4 (100.0), 565.4 (26.1), 564.3 (81.3), 517.2 (6.8), 322.2 8 (11.9), 244.2 (17.1), 243.2 (67.0), 165.1 (10.3), 136.1 (5.1), 105.0 (5.9)

TLC- system (R_f): CH_2Cl_2/ MetOH 65: 10 (0.69)

Monotrityltrideca(ethylene glycol)acetic acid N,N-dimethylaminoethanol ester

A small piece of sodium was dissolved in 4 ml (40 mmol) of freshly distilled N,N-dimethylaminoethanol. 3.26 g (3.2 mmol) of monotrityltrideca(ethylene glycol)acetic acid ethylester in 2 ml (20 mmol) of freshly distilled N,N-dimethylaminoethanol were added and the reaction mixture stirred at 100^0 C for 1 1/2 hours. Excess dimethylaminoethanol was evaporated, the viscous residue suspended in dichloromethane, which was decanted and evaporated. this residue was suspended in 15 ml of diethyl ether and stored over night at 4^0 C. the supernatant was decanted, the ether evaporated and the crude product extracted with seven times 15 ml of pentane. The pentane insoluble residue is monotrityltrideca(ethylene glycol)acetic acid N,N-dimethylaminoethanol ester (yield: 84 %).

Molecular weight: 962.2 ($C_{51}H_{79}O_{16}N$)

^{1}H-NMR ($CDCl_3$): 2.3 (s, 6 H), 2.6 (t, J = 5.7 Hz, 2 H), 3.3 (t, J = 5.7 Hz, 2 H), 3.7 (m, 50 H), 4.18 (s, 2 H), 4.25 (t, J = 5.7 Hz, 2 H), 7.3 (m, 9 H), 7.5 (m, 6 H)

^{13}C-NMR ($CDCl_3$): 45.86, 57.63, 62.57, 63.29, 68.75, 70.51, 70.67, 70.70, 86.58, 126.91, 127.74, 128.71, 144.08, 170.72

MS (FAB^+): 962.5 (100.0), 961.5 (18.7), 960.5 (38.8), 948.5 (5.2), 942.5 (10.3), 941.5 (21.2), 940.4 (8.9), 919.5 (7.4), 918.5 (14.4), 916.5 (6.3), 897.4 (9.8), 896.4 (14.5), 875.5 (12.4), 874.4 (24.6), 873.4 (5.6), 872.4 (11.3), 856.4 (7.9), 855.4 (15.6), 853.4 (8.1), 786.4 (5.2), 718.4 (9.0), 586.3 (9.2), 244.1 (19.8), 243.1 (56.3), 165.1 (12.9), 136.0 (5.6), 131.1 (5.1), 105.0 (8.9)

TLC- system (R_f): CH_2Cl_2/ MetOH 65: 10 (0.71)

Monotrityltetra(ethylene glycol)acetic acid choline ester bromide salt

0.35 g (3.5 mmol) of methylbromide in 8 ml of diethyl ether were dropwise added to 428 mg (0.75 mmol) of monotrityltetra(ethylene glycol) acetic acid N,N-dimethylaminoethanol ester. The solution was never clear as the choline ester formed is not soluble in ether. After stirring over night at room temperature the solvent and excess methylbromide was evaporated. After extraction with four times 4 ml of diethyl ether the ether insoluble residue was dissolved in 0.5 ml of dichloromethane and the product precipitated by addition of 7 ml of ether upon storing at 4^0 C. The supernatant was decanted, the residue dissolved in dichloromethane and filtered. The precipitation step with ether was repeated three times. Evaporation of the solvent yielded then 327 mg (66 %) of pure monotrityltetra(ethylene glycol)acetic acid choline ester bromide salt.

Molecular weight: 660.7 ($C_{34}H_{46}O_7NBr$)

^{1}H-NMR ($CDCl_3$): 3.2 (t, J = 5.7 Hz, 2 H), 3.4 (s, 9 H), 3.65 (m, 14 H), 4.15 (m, 2 H), 4.2 (s, 2 H), 4.6 (m, 2 H), 7.3 (m, 9 H), 7.5 (m, 6 H)

^{13}C-NMR ($CDCl_3$): 54.42, 58.20, 63.35, 65.0, 68.62, 70.56, 70.60, 70.65, 70.76, 71.10, 86.5, 127.01, 127.81, 128.72, 144.10, 169.5

MS (FAB^+): 580.3 (100.0), 243.0 (12.6), 160.1 (6.2)

TLC- system (R_f): CH_2Cl_2/ MetOH 65: 15 (0.58)

Monotrityltrideca(ethylene glycol)acetic acid choline ester bromide salt

2.4 g (2.5 mmol) of monotrityltrideca(ethylene glycol) acetic acid N,N-dimethylaminoethanol in 10 ml of absolute diethyl ether were added to a solution of 1.6 g (16 mmol) of methylbromide in 20 ml of absolute ether and stirred at room temperature for 44 hours. After keeping the reaction mixture over night at 4^0 C the supernatant was decanted. The viscous residue was dried at 12 mbar and 55^0 C, dissolved in 5 ml of dichloromethane and dropwise added to 35 ml of absolute diethyl ether. The suspension was stored over night at 4^0 C and the clear supernatant decanted the next day. The residue was dried yielding 1.3 g (49 %) monotrityltrideca(ethylene glycol)acetic acid choline ester bromide salt as a brown resin.

Molecular weight: 1057.1 ($C_{52}H_{82}O_{16}NBr$)

^{1}H-NMR ($CDCl_3$): 3.2 (t, J = 5.7 Hz, 2 H), 3.4 (s, 9 H), 3.65 (m, 50 H), 4.15 (m, 2 H), 4.2 (s, 2 H), 4.7 (m, 2 H), 7.3 (m, 9 H), 7.5 (m, 6 H)

^{13}C-NMR ($CDCl_3$): 54.51, 58.32, 63.33, 64.04, 68.67, 70.07, 70.52, 70.56, 70.58, 70.66, 70.77, 71.10, 86.54, 126.93, 127.76, 128.72, 169.64

MS (FAB^+): 976.39, 933.4 (8.7), 932.3 (16.2), 890.4 (5.2), 889.4 (16.1), 888.3 (32.9), 800.3 (9.3), 734.3 (5.6), 531.3 (12.5), 530.3 (26.3), 529.3 (5.7), 307.0 (8.8), 244.0 (6.6), 243.0 (23.2), 219.1 (5.9)

TLC- system (R_f): CH_2Cl_2/ MetOH 65: 10 (0.20)

Tetra(ethylene glycol)monoacetic acid choline ester bromide salt

64 µl (0.4 mmol) of triethylsilane and 0.2 ml of TFA were added to a solution of 123 mg (0.2 mmol) of monotetra(ethylene glycol) acetic acid choline ester bromide salt in 3 ml of absolute dichloromethane and stirred for 30 minutes at room temperature. After evaporation of the solvent the residue was extracted with three times 2 ml of absolute diethyl ether and the residue dried at reduced pressure yielding 78 mg (100 %) of tetra(ethylene glycol)monoacetic acid choline ester bromide salt as a yellowish resin.

Molecular weight: 418.7 ($C_{15}H_{32}O_7NBr$)

^{1}H-NMR ($CDCl_3$): 3.35 (s, 9 H), 3.6 (m, 16 H), 4.0 (m, 2 H), 4.18 (s, 2 H), 4.6 (m, 2 H)

^{13}C-NMR ($CDCl_3$): 54.30, 58.18, 61.04, 64.69, 68.38, 70.16, 70.28, 70.32, 70.34, 70.37, 70.40, 70.43, 70.63, 70.92, 72.53, 169.74

MS (FAB^+): 338.3 (100.0), 275.2 (5.1), 154.1 (16.8), 138.1 (5.5), 137.1 (8.9), 136.1 (13.3)

TLC- system (R_f): CH_2Cl_2/ MetOH 65: 10 (0.32)
CH_2Cl_2/ MetOH 65: 10 (0.60, RP-8!)

Trideca(ethylene glycol)monoacetic acid choline ester bromide salt

0.3 ml (1.8 mmol) of triethylsilane and 1 ml of TFA were added to a solution of 973 mg (0.92 mmol) of monotrityltrideca(ethylene glycol) acetic acid choline ester bromide salt in 15 ml of absolute dichloromethane. After stirring at room temperature for 15 minutes the solvent was evaporated. The residue was extracted with three times 15 ml of absolute diethyl ether, dissolved in 2 ml of dichloromethane and added to 25 ml of ether. The suspension was kept at 4^0 C until the supernatant was clear. The latter was decanted, the crude product (100 %), a the brown resin dried and dissolved in acetone at a concentration of 0.16 g/ml. 0.5 ml fractions thereof were then purified by chromatography (Sephadex LH-20, 8 g) eluting with acetone. This yielded 215 mg (28 %) of pure trideca(ethylene glycol)monoacetic acid choline ester bromide salt as a slightly yellow solid.

Molecular weight: 814.8 ($C_{33}H_{68}O_{16}NBr$)

^{1}H-NMR ($CDCl_3$): 3.4 (s, 9 H), 3.65 (m, 52 H), 4.05 (m, 2 H), 4.2 (s, 2 H), 4.6 (m, 2 H)

^{13}C-NMR ($CDCl_3$): 54.41, 58.18, 61.64, 64.79, 68.60, 70.28, 70.50, 70.58, 71.07, 72.47, 169.66

MS (FAB^+): 734.4 (100.0), 733.3 (6.9), 732.4 (17.2), 691.3 (6.4), 690.3 (16.3), 688.3 (7.2), 671.2 (5.2), 647.3 (10.0), 646.3 (27.7), 644.3 (9.8), 602.3 (6.8), 601.3 (10.5), 600.3 (31.1), 104.0 (20.2)

TLC- system (R_f): CH_2Cl_2/ MetOH 65: 10 (0.64, RP-8!)

3,6,9,12,15-pentaoxa-16-carbonyl-31-(2-pyridyldithio)-hentriacontanoic acid choline ester bromide salt (PyP-PEG$_4$-ACh)

20 mg (47.5 µmol) of tetra(ethylene glycol)monoacetic acid choline ester bromide salt, 40 mg (0.1 mmol) of 1-(2-pyridyldithio)hexadecanoic acid, 12 mg (0.1 mmol) of DMAP, and 30 mg (0.15 mmol) of DCC were suspended in 1 ml of absolute dichloromethane and stirred at room temperature for 20 hours. After filtration the solvent was evaporated and the residue extracted with pentane and ether. Dichloromethane was then added to the residue and the resulting suspension filtered. The solvent was evaporated, the residue redissolved in 0.2 ml of dry dichloromethane and added to 2 ml of diethyl ether. The suspension was stored at 4^0 C and the clear supernatant decanted. The residue was dried yielding 35 mg (92 %) of 3,6,9,12,15-pentaoxa-16-carbonyl-31-(2-pyridyldithio)-hentriacontanoic acid choline ester bromide salt.

Molecular weight: 798.0 ($C_{36}H_{65}O_8N_2S_2Br$)

^{1}H-NMR ($CDCl_3$): 1.3 (m, 22 H), 1.7 (m, 4 H), 2.3 (t, J = 6.7 Hz, 2 H), 2.8 (t, J = 6.7 Hz, 2 H), 3.4 (s, 9 H), 3.65 (m, 14 H), 4.05 (m, 2 H), 4.2 (s/m, 4 H), 4.65 (m, 2 H), 7.05 (m, 1 H), 7.65 (m, 2 H), 8.4 (m, 1 H)

^{13}C-NMR ($CDCl_3$): 24.89, 28.43, 28.89, 29.09, 29.12, 29.24, 29.42, 29.51, 29.56, 29.59, 33.96, 39.02, 54.22, 58.29, 63.24, 64.6, 68.3, 69.17, 70.29, 70.32, 70.38, 70.83, 119.50, 120.47, 136.94, 149.50, 160.69, 169.89, 173.88

MS (FAB^+): 717.5 (100.0), 715.5 (6.1), 608.5 (10.3), 607 (8.1), 606.5 (18.1), 574.5 (9.2), 484.4 (9.6), 483.4 (28.8), 380.3 (5.4), 320.3 (8.2), 276.2 (5.6), 232.2 (5.2), 160.1 (11.4), 154.1 (9.8), 145.1 (8.5), 137.1 (6.6), 136.1 (9.6), 123.1 (12.5), 112.0 (5.6), 111.0 (7.8), 107.0 (5.9)

TLC- system (R_f): CH_2Cl_2/ MetOH 65: 20 (0.71)

3,6,9,12,15,18,21,24,27,30,33,36,39,42-tetradecaoxa-43-carbonyl-58-(2-pyridyldithio)-octapentacontanoic acid choline ester bromide salt (PyP-PEG$_{13}$-ACh)

127 mg (0.16 mmol) of trideca(ethylene glycol)monoacetic acid choline ester bromide salt dissolved in 3 ml of dichloromethane were added to 30 mg (0.24 mmol) of DMAP and 103 mg of DCC. 95 mg (0.24 mmol) of 1-(2-pyridyldithio)hexadecanoic acid were added and the mixture was stirred at room temperature for 25 hours. The solvent was evaporated, the residue extracted with three times 5 ml of diethyl ether and then dried. the extracted residue was suspended in 2 ml of dichloromethane, filtered and the solvent evaporated. The residue was redissolved in 0.5 ml of dichloromethane and 7.5 ml of ether were dropwise added to the solution. After storage at 4^0 C the clear supernatant was decanted. The residue was dried, suspended in 1 ml of dichloromethane, and filtered. The solvent was evaporated yielding 188 mg (98 %) of 3,6,9,12,15,18,21,24,27,30,33,36,39,42-tetradecaoxa-43-carbonyl-58-(2-pyridyldithio)-octapentacontanoic acid choline ester bromide salt.

Molecular weight: 1194.5 ($C_{54}H_{101}O_{17}N_2S_2Br$)

^{1}H-NMR ($CDCl_3$): 1.25 (m, 22 H), 1.6 (m, 4 H), 2.25 (t, J = 6.7 Hz, 2 H), 2.75 (t, J = 6.7 Hz, 2 H), 3.4 (s, 9 H), 3.65 (m, 50 H), 4.1 (m, 2 H), 4.2 (s/m, 4 H), 4.65 (m, 2 H), 7.05 (m, 1 H), 7.65 (m, 2 H), 8.4 (m, 1 H)

^{13}C-NMR ($CDCl_3$): 24.85, 28.41, 28.86, 29.07, 29.09, 29.20, 29.39, 29.48, 29.55, 34.15, 38.99, 54.33, 58.25, 63.28, 64.48, 68.53, 69.12, 70.43, 70.47, 70.4, 71.00, 119.46, 120.45, 136.90, 149.49, 160.69, 169.66, 173.52

MS (FAB^+): 1113.5 (100.0), 1070.5 (11.2), 1069.5 (19.0), 1027.5 (12.9), 1026.5 (24.6), 1025.5 (43.5), 1004.5 (10.3), 1002.5 (15.8), 938.4 (11.4), 937.4 (21.3), 893.4 (12.4), 688.3 (11.3), 688.3 (11.3), 644.3 (15.9), 628.2 (10.1), 601.2 (32.0), 600.2 (93.2), 483.2 (21.0), 380.1 (45.3), 276.1 (23.7), 225.1 (26.6), 160.0 (44.0)

TLC- system (R_f): CH_2Cl_2/ MetOH 65: 10 (0.0.29)

20-Hydroxy-18,15,12,9,6,3-hexaoxaeicosanoic acid (PEG_6Ac)

0.8 g (35 mmol) of sodium were added to 13.00 g (46 mmol) of hexa(ethylene glycol) dissolved in 200 ml of dry diethyleneglycoldimethylether and stirred at 100^0 C under argon until no more hydrogen was developed (ca. 9 hours). To the dark brown solution 10 ml (90.5 mmol) of bromoacetic acid ethylester were added and stirring was continued over night under argon at 80^0 C until the pH was neutral. The solvent was then evaporated, the dark brown oil dried on high vacuum, suspended in chloroform, filtered and the chloroform completely evaporated. The residue was dissolved in 50 ml of 2 M NaOH and the solution stirred for 2 hours at 80 ^{0}C until the ester was completely hydrolyzed as monitored by TLC. Water was evaporated and the remaining oil extracted with toluene using a modified Kutscher-Steudel extraction set-up until the toluene extract contained no more hexa(ethylene glycol). The residue was then dissolved in water, cooled on ice, the pH adjusted to 2 with HCl, and the water carefully evaporated at 20^0 C. After drying of the residue on high vacuum for several hours dichloromethane was added. It was dried from anhydrous sodium sulfate, the suspension was filtered and the solvent evaporated again. The residual oil was dissolved in methanol and activated charcoal was added. After stirring for 1 hour at ambient temperature the coal was removed by filtration through Celite yielding a slightly yellow oil after evaporation of the methanol. This oil was purified by chromatography (alkaline aluminiumoxide, Machery-Nagel) eluting with CH_2Cl_2/ MetOH 65: 25 followed by CH_2Cl_2/ MetOH/ NH_4OH 65:25: 2. The product fractions were acidified to pH 2 with HCl, the solvents were evaporated and the residue was again extracted with dichloromethane. The organic phase was dried from anhydrous sodium sulfate, filtered and evaporated to dryness yielding (48 %) 20-hydroxy-18,15,12,9,6,3-hexaoxaeicosanoic acid.

Molecular weight: 340.4 ($C_{14}H_{28}O_9$)

^{1}H-NMR ($CDCl_3$): 3.6 -3.7 (m, 24 H), 4.25 (s, 2 H)

^{13}C-NMR ($CDCl_3$): 62.2 , 68.9, ca. 70.7, 73.7, 174.2

IR (ATR-FTIR) 2919.1 (m), 2879.4 (m), 1739.7 (m), 1633.8 (m), 1438.2 (m), 1338.2 (m), 1250.0 (m), 1083.8 (s), 944.1 (m), 825.0 (w)

MS (NH_3): 341 (2.3), 253 (4.2), 117 (6.0), 104 (5.4), 103 (78.1), 102 (35.5), 101 (16.8), 90 (6.8), 89 (100.0), 88 (18.8), 87 (77.9), 86 (5.9), 75 (8.6), 73 (27.9), 72 (18.0), 70 (6.7)

TLC- system (R_f): CH_2Cl_2/ MetOH/ NH_4OH 65: 25: 2 (0.55)

3,6,9,12,15,18,21-heptaoxa-22-carbonyl-37-(2-pyridyldithio)-heptatriacontanoic acid (PyP-PEG$_6$Ac)

1.065 g (2.68 mmol) of 1-(2-pyridyldithio)hexadecanoic acid and 0.434 g (2.68 mmol) of CDI in 50 ml of dry dichloromethane were refluxed over night under argon. 902 mg (2.65 mmol) of 20-hydroxy-18,15,12,9,6,3-hexaoxaeicosanoic acid were added and refluxing under argon was continued for another 12 hours. The solvent was evaporated and the residue extracted with pentane using a modified Kutscher-Steudel set- up. The residue was then suspended in little THF and stored at 4^0 C until no more turbid. The THF phase was decanted and the solvent evaporated. The well dried residue was twice extracted with pentane followed by repeated extraction with little diethyl ether always storing the turbid mixture at 4^0 C until the supernatant was completely clear. The residue was dried yielding 3,6,9,12,15,18,21-heptaoxa-22-carbonyl-37-(2-pyridyldithio)-heptatriacontanoic acid (50 - 70 %), which could be further purified by preparative TLC (silicagel 60 F_{254}) using CH_2Cl_2/ MetOH 65:10 to develop the plate and eluting the isolated band with CH_2Cl_2/ MetOH 1:1.

Molecular weight: 720.0 ($C_{35}H_{61}O_{10}NS_2$)

^{1}H-NMR ($CDCl_3$): 1.25 (m, 22 H), 1.6 (m, 4 H), 2.25 (t, J = 6.7 Hz, 2 H), 2.8 (t, J = 6.7 Hz, 2 H), 3.65 (m, 22 H), 4.2 (s/m, 4 H), 7.05 (m, 1 H), 7.65 (m, 2 H), 8.4 (m, 1 H)

^{13}C-NMR ($CDCl_3$): 24.93, 28.45, 28.90, 29.13, 29.25, 29.43, 29.51, 29.58, 34.17, 39.05, 63.2, 68.94, 69.12, 69.18, 39.36, 69.51, 69.76, 69.85, 69.99, 70.09, 70.11, 70.22, 70.36, 70.48, 70.55, 70.57, 70.62, 70.92, 71.15, 119.53, 120.42, 136.87, 149.53, 173.74, 175.22

TLC- system (R_f): CH_2Cl_2/ MetOH 65: 15 (0.32)

3,6,9,12,15,18,21-heptaoxa-22-carbonyl-37-(2-pyridyldithio)-heptatriacontanoic acid choline ester tosylate salt (PyP-PEG$_6$-ACh)

225 mg (0.32 mmol) of 3,6,9,12,15,18,21-heptaoxa-22-carbonyl-37-(2-pyridyldithio)-heptatriacontanoic acid , 300 mg (1.1 mmol) of choline tosylate, 445 mg (2.2 mmol) of DCC, and 40 mg (0.33 mmol) of DMAP were stirred at room temperature in 4 ml of dichloromethane in the dark during 6 days. The suspension was then filtered and the solvent evaporated. The residue was repeatedly extracted with diethyl ether by heavy shaking and subsequent storage at 4^0 C until the supernatant was clear. The ether phases were decanted. Absolute THF was added to the residue. The mixture was well mixed, stored at 4^0 C until the supernatant was clear and then filtered through celite. This ether/THF extraction cycle was repeated. 3,6,9,12,15,18,21-heptaoxa-22-carbonyl-37-(2-pyridyldithio)-heptatriacontanoic acid choline ester tosylate salt (37 %) was isolated after prolonged extraction of the residue with ether using a modified Kutscher-Steudel extraction set-up.

Molecular weight: 977.4 ($C_{47}H_{80}O_{13}N_2S_3$)

^{1}H-NMR ($CDCl_3$): 1.3 (m, 22 H), 1.65 (m, 4 H), 2.3 (m, 5 H), 2.8 (t, J = 6.7 Hz, 2 H), 3.4 (s, 9 H), 3.65 (m, 22 H), 4.0 (m, 2 H), 4.2 (s/m, 4 H), 4.6 (m, 2 H), 7.05 (m, 1 H),7.16 (d, J = 7.0 Hz, 2 H), 7.65 (m, 2 H), 7.75 (d, J = 7.0 Hz, 2 H), 8.4 (m, 1 H)

^{13}C-NMR ($CDCl_3$): 21.3, 24.91, 28.47, 28.92, 29.15, 29.28, 29.46, 29.55, 29.61, 29.63, 33.93, 39.05, 54.17, 58.37, 63.29, 64.44, 68.41, 69.16, 70.35, 70.40, 70.45, 70.49, 70.87, 119.53, 120.46, 125.883, 128.72, 136.94, 139.50, 143.49, 149.56, 160.69, 168.63, 170.0

MS (FAB^+): 805.4 (100.0), 762.4 (5.1), 761.4 (11.1), 696.4 (7.6), 694.4 (7.6), 662.5 (5.8), 483.3 (5.8), 306.3 (6.9), 246.1 (10.1), 229.2 (22.9), 170.1 (12.5), 160.1 (12.9), 145.1 (7.9), 136.1 (5.4), 104.1 (26.6), 102.0 (5.8)

TLC- system (R_f): CH_2Cl_2/ MetOH 65: 15 (0.22)
CH_2Cl_2/ MetOH 65: 10 (0.46, RP-8!)

Bromoacetylcholine bromide [Her90]

5 ml (57.4 mmol) of bromoacetylbromide were dropwise added under nitrogen to 8.8 g (48 mmol) of dried choline bromide cooled on ice. Hydrogen bromide formed was trapped in gas washing bottles containing sodium hydroxide. After 4 hours of stirring at 0^0 C the reaction mixture was stirred for one hour at 60^0 C and then cooled to ambient temperature. 27 ml of absolute ethanol were added and the solution stored at 4^0 C . The precipitate was filtered off, recrystallized twice from absolute isopropanol, and dried yielding 12.77 g (88 %) of bromoacetylcholine bromide as a white, hygroscopic solid.

Molecular weight: 305.0 ($C_7H_{15}O_2NBr_2$)

^{1}H-NMR ($CDCl_3$): 3.3 (s, 9 H), 3.86 (m, 2 H, 4.13 (s, 2 H), 4.70 (m, 2 H)

^{13}C-NMR ($CDCl_3$): 26.5, 65.8, 60.6, 168.1

IR (ATR-FTIR) 3016.2 (m), 2969.1 (m), 2070.6 (br, w), 1750 (vs), 1633.8 (vs), 1473.5 (vs), 1416.2 (s), 1282.4 (vs), 1147.1 (vs), 1032.4 (s),969.1 (vs), 867.7 (s)

MS (NH_3):	224.0 (100.0), 167.0 (13.9), 165.0 (14.3), 146.1 (11.2), 145.1 (12.3), 104.1 (11.1), 102.0 (5.8)
m.p.:	131^0 C
TLC- system (R_f):	CH_2Cl_2/ MetOH/ NH_4OH 65: 25: 4 (0.14)

9. Determination of Phase transition temperatures in Liposomes by Calorimetry

Phase transition temperatures of vesicles of the synthesized thiolipids were measured by calorimetry using a MicroCal Inc. Calorimetry system. Vesicles were prepared by sonifying completely dried lipids for five minutes in buffer (10 mM potassium phosphate (pH 7.25)/ 100 mM NaCl). The final lipid concentration was 1.0 mg/ml. Vesicle solutions were degassed for 15 minutes prior to measurement. Samples were heated at a rate of 80^0 C/ hr from 11 to 60^0 C. Table 9.1 summarizes the phase transition temperatures found.

lipid	concentration (mM)	phase transition temperature	remarks
BPyPPC	0.89	44.5^0 C	in 10 mM Hepes (pH 7.4)
BmPPC	1.3	48.0^0 C	
PmPPC	1.3	44.0^0 C	
LmPPC	1.4	-	very broad band
PhymPPC	1.2	-	
mPPhyPC	1.2	-	
LPPC	-	21.5^0 C	[Cev93]
DPPC	-	41.5^0 C	[Blu83]

Tab. 9.1. Phase transition temperatures for vesicles of the synthesized thiolipids.

From the phase transition temperatures measured it can be concluded that substitution of the ω-standing methyl groups on the palmitic acid chains of DPPC by thiol groups increases the phase transition temperature. Removal of the bulky protective groups of the thiols (BPyPPC -> BmPPC) surprisingly leads to an increase of the phase transition temperature of 3.5^0 C. No phase transition between 10 and 60^0 C was found for polymerized vesicles of BmPPC [Sam85].

No phase transition was observed between 11 and 60^0 C for PhymPPC and mPPhyPC. DPhyPC is reported to have no phase transition between - 120^0 C and + 80^0 C [Ava94]. No sharp peak, but only a very broad band was observed for LmPPC even though the analogous lipid without thiol is reported to have a phase transition at 21.5^0 C.

10. Characterization of Self-assembled thiolipid Monolayers

10.1. Impedance Spectroscopy

Glass slides, cleaned according to the protocol described in annex A, were silanized by vapor phase deposition using the thiosilane $HS(CH_2)_3Si(OCH_3)_3$. Resistive evaporation of about 40 nm of gold (procedure as described for SPR) using a mask yielded point electrodes with a radius of 1.0 mm and thus an area of 0.0314 cm^2. The measurement cell was immediately assembled and thiolipids were self-assembled at a concentration of 0.5 mg/ml in ethanol over night. Layers were then rinsed with ethanol followed by methanol and electrolyte (0.1 M KCl). Impedance spectroscopy was performed using the set-up depicted in figure 10.1. It consists of a phase-sensitive lock-in amplifier (Stanford Research, SR850), which generates the alternating voltage applied and records the response, a measurement cell composed of the coated gold electrode and a Ag/AgCl reference electrode, and a combined amplifier/converter unit, which amplifies the measured current and converts it into a tension. Frequency spectra between 1 and 20 000 Hz were recorded applying a sinusoidal voltage with an amplitude of 10 mV. Frequency spectra show the amplitude of the measured signal and its phase shift with respect to the applied voltage.

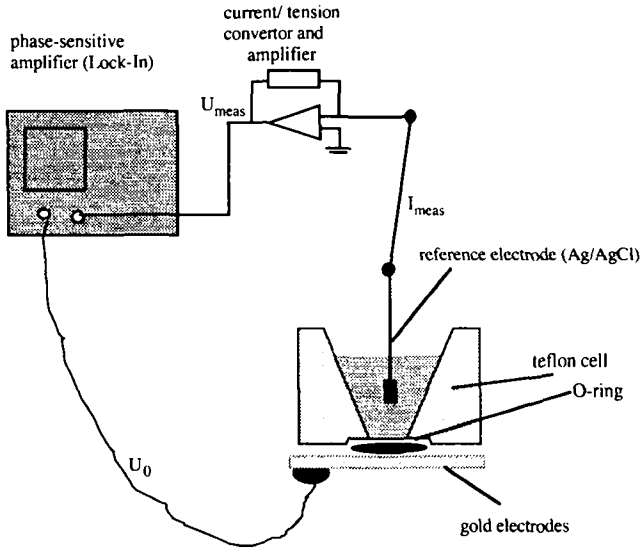

Fig. 10.1. Electrochemical cell for impedance spectroscopy. U_0 is the applied tension, U_{meas} and I_{meas} the measured tension and current, respectively.

10.2. FTIR

Instrumental details are described in chapter 7.2, acquisition parameters and data treatment in annex B and C. Spectra are shown in annex D.

10.2.1. Transmission FTIR

KBr-pellets were prepared by adding a few drops of the lipid dissolved in CH_2Cl_2 to 200 mg of KBr (Fluka, for IR). After evaporation of the solvent and complete drying (< 0.01 mbar/ P_2O_5/ 3 hrs) the samples were molded, pressed and immediately measured in the nitrogen purged measurement chamber using the same acquisition parameters as for the grazing incidence measurements, but a DTGS detector and only 300 scans.

10.2.2. GI-FTIR on Self-assembled Thiolipid Monolayers

Microscopy slides were used as substrates for the deposition of 1.0 nm of chromium (deposition rate < 0.1 nm/ sec) followed by about 100 nm of gold (rate < 0.1 nm/sec for the first and the last 5 nm, else 0.2 - 0.3 nm/sec). The freshly prepared slides were immediately immersed into an ethanolic solution of the synthesized thiolipids (0.5 mg/ml). Layers were self-assembled over night at room temperature. After thorough rinsing with ethanol followed by dichloromethane samples were dried for one hour at 0.01 mbar over phosphorous pentoxide and immediately put into the measurement chamber flushed with dry nitrogen. A self-assembled monolayer of fully deuterated hexadecanethiol $HS(CD_2)_{16}D$ (0.5 mg/ml chloroform) was prepared accordingly and used as a reference.

10.2.3. GI-FTIR of transferred Langmuir-Blodgett Layers

Monolayers of the synthesized thiolipids were formed at the air-water interface of a Langmuir balance (Riegler and Kirstein, Mainz, Germany) at a water temperature of 22^0 C and transferred at a pressure of about 30 mN/m onto a self-assembled monolayer of 11-hydroxy-undecane-1-thiol ($HS(CH_2)_{11}OH$), which had been prepared according to the procedure described for self-assembled thiolipid monolayers investigated by GI-FTIR (0.5 mg/ml chloroform/ over night/ ambient temperature// drying after washing with CH_2Cl_2). For the transfer of the LB-layers the substrate was immersed at maximum speed and very slowly withdrawn.

10.2.4. ATR-FTIR of transferred Langmuir-Blodgett Layers

A monolayer of DPPC was formed at the air-water interface of a Langmuir balance (Riegler and Kirstein, Mainz, Germany) at a water temperature of 22^0 C and transferred onto a germanium crystal at a pressure of about 30 mN/m. The substrate was immersed at maximum speed through the lipid monolayer and subsequently slowly transferred to the substrate at about 30 mN/m.

10.2.5. Temperature dependent GI-FTIR

A thermostated copper element was placed onto a microscopy slide with the lipid layer prepared as described above. To improve heat transfer between copper element and glass a heat sink compound (Dow Corning 340 silicone) was used (fig. 10.2).

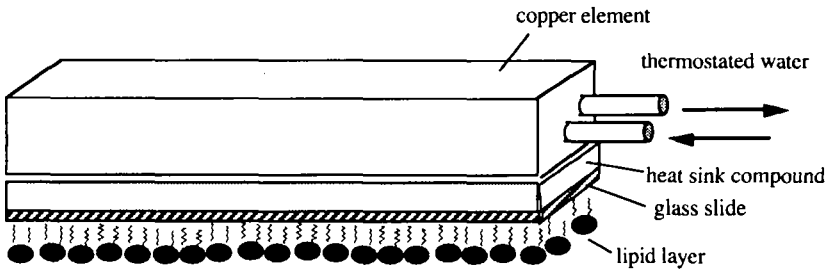

Fig. 10.2. Set-up used for temperature dependent GI-FTIR.

10.3. Contact Angle Measurements

Contact angle measurements were performed using a G10 contact angle measurement system (Krüss). 15 µl droplets of water were deposited on the sample using a Hamilton syringe and the advancing contact angle was determined after 10 seconds with a precision of 0.5^0. 10 seconds after retraction the receding contact angles were read. Each value corresponds to the mean of 15 to 20 readings.

10.4. Surface Plasmon Resonance Spectroscopy

Surface plasmon resonance spectroscopy was performed on a home-built set-up described in detail by Terrettaz et al. [Ter93]. The Kretschmann coupling scheme [Kre72] was used with a p-polarized He-Ne laser (632.8 nm) and a unilateral, high index prism (SF-10, Leica; n = 1.723). Optical parameters were deduced by fitting the ATR scans to the Fresnel equations.

10.4.1. Self-assembly of Lipid Monolayers and Nonspecific Binding of Proteins

Quartz slides (SF-10, EPL) were cleaned according to the protocol described in annex A. Resistive vapor deposition of 0.7 to 1.0 nm of chromium at a rate of < 0.1 nm/sec was followed by 37 nm of gold (rate < 0.1 nm/ sec for the first 5 and the last 2 nm, else 0.2 - 0.3 nm/sec). Measurement cells were immediately assembled. Angle scans of bare gold both in water and in ethanol were recorded. Self-assembly of the synthesized thiolipids from an ethanolic solution at a lipid concentration of 0.5 mg/ ml was followed by monitoring reflectivity as a function of time at a constant angle slightly below the resonance angle of bare gold(time scan). A stable signal was usually reached after at least 6 to 7 hours. The layer was then thoroughly washed with ethanol (angle scan in ethanol) and the ethanol exchanged against water (angle scan in water). Water was then replaced by buffer (10 mM potassium phosphate (pH 7.4)/ 100 mM NaCl). Protein adsorption was again monitored with a time scan. After one hour of incubation - a stable signal was usually already reached after a few minutes- the layers were thoroughly rinsed with buffer and the adsorbed amount of protein determined with an additional angle scan. Bovine serum albumin (Fluka BioChemika), immunoglobulin G from rabbit serum (Fluka BioChemika), fibrinogen from bovine plasma (fraction I, Type I-S, 75 % protein; Sigma), and rabbit serum (Sigma) reconstituted with deionized water were used.

10.4.2. Self-assembly of Mixed Lipid/ Ligand Molecule Layers and specific Binding of the Acetylcholine Receptor

Mixed layers of ligand molecules and thiolipids were prepared by self-assembly over night at room temperature on freshly prepared gold substrates using a solution of 0.5 mg/ml mPPhyPC and 0.25 mg/ml PyP-PEG_{13}-ACh (molar ratio: 2.9:1) in dichloromethane. The slides were then rinsed with CH_2Cl_2 followed by ethanol, water and buffer and immediately used for adsorption experiments.

Enriched membranes of the electric organ of *Torpedo Californica* were a generous gift from Prof. F. Hucho (Freie Universität Berlin). Purified nicotinic acetylcholine receptor from *Torpedo californica* solubilized in detergent or reconstituted in vesicles according to [Sch92] was a generous gift from Dr. T. Schürholz (Universität Bielefeld).

Annex A: Cleaning Protocol for Glass Slides

Glass slides used for the evaporation of thin metal films were cleaned according to the following protocol:

1. rinsing: 20 x with water
2. ultrasound: 15 minutes in water
3. rinsing: 10 x with water
4. ultrasound: 30 minutes in 2 % Hellmanex
5. rinsing: 20 x with water
6. ultrasound: 20 minutes in water
7. rinsing: 20 x with water
8. ultrasound: 40 minutes in 2 % Hellmanex
9. rinsing: 20 x with water
10. ultrasound: 10 minutes in water
11. rinsing: 20 x with water
12. ultrasound: 10 minutes in methanol

water: ultrafiltered type I water of a NANOpure ultrapure water system from Barnstead
detergent: Hellmanex II from Hellma
methanol: ROMIL SPS (non-volatile residue < 0.0001 %)

Annex B: Acquisition parameters for FTIR

acquisition parameters:	acquisition mode: double sided, fast return
	no correlation test mode
	low pass filter: 16 kHz
	multiplexed data ADC 1
	resolution: 1 cm^{-1}
optic parameters:	source settings: globar (MIR)
	beam splitter setting: KBr
	stabilization delay: 0
	scanner velocity: 60 kHz
FT-parameters:	phase resolution 32
	phase correction mode: power spectrum
	apodization function: triangular

Annex C: Treatment of FTIR spectra after acquisition

1. water subtraction
2. calculation of exponential of spectrum: $10^{spectrum}$
3. inverse Fourrier transformation
4. Fourier transformation with a reduced resolution of 4 cm^{-1}, zero filling factor 2, triangular apodization
5. calculation of logarithm of spectrum: log(spectrum)

Annex D: Infrared Spectra

SA/GI : self-assembled thiolipid layer, measured with GI-FTIR
LB/GI : transferred LB-layer, measured with GI-FTIR
KBr : transmission spectrum of KBr pellet

x-axes : wavenumber in cm^{-1}
y-axes : absorption (logarithm of the relative intensity): $A = -\log(I/I_0)$

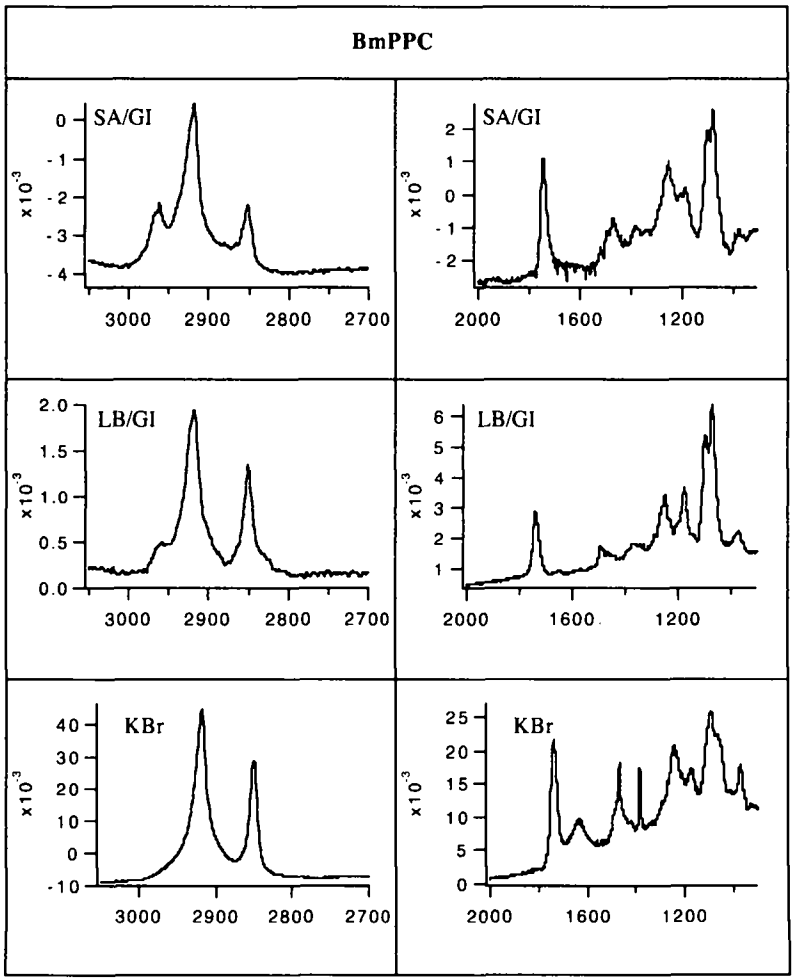

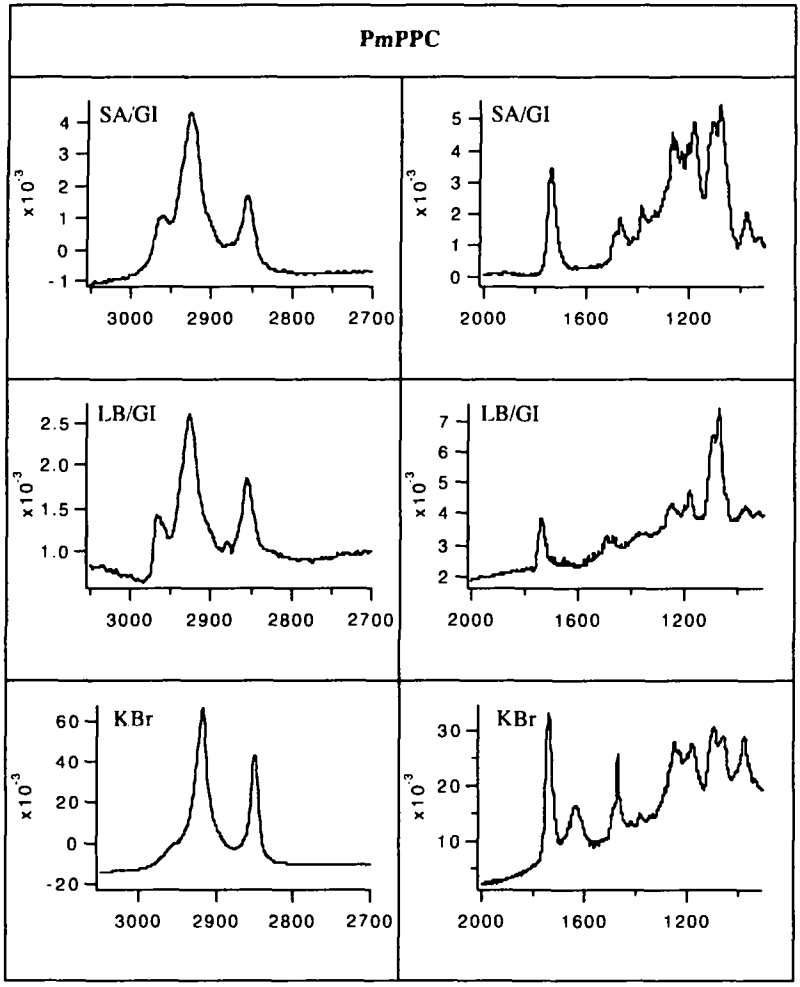
PmPPC
SA/GI
x10-3
4
3
2
1
0
-1
3000
2900
2800
2700
SA/GI
x10-3
5
4
3
2
1
0
2000
1600
1200
LB/GI
x10-3
2.5
2.0
1.5
1.0
3000
2900
2800
2700
LB/GI
x10-3
7
6
5
4
3
2
2000
1600
1200
KBr
x10-3
60
40
20
0
-20
3000
2900
2800
2700
KBr
x10-3
30
20
10
2000
1600
1200

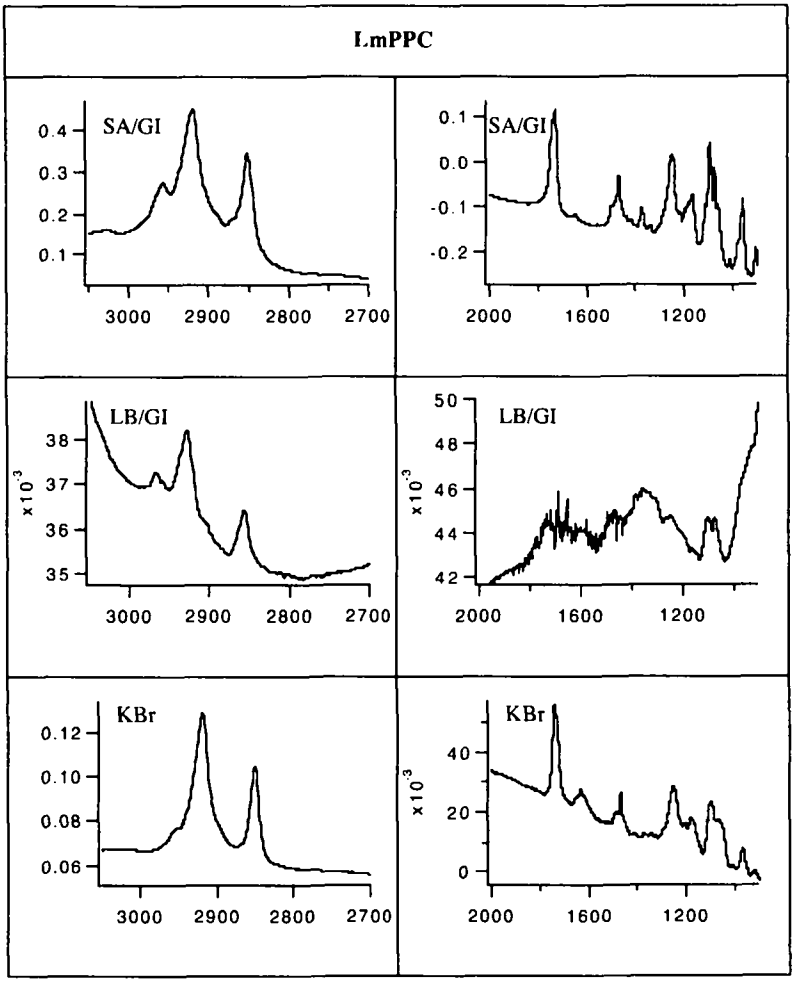
LmPPC
SA/GI
0.4
0.3
0.2
0.1
3000
2900
2800
2700
SA/GI
0.1
0.0
-0.1
-0.2
2000
1600
1200
LB/GI
x10-3
38
37
36
35
3000
2900
2800
2700
LB/GI
x10-3
50
48
46
44
42
2000
1600
1200
KBr
0.12
0.10
0.08
0.06
3000
2900
2800
2700
KBr
x10-3
40
20
0
2000
1600
1200

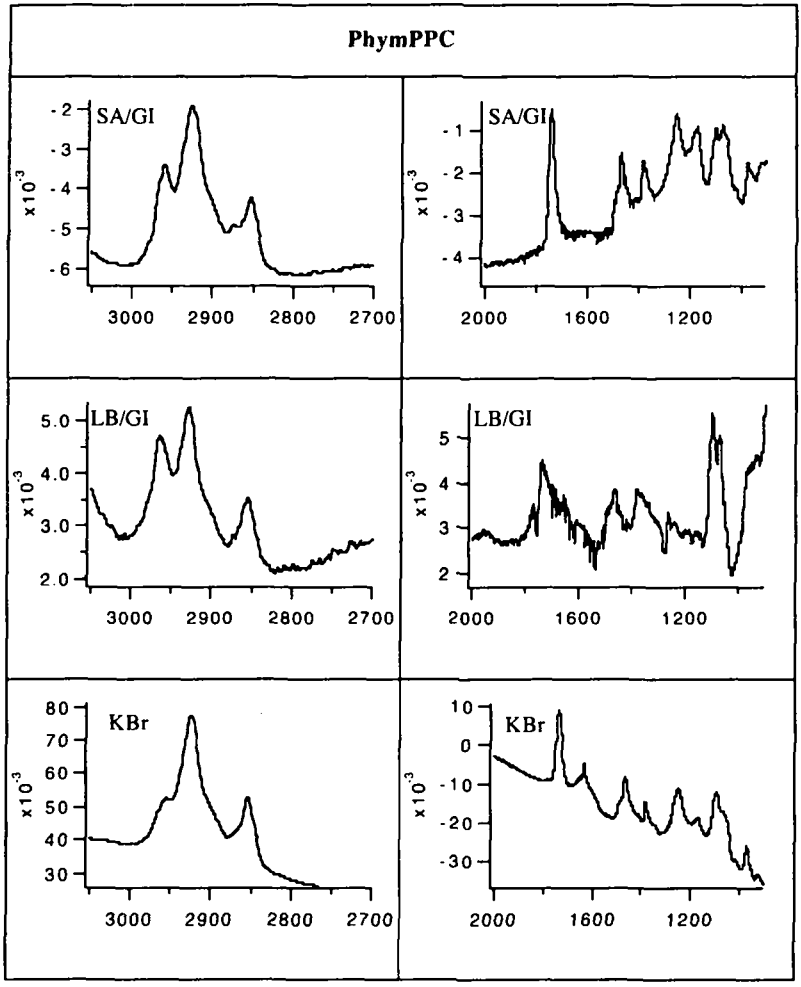
PhymPPC
SA/GI
x10-3
-2
-3
-4
-5
-6
3000
2900
2800
2700
SA/GI
x10-3
-1
-2
-3
-4
2000
1600
1200
LB/GI
x10-3
5.0
4.0
3.0
2.0
3000
2900
2800
2700
LB/GI
x10-3
5
4
3
2
2000
1600
1200
KBr
x10-3
80
70
60
50
40
30
3000
2900
2800
2700
KBr
x10-3
10
0
-10
-20
-30
2000
1600
1200

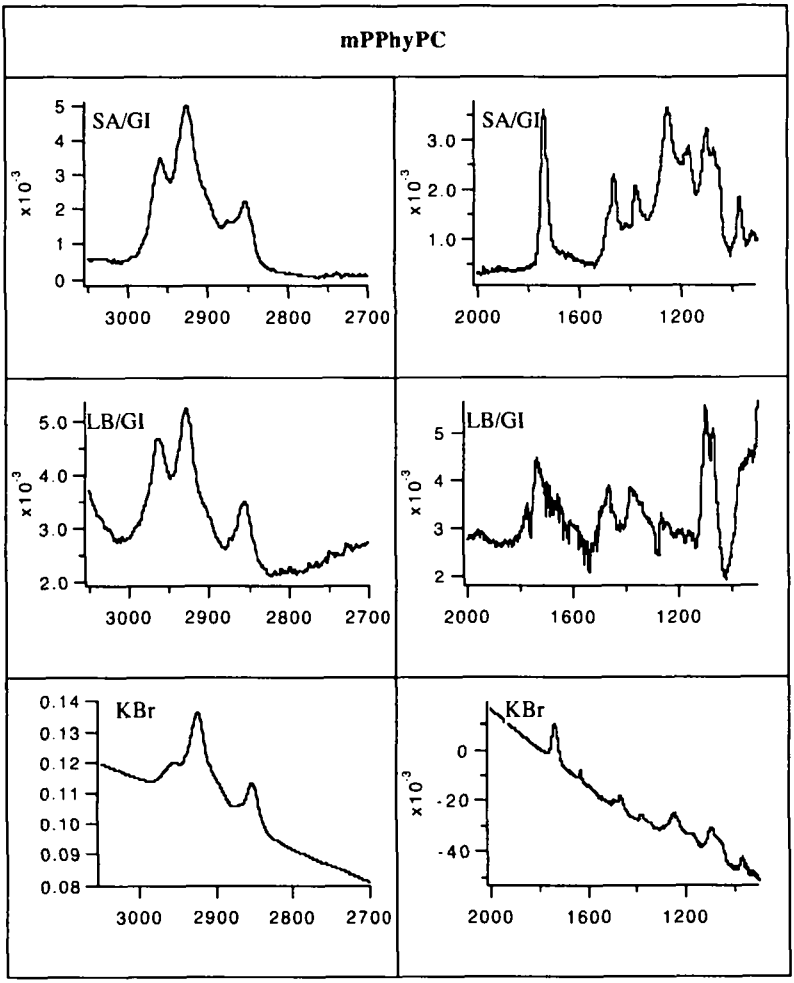
mPPhyPC
SA/GI
x10-3
5
4
3
2
1
0
3000
2900
2800
2700
SA/GI
x10-3
3.0
2.0
1.0
2000
1600
1200
LB/GI
x10-3
5.0
4.0
3.0
2.0
3000
2900
2800
2700
LB/GI
x10-3
5
4
3
2
2000
1600
1200
KBr
0.14
0.13
0.12
0.11
0.10
0.09
0.08
3000
2900
2800
2700
KBr
x10-3
0
-20
-40
2000
1600
1200

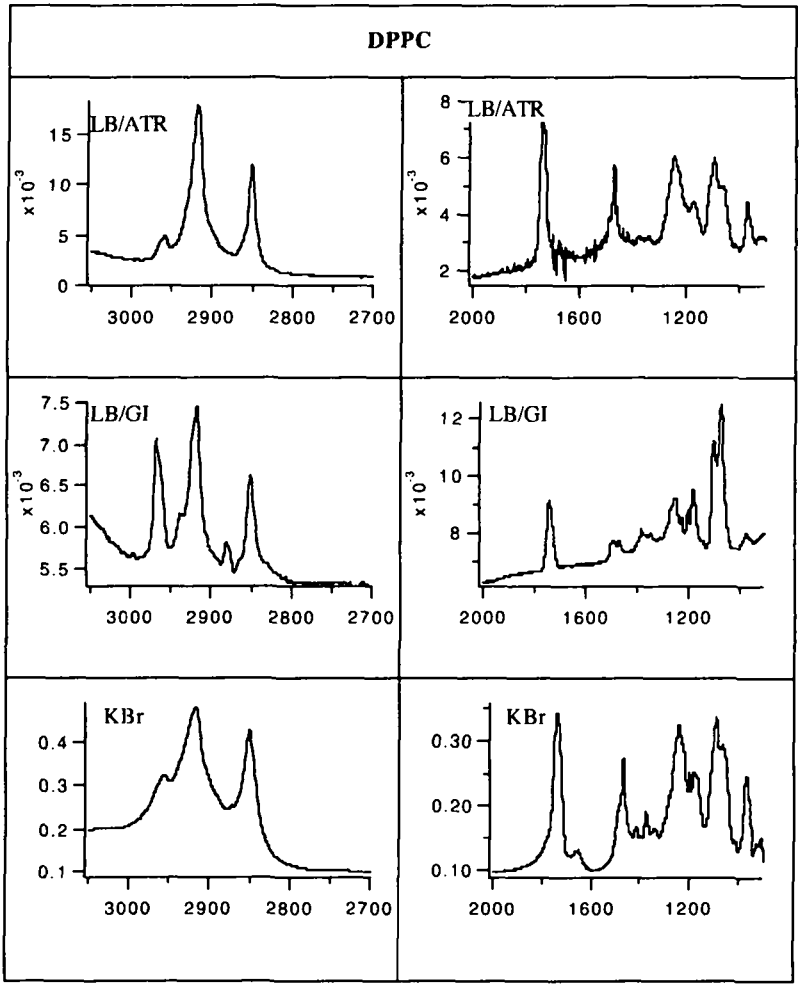
DPPC
LB/ATR
x10-3
15
10
5
0
3000
2900
2800
2700
LB/ATR
x10-3
8
6
4
2
2000
1600
1200
LB/GI
x10-3
7.5
7.0
6.5
6.0
5.5
3000
2900
2800
2700
LB/GI
x10-3
12
10
8
2000
1600
1200
KBr
0.4
0.3
0.2
0.1
3000
2900
2800
2700
KBr
0.30
0.20
0.10
2000
1600
1200

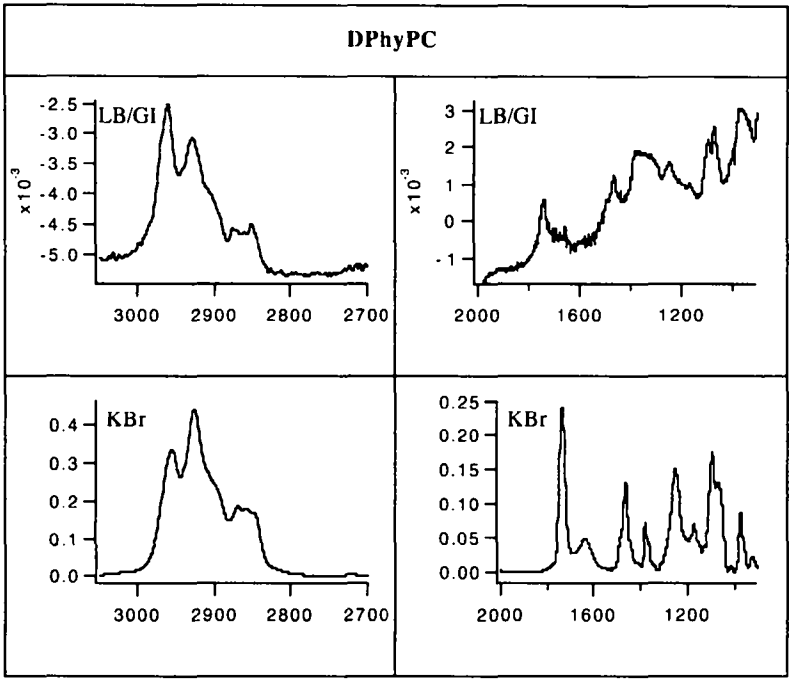

Annex E: TLC Reagents

The following reagents were used for the development of analytical thin layer chromatograms:

1. 15 % **sulfuric acid**, spraying followed by heating
-> general carbon, brown spots

2. 0.1 g of **bromecresolgreen** in 500 ml of ethanol and 5 ml of 0.1 M aqueous sodium hydroxide solution; spraying.
-> carboxylic acids turn yellow, bases light blue [Mac93]

3. 4 mg of **Ellman's reagent** (5,5'-dithio-bis(dinitrobenzoic acid)) per ml of 0.1 M phosphate buffer (pH 8); spraying.
-> thiols turn brown-purple

4. **Hydroxylamine/ Iron(III) chloride**

Solution A: 0.1 mole of hydroxylammonium chloride in 100 ml of methanol is mixed with 0.13 mole of potassium hydroxide in 100 ml of methanol. The precipitating KCl is filtered off.
Solution B: 2 % iron(III) chloride in 1 % aqueous hydrochloric acid.
The TLC plate is sprayed with solution A followed by solution B.
-> esters turn brown-red [Mac93]

5. 0.2 g of **ninhydrin** in 100 ml of ethanol, spraying followed by heating.
-> amines turn red-purple [Mac93]

6. **Zinzade's reagent**

6.85 g of sodium molybdate dihydrate ($Na_2MoO_4 \cdot 2\ H_2O$) and 400 mg of hydrazine sulfate are dissolved in 100 ml of water and 250 ml of conc. sulfuric acid, cooled, and then diluted with 600 ml of water. Immersion of the TLC plate for several minutes, rinsing with water, drying in fume hood.
- > phosphorus containing lipids turn blue [Kat86]

7. **Dragendorff reagent**

Solution A: 7 g of $Bi(NO_3)_3$ in 20 ml of acetic acid and 80 ml of water are mixed with 40 g of KI in 200 ml of acetic acid and 100 ml of water and diluted to 1 liter with water.
Solution B: 20 g of $BaCl_2$ are dissolved in 100 ml of water.
TLC plates are sprayed with a mixture of solution A and B of a ratio of 2:1 (v/v).
-> quarternary amines turn dark red, poly(ethylene glycol) containing compounds orange-red.

Annex F: Synthesis of Quipazinbutyrate for Affinity Purification of the 5-HT$_3$ Receptor

1. Introduction

Serotonin (5-Hydroxytryptamine, 5-HT) is a biogenic amine involved in various physiological actions including signal transmission in the peripheral and central nervous system. Four major serotonin receptor groups have been identified: 5-HT$_1$, 5-HT$_2$ and 5-HT$_4$ receptors transduce extracellular signals by activating G proteins and mediate responses via secondary messenger pathways whereas the 5-HT$_3$ receptor acts as a ligand-gated cation channel. It occurs throughout the central and peripheral nervous system where it mediates the excitatory effects of serotonine [Cac85]. The gene for the murine 5-HT$_3$ receptor has been cloned and sequenced [Mar91]. It shares many features with other ligand-gated ion channels, notably the nicotinic acetylcholine receptor. Affinity chromatography using serotonin or its competitors as ligands allowed the purification of the 5-HT$_3$ receptor from NCB20 cells [McK90] and from the mouse neuroblastoma x rat glioma hybrid cell line NG108-15 [Boe92].

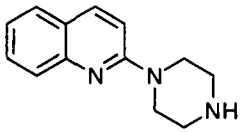

Fig. G.1. Quipazine

Purification of the 5HT$_3$ receptor from pig brain was aimed at by affinity chromatography. The antagonist quipazine was chosen as a ligand because it binds several subunits of the 5HT$_3$ receptor. Quipazine itself (fig. G.1) is thus not very selective, but N-methyl-quipazine is. In analogy selectivity was therefore hoped to be increased by immobilization of quipazine via the same amino group which is methylated in methyl-quipazine. In order to immobilize quipazine the dimaleate salt had to be modified in a three-step synthesis (scheme G.1). The resulting quipazinebutyrate was then coupled in a carbodiimide-mediated reaction to the terminal amine group of diaminodipropylamine agarose (Pierce). This gel is a Sepharose CL 4B to with a hydrophilic spacer (fig. G.22). The final concentration of available amino groups is 16 - 20 µmoles per ml of gel.

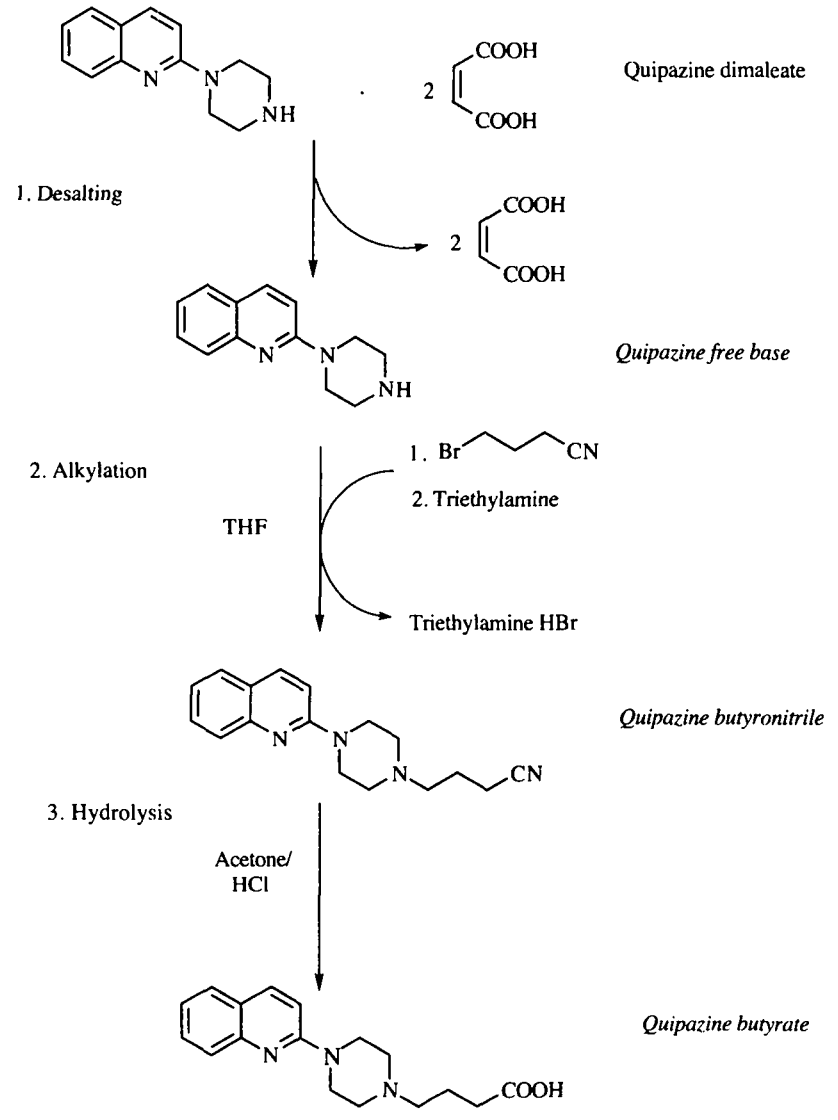

Scheme G.1. Synthesis of Quipazinebutyrate.

2. Synthesis of Quipazinebutyrate

a) Materials

Quipazine dimaleate was purchased from Cookson, 1-bromo-4-butyronitrile (purum) and triethylamine (purum) from Fluka, 1-ethyl-3-(3-dimethylaminopropyl) carbodiimide (EDC) from Pierce. Thin layer chromatography plates (Silicagel 60 F 254, 0.2 mm, Merck) were developed in CH_2Cl_2 (10) : methanol (1) : NH_4OH (0.1) and analyzed with UV or by spraying with 15% sulfuric acid or with an ethanolic solution of bromecresolgreen.

b) Desalting of Quipazine dimaleate

500 mg (1.1 mmol) of Quipazine dimaleate were dissolved upon slight warming in 10 ml of 100 mM $NaHCO_3$ buffer (pH 10.3). pH was readjusted to about 10 with NaOH. The turbid suspension was extracted with five times 25 ml of ether. The united ether fractions were dried from potassium carbonate and evaporated to dryness yielding Quipazine free base.

Molecular weight:	213.3 ($C_{13}H_{15}N_3$)
Yield:	97 %
^{1}H-NMR (D_2O):	3.55 (t, 4 H), 4.2 (t, 4 H), 7.4 (d, 1 H), 7.6 (m, 1 H), 7.9 (m, 3 H), 8.4 (d, 1 H)
TLC-system(R_f)	CH_2Cl_2/ MetOH/ NH_4OH 10:1:0.1 (0.46)

c) Synthesis of Quipazinebutyronitrile

233 mg (1.1 mmol) of Quipazine free base were dissolved in 15 ml of tetrahydrofurane (freshly distilled from CaH_2). 1 ml (10 mmol) of 4-bromobutyronitrile and 0.4 ml (3 mmol) of triethylamine were added and the mixture refluxed over night. After evaporation of the solvent the residue was resuspended in 20 ml of ether, filtered and the residue washed with ether. The ether phase was then extracted with three times 10 ml of 1 M NaOH followed by 4 M H_2SO_4. The acidic phase was made alkaline and subsequently extracted with 6 times 30 ml of ether. The united ether fractions were dried from K_2CO_3 and evaporated almost to dryness. Upon cooling Quipazinebutyronitrile was isolated as yellowish crystals, soluble in chloroform, methylene chloride, acetone and warm ether.

Molecular weight:	280.4 ($C_{17}H_{20}N_4$)
Yield:	58 %
^{1}H-NMR ($CDCl_3$):	1.9 (q, 2 H), 2.5 (m, 8 H), 3.7 (t, 4 H), 7.0 (d, 1 H), 7.2 (t, 1 H), 7.6/ 7.7 (m, 3 H), 7.9 (d, 1 H)
IR (ATR-FTIR):	2940 (m), 2730 (w), 2690 (m), 2590 (m), 1730 (s), 1450 (w), 1420 (w), 1400 (w), 1260 (w), 1165 (s)
TLC-system(R_f)	CH_2Cl_2/ MetOH/ NH_4OH 10:1:0.1 (0.94)

d) Synthesis of Quipazinebutyrate

48.5 mg (0.17 mmol) of quipazinebutyronitrile were dissolved in little acetone and 3 ml of concentrated hydrochloric acid were added. The mixture was refluxed over night. 36.2 mg of Quipazinebutyrate·3 HCl were isolated by preparative TLC (Silicagel 60, eluent: CH_2Cl_2/ MetOH/ NH_4OH 10:1:0.1).

Molecular weight:	299.4 ($C_{17}H_{21}N_3O_2$)
Yield:	58 %
^{1}H-NMR (D_2O):	2.0 (m, 2 H, b), 2.35 (m, 2 H, a), 3.15 (m, 2 H, c), 3.4 (m, 4 H, d), 3.95 (m, 4 H, e), 7.0 (d, 1 H), 7.4 (m, 1 H), 7.65 (m, 3 H), 8.0 (d, 1 H) *For attribution of peaks see fig. G.3.*
^{13}C-NMR (D_2O):	20.8, 35.1, 44.0, 51.9, 57.9, 111.5, 122.5, 123.3, 125.7, 129.1, 132.6, 142.3, 155.3, 181.7
IR (KBr):	2960 (m), 2920 (m), 2850 (w), 2670 (w), 2590 (m), 2460 (m), 1720 (m), 1645 (s), 1605 (s), 1565 (m), 1510 (s), 1430 (s), 1400 (s), 1345 (w), 1320 (w), 1280 (w), 1240 (w) cm^{-1}
MS (EI):	299 (2), 196 (3), 183 (7), 169 (17), 157 (100), 144 (10), 128 (46),
101	(16), 77 (14), 75 (14), 56 (28)

TLC-system(R_f) : CH_2Cl_2/ MetOH/ NH_4OH 10:1:0.1 (0.06)

Elemental analysis:		C	H	N
	% calculated[1]:	50.33	5.96	10.36
	% found:	50.01	5.88	10.18

1) calculated for quipazinebutyrate · 3 HCl!

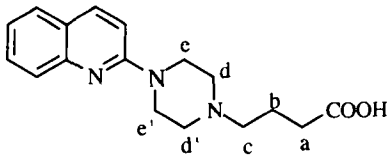

Fig. G.3. Attribution of ^{1}H-NMR peaks.

c) Coupling of Quipazinbutyrate to Diaminodipropylamineagarose

For dehalogenation of the quipazinebutyrate·3 HCl fresh silver oxide was prepared by reacting silver nitrate with sodium hydroxide. After stirring of the aqueous mixture for 15 minutes the black precipitate was filtered, washed with water and added to the hydrochloride salt of quipazinebutyrate dissolved in 0.1 M sodium hydroxide. Stirring was continued overnight at 40 ^{0}C. The black suspension was filtered twice and the filtrate evaporated to dryness yielding quipazinebutyrate sodium salt.

This was then coupled to the primary amine of the diaminodipropylamine agarose (Pierce) in a carbodiimide-mediated reaction forming an amide bond (scheme G.2). 10 ml gel suspension corresponding to 5 ml settled gel were therefore washed with water. 8.24 ml of 0.1 M piperazine buffer (pH 4.8) were added to 160 µl of 54.8 mM quipazinebutyrate (8.76 µmole), followed by 100 mg of EDC (600 µmole) in 400 µl of piperazine buffer. The solution was added to the washed gel and shaken vigorously. Assuming that quipazinebutyrate which has disappeared from the supernatant is covalently bound to the gel, the coupling reaction was followed by taking samples from the supernatant for measurement of UV absorbance at 340 nm (ε = 5974). The reaction was stopped by filtration at the desired concentration of coupled ligand (0.6 µmole/ ml gel, [1]). A 20-fold excess of acetic acid and 100 mg (600 µmol) EDC in 4.7 ml

piperazine buffer was used to block the remaining free amino groups of the resin. After shaking over night the gel was filtered, washed with 0.1 M acetate (pH 4), a solution of NaOH (pH 8.3) and 0.5 M NaCl. The gel was stored in 100 mM Tris buffer (pH 6.5) containing 1 mM EDTA, 0.5% Triton x-100 and 0.2 % NaN_3.

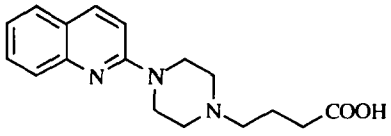

Quipazine butyrate

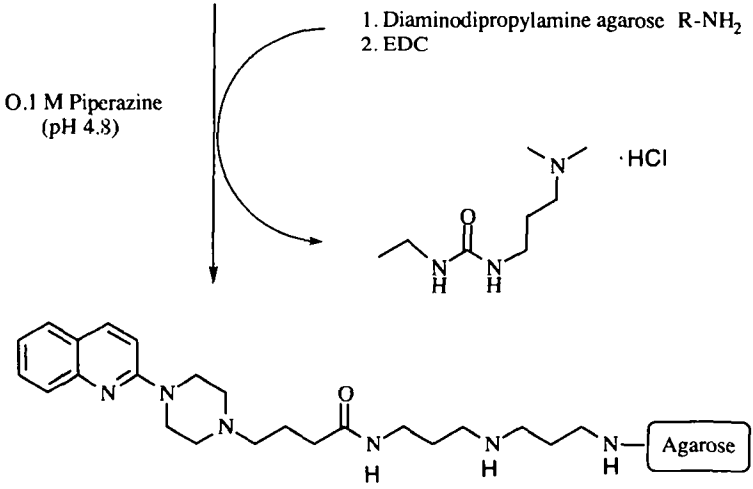

Quipazine butyrate agarose

Scheme G.2. Coupling of Quipazinebutyrate to diaminodipropylamine agarose (Pierce).

Literature

[Alb82] O. Albrecht, D.S. Johnston, C. Villaverde, D. Chapman, *Biochim. Biophys. Acta* 687 (1982) 165

[All78] D.L. Allara, A. Baca, C.A. Pryde, *Macromolecules* 11 (1978) 1215

[All82] D.L. Allara, J.D. Swalen, *J. Phys. Chem.* 86 (1982) 2700

[All85a] D.L. Allara, R.G. Nuzzo, *Langmuir* 1 (1985) 45

[All85b] D.L. Allara, R.G. Nuzzo, *Langmuir* 1 (1985) 52

[And73] J.D. Andrade, *Med. Instr. (Baltimore)* 7 (1973) 110

[And76] J.D. Andrade, *Med. Instr.* 7 (1976) 110

[And85a] J.D. Andrade, *Surface and Interfacial Aspects of Biomedical Polymers* 2 (1985), Plenum Press, New York

[And85b] J.D. Andrade, *Protein Adsorption* (1985) Plenum Press, New York

[And86] J.D. Andrade, V. Hlady, *Adv. Polymer Sci.* 79 (1986) 1

[And87] J.D. Andrade, V. Hlady, *Ann. N. Y. Acad. Sci.* 516 (1987) 158

[And90] J.D. Andrade, J.-N. Lin, V. Hlady, J. Herron, D. Christensen, J. Kopecek in *Biosensor Technology: Fundamentals and Applications* (1990) 219, R.P. Buck (editor), Dekker

[And92] J.D. Andrade, V. Hlady, A.-P. Wei, C.-H. Ho, A.S. Lea, S.I. Jeon, Y.S. Lin, E. Stroup, *Clinical Materials* 11 (1992) 67

[And93] J.D. Andrade, *J. Ass. Adv. Med. Inst.* 7 (1993) 110

[Arn85] T. Arnebrant, B. Ivarsson, K. Larsson, I. Lundström, T. Nylander, *Progr. Colloid Polym. Sci.* 70 (1985) 62

[Ava94] catalogue of Avanti Polar Lipids, Inc. (1994)

[Bai72] R.E. Baier, *Bull. N.Y. Acad. Med.* 48 (1972) 257

[Bai88] C.D. Bain, G.M. Whitesides, *Science* 240 (1988) 62

[Bai89a] C.D. Bain, E.B. Troughton, Y.-T. Tao, J. Evall, G.M. Whitesides, *JACS* 111 (1989) 321

[Bai89b] C.D. Bain, J. Evall, G.M. Whitesides, *JACS* 111 (1989) 7155

[Bai88c] C.D. Bain,G.M. Whitesides, *JACS* 111 (1989) 7164

[Ben75] R. Benz, O. Fröhlich, P. Läuger, M. Montal, *Biochim. Biophys. Acta* 394 (1975) 323

[Ber92] K. Bergström, K. Holmberg, A. Safranj, A.S. Hoffman, M.J. Edgell, A. Kozlowski, B.A. Hovanes, J.M. Harris, *J. Biomed. Mat. Res.* 26 (1992) 779

[Ber93] L. Bertilsson, B. Liedberg, *Langmuir* 9 (1993) 141

[Bla85] P. Blake, J. Ralston, *Coll. Surf.* 15 (1985) 101

[Blu83] A. Blume, *Biochemistry* 22 (1983) 5436

[Boe92] F.G. Boess, S.C.R. Lummis, I.L. Martin, *J. Neurochem.* 59 (1992) 1692

[Bok76] L. Boksànyi, O. Liardon, E.sz. Kovàts, *Advan. Colloid Interface Sci.* 6 (1976) 95

[Bon97] M. Bontcheva, H. Vogel, *Biophys. J.* 73 (1997) 1056

[Bül81] G. Büldt, R. Wohlgemuth, *J. Membrane Biol.* 58 (1981) 81

[Cac85] S. Caccia et al., *J. Pharm. Pharmacol.* 37 (1985) 567

[Cas83] H.L. Casal, H.H. Mantsch, *Biochem. Biophys. Acta* 735 (1983) 387

[Cev93] G. Cevc, *Phospholipids Handbook* (1993), Marcel Dekker Inc., N.Y.

[Cha84] D. Chapman, A.A. Durrani, *European Patent* 157469 (1984)

[Che89] S.H. Chen, C.F. Frank, *Langmuir* 5 (1989) 978

[Chu91] Y.-C. Chung, S.L. Regen, *Macromolecules* 24 (1991) 5738

[Coh86] S.R. Cohen, R. Naaman, J. Sagiv, *J. Phys. Chem.* 90 (1986) 3054

[Cib79] Wissenschaftliche Tabellen Geigy: *Hämatologie und Humangenetik* (1979) Ciba-Geigy limited, Basel

[Col80] B.S. Coller, *Blood* 55 (1980) 169

[Col82] D.L. Coleman, D.E. Gregonis, J.D. Andrade, *J. Biomed. Mat. Res.* 16 (1982) 381

[Cos70] M. Costello, B. Stanczewski, P. Vriesman, S. Lucas, S. Srinivasan, P.N. Sawyer, *Trans. Am. Soc. Artif. Intern. Organs 16 (1970) 1*

[Coy89] L.C. Coyle, Y.N. Danilov, R.L. Juliano, S.L. Regen, *Chem. Mat.* 1 (1989) 606

[Cuy78] P.A. Cuypers, W.T. Hermens, H.C. Hemker, *Anal. Biochem.* 84 (1978) 56

[Deb82] M.K. Debe, *Appl. Surf. Sci.* 14 (1982) 1

[Deb84] M.K. Debe, *J. Appl. Phys.* 55 (1984) 3354

[DeG85] P.G. De Gennes, *Rev. Mod. Phys.* 57 (1985) 827

[Dem75] R.A. Demel, W.S.M. Geurts van Kessel, R.F.A. Zwaal, B. Roelofsen, L.M.M. Van Deenen, *Biochim. Biophys. Acta* 406 (1975) 97

[Die86] T. Diem, B. Czajka, B. Weber, S.L. Regen, *JACS* 108 (1986) 6094

[Dil82] J.P. Dilger, L.R. Fisher, D.A. Haydon, *Chem. Phys. Lipids* 30 (1982) 159

[Din81] M.B. Dines, P.M. Di Giacomo, *Inorg. Chem.* 20 (1981) 92

[Dur86] A.A. Durrani, J.A. Hayward, D. Chapman, *Biomaterials* 7 (1986) 121

[Dur87] A.A. Durrani, *European Patent* 275293 B1 (1987)

[Dus96a] C. Duschl, M. Liley, H. Lang, A. Ghandi, S.M. Zakeeruddin, H. Stahlberg, J. Dubochet, A. Nemetz, W. Knoll, H. Vogel, *Mat. Sci. Eng.* C4 (1996) 7

[Dus96b] C. Duschl, A.-F. Sévin-Landais, H. Vogel, *Biophys. J.* 70 (1996) 1985

[Eib81] H. Eibl, Chapter 2 in *Liposomes: From Physical Structure to Therapeutic Applications* (1981), C.G. Knight (editor), Cambridge

[Eva91] S.D. Evans, E. Urankar, A. Ulman, N. Ferris, *JACS* 113 (1991) 4121

[Eve94] R.P. Evershed, *Development in the Analysis of Lipids* (1996) 123, Royal Society of Chemistry

[Fab89] W. Fabianowski, L.C. Coyle, B.A. Weber, R.D. Granata, D.G. Castner, A. Sadownik, S.L. Regen, *Langmuir* 5 (1989) 35

[Fäg90] L.G. Fägerstam, Å. Frostell, R. Karlsson, M. Kullman, A. Larsson, M. Malmqvist, H. Butt, *J. Molec. Recog.* 3 (1990) 208

[Fen83] G.R. Fenwick, J. Eagles, R. Self, *Biomed. Mass Spectr.* 10 (1983) 382

[Fin86] H.O. Finklea, L.R. Robinson, A. Blackburn, B. Richter, D. Allara, T. Bright, *Langmuir* 2 (1986) 239

[Fri77] U.P. Fringeli, *Z. Naturforsch.* 32 c (1977) 20

[Fri79] U.P. Fringeli, *Infrared Membrane-Spectroscopy*, Habilitationsschrift ETHZ (1979)

[Fri81] U.P. Fringeli, Hs.H. Günthard, in *Membrane Spectroscopy* (1981) 270, E. Grell (editor), Springer, Berlin Heidelberg

[Fuj81] T. Fujisawa, T. Sato, T. Kawara, K. Ohashi, *Tetrahedron Letters* 22 (1981) 4823

[Gen82] R.M. Gendreau, R.I. Leininger, S. Winters, R.J. Jakobsen, *Biomat. Adv. Chem. Series* 199 (1982) 371

[Gen89] R.B. Gennis, *Biomembranes: Molecular Structure and Function* (1989) Springer-Verlag, New York

[Gom91] W.R. Gombotz, W. Guanghui, T.A. Horbett, A.S. Hoffman, *J. Biomed. Mat. Res.* 25 (1991) 1547

[Gre66] R.G. Greenler, *J. Chem. Phys.* 44 (1966) 310

[Gre69] R.G. Greenler, *J. Chem. Phys.* 50 (1969) 1963

[Gri74] O.H. Griffith, P.J. Dehlinger, S.P. Van, *J. Membrane. Biol.* 15 (1974) 159

[Gom91] W.R. Gombotz, W. Guanghui, T.A. Horbett, A.S. Hoffman, *J. Biomed. Mat. Res.* 25 (1991) 1547

[Gun94] F.D. Gunstone, *Development in the Analysis of Lipids* (1996) 109, Royal Society of Chemistry

[Ham92] R.J. Hamilton, S. Hamilton, *Lipid Analysis- A Practical Approach* (1992) IRL Press, Oxford

[Han64] T. Hanai, D.A. Haydon, J. Taylor, *Proc. R. Soc. London* A281 (1964) 377

[Han65] T. Hanai, D.A. Haydon, J. Taylor, *J. Theoret. Biol.* 9 (1965) 278

[Hau81] H. Hauser, I. Pascher, I.H. Pearson, S. Sundell, *Biochim. Biophys. Acta* 650 (1981) 21

[Hay84] J.A. Hayward, D. Chapman, *Biomaterials* 5 (1984) 135

[Her90] S. Hertling-Jaweed, G. Bandini, F. Hucho in E.C. Hulme, *Receptor Biochemistry - A practical Approach* (1990), Oxford Univesity Press

[Hey97] S. Heyse, *Investigation of Biomolecular Interactions at Supported Membranes by Evanescent Wave Techniques: Self-Asssembly, Reconstitution of Receptors, and Molecular Recognition* (1997), Thesis EPFL, Lausanne

[Hil84] B. Hille, *Ionic Channels of Excitable Membranes* (1984) Sinauer Associates, Inc., Sunderland, Massachusetts

[Hof82] A.S. Hoffman, *Adv. Chem. Series* 199 (1982) 1

[Hol89] F. Holler, J.B. Callis, *J. Phys. Chem.* 93 (1989) 2053

[Hop65] C.Y. Hopkins, *Progress in Chemistry of Fats and other Lipids* 8 (1965) 213

[Hor87] T.S. Horbett, J. Brash, *Am. Chem. Soc. Symp. Series* 343 (1987), Proteins at Interfaces

[Hüb91] W. Hübner, H.H. Mantsch, *Biophys. J.* 59 (1991) 1261

[Ika84] Y. Ikada, *Adv. Polym. Sci.* 57 (1984) 103

[Ima92] Y. Imanishi (editor), *Synthesis of Biocomposite Materials: Chemical and Biological Modification of Natural Polyers* (1992) CRC Press

[Ish90] K. Ishihara, R. Aragaki, T. Ueda, A. Watenabe, N. Nakabayashi, *J. Biomed. Mat. Res.* 24 (1990) 1069

[Ish92] K. Ishihara, S.-I. Ohta, T. Yoshikawa, N. Nakabayashi, *J. Polym Sci. Part A: Polym. Chem.* 30 (1992) 929

[Ish93] K. Ishihara, N. Nakabayashi, K. Nishida, M. Sakakida, M. Shichiri, *Chemtech* (Oct. 1993) 19

[Isr92a] J.N. Israelachvili, *Intermolecular Forces and Surface Forces* (1992) second edition, Academic Press

[Isr92b] J. N. Israelachvili, H. Wennerström, *J. Phys. Chem.* 96 (1992) 520

[Ito86] Y. Ito, M. Sisidio, Y. Imanishi, *J. Biomed. Mat. Res.* 20 (1986) 1139

[Ito90] Y. Ito, M. Sisidio, Y. Imanishi, *J. Biomed. Mat. Res.* 24 (1990) 229

[Jac89] R.E. Jacobs, S.H. White, *Biochemistry* 28 (1989) 3421

[Jay90] N. Jayasuriya, S. Bosak, S.L. Regen, *JACS* 112 (1990) 585

[Jeo91] S. I. Jeon, J.H. Lee, J.D. Andrade, P.G. De Gennes, *J. Colloid Interface Sci.* 142 (1991) 149

[Joh80] D.S. Johnston, S. Sanghera, M. Pons, D. Chapman, *Biochim. Biophys. Acta* 602 (1980) 57

[Jön85] U. Jönsson, G. Olofsson, M. Malmqvist, I. Rönnverg, *Thin Solid Films* 124 (1985) 117

[Kal87] K.M.R. Kallury, U.J. Krull, M. Thompson, *J. Org. Chem.* 52 (1987) 5478

[Kat86] M. Kates, *Techniques of Lipidology - Isolation, Analysis, and Identification of Lipids* (1986) Elsevier

[Kes91] C.R. Kessel, S. Granick, *Langmuir* 7 (1991) 532

[Kno91] W. Knoll, *MRS Bull.* 16 (1991) 29

[Koj91] M. Kojima, K. Ishihara, A. Watanabe, N. Nakabayashi, *Biomaterials* 12 (1991) 121

[Kre94] E. Kretschmann, *Opt. Commun.* 6 (1972) 185

[Kuh94] T.L. Kuhl, D.E. Leckband, D.D. Lasic, J.N. Israelachvili, *Biophys. J.* 66 (1994) 1479

[Kyt95] J. Kyte, *Structure in Protein Chemistry* (1995) Garland Publishing, Inc., N.Y. & London

[Lai89] P.E. Laibinis, J.J. Hickman, M.S. Wrighton, G.M. Whitesides, *Science* 245 (1989) 845

[Lai92a] P.E. Laibinis, R.G. Nuzzo, G.M. Whitesides, *J. Phys. Chem.* 96 (1992) 5097

[Lai92b] P.E. Laibinis, G.M. Whitesides, *JACS* 114 (1992) 1990

[Lai95] P.E. Laibinis, C.D. Bain, R.G. Nuzzo, G.M. Whitesides, *J. Phys. Chem.* 99 (1995) 7663

[Lan94a] H. Lang, *Supported Lipid Bilayers; An Approach for the Development of Biosensors Based on Membrane Proteins* (1992) Thesis, EPFL, Lausanne

[Lan92b] H. Lang, C. Duschl, M. Grätzel, H. Vogel, *Thin Solid Films* 210/211 (1992) 818

[Lan94] H. Lang, C. Duschl, H. Vogel, *Langmuir* 10 (1994) 197

[Lec94] D. E. Leckband, F.-J. Schmitt, J.N. Israelachvili, W. Knoll, *Biochemistry* 33 (1994) 4611

[Lee95] J.H. Lee, H.B. Lee, J.D. Andrade, *Prog. Polym. Sci.* 20 (1995) 1043

[Lee88a] H. Lee, L.J. Kepley, H.-G. Hong, S. Akhter, T.E. Mallouk, *J. Phys. Chem.* 92 (1988) 2597

[Lee88b] H. Lee, L.J. Kepley, H.-G. Hong, T.E. Mallouk, *JACS* 110 (1988) 618

[Lee89] J.H. Lee, J. Kopecek, J.D. Andrade, *J. Biomed. Mat. Res.* 23 (1989) 351

[Lee88] J.H. Lee, P. Kopeckova, J. Zhang, J. Kopecek, J.D. Andrade, *Proc. Polym. Mat. Sci. Eng.* (1988) 234

[Lei87] R.I. Leininger, T.B. Hutson, R.J. Jakobsen, *Ann. N.Y. Acad. Sci.* 516 (1987) 173

[Len89] T.J. Lenk, B.D. Ratner, R.M. Gendreau, K.K. Chittur, *J. Biomed. Mat. Res.* 23 (1989) 549

[Lew90] R.N.A.H. Lewis, R.N. McElhaney, *Biochemistry* 29 (1990) 7946

[Lew94] R.N.A.H. Lewis, R.N. McElhaney, M.A. Monck, P.R. Cullis, *Biophys. J.* 67 (1994) 197

[Lew96] R.N.A.H. Lewis, R.N. McElhaney in H.H. Mantsch, D. Chapman, *Infrared Spectroscopy of Biomolecules*, Wiley-Liss, New York (1996)

[Lie93] B. Liedberg, I. Lundström, E. Stenberg, *Sensors and Actuators B* 11 (1993) 63

[Lil97] M. Liley, T.A. Keller, C. Duschl, H. Vogel, *Langmuir*, in press

[Löf90] S. Löfås, B. Johnsson, *J. Chem. Soc. Chem. Commun.* (1990) 1526

[Lou75] A.K. Lough, *Progress in the Chemistry of Fats and Other Lipids* 14 (1975) 5

[Lyk84] J. Lyklema, *Colloids and Surfaces* 10 (1984) 33

[Lym65] D.J. Lyman, W.M. Muir, I.J. Lee, *Trans. Am . Soc. Artif. Int. Organs* 11 (1965) 301

[Mac87] J.R. Macdonald (editor), *Impedance Spectroscopy: Emphasizing Solid Materials and Systems*" (1987) John Wiley and Sons., Inc.

[Mac93] Macherey-Nagel, TLC Catalogue (1993)

[Mal96] M. Malmsten, J.-A. Johansson, N.L. Burns, H.K. Yasada, *Colloids Surf. B: Biointerf.* 6 (1996) 191

[Man91] H.H. Mantsch, W. Hübner, *Spectroscopy of Biological Molecules* , Royal Society of Chemistry (1991) 147

[Mao84] R. Maoz, J. Sagiv, *J. Colloid Interf. Sci.* 100 (1984) 465

[Mao85] R. Maoz, J. Sagiv, *Thin Solid Films* 132 (1985) 135

[Mao87a] R. Maoz, J. Sagiv, *Langmuir* 3 (1987) 1034

[Mao87b] R. Maoz, J. Sagiv, *Langmuir* 3 (1987) 1045

[Mao88] R. Maoz, L. Netzer, J. Gun, J. Sagiv, *J. Chim. Phys.* 85 (1988) 1059

[Mar85] J. Marra, J. Israelachvili, *Biochemistry* 24 (1985) 4608

[Mar90] D. Marsh, *CRC Handbook of Lipid Bilayers* (1990) CRC Press

[Mar91] A.V. Maricq, A.S. Peterson, A.J. Brake, R.M. Myers, D. Julius, *Science* 254 (1991) 432

[McK90] R.M. McKernan, N.P. Gillard, K. Quirk, C.O. Kneen, G.I. Stevenson, *J. Biol. Chem.* 265 (1990) 13572

[Men91] R. Mendelsohn, *Spectroscopy of Biological Molecules* , Royal Society of Chemistry (1991) 151

[Mes96] U. Meseth, *Structural and Functional Investigations of Channel-Forming Peptides in Lipid Membranes* (1996) Thesis N° 1538, EPFL, Lausanne

[Mie93] J.A. Mielczarski, *J. Phys. Chem.* 97 (1993) 2649

[Mor77] B.W. Morrissey, *Ann. N. Y. Acad. Sci.* 288 (1977) 50

[Mur93] R.C. Murphy, *Handbook of Lipid Research* 7 (1993)

[Nag84] S. Nagaoka, Y. Mori, H. Takiuchi, K. Yokota, H. Tanzawa, S. Nishiumi, *Polymers as Biomaterials* (1984) 361

[Net83a] L. Netzer, R. Iscovici, J. Sagiv, *Thin Solid Films* 99 (1983) 235

[Net83b] L. Netzer, R. Iscovici, J. Sagiv, *Thin Solid Films* 100 (1983) 67

[Net83c] L. Netzer, J. Sagiv, *JACS* 105 (1983) 674

[Nor80] W. Norde, *Adhesion and Adsorption of Polymers* 2 (1980) 801, L.-H. Lee (ed.), Plenum Press, New York

[Nuz83] R.G. Nuzzo, D.L. Allara, *JACS* 105 (1983) 4481

[Nuz87] R.G. Nuzzo, B.R. Zegarski, L.H. Dubois, *JACS* 109 (1987) 733

[Nuz90] R.G. Nuzzo, L.H. Dubois, D.L. Allara, *JACS* 112 (1990) 558

[Oka78] T. Okano, S. Nishiyama, I. Shinohara, T. Aikaike, Y. Sakurai, *Polymer J.* 10 (1978) 223

[Paw94] M. Pawlak, A. Kuhn, H. Vogel, *Biochemistry* 33 (1994) 283

[Pea79] R.H. Pearson, I. Pascher, *Nature* 281 (1979) 499

[Pet82] R. Peters, K. Beck, *Proc. Natl. Acad. Sci. USA* 80 (1983) 7183

[Pid89] C. Pidgeon, U.V. Venkataram, *Anal. Biochem.* 176 (1989) 36

[Pid90] C. Pidgeon, *United States Patent* 4 931 498 (1990) and 4 927 879 (1990)

[Por87] M.D. Porter, T.B. Bright, D.L. Allara, C.E.D. Chidsey, *J. Am. Chem. Soc.* 109 (1987) 3559

[Pow77] L. Powers, P.S. Persham, *Biophys. J.* 20 (1977) 137

[Pri91] K.L. Prime, G.M. Whitesides, *Science* 252 (1991) 1164

[Pri93] K.L. Prime, G.M. Whitesides, *JACS* 115 (1993) 10714

[Pri95] K.L. Prime, G.M. Whitesides, *JACS* 115 (1995) 10714

[Rat82] B.D. Ratner, *Adv. in Chemistry (Am. Chem. Soc.)* 199 (1982) 9

[Rat96a] B.D. Ratner, *Molecular Engineering of Polymers: Directing Biological Response*, Conference Proceedings (1996) Santa Barbara, CA

[Rat96b] B.D. Ratner, *Lecture Series* (1996) Lausanne, EPFL

[Red71] W.R. Redwood, F.R. Pfeiffer, J.A. Weisbach, T.E. Thompson, *Biochem. Biophys. Acta* 233 (1971) 1

[Rei93] R. Reiter, H. Motschmann, W. Knoll, *Langmuir* 9 (1993) 2430

[Rui97] L. Ruiz, J.G. Hilborn, D. Léonard, H.J. Mathieu, submitted to *Biomaterials*

[Ryh60] R. Ryhage, E. Stenhagen, *J. Lipid Res.* 1 (1960) 361

[Sad86] A. Sadownik, J. Stefely, S.L. Regen, *JACS* 108 (1986) 7789

[Sag80] J. Sagiv, *JACS* 102 (1980) 92

[Sak80] Y. Sakurai, T. Akaike, K. Kataoka, T. Okano, *Biomed. Polym.* (1980) 335, E.P. Goldberg, A. Nakajima (eds.), Academic Press, New York

[Sak92] B. Sakman, *The EMBO Journal* 11 (1992) 2003

[Sam85] N.K.P. Samuel, M. Singh, K, Yamaguchi, S.L. Regen, *JACS* 107 (1985) 42

[San86] T. Sanada, Y. Ito, M. Sisido, Y. Imanishi, *J. Biomed. Mater. Res.* 23 (1986) 1261

[Sat80] T. Sato, R. Ruch, *Stabilization of Colloidal Dispersions by Polymer Adsorption* (1980) Marcel Dekker, New York

[Sch82] M. Schmid, F. Gerber, G. Hirth, *Helvetica Chimica Acta* 65 (1982) 684

[Sch86] N.E. Schlotter, M.D. Porter, T.B. Bright, D.L. Allara, *Chem.Phys. Lett.* 132 (1986) 93

[Sch90] P. Schneider, R. Cloux, K. Fòti, E.sz. Kovàts, *Synthesis* (1990) 1027

[Sch92] T. Schürholz, J. Kehne, A. Gieselmann, E. Neumann, *Biochemistry* 31 (1992) 5067

[See77] J. Seelig, *Quart. Rev. Biophys.* 10 (1977) 353

[See80] J. Seelig, A. Seelig, *Quart. Rev. Biophys.* 13 (1980) 19

[Sev83] V.I. Sevastianov, Z.M. Belomestnaia, N.K. Zimin, *Artif. Organs* 7 (1983) 126

[Sev84] V.I. Sevastianov, E.A. Tseytlina, A.V. Volkov, V.I. Shumakov, *Trans. Am Soc. Artif. Intern. Organs* 30 (1984) 137

[Sha88] J.A. Shafer, D.L. Higgins, *CRC Crit. Rev. Clin. Lab. Sci.* 26 (1988) 1

[She92] C.W. Sheen, J.-X. Shi, Y. Martensson, A.N. Parikh, D.L. Allara, *JACS* 114 (1992) 1514

[Sny82] R.G. Snyder, H.L. Strauss, C.A. Elliger, *J. Phys. Chem.* 86 (1982) 5145

[Sny86] R.G. Snyder, M. Maroncelli, H.L. Strauss, V.M. Hallmark, *J. Phys. Chem.* 90 (1986) 5623

[Spi92] J. Spinke, J. Yang, H. Wolf, M. Liley, H. Ringsdorf, W. Knoll, *Biophys. J.* 63 (1992) 1667

[Spi93] J. Spinke, M. Liley, H.J. Guder, L. Angermaier, W. Knoll, *Langmuir* 9 (1993) 1821

[Spi95] U.E. Spichiger, *Grundlagen zum Verständnis der Funktionsweise von chemischen Sensoren und Biosensoren* (1995) Course ETH Technopark, Zürich

[Ste96] C. Steinem, A. Janshoff, W.-P. Ulrich, M. Sieber, H.-J. Galla, *Biochim. Biophys. Acta* 1279 (1996) 169

[Swa85] J.D. Swalen, J.F. Rabolt, *Fourier Transform Infrared Spectroscopy* 4 (1985) 283

[Swa87] J.D. Swalen, D.L. Allara, J.D. Andrade, E.A. Chandross, S. Garoff, J. Israelachvili, T.J. McCarthy, R. Murray, R.F. Pease, J.F. Rabolt, K.J. Wynne, H. Yu, *Langmuir* 3 (1987) 932

[Sza84] K. Szabò, N.L. Ha, P. Schneider, P. Zeltner, E.sz. Kovàts, *Helv. Chim. Acta* 67 (1984) 2128

[Ter88] Y. Terao, M. Murata, K. Achiwa, T. Nishio, M. Akamtsu, M. Kamimura, *Tetrahedron Letters* 29 (1988) 5173

[Ter93] S. Terrattaz, T. Stora, C. Duschl, H. Vogel, *Langmuir* 9 (1993) 1361

[Thi97] J. Thiele, *Aufbau und Charakterisierung monomolekularer Schichten aus Polysiloxanen mit funktionalisierten Seitenketten zur Verbesserung der Biokompatibilität von Materialien* (1997) Thesis, Johannes Gutenberg Universität, Mainz

[Til89] N. Tillman, A. Ulman, T.L. Penner, *Langmuir* 5 (1989) 101

[Til90] N. Tillman, A. Ulman, J.F. Elman, *Langmuir* 6 (1990) 1512

[Tro88] E.B. Troughton, C.D. Bain, G.M. Whitesides, R.G. Nuzzo, D.L. Allara, M.D. Porter, *Langmuir* 4 (1988) 365

[Ulm88] A. Ulman, D.J. Williams, T.L. Penner, D.R. Robello, J.S. Schildkraut, M. Scazzafava, C.S. Willand, *US Patent 4 792.208* (1988)

[Ulm89] A. Ulman, N. Tillman, *Langmuir* 5 (1989) 1418

[Ulm91] A. Ulman, *An Introduction to Ultrathin Organic Films: From Langmuir-Blodgett to Self-Assembly* (1991) Academic Press, San Diego, CA

[Ulm92] A. Ulman, S.D. Evans, R.G. Snyder, *Thin Solid Films* 210/211 (1992) 806

[Van81] P. Van Dulm, W. Norde, J. Lyklema, *J. Colloid Interface Sci.* 82 (1981) 77

[Val85] G. P. Valencia, *European Patent* 247114 (1985)

[Wal91] M.M. Walczak, C. Chung, S.M. Stole, C.A. Widrig, M.D. Porter, *JACS* 113 (1991) 2370

[Was89a] S.R. Wasserman, G.M. Whitesides, I.M. Tidswell, B.M. Ocko, P.S. Pershan, J.D. Axe, *JACS* 111 (1989) 5852

[Was89b] S.R. Wasserman, Y.-T. Tao, G.M. Whitesides, *Langmuir* 5 (1989) 1074

[Wea73] R.C. Weast (Editor), *Handbook of Chemistry and Physics* (1973) CRC, Cleveland, OH

[Wei95] G. Weissmüller, *Determination of Structural and Electrical Properties of Supported Lipid Films by Impedance Analysis, Surface Plasmon Spectroscopy and Reflection Interference Contrast Microscopy* (1995) Thesis, Technische Universität München

[Whi88] G.M. Whitesides, G.S. Ferguson, *Chemtracts* 1 (1988) 171

[Whi94] S. White, W.C. Wimley, *Curr. Opin. Struct. Biol.* 4 (1989) 3421

[Wie89] M.C. Wiener, R.M. Suter, J.F. Nagle, *Biophys. J.* 55 (1989) 315

[Wil91] G.M. Willems, W.T. Hermens, H.C. Hemker, *Biomat. Sci. Polym. Ed.* 2 (1991) 217

[Win96] E. Wintermantel, S.-W. Ha, *Biokompatible Werkstoffe und Bauweisen* (1996) Springer Verlag Berlin Heidelberg

[Woj93] P.W. Wojciechowski, J. Brash, *Colloids Surf. B: Biointerf.* 1 (1993) 107

[Wor76] D.L. Worcester, N.P. Franks, *J. Mol. Biol.* 100 (1976) 359

[Yam94] K. Yamamoto, H.Ishida, *Appl. Spectr.* 48 (1994) 775

[Yen89] Y.-S. Yen, J.S. Wong, *J. Phys. Chem.* 93 (1989) 7208

Curriculum Vitae

date of birth:	:	6. 7. 1966 (Männedorf, Switzerland)
1973- 1979	:	primary school in Männedorf
1979 - 1985	:	high school in Zurich
1985 - 1986	:	Au-pair in Denver, Colorado (USA)
1986 - 1991	:	studies of chemistry at the Swiss Federal Institute of Technology in Zurich (ETH)
1991	:	- research assistant at the Institute of Biochemistry, Academica Sinica, Shanghai (China) - research assistant at the Eidgenössische Anstalt für Wasser, Abwasser und Gewässerschutz (EAWAG) in Dübendorf
1992	:	research assistant at the Heart Research Institute, Sydney (Australia)
1993 -	:	Ph. D. student and teaching assistant at the Swiss Federal Institute of Technology in Lausanne (EPFL)